

The Geology and Mechanics of Formation of the Fort Rock Dome, Yavapai County, Arizona

U.S. GEOLOGICAL SURVEY PROFESSIONAL PAPER 1266



**THE GEOLOGY AND MECHANICS OF
FORMATION OF THE FORT ROCK DOME,
YAVAPAI COUNTY, ARIZONA**



Aerial view of the Fort Rock dome, looking southeastward. Muddy Creek crosses the center of the photo. On the horizon are the Juniper Mountains. Mt. Hope is the dark conical butte near the horizon on the right.

The Geology and Mechanics of Formation of the Fort Rock Dome, Yavapai County, Arizona

By GARY S. FUIS

U.S. GEOLOGICAL SURVEY PROFESSIONAL PAPER 1266

*A study of the geology of the Fort Rock dome and nearby Aquarius Mountains
in west-central Arizona; a theoretical study of the process of doming by intrusion*



UNITED STATES GOVERNMENT PRINTING OFFICE, WASHINGTON : 1996

U.S. DEPARTMENT OF THE INTERIOR

BRUCE BABBITT, *Secretary*

U.S. GEOLOGICAL SURVEY

GORDON P. EATON, *Director*

Any use of trade, product, or firm names in this publication
is for descriptive purposes only and does not imply endorsement
by the U.S. Government

Library of Congress Cataloging-in-Publication Data

Fuis, Gary S.

The geology and mechanics of formation of the Fort Rock dome, Yavapai County, Arizona.

(Contributions to general geology) (Geological Survey professional paper ; 1266)

Includes bibliographical references.

Supt. of Docs no.: I 19.16:1266

1. Domes (Geology)—Arizona—Yavapai County.

I. Title. II. Series. III. Series: Geological Survey professional paper ; 1266.

QE611.5.U6F84 1991

551.4'3

84-600065

For sale by
U.S. Geological Survey, Information Services
Box 25286, Federal Center
Denver, CO 80225

CONTENTS

| | Page | | Page |
|---|------|--|------|
| Abstract | 1 | Tertiary volcanic and sedimentary rocks—Continued | |
| Introduction | 2 | Miscellaneous units—Continued | |
| Location, accessibility, and culture | 2 | Basalt of Buttox Hills | 56 |
| Physical features | 2 | Quaternary sedimentary deposits | 57 |
| Climate, vegetation, and exposure | 5 | Structure | 58 |
| Previous work | 5 | Precambrian structures | 58 |
| Fieldwork | 6 | Folds | 58 |
| Acknowledgments | 6 | Shear zone | 58 |
| Geologic setting | 6 | Tertiary pre-dome faults | 59 |
| Precambrian rocks | 7 | The Fort Rock dome | 60 |
| Layered metamorphic rocks | 7 | The monocline | 60 |
| Cataclasites | 9 | Mapped faults | 62 |
| Granite and granite pegmatite | 12 | Unmapped faults and breccia lenses | 66 |
| Veined rocks | 14 | Uplift and tilting of the Fault Canyon flow and units of the Fort Rock Creek Rhyodacite | 66 |
| Tertiary volcanic and sedimentary rocks | 17 | Major normal faults | 66 |
| Middle Tertiary erosion surface | 17 | Geologic history | 68 |
| Crater Pasture Formation | 17 | History before Tertiary volcanism | 68 |
| Type section | 18 | Tertiary volcanic history | 69 |
| Reference section | 19 | Beginning of volcanism and eruption of the Crater Pasture Formation | 69 |
| Basal tuffaceous breccia and sandstone | 20 | Eruption of the Fort Rock Creek Rhyodacite | 79 |
| Volcanic breccia and flow of Road End Gap | 20 | Eruption of the basalt of Buttox Hills | 80 |
| Flow of Eight O'Clock Gorge | 22 | Eruption of other volcanic rocks | 80 |
| Flow of Meadow Dam | 25 | Late geologic history | 80 |
| Tuff and flow of Two O'Clock Gap | 26 | Mechanics of formation of the Fort Rock dome | 81 |
| Pyroxene-trachyandesite sandstone and conglomerate | 27 | Formulation and solution of the problem | 81 |
| Flow of Annex Ridge | 28 | Behavior of the dome | 84 |
| Flow of Buffalo Ridge | 29 | Dependence on radius | 84 |
| Flow of Lion Ridge | 31 | Dependence on γ and τ' | 84 |
| Tuff and conglomerate of Hidden Pasture | 33 | Acceleration | 85 |
| Sedimentary breccia of One O'Clock Wash | 34 | Velocity and stresses | 85 |
| Tuff and agglomerate of Cinder Basin | 36 | Processes for halting doming | 87 |
| Flow of Fault Canyon | 38 | Formation of a vent | 87 |
| Miscellaneous units | 40 | Crystallization of the magma | 89 |
| Fort Rock Creek Rhyodacite | 41 | Comparison of the Fort Rock dome with the model | 89 |
| Type section | 41 | Depth and dimensions of the magma chamber and driving pressure | 89 |
| Reference section | 43 | Effective viscosity of fractured Precambrian and Tertiary rocks | 90 |
| Sedimentary breccia of Noon Gorge | 46 | Faults and breccia lenses | 90 |
| Old Stage Road Member | 50 | Crystallization of the magma | 92 |
| Three Sisters Butte Member | 52 | History of doming | 92 |
| Breccia and conglomerate of the Crossing | 53 | Summary | 92 |
| Miscellaneous units | 53 | References cited | 93 |
| Source of the Fort Rock Creek Rhyodacite | 54 | | |
| Mode of emplacement of extrusive rocks | 55 | | |
| Miscellaneous units | 56 | | |
| Rhyodacite intrusion of Five O'Clock Wash | 56 | | |

 ILLUSTRATIONS

[Plates are in pocket]

| | Page |
|---|------|
| PLATE 1. Geologic map of Fort Rock dome, Yavapai County, Arizona, and explanation of map units and symbols | |
| 2. Cross sections <i>A-A'</i> , <i>B-B'</i> , <i>C-C'</i> , and <i>D-D'</i> | |
| FIGURE 1. Index map showing location of Fort Rock Dome ----- | 3 |
| 2. Aerial photograph of Fort Rock dome and vicinity ----- | 4 |
| 3. Reconnaissance geologic map of Aquarius Mountains and vicinity ----- | 10 |
| 4. Map showing Precambrian structures on Fort Rock dome ----- | 15 |
| 5. Structure contour map of Fort Rock dome ----- | 62 |
| 6. Uplift map of Fort Rock dome ----- | 63 |
| 7. Diagram showing author's conception of One OClock Hill fault ----- | 64 |
| 8. Graphs showing average spatial density of small faults and maximum thicknesses of breccia lenses on Fort Rock dome ----- | 67 |
| 9. Paleogeologic-paleotopographic maps of Fort Rock dome ----- | 70 |
| 10. Map showing composition of the One OClock Wash sedimentary breccia at various places around Fort Rock dome ----- | 77 |
| 11. Diagram showing stream profiles on dome undergoing accelerating uplift ----- | 78 |
| 12. Diagram showing model used in mathematical formulation of doming ----- | 82 |
| 13-15. Graphs showing: | |
| 13. Amplitude factors in equations (4) and (5) ----- | 83 |
| 14. Normalized amplitude of dome and magma chamber ----- | 85 |
| 15. Normalized velocity in layer of fluid ----- | 86 |
| 16. Diagram showing coordinate system used to describe principal stresses in layer of fluid ----- | 87 |
| 17. Diagram summarizing table 8 ----- | 89 |
| 18. Diagram showing hypothetical graphs of σ_0 and σ_t versus time ----- | 89 |

 TABLES

| | Page |
|--|------|
| TABLE 1. Estimated modal composition of cataclasites ----- | 13 |
| 2. Modal composition of Crater Pasture Formation ----- | 22 |
| 3. Chemical and normative composition of Crater Pasture Formation ----- | 23 |
| 4. Contrasts between lithology of sedimentary breccia of One OClock Wash (Crater Pasture Formation) and sedimentary breccia of Noon Gorge (Fort Rock Creek Rhyodacite) ----- | 48 |
| 5. Chemical and normative composition of Fort Rock Creek Rhyodacite and other units ----- | 49 |
| 6. Dips of volcanic units older than Fault Canyon flow on the dome ----- | 61 |
| 7. Dips of units in Fort Rock Creek Rhyodacite on the dome ----- | 68 |
| 8. Inclination <i>i</i> of principal stress system; maximum shear stress S/σ_0 ; and direction of shear planes in principal stress system ----- | 88 |

THE GEOLOGY AND MECHANICS OF FORMATION OF THE FORT ROCK DOME, YAVAPAI COUNTY, ARIZONA

By GARY S. FUIS

ABSTRACT

The Fort Rock dome, in Yavapai County, Ariz., is a circular geologic structure, 2.5 km in diameter, that is similar in many ways to an impact crater; however, it is a structural dome caused by an intrusion at depth, and the craterlike depression in its center is erosional in origin.

Rocks exposed in the vicinity of the Fort Rock dome range in age from Precambrian to Quaternary. The chief rock units are Precambrian igneous and metamorphic rocks and Tertiary volcanic rocks. Volcanic rocks crop out over an area about 2,600 km² in extent largely west and south of the dome. Numerous volcanic centers are scattered throughout this area; the Fort Rock dome is one relatively small center. The chief structures in the region are basin-and-range faults. Most Phanerozoic rocks are relatively flat lying. The Fort Rock dome is an anomalous area where Tertiary rocks are highly deformed.

Precambrian rocks on or near Fort Rock dome include layered metamorphic rocks, of epidote-amphibolite facies, intruded or apparently intruded by two separate groups of granitic rocks. The first group was crushed and foliated along with the host rocks; these rocks are termed cataclasites. Intrusive relations are only suggested by outcrop patterns. The second group intrudes both older groups of rocks and is crushed but not foliated. The entire assemblage of rocks resembles older Precambrian rocks of the Grand Canyon. On the dome, the Precambrian rocks are fractured and veined in an east-west-trending shear zone that crosses the south half of the dome. Most fracturing and veining in this zone is Precambrian in age.

Tertiary volcanic rocks lie on a middle Tertiary erosion surface that covered most of northwest Arizona. In the vicinity of the Fort Rock dome, these rocks comprise chiefly two formations, the Crater Pasture Formation and Fort Rock Creek Rhyodacite; the Crater Pasture Formation is older. Younger volcanic rocks in the region include the Peach Springs Tuff, of middle Miocene age, which overlies the Fort Rock Creek Rhyodacite 16 km west of the dome, and the Mohon Mountains volcanic field, south of Trout Creek, which overlies the Peach Springs Tuff.

The Crater Pasture Formation includes a series of ultrabasic to intermediate lava flows, agglomerates, tuffs, and associated intrusive and sedimentary rocks on the Fort Rock dome in an area of about 300 km² west and north of the dome. Eleven subunits are recognized in the vicinity of the dome. Most of the rocks in these subunits originated from vents on or near the

periphery of the Fort Rock dome and are traceable for distances of 2 km or less. The youngest unit in the formation is an olivine-sanidine-trachybasalt flow, herein referred to as the flow of Fault Canyon. This flow was erupted from a vent on the southwest flank of the dome; it apparently came from a magma beneath the dome that is believed to have caused doming.

The Fort Rock Creek Rhyodacite includes a series of ash-flow and other massive tuffs, volcanic breccias, lava flows, and associated intrusive and sedimentary rocks in the Aquarius Mountains and vicinity. Four subunits are recognized; two are major rock units in the area and are designated members. The older member is the Old Stage Road Member, a unit consisting chiefly of nonwelded ash-flow tuff. The younger member is the Three Sisters Butte Member, a unit of interbedded volcanic breccia and massive tuff. Most of the Fort Rock Creek Rhyodacite was erupted from a large center in the Aquarius Mountains about 4 km southwest of Fort Rock dome.

Precambrian structures on the dome include folds of different amplitudes in the layered metamorphic rocks and an east-west-trending shear zone in the south half of the dome that brings together different rock assemblages and also rocks of slightly different metamorphic grade. This shear zone appears to be part of a major aeromagnetic discontinuity in Precambrian rocks in northwest Arizona. The discontinuity is associated with Tertiary normal faults and may be an ancient strike-slip fault zone in the Precambrian rocks. It was presumably a zone of weakness along which the body of magma was intruded that ultimately created the Fort Rock dome.

Tertiary structures on the dome include relatively minor faults that predate the uplift of the dome and the dome itself, with its associated folds and faults. The dome is a structural dome with its central part now deeply eroded. Its edge is, in most places, a sharp monocline. Structural relief on the dome is 400 m. Dips on the steeply dipping limb of the monocline, where dips can be measured accurately, range from about 40° to nearly vertical and average about 66°. Units of the Crater Pasture Formation older than the Fault Canyon flow reflect these strong dips, whereas the Fault Canyon flow and units of the Fort Rock Creek Rhyodacite dip much more gently on the monocline. Most faults mapped on the dome are confined to the vicinity of the monocline, perhaps partly as a result of poor exposure and lack of structural control in the deeply eroded central part of the dome. These faults have chiefly radial and tangential strikes and steep dips, where attitudes can be determined. Normal dip-slip movement appears to have been dominant, although radial faults may have had a strike-slip component of movement. Block rotations are observed along relatively long faults. Ages of faults, where

they can be determined, range from the beginning of uplift, which was signaled by deposition of sedimentary breccia on the flanks of the dome, to after the emplacement of the ash-flow tuff of the Fort Rock Creek Rhyodacite. The major offsets, however, appear to have occurred during the emplacement of sedimentary breccia. In addition to mapped faults on the rim of the crater, abundant small faults with displacements of centimeters to several meters and lenses of largely unmineralized breccia were formed during doming. These are best seen in the Precambrian rocks within the crater.

In a mathematical model of doming described in this report, the Pre-cambrian and Tertiary rocks underlying the Fort Rock dome are treated as a layer of Newtonian-viscous fluid above an inviscid magma. Intrusion of the magma is modeled by applying an axisymmetric pressure distribution on the bottom of the layer, creating a dome on the surface that has a smaller amplitude than the arch created on the bottom of the layer by the intrusion. It can be shown that a dome like the Fort Rock dome cannot be created unless the radius of the applied pressure is roughly equal to the thickness of the overlying layer. In addition, given a cooling time of around 10^4 years for the magma that uplifted the Fort Rock dome, an effective viscosity for the Precambrian and Tertiary rocks underlying the dome is calculated to be around 4×10^{20} poises. Planes of maximum shear generated in the model are consistent in attitude and sense of displacement with most faults mapped on the Fort Rock dome. The history of doming predicted by the model is consistent in large part with the history of doming at the Fort Rock dome. It includes an initial stage of accelerating uplift followed by slower uplift or collapse upon formation of a vent for the magma. Uplift ceased upon crystallization of the magma.

INTRODUCTION

The Fort Rock dome, in Yavapai County, Arizona, is a circular geologic structure, 2.5 km in diameter,¹ discovered from the air in the early 1960's. Many features suggest that it is of impact origin. It has a craterlike center underlain by brecciated Precambrian igneous and metamorphic rocks. In its rim, Tertiary volcanic flows and sedimentary rocks are upturned and are offset by radial and tangential faults. On its flanks is an apron of breccia in which clasts occur stratigraphically in the reverse order of the rock units in the rim from which they were derived. The record of volcanic activity in and around the dome, however, points to a different origin.

LOCATION, ACCESSIBILITY, AND CULTURE

Fort Rock dome is centered approximately at lat. $35^{\circ}8.25' N.$, long. $113^{\circ}18.5' W.$, near the west boundary of Yavapai County, Ariz. (fig. 1). It lies immedi-

¹ Measurements in this report were originally made in English units and have been converted to metric (SI) units of comparable accuracy.

ately southeast of the headquarters of Fort Rock Ranch (see fig. 3). A gravel road connects Fort Rock Ranch with Seligman, Ariz., about 50 km to the northeast. This gravel road has been largely supplanted by U.S. Interstate Highway 40 (not shown in fig. 1), which connects Seligman to Kingman and passes 6.5 km north of the ranch headquarters. The dome is accessible from the north and east by a dirt road from the ranch headquarters to Number One Well (pl. 1). Two jeep trails extend into the interior of the dome from this road; one enters from the north through Noon Gorge, and the other passes over Two O'clock Gap from Number One Well. The residence of W. Becker, owner of the ranch, is situated on the west flank of the dome, about 1 km south of the ranch headquarters.

A location called "Fort Rock" by early settlers is the site of the present Fort Rock Ranch headquarters. It was established in 1864 as a way station on the Old Beale Wagon Road, which was a stage route between Prescott and Hardyville, Ariz. (Rascoe, 1968, p. 54). (Hardyville is presently a ghost town on the Colorado River near Bullhead City, Ariz.) Remnants of this old road are still preserved as deep ruts in the white ash-flow tuff in this area and are labeled "old stage road" on the geologic map in this report (pl. 1). The name "Fort Rock" is not of military origin but stems from a stone playhouse in which the proprietors of the way station were forced to defend themselves against a surprise attack by Hualapai Indians in the fall of 1866 (Barnes, 1960, p. 343).

PHYSICAL FEATURES

The Fort Rock dome is in the Mexican Highland section of the Basin and Range physiographic province (Fenneman, 1931). The Colorado Plateau province lies to the north and northeast; in the area covered by figure 1, it lies roughly north of a line between the Aubrey Cliffs and the Lower Grand Wash Cliffs. The most prominent topographic feature in the vicinity of the dome is Cross Mountain (elevation 1,970 m, 6,463 ft), which is a 240-m-high butte 5 km to the northeast. The rugged Aquarius Mountains lie west and southwest of the dome, rising from an elevation 1,200 m (4,000 ft) on the east edge of Big Sandy Wash, 21 km west of the dome, to over 1,800 m (6,000 ft) several kilometers southwest of the dome.

Fort Rock Creek, which flows along the west flank of the dome, is the only permanent stream in the area. This stream joins Muddy Creek and Cow Creek about 8 km south of the dome to form Trout Creek

(fig. 1). The area south and southeast of the dome is, for the most part, a plateau into which Fort Rock, Muddy, Cow, and Trout Creeks have cut deep, spectacular canyons. Mt. Hope, 26 km southeast of the dome, and the Mohon Mountains, 19 km south, are prominent features rising from this plateau. The

Juniper Mountains, 32 km east of the dome, form the east boundary of this plateau.

Fort Rock dome is expressed topographically as a ring of ridges and hills (fig. 2). In the center of the dome is an elevated craterlike depression formed by erosion. The depression is divided by a drainage di-

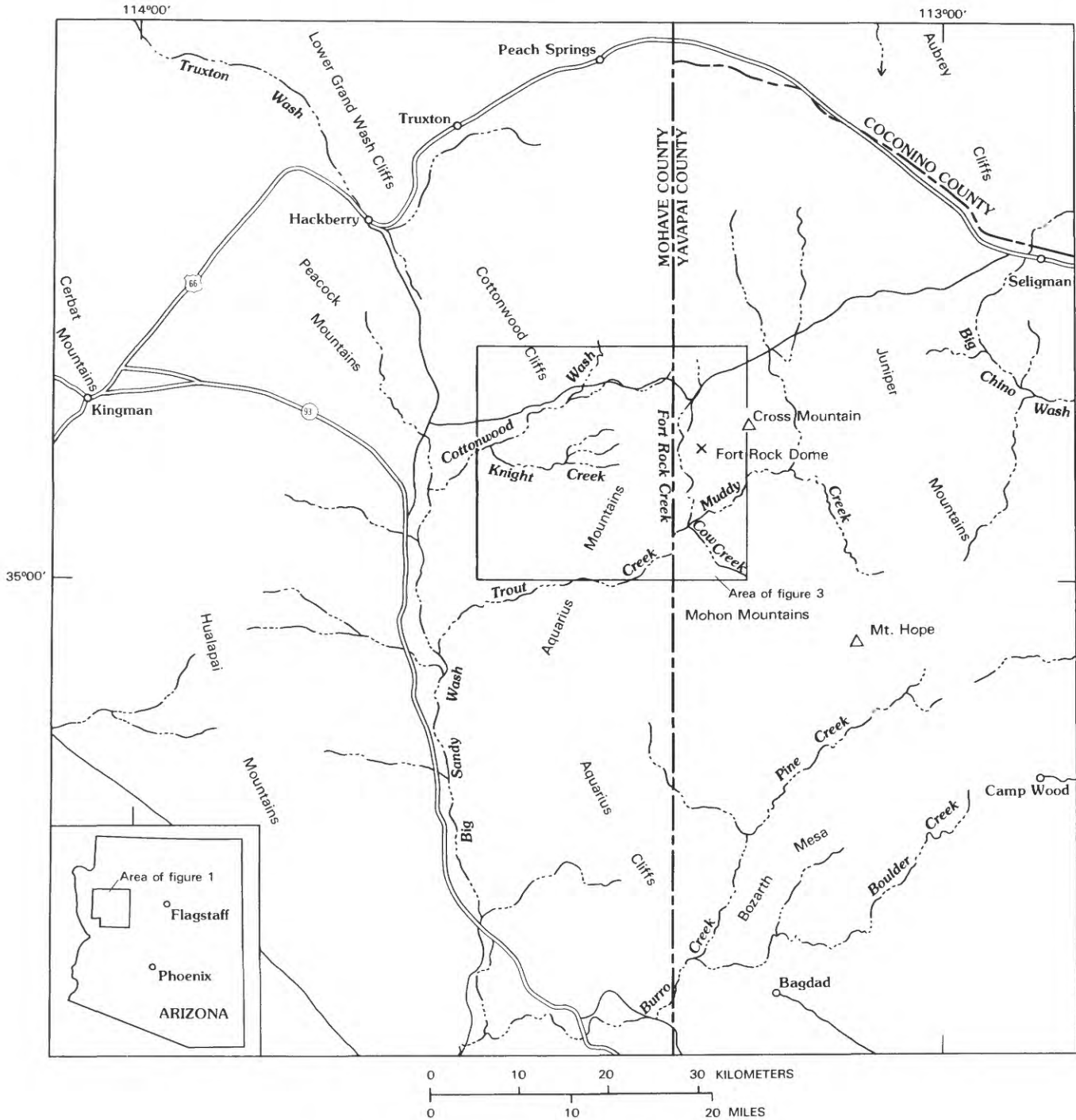


Figure 1.—Index map showing location of Fort Rock dome.

vide, Crater Divide (pl. 1), into two morphologically distinct halves. The southeast half is a topographically low, gently undulating surface encircled by ridges. This low surface, referred to in this report as Crater Pasture, slopes to the southeast at a few degrees and is drained by two washes that pass through gaps between the ridges on its southeast side. The ridges reach maximum elevations of about 1,650 m (5,400 ft) on both the northeast and southwest sides of Crater Pasture. The northwest half of the depres-



Figure 2.—Aerial photograph of Fort Rock dome and vicinity.

sion is broken up into a number of basins with intervening hills and ridges; it is surrounded by flat-iron-shaped hills arranged in a semicircle. Some of the hills in the interior of the depression exceed the encircling hills in elevation. One such hill, Ten O'Clock Peak, is the highest hill on the dome; it rises 130 to 160 m above outlying terrain to the northwest. The northwest half of the depression has eight drainages that exit between the flat-iron-shaped hills. Elevation in the mapped area ranges from 1,450 to 1,660 m (4,760-5,450 ft).

CLIMATE, VEGETATION, AND EXPOSURE

The climate of this region is mild, and fieldwork usually can be conducted all year. The annual precipitation at Seligman is about 28 cm (Green and Sellers, 1964, p. 387). The average daily temperature ranges from about 2°C in January to about 23°C in July. Winds are sometimes strong.

Fort Rock dome is sparsely to densely forested with juniper and scattered piñon. The trees have been uprooted to provide better pasture on Crater Pasture and on the more accessible flanks of the dome to the west, north, and east. Prominent shrubs include shrub live oak, which is very common in areas where larger trees have been uprooted, and cliffrose, or "quinine-bush." Cliffrose flourishes in areas underlain by breccia and delineates breccia outcrops well. Succulents include yucca, prickly pear, and cholla.

The rocks of the dome are well exposed. Alluvium and colluvium cover only about 35 percent of the area mapped.

PREVIOUS WORK

Prior to the time the author began work in this area, in 1967, no detailed geologic investigation of Precambrian or Tertiary rocks had been carried out in the area bounded by Cross Mountain on the east, Big Sandy Wash on the west, the Cottonwood Cliffs on the north, and the Mohon Mountains on the south (fig. 1). Several major geologic features were unmapped, including a large rhyodacite eruptive center in the Aquarius Mountains (fig. 3) and a large volcanic center in the Mohon Mountains. Several studies and mapping projects had been carried out in the peripheral areas, however. A detailed study had been conducted by Anderson and others (1956) of the geology and ore deposits of the Bagdad area,

Arizona, about 50 km south of the dome. Krieger (1967) mapped, in reconnaissance, seven 15-minute quadrangles east of the Fort Rock area. Her nearest mapping was about 26 km east of the Fort Rock dome. Wilson (Wilson and others, 1969) completed reconnaissance mapping, for the purpose of publishing a State geologic map, in an area extending from the area mapped by Krieger to the western boundary of the State. Young (1966) studied Cenozoic geology of the Colorado Plateau between the Grand Wash Cliffs and Peach Springs, Ariz. Peach Springs is 45 km north-northwest of the dome (fig. 1). Davis (1931) studied the Peacock Mountains, 40 km northwest of the dome. Hobbs (1944) reported on a tungsten mine in Precambrian rocks in the Aquarius Mountains south of Trout Creek, about 32 km southwest of the Fort Rock dome.

Since this report was completed, in 1973, considerable geologic investigation has taken place in the region. The most detailed work near the Fort Rock dome is a strip geologic map 10 km wide that extends from Kingman, Arizona, 160 km eastward, passing a few kilometers north of the dome (Goff and others, 1983). In this strip map and accompanying report, an olivine basalt dike that intrudes the Fort Rock Creek rhyodacite (see below) yields a whole-rock K-Ar age of 22.0 ± 0.7 Ma. This age would make most of the volcanic rocks discussed herein early Miocene or older. Detailed geologic mapping has also been done in the Mohon Mountains and Mt. Hope region, south and southeast of the Fort Rock dome (fig. 1) by Simmons (1986, 1990) and by Ward and Neeley (1990a, 1990b). Petrochemistry of rocks in this region are summarized by Nealey and others (1986). Simmons (1988) and Ward and Nealey (1990a, 1990b) describe a two-part volcanic history for the Mohon Mountains - Mt. Hope region. First, in the early to middle Miocene (22-20 Ma), andesites and dacites were erupted. Secondly, in the late Miocene to early Pliocene (13-5 Ma), accompanying and following extension in the region, bimodal volcanic rocks (basalt and rhyolite) were erupted. Bimodal volcanism in the region of the Aquarius Cliffs (fig. 1) also has been described by Moyer and Esperanca (1989). The geology in the region southeast of the Juniper Mountains (fig. 1) has recently been compiled by Billingsley and others (1988).

Precambrian geology of Arizona was recently summarized by Conway and Karlstrom (1986) and Conway (1986); Conway and others (1986) have studied in detail Early Proterozoic rocks in the Bagdad area that host massive sulfide deposits. A new geologic map of Arizona was recently compiled by Reynolds (1988).

FIELDWORK

Fieldwork was started in the Fort Rock area in the summer of 1967. Eight weeks were spent mapping, in reconnaissance, a large rhyodacite eruptive center in the Aquarius Mountains (fig. 3). The Fort Rock dome was discovered on the aerial photographs used in this study and was also mapped in reconnaissance. The dome had been seen earlier in the 1960's from the air and had been visited once by David Cummings of the U.S. Geological Survey. Fieldwork was continued the following summer, during which period Precambrian rocks were investigated in an area extending from Cross Mountain westward to where these rocks are buried by Tertiary volcanic rocks in the Aquarius Mountains. Detailed fieldwork on the dome was begun in the summer of 1969 and was completed in the fall of 1971. A total of 280 days was spent in fieldwork on the dome.

Aerial photographs were used for field compilation. Initial mapping was done on Army Map Service aerial photographs (for example, fig. 2; original scale, 1:62,500) enlarged five times. About one-fifth of the geology of the dome was compiled on these enlargements. In June 1970, new aerial photographs were made and topographic field control was established by the U.S. Geological Survey, preparatory to making a detailed topographic map of the dome. The remainder of the geology of the dome was compiled in the field on enlargements of this new photography (original scale, 1:11,400). All of the geology was subsequently compiled photogrammetrically onto a topographic map of the dome at a scale of 1:5,000 by photogrammetrists at the U.S. Geological Survey at Flagstaff, Ariz., and was edited by the author.

Deposits of colluvium and alluvium exceeding 30 to 45 cm in thickness are shown on the geologic map. Bedrock underlying thinner surficial deposits can be identified with reasonable accuracy either from float or by digging shallow pits. About 3,000 pits were dug. The use of pits was essential in mapping compositional changes in breccias on the north flank of the dome, where composition is not accurately reflected in the float.

ACKNOWLEDGMENTS

This study was funded by fellowships from the National Science Foundation, project money from the National Aeronautics and Space Administration, and graduate assistantships from the California Institute of Technology. The U.S. Geological Survey sup-

plied logistical support for fieldwork and also laboratory work, including chemical analyses and preparation of thin sections, and photogrammetric work, including compilation of a topographic base map.

Three persons to whom I am most indebted for their efforts in matters of funding and other support for this study are Eugene Shoemaker, the late Alfred Chidester, and John McCauley, of the U.S. Geological Survey. Fieldwork was facilitated in many ways by Robert Orr, former foreman of the Fort Rock Ranch, and his wife, Norma, and by William Becker, present owner of the ranch, and his wife, Joan. Arthur Dial, of the U.S. Geological Survey, was of welcome assistance in the field for several weeks near the end of the study. My dog Sam helped me maintain sanity during long sessions in the field. Donna Barton, Elsie Hirscher, Suzan Hotop, Marty Sanders, and Susan Larsen patiently typed the manuscript.

GEOLOGIC SETTING

Rocks exposed in the region around the Fort Rock dome (fig. 3) range in age from Precambrian to Quaternary. The Precambrian rocks are part of a broad belt of Precambrian rocks exposed in the mountains of central Arizona that border the southwest margin of the Colorado Plateau. The Precambrian rocks in the vicinity of the dome consist of layered metamorphic rocks, cataclasites, granites, granite pegmatites, and veined rocks. These rocks more closely resemble older Precambrian rocks in the Grand Canyon than Precambrian rocks to the south and southeast of the dome.

Early and middle Paleozoic sedimentary formations recognized in the Grand Canyon underlie Cross Mountain, east of the dome. The formations represented are the Tapeats Sandstone, Bright Angel Shale, and Muav Limestone all of Cambrian age, unnamed Devonian carbonate rocks, and the Redwall Limestone, of Mississippian age. Cross Mountain is the southwesternmost outcrop of these rocks in the region.

Tertiary volcanic rocks in the vicinity of the Fort Rock dome form a large (about 2,600 km²) dissected field extending from Big Sandy Wash on the west to the Juniper Mountains on the east and from about 20 km north of the dome to about 40 km south of the Mohon Mountains (fig. 1; Wilson and others, 1969; Reynolds, 1988). This field includes lava flows, pyroclastic rocks, volcanic necks, and sedimentary rocks. Numerous volcanic centers are scattered across it. Fort Rock dome is one such center, although it is

small compared to some of the others. The nearest large center is in the Aquarius Mountains about 4 km southwest of the dome (fig. 3). The Mohon Mountains and Mt. Hope are also large centers (see Simmons, 1986, 1990; Ward and Nealey, 1990a, 1990b).

Quaternary deposits in the area include, in addition to modern alluvium and colluvium, alluvial terrace deposits, which are extensively developed east of the dome and south of Cross Mountain (fig. 3). The terrace deposits contain abundant Paleozoic clasts and were derived either from Cross Mountain or from the Paleozoic terrane to the northeast or east.

The Fort Rock dome lies within a region of basin-and-range faulting. Between the dome and Seligman, Ariz., about 50 km to the northeast, a series of north-south-trending normal faults with displacements of up to a couple hundred meters are responsible for a series of ridges and valleys (Goff and others, 1983). Sixteen km west of the dome, one or more north-south-trending normal faults with a displacement of 300 m or more are responsible for the large west-facing escarpment of the Cottonwood Cliffs and Aquarius Mountains that bounds the valley of Big Sandy Wash (figs. 1, 3).

The chief structures in the more immediate vicinity of the dome include Precambrian shear zones and Tertiary normal faults (fig. 3). The largest Precambrian shear zone is an east-west-trending zone that runs through the Fort Rock dome. A second shear zone trends northwest-southeast in the Precambrian rocks on the northwest side of Cross Mountain. Normal faults include several northwest-southeast-trending faults south and southeast of the dome and a number of approximately east-west-trending faults west of the dome. The southwest and south sides of these faults, respectively, are downthrown.

Paleozoic and Tertiary rocks in the area around the dome are nearly flat lying or dip gently eastward (Goff and others, 1983). The dome is an anomalous small area of highly deformed rocks.

PRECAMBRIAN ROCKS

Precambrian rocks in the area include layered metamorphic rocks and subordinate cataclasites and plutonic rocks. These rocks resemble older Precambrian rocks of the Grand Canyon described by Noble and Hunter (1917), Maxson (1961), Boyce (1972), Babcock and others (1974), and Brown and others (1974). They do not resemble as closely the geographically nearer Precambrian rocks of the Yavapai Series to the south and southeast described by

Anderson (Anderson and others, 1956, 1971) and Anderson and Creasey (1958).

The layered metamorphic rocks probably represent a metasedimentary and metavolcanic assemblage, as do the older Precambrian metamorphic rocks of the Grand Canyon and the Yavapai Series to the south and southeast. The layered metamorphic rocks on the dome belong to the epidote-amphibolite metamorphic facies; a secondary foliation is due to cataclastic deformation. Rocks referred to in this text as "cataclasites" are small, uniform bodies of crushed, foliated rock within the layered metamorphic rocks that have granitic compositions and outcrop patterns suggesting that they were intruded into the layered metamorphic rocks. Some cataclasites may, however, be metamorphosed beds of very homogeneous sedimentary or volcanic rocks having granitic compositions. These cataclasites may be correlative with some of the granite gneisses in the Grand Canyon, such as the Zoroaster Granite of Campbell and Maxson (1936) and the Trinity Creek-Elves Chasm gneisses. Plutonic rocks on Fort Rock dome include small bodies of granite and granite pegmatite that intrude both the layered metamorphic rocks and the cataclasites. They may be correlative with the younger series of granite and granite pegmatite intrusions at the Grand Canyon.

LAYERED METAMORPHIC ROCKS

DISTRIBUTION AND PHYSICAL FEATURES

Layered metamorphic rocks in the area of Fort Rock dome include amphibolite, schist, phyllonite, and gneiss. They constitute on the average about 75 percent of the Precambrian rocks in the area mapped; the proportion is somewhat higher on the south half of the dome and somewhat lower on the north half. These rocks are usually covered by colluvium and are generally best exposed in gullies and washes. In places, however, metamorphic rocks underlie bouldery slopes and ridges (pl. 1).

FIELD RELATIONS

Field relations among the layered metamorphic rocks are obscure because of poor exposure. Interlayering between amphibolite and schist occurs at a scale of centimeters in some places. In other places, areas as large as 90 m across are composed predominantly of either amphibolite or schist. Phyllonite and gneiss form bodies of indefinite shape up to 150

m across. Phyllonite appears to grade in several places into bodies of cataclasite.

In the petrographic descriptions below, rock types are described in order of their apparent abundance.

AMPHIBOLITE

Amphibolite appears to be the most abundant. It is a gray, medium-grained, banded rock. Black hornblende grains distributed abundantly among white plagioclase grains give a salt-and-pepper appearance to hand specimens. The rock weathers to thin slabs. In a typical sample, the amphibolite is composed of 60 percent albite, 20 percent blue-green hornblende (ferrohastingsite), 15 percent quartz, 5 percent epidote, and a trace of zircon.² Weakly developed planes of very fine grained (75 μm) crushed material, constituting a weak "cataclastic foliation," parallel the banding in this rock. All grains in the rock have ragged or irregular boundaries. Albite grains commonly are very finely crushed on their borders, giving them a ragged appearance. Where they are not crushed, they have irregular contacts with other grains. They are fractured and commonly displaced. Extinction is undulatory to patchy. Quartz grains generally occur in groups of uniform grain size and tend to be segregated into bands. Grain boundaries are irregular but not crushed.

Some recrystallization apparently took place during or after crushing. In places, grains of epidote and rarely hornblende are strung out along fractures in albite grains where there has not been any significant displacement of the grains.

HORNBLLENDE-MICA SCHIST

Hornblende-mica schist is the most poorly exposed subunit. It is seen less commonly than amphibolite but may be as abundant or more abundant than amphibolite. A weakly and a strongly foliated type are recognized. The weakly foliated type appears to be more abundant.

The weakly foliated type is commonly quartz-hornblende-biotite-oligoclase schist.³ The rock is dark greenish brown to dark grayish brown and medium grained. In hand specimen, black hornblende grains and bronze biotite flakes are distributed abundantly among white plagioclase grains. The rock contains

40 percent oligoclase, 25 percent biotite, 20 percent blue-green hornblende (ferrohastingsite), 15 percent quartz, and a trace of epidote and sphene. Ragged biotite flakes are oriented in four or five intersecting directions, making successive angles of 20° to 40° with each other and giving the impression of a house of cards. Some of these directions coincide with weakly developed planes of crushed grains. Evidence for recrystallization during crushing is stronger in this rock than in the amphibolite. Although some of the biotite is kinked, much of it is not. Biotite flakes commonly penetrate deeply into cracks in the oligoclase.

The strongly foliated type is commonly hornblende-albite-biotite-quartz-microcline schist. It is similar to the schist described above but is fine grained, strongly schistose and has abundant quartzofeldspathic bands. It contains 35 percent microcline, 30 percent quartz, 15 percent biotite, 15 percent albite, 5 percent blue-green hornblende (ferrohastingsite?), and a trace of epidote and sphene. Only one major orientation of biotite flakes is apparent in thin section. Weakly developed planes of crushed grains are parallel to the foliation.

PHYLLONITE

Phyllonite occurs as relatively large (90 m) bodies of indefinite shape on the dome. Specimens from several bodies are described below.

Quartz-feldspar phyllonite underlies Crater Divide southeast of Eight O'Clock Basin. It is a hard fine-grained rock that is olive on fresh surfaces but commonly weathers red. The quartzofeldspathic minerals characteristically form minute streaks. It contains 69 percent potassium feldspar, 25 percent quartz, 4 percent biotite, 2 percent epidote, and a trace of allanite and chlorite. Cataclastic foliation is strong, and all grains have ragged or irregular outlines. Some feldspar occurs as small porphyroclasts. Quartz occurs in strings of grains that follow the foliation. Generally the feldspar has patchy extinction and the quartz undulatory extinction. Feldspar appears to be dominant among finer grained crushed material. Biotite, commonly associated with epidote, occurs as narrow stringers of small, ragged, usually bent flakes parallel to the foliation. Chlorite grades optically into biotite. Minor recrystallization has apparently accompanied cataclastic deformation. Epidote and biotite in some places invade cracks in feldspar. The name "phyllonite" was chosen for this rock rather than "mylonite" to reflect the small amount of recrystallization.

² All percentages are estimates made from thin sections unless otherwise noted.

³ In this report, rock names include minerals that are present in amounts of 5 percent or more; last-named minerals are most abundant.

A biotite-epidote-albite-microcline phyllonite underlies the divide between Ten O'Clock Wash and Eight O'Clock Basin. It is olive, fine grained, lineated, and weakly banded. It consists of 40 percent microcline, 39 percent albite, 12 percent epidote, 6 percent biotite, and 3 percent chlorite. Microcline and albite occur both as small porphyroclasts and as fine crushed material. Three or more planes parallel to a single direction are defined by lenses of crushed grains and by preferred orientation of biotite, chlorite, and prismatic epidote, giving a strong lineation to the rock. The prismatic form of epidote is an indication of recrystallization during crushing.

A hornblende-chlorite-feldspar-biotite-epidote phyllonite crops out in the west part of Eight O'Clock Basin. It is a dark olive-brown fine-grained rock with a very weak foliation containing 45 percent epidote, 35 percent biotite, 10 percent feldspar (including albite), 5 percent chlorite, 5 percent blue-green hornblende (ferrohastingsite?), and a trace of sphene. Feldspar occurs as medium- to fine-grained porphyroclasts. Fine-grained epidote is scattered throughout the rock but occurs in some places as medium- to fine-grained aggregates. Biotite occurs as larger (0.3 mm) dark-brown largely altered(?) elongate flakes parallel to the weak foliation and also as smaller (0.1 mm) light-brown equant flakes of random orientation which are commonly found in aggregates and accompanied by chlorite. Hornblende occurs as ragged, medium- to fine-grained porphyroclasts that are invaded by biotite. Recrystallization of biotite, which is indicated by the formation of granular aggregates, and alteration of hornblende in this rock seem to indicate retrograde metamorphism from epidote-amphibolite to greenschist facies. Greenschist is found near this area, in Eight O'Clock Gorge.

GRANITIC GNEISS

Granitic gneiss, a subordinate rock type on Fort Rock dome, is a hard medium-grained strongly banded pink and black rock. The bands are isoclinally folded. Examples of injection banding are present in the gneiss on the northeast flank of Lion Ridge. In a sample collected from Ten O'Clock Wash, the granitic bands have both sharp and gradational boundaries. Averaging light and dark bands, the specimen from Ten O'Clock Wash is composed of 57 percent microcline, 22 percent quartz, 13 percent oligoclase, 6 percent biotite, 2 percent hornblende (ferrohastingsite), and traces of sphene, epidote, and magnetite. The gneiss has a secondary foliation pro-

duced by cataclastic deformation that, in the samples examined, coincides with axial planes of folds. All grains have ragged or irregular boundaries. Microcline and oligoclase occur as porphyroclasts as well as very fine grained crushed material. The porphyroclasts are fractured and displaced and show patchy extinction. Quartz occurs as irregular groups of grains of fairly even size, commonly bordering or surrounding ragged feldspar porphyroclasts. Biotite occurs in two size groups. Larger grains in some places show idiomorphic or idioblastic outlines against feldspars. Fine, ragged flakes of biotite follow cataclastic folia, which transect the banding where it is folded.

GREENSCHIST

A single outcrop of greenschist occurs in Eight O'Clock Gorge. This rock is medium to coarse grained and lineated, owing to the presence of blades of bluish-green actinolite. Porphyroclasts of pink feldspar are visible in hand specimen. It contains 71 percent actinolite, 20 percent albite(?) (heavily sericitized), 8 percent chlorite (after biotite), 1 percent epidote, and a trace of biotite. The rock is seen in thin section to be diffusely crushed.

METAMORPHIC FACIES

All of the rocks described above belong to the epidote-amphibolite metamorphic facies, with the exception of the greenschist in Eight O'Clock Gorge and the phyllonite showing extensive retrograde greenschist metamorphism in the west part of Eight O'Clock Basin. All have undergone cataclastic deformation, which has superimposed weak to strong cataclastic foliations. In some cases, cataclastic foliation is parallel to original layering or schistosity. In other cases, several different cataclastic foliations parallel to a single direction obscure the original rock fabric and produce a lineation in the rock. Some recrystallization of biotite and epidote accompanied cataclastic deformation. In the west and southwest part of the crater, extensive retrograde greenschist metamorphism may have accompanied cataclastic deformation.

CATACLASITES

A number of small, uniform bodies of Precambrian rocks have granitic mineralogy and outcrop patterns similar to that of small intrusions but do not exhibit

clear intrusive relations with the metamorphic rocks around them. Contacts are rarely exposed but appear to be concordant or gradational. Because all of these bodies have weak to moderate cataclastic foliations and lineations, they have been termed "cataclasites." In the terminology of Spry (1969, p. 229) these rocks are "protomylonites." Cataclasites with distinctive physical features and petrography have been informally named after localities where they are most typically developed. These include the cataclasites of Noon Basin, Lion Ridge, Eight O'Clock Basin, Eight O'Clock Gorge, and Sams Camp Rise. Other cataclasites are distinguished only on the ba-

sis of grain size. Altogether, cataclasites constitute only a few percent of the Precambrian rocks.

DISTRIBUTION

Outcrop patterns of the cataclasites differ in the north and south halves of the crater (see pl. 1). The cataclasites of Noon Basin and Lion Ridge, which crop out in the north half, are clusters of small, elongate bodies. The Noon Basin cluster is elongate in an east-northeast–west-southwest direction; it is 120 m wide and 490 m long. The Lion Ridge cluster

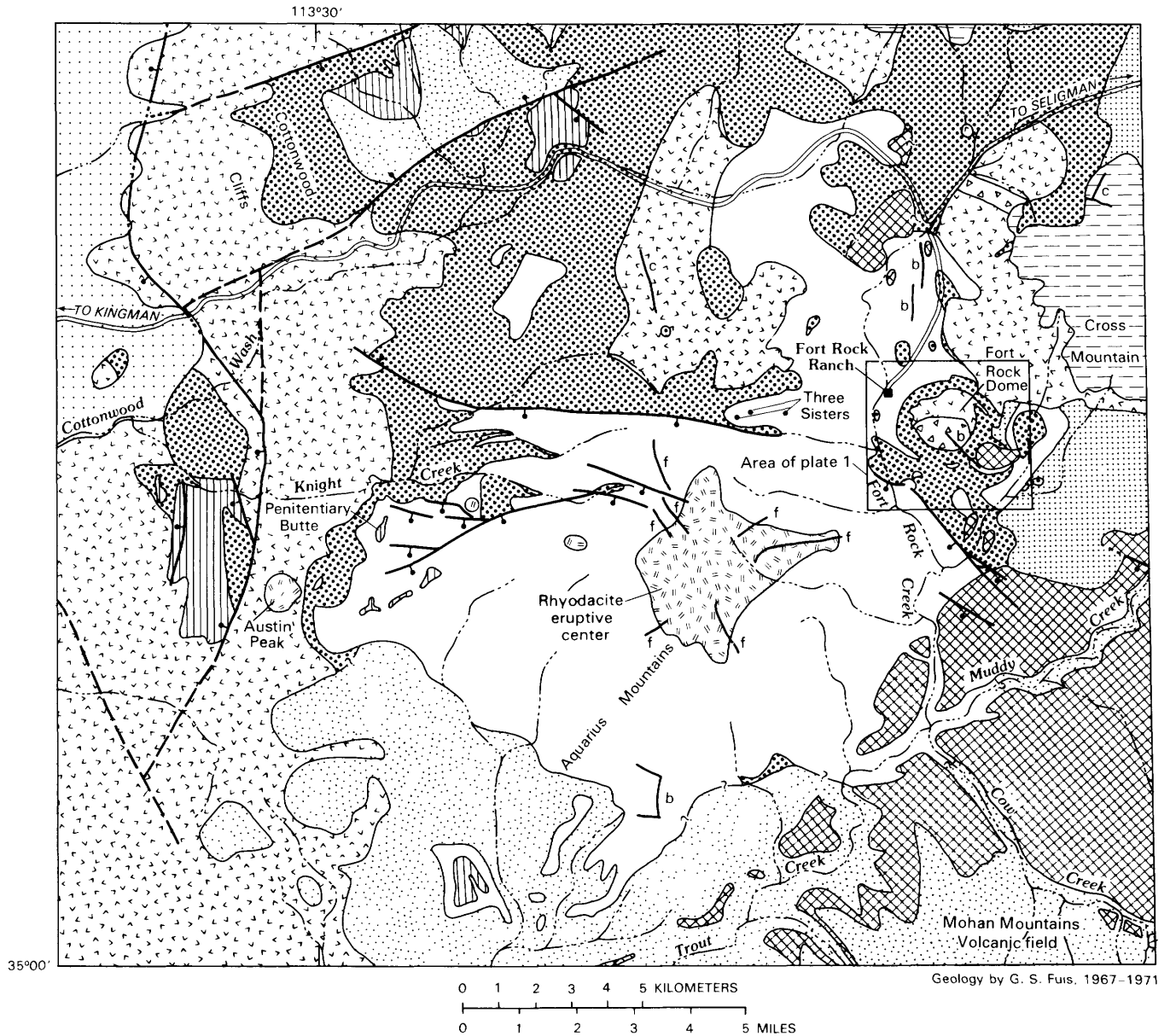


Figure 3.—Reconnaissance geologic map of the Aquarius Mountains and vicinity.

is almost equidimensional, with a diameter of about 140 m. Individual bodies within the Noon Basin and Lion Ridge clusters commonly are about 20 m wide and about 75 m long.

The cataclasites of Eight O'Clock Basin, Eight O'Clock Gorge, and Sams Camp Rise crop out in the south half of the crater. Each of these cataclasites consists of a relatively large elongate body oriented east-west and smaller satellitic bodies. The main bodies of the cataclasites of Eight O'Clock Basin and Sams Camp Rise are each about 400 m long and 75 m and 120 m wide, respectively. The cataclasite of Eight O'Clock Gorge is 150 m long and 75 m wide.

PHYSICAL FEATURES

The cataclasites also differ in gross physical features between the north and south halves of the crater. The cataclasites of Noon Basin and Lion Ridge both form bouldery outcrops, and the cataclasites of Eight O'Clock Basin and Sams Camp Rise form low outcrops. The Eight O'Clock Basin body is slightly more resistant than the surrounding metamorphic rocks and forms low knobs; it weathers to gruss and breaks up easily under the blow of a hammer. The cataclasite of Sams Camp Rise forms low outcrops

and weathers to angular cobbles. The cataclasite of Eight O'Clock Gorge crops out as resistant angular blocks.

FIELD RELATIONS

The cataclasites have both sharp and gradational contacts, but contacts are rarely exposed. A contact between the cataclasite of Noon Basin and adjacent schist is exposed on the divide extending south from Noon Hill. It is concordant, although two small quartz veins in the cataclasite terminate against the schist. The cataclasite of Lion Ridge appears to grade, by the development of a strong foliation and lineation and increase in biotite, into poorly resistant phyllonite. The main body of the cataclasite of Eight O'Clock Basin also grades into phyllonite on its eastern border. Contacts on the north, south, and west sides of this body, however, appear to be sharp. The cataclasite of Eight O'Clock Gorge exhibits a concordant contact with gneiss in a gully near the contact with Tertiary volcanic rocks on the southeast side of Eight O'Clock Gorge. The cataclasite of Sams Camp Rise grades, by the development of a strong foliation and a slight increase in biotite content, into mylonite and phyllonite. Distinction between the mylonite and

EXPLANATION

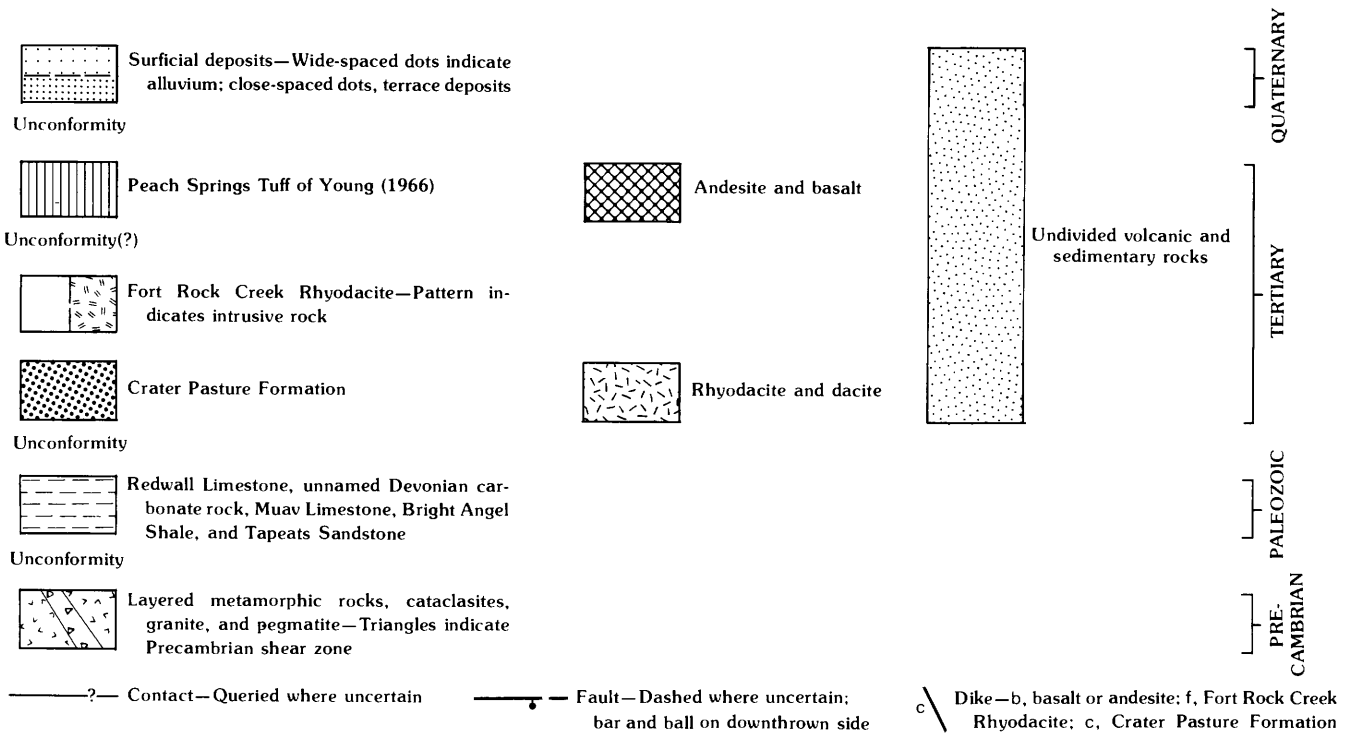


Figure 3.—Continued.

the phyllonite is arbitrary at best. The mylonite was mapped as part of this cataclasite, and the phyllonite was mapped as part of the layered metamorphic rocks.

PETROGRAPHY

A cataclastic fabric characterizes all of these rocks. One or more foliations are commonly developed by the alinement of lenticular grains and of stringers of grains less than about 0.5 mm across. The foliation is enhanced by alinement of biotite, although in most bodies, biotite occurs in amounts less than 5 percent. The development of two intersecting foliations gives rise to a lineation. Generally one foliation is stronger than the other. Feldspar occurs as porphyroclasts, although some porphyroblasts occur in the cataclasite of Eight O'Clock Gorge. Porphyroclasts have crushed and ragged boundaries. They are commonly fractured and, in places, displaced and have undulatory to patchy extinction in thin section. Porphyroblasts in the cataclasite of Eight O'Clock Gorge are grains of microcline containing a complete or partial ring of quartz inclusions. Quartz grains in the cataclasites occur in groups of relatively uniform grain size and generally do not show strongly undulatory extinction. Biotite is ragged and locally bent and kinked. The interstices between feldspar porphyroclasts and porphyroblasts and quartz-grain aggregates are occupied by finely crushed grains of quartz and feldspar. The fabric might be described as "mortar texture" (see Spry, 1969, pl. XXVIII and XXX) coupled with a foliation or lineation.

Distinctions among the various cataclasites are based on color, overall grain size, size and percentage of porphyroclasts, and degree of foliation or lineation. To a lesser extent, distinctions are based on mineralogic composition. Mineralogic compositions are given in table 1.

The cataclasite of Noon Basin is a dark-brown medium-grained rock with the composition of a granite. It is characterized by scattered coarse-grained augen of twinned microcline and relatively abundant (4 percent) black biotite. It has weak foliation and lineation that are best seen on a fresh surface.

The cataclasite of Lion Ridge is a red medium- to fine-grained rock with the composition of a quartz monzonite. It is characterized by rare augen like those of the Noon Basin cataclasite. Fresh surfaces are mottled pink and red-brown to olive from microcline and finely divided biotite, respectively. Foliation is weak to moderate. Moderately foliated specimens contain a few percent biotite (see table 1).

The cataclasite of Eight O'Clock Basin is a white medium-grained rock with the composition of a leucocratic quartz monzonite. A strong lineation is developed by parallel alinement of stringers of quartz grains and finely divided biotite.

The cataclasite of Eight O'Clock Gorge includes two rock types. The more abundant has the composition of a quartz monzonite and is characterized by pink medium-grained microcline augen in a fine-grained dark red-brown matrix. The second rock type has the composition of a granodiorite and consists of closely spaced plagioclase augen in a scant dark-green fine-grained matrix. The quartz-monzonitic rock is poorly foliated, but the granodioritic rock is moderately well foliated. The relation between these two rock types is unknown.

The Cataclasite of Sams Camp Rise is of varied appearance in hand specimen. Specimens range from (a) dark pink, medium grained, and unfoliated, to (b) mottled pink and olive, medium grained, and weakly foliated, to (c) olive (fresh surface) or red (weathered surface), fine grained, well foliated, and lineated by streaks of fine-grained biotite; this last specimen is termed a mylonite. Strongly foliated specimens of this unit contain a few percent biotite (table 1). This cataclasite has the mineralogic composition of a granite.

Several bodies of cataclasite have been distinguished only on the basis of grain size. The largest is a topographically and petrographically undistinctive body southwest of Thunder Camp. It is a medium- to fine-grained poorly to moderately foliated granitic rock. A more distinctive cataclasite in this group is found in several locations, but its largest outcrop is at the head of Ten O'Clock Wash. It is a white coarse-grained weakly banded rock, consisting dominantly of white feldspar.

Some recrystallization is indicated in most of the cataclasites by invasion of biotite into fractures in feldspar. In the Eight O'Clock Gorge cataclasite, some recrystallization to form microcline porphyroblasts is indicated.

GRANITE AND GRANITE PEGMATITE

Granite and granite pegmatite clearly intrude the layered metamorphic rocks and some of the cataclasites on the Fort Rock dome. Like the older rocks, these intrusive rocks are crushed, but only in the granite are there instances of cataclastic foliation. Both the granite and granite pegmatite are leucocratic and resistant to weathering, and they tend to occur in close association with one another. These

Table 1.—Estimated modal composition of cataclasites

[Estimates are made from thin sections (unstained). Tr., trace.; --, not present]

| Mineral | Cataclasite of | Cataclasite of | Cataclasite of | Cataclasite of | Cataclasite of | Cataclasite of |
|-----------------|----------------|----------------|--------------------|--|---|----------------|
| | Noon Basin | Lion Ridge | Eight OClock Basin | Eight OClock Gorge: quartz-monzonitic rock | Eight OClock Gorge: grano-dioritic rock | Sams Camp Rise |
| | Percent | | | | | |
| Quartz | 15 | 25 | 39 | 25 | 40 | 35 |
| Microcline | 55 | 43 | 33 | 32 | 10 | 55 |
| Plagioclase | 25 | 30 | 27 | 28 | 45 | 9 |
| Biotite | 4 | 1-1/2 | 1/2 | 15* | 2 | 3/4 |
| Muscovite | Tr. | Tr. | 1/2 | Tr. | -- | Tr. |
| Chlorite | Tr. | -- | Tr. | -- | 3 | Tr. |
| Epidote | Tr. | Tr. | -- | -- | -- | Tr. |
| Allanite | Tr. | -- | -- | -- | -- | Tr.-1/4 |
| Sphene | Tr. | Tr. | -- | Tr. | Tr. | -- |
| Zircon | Tr. | -- | -- | -- | -- | -- |
| Apatite | -- | Tr. | -- | -- | -- | -- |
| Opaque minerals | Tr. | 1/2 | Tr. | -- | -- | 1/4 |
| Total | 99 | 100 | 100 | 100 | 100 | 100 |
| Plagioclase is | oligo-clase | albite | albite | albite | albite | albite |

* Includes opaque minerals

characteristics help to distinguish the granite from the cataclasite in places where the granite is foliated.

DISTRIBUTION AND PHYSICAL FEATURES

Granite is most abundant northeast of the dome and in the northwest quadrant of the dome (pl. 1). It tends to form small bodies and irregular dikes. The rock is more resistant than the surrounding metamorphic rocks and underlies hills, spurs, and irregular ridges. The largest body underlies Ten OClock Peak, which is the highest hill in the area mapped. Outcrops of granite are generally bouldery or blockly.

Granite pegmatite in the area mapped is almost exclusively confined to the north half of the dome and the exposure northeast of the dome (pl. 1). It forms narrow, linear to irregularly shaped dikes. Three swarms of larger dikes can be identified. The largest swarm is found on Noon Hill, on the hill south of Noon Hill, and on One OClock Hill. The second largest swarm occurs in the vicinity of Crater Divide just north of the center of the dome. A smaller swarm occurs on the west flank of the small knob extending southwest of Lion Ridge. The pegmatites are more resistant to weathering than

the metamorphic rock they intrude and underlie topographic ribs, ridges, and hills. Outcrops of pegmatite are blocky; very coarse crystals in the rock weather to sharp, angular faces.

FIELD RELATIONS

Granite and granite pegmatite clearly intrude the layered metamorphic rocks. In addition, granite pegmatite intrudes the cataclasites of Noon Basin and Lion Ridge. The virtual absence of pegmatite in the south half of the crater precludes determining the age of this rock relative to the cataclasites in that area, although the pegmatite is almost certainly younger.

The pegmatite and granite occur in close association in most places. In some cases, the pegmatite intrudes the granite, and in other cases, it grades texturally into the granite. In cases of either intrusion or gradation, mixtures of nearly equal proportions of both rocks are found in some localities and are mapped as "mixed granite and granite pegmatite." This mixed unit is formally defined to include mixtures of between 30 and 70 percent of either component. Mixtures falling outside of this range are mapped simply as "granite" or "granite pegmatite."

Mixture occurs on the scale of centimeters to meters. The unit of "mixed granite and granite pegmatite" is only common northeast of the dome.

GRANITE

The granite on Ten O'Clock Peak is a very hard pink fine-grained lineated (or streaked) rock. All minerals that are visible in hand specimen form stringers, giving the rock its lineation. Finely divided biotite produces black streaks or specks, depending on the orientation in which the rock is viewed. Stringers of feldspar and quartz grains form light-colored streaks. The rock is a leucogranite and contains 60 percent microcline, 38 percent quartz, $\frac{1}{2}$ percent albite or oligoclase, $\frac{3}{4}$ percent biotite, $\frac{1}{4}$ percent opaque minerals, and traces of muscovite, epidote, and zircon. In thin section, the rock appears crushed, but lineation does not show up as strongly in thin section as it does in hand specimen. Most of the biotite forms sharply defined, undeformed flakes, which may be recrystallized. Rare strings of quartz inclusions are found in microcline grains and are parallel to the lineation of the rock; these may be evidence for recrystallization of microcline.

A specimen of granite from near the center of the dome is white (fresh surface) to light brown (weathered surface), medium grained, and poorly to moderately foliated. Albite content reaches about 20 percent, and there is a trace of garnet.

A few of the rocks mapped as granite are leucocratic quartz monzonite and granodiorite.

GRANITE PEGMATITE

Granite pegmatite on the Fort Rock dome is pink and massive with a grain size ranging from medium to very coarse. Crystals of microcline with dimensions up to 10 cm or more are characteristic. These large crystals are frequently graphically intergrown with quartz and sometimes appear to be a mosaic in hand specimen. Quartz is occasionally segregated into large white bodies within the pegmatite. Since this rock is of varied grain size and since mineral segregation occurs on several scales, it is difficult to determine the overall mineral percentages. One medium-grained specimen contains 40 percent quartz, 40 percent microcline, $19\frac{1}{2}$ percent plagioclase, $\frac{1}{2}$ percent biotite, and traces of muscovite and opaque minerals. All pegmatites are crushed; they have a "mortar texture." Cataclastic foliation is rare, however. Feldspar, especially microcline, forms porphyro-

clasts. In thin section these porphyroclasts have either crushed and ragged or irregular boundaries. Irregular boundaries occur adjacent to groups of quartz grains. Feldspars are more commonly fractured and displaced in the pegmatites than in the cataclasites and show rotation of internal grain segments. Displacements and rotations have the effect of breaking up grains into mosaics, hence the mosaiclike appearance of large microcline crystals in hand specimens. The fractures in the grains are occupied by very fine grained crushed material but are frequently invaded by coarser grained quartz, which may indicate some recrystallization of quartz during deformation.

A minor outcrop of flaser granite, mapped in the south half of the crater near the crest of Buffalo Ridge, may be a sheared granite pegmatite. The rock is a pink, coarse-grained granite consisting of microcline augen in a rust-colored matrix. The contacts of this rock are intrusive.

VEINED ROCKS

Numerous small faults and fractures in the Precambrian rocks in shear zones in this area are veined by epidote, hematite, quartz, and other minerals. Veins have thicknesses ranging from micrometers to several centimeters. In places, veins are so dense that the original rock can no longer be distinguished, and a separate geologic map unit, "veined rocks," is used.

DISTRIBUTION AND PHYSICAL FEATURES

Veined rocks occur in an east-west-trending zone that occupies the south half of the exposure of Precambrian rocks on the Fort Rock dome; they also occur in a half-mile-wide northwest-southeast-trending zone on the northwest side of Cross Mountain (fig. 3). Veined rock tends to break up along veins during weathering and forms small (pebble and cobble size) angular float. This weathering characteristic distinguishes it from most of the rest of the Precambrian rocks, which weather to blocks and boulders. Outcrops of veined rocks are generally topographically low. Where quartz is the chief vein mineral, however, low ridges may occur.

FIELD RELATIONS

Several levels of spatial density of veins were defined and mapped on the Fort Rock dome (fig. 4).

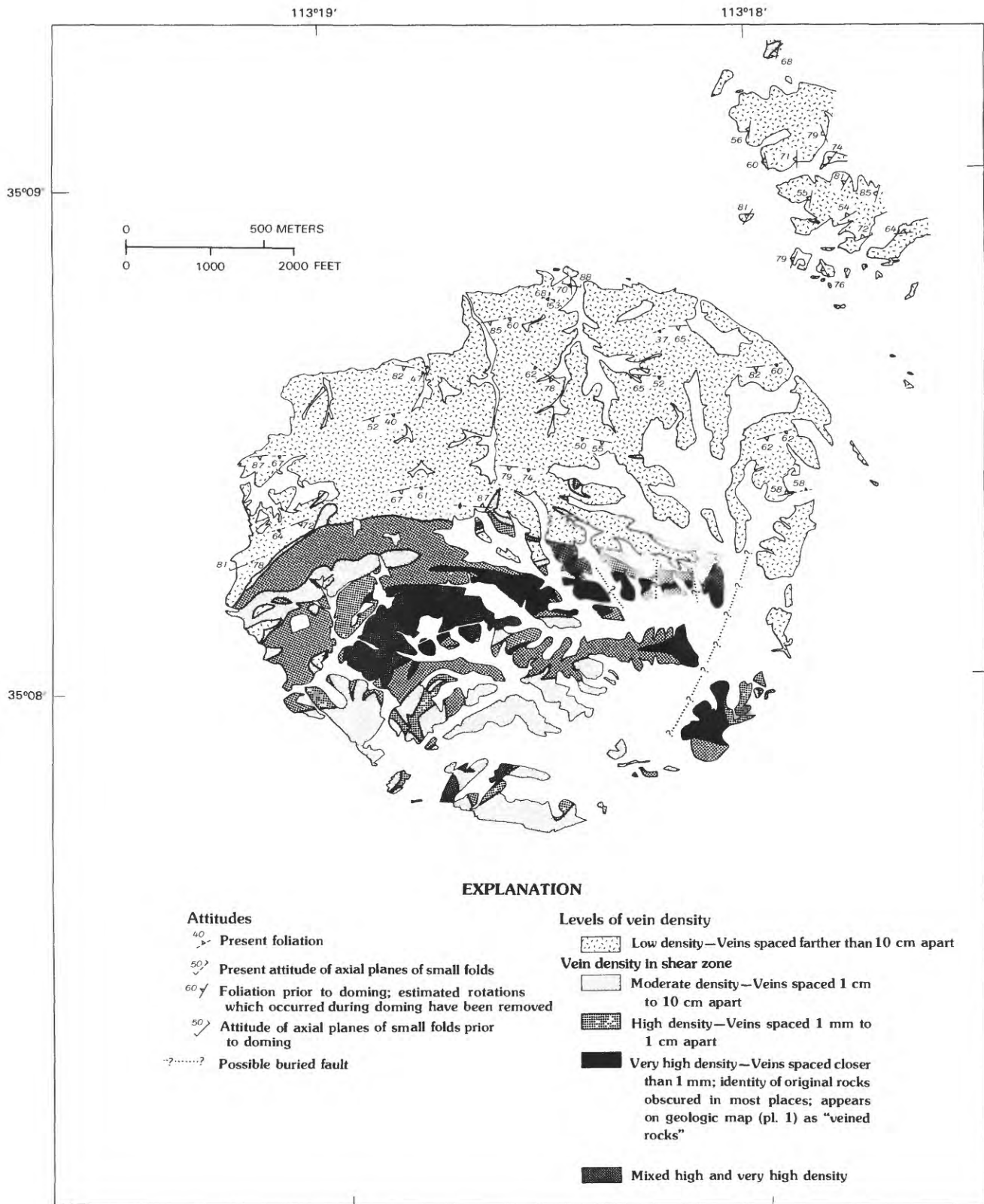


FIGURE 4.— Map showing Precambrian structures on Fort Rock dome.

Owing to poor exposure of veined rocks on the dome, mapping of these levels was based largely on float. In a given small area, about 6 by 6 m, the highest possible level was assigned if 20 percent or more of the float (or 10 percent or more of the outcrop, if present) had a vein density of that level. At some localities adjacent small areas could be assigned to different levels. These localities were mapped as "mixed." Only one mixed level occurs on the dome, "mixed high and very high density" veined rocks. The level designated "very high density" was mapped as a geologic unit (pl. 1). Each level can be seen in an easily mappable, regular sequence on the east end of the low rise north of Sams Camp Rise. This area was used as a reference for mapping levels in the rest of the shear zone in the crater.

A discussion of the outcrop pattern of the various levels of vein density is found below in the section entitled "Precambrian Structures."

PETROGRAPHY

Veins range in width from 20 micrometers to several centimeters. Vein minerals include, in order of abundance, olive-green epidote, clear to milky quartz, dark-red to specular hematite, pinkish-orange adularia, bluish-black chlorite (rare), and sericite (rare). Fractures are continuous through many grains in the rock and generally extend throughout a hand specimen, cutting both porphyroclasts and the finer grained matrix. They commonly offset grains and other fractures, although offsets are usually less than 1 cm. Some fractures are zones of crushing and diffuse to heavy mineralization. Others are cracks lined with druzey vein minerals. Where crushing occurs, the fractures are distinguished from older cataclastic foliation in the host rock in that the younger fractures (1) are localized (or bounded by two discrete planes), (2) have a broad grain-size distribution, with a minimum grain size much smaller than seen in the host rock (less than a few micrometers), and (3) are mineralized. Zones of crushing are mineralized by only epidote or hematite. Fractures lined by druzey vein minerals may contain any of the minerals listed above.

PARAGENESIS OF VEIN MINERALS

The following are examples of paragenesis of vein minerals in rocks on the Fort Rock dome. In each example, the level of vein density in the particular rock sample is given first, followed by a numbered

sequence of events that can be recognized in the rock. The oldest event is listed first.

- A. Rock with a "moderate density" of veins.
 1. Fracturing and veining by very fine grained epidote.
 2. Fracturing and veining by druzey quartz followed by druzey epidote.
- B. Rock with a "moderate density" of veins.
 1. Fracturing and veining simultaneously by adularia, chlorite, and sericite.
- C. Rock with a "high density" of veins.
 1. Fracturing and veining by epidote.
 2. Fracturing and veining by hematite.
- D. Rock with a "high density" of veins.
 1. Fracturing and veining by epidote, including some druzey epidote.
 2. Fracturing and veining by quartz and (or) adularia(?).
- E. Rock with a "high density" of veins.
 1. Fracturing with extensive crushing and mineralization by very fine grained epidote.
 2. Fracturing and veining by clear quartz.
 3. Fracturing and veining by druzey milky quartz followed, but in some cases preceded by, druzey adularia(?).
- F. Rock with a "high density" of veins.
 1. Fracturing with extensive crushing and mineralization by epidote.
- G. Rock with a "very high density" of veins.
 1. Fracturing with some crushing and mineralization by epidote.
 2. Fracturing and veining by hematite and quartz.
 3. Fracturing and veining by druzey quartz followed by druzey adularia(?); simultaneous filling of hairlike veins by quartz.
 4. Fracturing with crushing and mineralization by hematite.
- H. Rock with a "very high density" of veins.
 1. Fracturing with extensive crushing and mineralization by very fine grained epidote in one case and hematite in another; relative ages of epidote and hematite mineralization unknown.
 2. Fracturing and filling of hairlike veins by quartz; associated or somewhat younger fracturing and veining by milky quartz followed by druzey adularia(?).
 3. Minor fracturing and filling of hairlike veins by clear quartz.

SUMMARY

The oldest event in most of the examples of vein-mineral paragenesis is fracturing, generally with

crushing, and veining by epidote or, less commonly, hematite. The next event involves open fracturing and filling of the fractures by druzy quartz, minor adularia, and, rarely, epidote. An event succeeding these two events in at least one rock involves fracturing, with some crushing, and veining by hematite. The oldest event in this sequence is suggestive of higher pressures and temperatures than the second event because of the crushing involved and the abundance of epidote. Pressures in the second event apparently frequently dropped below local rock strengths, as evidenced by open cracks. A possible reversion to higher pressures is suggested by the third event.

TERTIARY VOLCANIC AND SEDIMENTARY ROCKS

Tertiary rocks in the vicinity of the Fort Rock dome comprise chiefly two formations. The older formation is here given the name Crater Pasture Formation; the younger, Fort Rock Creek Rhyodacite. In addition to these two formations, several lava flows and intrusive bodies are present in the vicinity of the dome that are younger than the Fort Rock Creek Rhyodacite (fig. 3). Other volcanic rocks in the region include the Peach Springs Tuff of Young (1966), a middle Miocene tuff which overlies the Fort Rock Creek Rhyodacite 16 km west of the Fort Rock dome, and the Mohon Mountains volcanic field, south of Trout Creek, which overlies the Peach Springs Tuff.

MIDDLE TERTIARY EROSION SURFACE

The Tertiary volcanic and sedimentary rocks in the Fort Rock area lie on a middle Tertiary erosion surface, parts of which are preserved in many places in the surrounding region. Cross Mountain formed a prominent butte that rose at least 240 m above the surrounding terrain on this ancient surface. South and west of Cross Mountain, a rolling to hilly surface was developed on Precambrian rocks that had a relief comparable to that of the present surface on these rocks. The paleotopography at the site of the present Fort Rock dome is discussed and mapped below.

The middle Tertiary erosion surface has been recognized in the Prescott-Jerome area, along the Mogollon Rim, in the Seligman-Ashfork area, and on the Hualapai Plateau. The present topography in the Seligman-Ashfork area and on the Hualapai Plateau is apparently similar to the middle Tertiary topography.

In the Prescott-Jerome area, this erosion surface has been described by Krieger (1965) and Anderson and Creasey (1958), where it is overlain by gravel and basalt of the Hickey Formation. A basalt flow in the Hickey Formation has a reported potassium-argon age of 10 to 11 million years (McKee and Anderson, 1971; Damon, 1968, p. 49). Gravels filling a broad ancient valley under the Mount Floyd volcanic field north and northeast of Seligman have been described by Koons (1948, 1964). The oldest basalt overlying these gravels has a reported potassium-argon age of 14 million years (McKee and McKee, 1972). Similar gravels on the east part of the Hualapai Plateau (Koons, 1948, 1964) are overlain in one location by the basalt of Blue Mountain, which has a reported age of 14 Ma (P.E. Damon, oral commun, 1973). On the west part of the Hualapai Plateau, deep canyons were present on the middle Tertiary erosion surface that were later filled by thick deposits of alluvial and colluvial deposits and locally by volcanic rocks (Young, 1966). Most of the volcanic rocks in this area postdate the gravels and include, from oldest to youngest, basalts or andesites, the Peach Springs Tuff, and younger basalts or andesites. The Peach Springs Tuff has a reported potassium-argon age of about 18 Ma (Damon, 1964, p. 19; Nielson and others, 1990). (A summary of Cenozoic erosion, sedimentation, and volcanism in the above areas is given by McKee and others, 1964.)

CRATER PASTURE FORMATION

Crater Pasture Formation is a name applied by Fuis (1973) to a series of lava flows, agglomerates, tuffs, and associated intrusive and sedimentary rocks on the Fort Rock dome and in an area of about 300 km² largely west and north of the dome (fig. 3). Composition of the volcanic rocks ranges from ultrabasic to intermediate. "Crater Pasture" is a local, informal name for a fenced area enclosing the dome that constitutes most of the area mapped (pl. 1). As used in this report, however, the name Crater Pasture refers to that part of the physiographic crater inside the dome southeast of Crater Divide (pl. 1).

On and near the Fort Rock dome, the Crater Pasture Formation is subdivided into 11 informally named members, listed below with the oldest at the bottom. Rock-unit names such as flow and agglomerate refer to the major rock units in each member. The general rock type in each member is listed in parentheses after the name. Relative ages are unknown in the two pairs of members at the bottom of the list.

- Flow of Fault Canyon (olivine-sanidine trachybasalt)
- Tuff and agglomerate of Cinder Basin (olivine trachybasalt)
- Sedimentary breccia of One OClock Wash (dominantly clasts of hornblende trachyandesite and clasts of Precambrian rocks)
- Tuff and conglomerate of Hidden Pasture (olivine and hornblende trachyandesite)
- Flow of Lion Ridge (hornblende trachyandesite)
- Flow of Buffalo Ridge (hornblende trachyandesite)
- Flow of Annex Ridge (hornblende trachyandesite)
- Flow of Meadow Dam (hornblende trachybasalt); tuff and flow of Two OClock Gap (pyroxene trachyandesite)
- Flow of Eight OClock Gorge (limburgite); volcanic breccia and flow of Road End Gap (olivine trachyandesite)

In addition to these informally named members, the Crater Pasture Formation on the dome includes a basal tuffaceous breccia and sandstone, a pyroxene trachyandesite sandstone and conglomerate, and four separate intrusive bodies, three of which appear to be related to three of the members.

Rocks of the Crater Pasture Formation originated from numerous scattered vents. Generally, flows are less than 2 km in length. Vents for these rocks on Fort Rock dome are located chiefly on the dome's periphery. The informally named members on the dome cannot be traced to the west and north.

TYPE SECTION

The type section is exposed in Eight OClock Gorge, which cuts through the southwest rim of the crater. The base of the section is located in the E¹/₂SW ¹/₄ NW¹/₄ sec. 10, T. 20 N., R. 10 W. The section extends to the southwest through the gorge and down the wash to its junction with Fort Rock Creek. About 180 m of this formation is exposed in the gorge; another 18 m of the youngest flow in the formation is exposed farther down the wash. In the gorge, the Crater Pasture Formation overlies Precambrian rocks, and all rocks in the formation dip about 50° to the southwest. On the southeast side of the gorge, rocks in this formation underlie the crest of Buffalo Ridge and its southwest flank. On the northwest side of the gorge, they underlie a flatiron-shaped knob below the peak of Eight OClock Hill and the

west flank of Eight OClock Hill. Five units are present in the type section: the flow of Eight OClock Gorge, the flow of Meadow Dam, the flow of Buffalo Ridge, the sedimentary breccia of One OClock Wash, and the flow of Fault Canyon.

The basal contact is well exposed (and slightly faulted) in a gully in the southeast wall of the gorge. Here, about 30 cm of buff to orange tuffaceous sandstone overlies Precambrian gneiss and cataclasite and is in turn overlain by black massive amygdaloidal limburgite of the Eight OClock Gorge flow. The limburgite ranges in thickness in the gorge from about 9 m on the southeast wall to about 20 m on the northwest wall. Just above the flow is a thin orange fine-grained tuffaceous sandstone.

The Eight OClock Gorge unit is overlain by about 41 m of gray hornblende trachybasalt of the Meadow Dam flow; the contact is well exposed in the northwest bank of the wash. This flow has excellent flow cleavage throughout, except in its basal 1 m. It is overlain by about 30 cm of maroon volcanic sandstone and conglomerate in the northwest wall of the gorge.

Blue-gray hornblende trachyandesite of the Buffalo Ridge flow, 62 m in thickness, overlies the Meadow Dam flow and the thin sandstone and conglomerate. Sixty to ninety centimeters of trachyandesite lapilli tuff, made up of yellow-brown clasts with abundant hornblende prisms, occurs at the base of the flow. The flow has flow cleavage near its base, is massive in its central and upper parts, and has a rough brownish varnished aa top.

The Buffalo Ridge flow contains two bodies of breccia and is offset by three reverse faults in this location. On the northwest wall of the gorge, one body of breccia extends upward from the base to deep within the flow; the other body is found in the central part of the flow. Both bodies are locally reddened and are probably flow breccias. Both bodies are exposed very near the wash bottom and are shown on the geologic map (pl. 1). Three shinglelike reverse faults in the upper part of the flow partly repeat the section (pl. 3). A sharp kink in the gorge appears to be controlled by the upper fault. In some places these faults apparently formed open fissures that were later filled by the sedimentary breccia of One OClock Wash.

The gorge walls diminish sharply in height past the kink in the gorge. Two breccia units are exposed in the walls of the wash where it traverses the flank of the dome; the older is the sedimentary breccia of One OClock Wash, of the Crater Pasture Formation, and the younger is the sedimentary breccia of Noon Gorge, of the Fort Rock Creek Rhyodacite. The basal contact of the One OClock Wash breccia is exposed

in the northwest wall of the gorge and is highly irregular owing to the rugged topography on the top of the underlying flow, which was offset by reverse faulting before deposition of the breccia. The thickness of the breccia, consequently, ranges from a meter or so to about 60 m in this area. The breccia consists of gray, red-brown, and yellow-brown clasts of Buffalo Ridge flow, a trace or more of black to light-green ash, and a few clasts of Precambrian rock. The contact between this breccia and the Noon Gorge sedimentary breccia is subtle and poorly exposed. It trends steeply down the hillside on the northwest side of the wash, intersecting the wash about 15 m downstream from the last outcrop of Buffalo Ridge flow. On the southeast side of the wash, almost all the breccia exposed belongs to the Noon Gorge sedimentary breccia; the One O'Clock Wash sedimentary breccia forms a few isolated pockets on top of the fault blocks in the Buffalo Ridge flow.

Farther down the wash, 120 m from the kink in the gorge, a higher member of the Crater Pasture Formation, the Fault Canyon flow, is exposed. This flow is presumed to overlie at some depth the One O'Clock Wash sedimentary breccia, although the contact is not exposed. At this location, the Fault Canyon flow is relatively flat lying, as it lies beyond the structural flank of the Fort Rock dome. The Fault Canyon flow is a black olivine-sanidine trachybasalt that forms the walls of a shallow canyon extending from this location to Fort Rock Creek. On top of the flow, pockets of distinctive agglomerate crop out that consist of vesicular grayish-brown clasts in a fine-grained white tuffaceous matrix. The contact between the Fault Canyon flow and the overlying Noon Gorge breccia of the Fort Rock Creek Rhyodacite (see below) is well exposed in the northwest bank of the wash. At the lower end of the wash, the Fault Canyon flow is directly overlain by the Old Stage Road Member of the Fort Rock Creek Rhyodacite.

REFERENCE SECTION

The reference section for the Crater Pasture Formation is exposed in Six Thirty Wash, on the south side of the crater. The base of this section is located in the S¹/₂NW¹/₄SE¹/₄ sec. 10, T. 20 N., R. 10 W.; it is 240 m west of Road End Gap, on Buffalo Ridge. About 250 m of the Crater Pasture Formation is exposed in this section, which dips about 75° to the south. At the base of the section these rocks underlie the rim of the crater. Six units are exposed: the volcanic breccia and flow of Road End Gap, the flow of Annex Ridge, the flow of Buffalo Ridge, the sedi-

mentary breccia of One O'Clock Wash, the agglomerate and tuff of Cinder Basin, and the flow of Fault Canyon.

The basal contact of the Crater Pasture Formation with Precambrian rocks runs precisely along the crest of Buffalo Ridge in this area and can easily be exposed by digging. The basal unit here is the volcanic breccia and flow of Road End Gap, estimated to be 90 m thick. Both the flow and the breccia are olivine trachyandesite. The volcanic breccia consists of black vesicular clasts in a reddened matrix. Flow rock varies from light grayish brown to black; the black variety is commonly vesicular. Flow is generally massive and rarely shows flow cleavage. In this locality, flow commonly grades into volcanic breccia; however, colluvium is fairly thick and internal contacts are difficult to follow.

The contact between the Road End Gap volcanic breccia and flow and the overlying Annex Ridge flow is well exposed on the east bank of the gully at the head of Six Thirty Wash. Here the upper part of the Road End Gap unit is sedimentary breccia containing clasts of Road End Gap trachyandesite up to 60 cm across. This breccia grades upward into a conglomerate with clasts no larger than 1 cm across. The next unit in this section is a bedded sedimentary breccia containing fragments of the Road End Gap unit, yellow-brown hornblende-bearing trachyandesite ash and lapilli, and clasts of Precambrian rock. The contact between the Annex Ridge and the Road End Gap units is placed at the base of this breccia. Above this breccia are thin beds of volcanic and sedimentary breccias, conglomeratic sandstone, and tuff. These beds are overlain by a light-gray hornblende trachyandesite lava flow that is approximately 105 m thick in this location. The upper part of the flow is soft, light-brown rock; it is seen best in the bed of the wash 120 m from the exposure of the basal contact. All of this flow is characterized by abundant hornblende prisms.

The Buffalo Ridge flow is exposed on the slope southwest of Six Thirty Wash, but it pinches out against the Annex Ridge flow before it reaches the wash. The geologic map (pl. 1) provides a cross section of this relationship owing to the steep dip of all units. The Buffalo Ridge flow is a somewhat darker blue-gray than the Annex Ridge flow; it, too, contains abundant hornblende prisms. The base of this unit includes several meters of yellow-brown ash. The base of the lava flow in this location is reddened and brecciated. The top of the flow is dark varnished aa.

The One O'Clock Wash sedimentary breccia overlies both the Buffalo Ridge and Annex Ridge flows

in this area. In Six Thirty Wash it forms a small flat-iron over the Annex Ridge flow with a dip of about 30° to the south. Here, it contains clasts of Annex Ridge flow, some of which are larger than 1.2 m across. About 30 m down the wash from the basal contact of the breccia, it contains clasts of Precambrian rocks and Road End Gap (?) olivine trachyandesite. The unit has an estimated thickness of 18 m here.

At a bend in Six Thirty Wash 40 m south of the Annex Ridge flow, the One OClock Wash breccia is in contact with an agglomeratic unit in the overlying tuff and agglomerate of Cinder Basin, although the contact is here covered by alluvium. Trachybasalt agglomerate, with bombs more than 3 m across, is exposed from the bend in the wash to the junction of Six Thirty and Six OClock Washes. Overlying the agglomerate on the ridge south of the bend is an orange volcanic sandstone and sedimentary breccia, of the Cinder Basin unit, which also crops out in Six OClock Wash. It contains clasts of Annex Ridge (?) flow (up to 1.2 m across) and Precambrian rocks in addition to trachybasalt clasts. The Cinder Basin tuff and agglomerate is about 20 m thick here.

The Cinder Basin tuff and agglomerate is overlain on the crest of the above-mentioned ridge by black, poorly banded trachybasalt of the flow of Fault Canyon. In this area, the Fault Canyon flow forms a low north-facing escarpment on the flank of the dome. Only about 6 m thickness is preserved here.

BASAL TUFFACEOUS BRECCIA AND SANDSTONE

DISTRIBUTION AND PHYSICAL FEATURES

In a few isolated localities along the contact between the Crater Pasture Formation and Precambrian rocks, tuffaceous breccia and sandstone are exposed. The thickest deposit, 9 m, is found in Nine OClock Wash. In Four OClock Wash, a shallow excavation in the wash bottom revealed more than 1.4 m of such deposits. In the southeast wall of Eight OClock gorge, about 30 cm of buff to orange basal tuffaceous sandstone is exposed. In places on Buffalo Ridge, Six OClock Hill, Five OClock Hill, and Three OClock Hill, a thin, bedded, dark-olive tuff is found; it is too thin to map separately, but it contains ash that is petrographically similar to ash found in the above localities. All of these basal deposits are poorly resistant to erosion and difficult to map separately, but they are important locally in determining structure in the rim owing to their bedding.

PETROGRAPHY

The lower part of the deposit in Nine OClock Wash is a crudely bedded breccia consisting of clasts of Precambrian rocks, up to 15 cm across, in a matrix of moderately sorted sandstone. The matrix contains a trace of red-brown ash and is cemented by caliche. This breccia is about 6 m thick and grades upward into a 3-m-thick maroon moderately well sorted thick-bedded tuffaceous sandstone consisting dominantly of red-brown ash. In Four OClock Wash, the lower part of the deposit is a breccia that shows an increase in both degree of sorting and ash content from base to top. It is about 1 m thick and is overlain by a 30-cm-thick bed of red moderately well sorted tuffaceous sandstone succeeded by a 15-cm-thick bed of olive-brown tuff.

The ash in these deposits is yellow-brown to dominantly red-brown in thin section and is microvesicular. It contains abundant (15 to 30 percent) serpentized(?) olivine grains as phenocrysts, microphenocrysts, and rarely groundmass grains in a glassy to opaque matrix. The ash in the deposits in Eight OClock Gorge contains in addition rare pyroxene phenocrysts and commonly has a groundmass of plagioclase laths and yellow-brown to red-brown glass. The ash in the Four OClock and Nine OClock Wash deposits contains no pyroxene and has a dark dusty to opaque matrix.

The bed of breccia in Four OClock Wash contains a few felsic volcanic clasts, up to 1 cm across, containing small phenocrysts and microphenocrysts of sanidine, plagioclase, biotite, and hornblende in a groundmass of sparse feldspar laths and cryptocrystalline felsic minerals. These clasts are either latite or rhyodacite and are petrographically similar to the rhyodacite intrusive body in the gully at the head of Five OClock Wash.

VOLCANIC BRECCIA AND FLOW OF ROAD END GAP

DISTRIBUTION, STRATIGRAPHY, AND PHYSICAL FEATURES

The volcanic breccia and flow of Road End Gap is exposed on the southeast and south parts of the rim of the crater from the south flank of Three OClock Hill to the crest of Buffalo Ridge. It consists of volcanic breccia interlayered with five relatively small flows, numbered in order of age (oldest=flow 1; pl. 1). There is a successive increase in maximum flow thickness from flow 1 (9-20? m) to flow 2 (20-35? m) to flow 3 (65 m), and there is also a successive shift southward of the centers of the outcrop areas of these

three flows. Flows 4 and 5 are west of the first three flows and have maximum thicknesses of 3 m and 11 m, respectively. The Road End Gap unit as a whole is thickest near the head of Six Thirty Wash, where it is estimated to be 90 m thick. The section exposed in Road End Gap is representative but not complete.

The volcanic breccia and flow of Road End Gap is more colorful than the rest of the Crater Pasture units; the rocks are black, red, red-orange, and yellow-brown. This unit also tends to be less resistant to erosion and is more commonly covered by colluvium than the adjacent flows in the formation. Except for a few outcrops of its flows, it rarely forms the blocky outcrops that are typical of other volcanic units.

RELATION TO OTHER UNITS

This unit overlies Precambrian rocks and pockets of the basal tuffaceous breccia and sandstone of the Crater Pasture Formation. Its age relative to the flow of Eight O'Clock Gorge is unknown. It is overlain on its northeast edge by pockets of tuff of the Two O'Clock Gap tuff and flow; these pockets are too small to be shown on the geologic map. It is overlain in several places, including its northeast edge, by pyroxene-trachyandesite sandstone and conglomerate of the Crater Pasture Formation. In most places, it is overlain by Annex Ridge flow. Its west part is overlain by Buffalo Ridge flow. A vent for the Buffalo Ridge flow cuts this unit, as does a sill of the Fault Canyon flow.

SOURCE

The thickest section of the Road End Gap unit and also the thickest sections of flows 2 and 3, which are the major flows in the unit, are located on the south rim of the crater. Unless these thicknesses represent merely fillings of a local depression, the vent for the Road End Gap lavas probably lies somewhere to the south of this area.

PETROGRAPHY

Volcanic breccia in this unit consists of black vesicular clasts in a scant tan to reddish matrix consisting of ash-size fragments similar to the larger clasts. Clasts rarely exceed 30 cm or so across. Flows 1 and 4 consist of rocks that are medium gray on fresh surfaces, grayish brown on weathered surfaces, and nonvesicular; these rocks have flow cleavage.

Rocks of flows 2 and 5 are dark brownish red or dark tan on fresh surfaces, reddish orange on weathered surfaces, and vesicular; they have no flow cleavage. Rocks of flow 3 are either black and vesicular or medium gray and nonvesicular. All rocks of the Road End Gap unit contains red-brown-rimmed phenocrysts of olivine up to 3 mm across.

Rocks of flow 1 contain plagioclase, sanidine, olivine, augite, opaque minerals, and apatite and have a color index of about 35 (table 2). Recognizable sanidine is subordinate to plagioclase but exceeds 10 percent of the total rock. On the basis of its color index, the lack of quartz, and the presence of more than 10 percent sanidine, the rock is classified as an olivine trachyandesite.⁴ The presence of sanidine in the groundmass, suggested by chemical and normative analyses (table 3), was confirmed using an electron microprobe. The sanidine occupies interstices between plagioclase laths and commonly contains abundant apatite needles. Plagioclase has a composition, as indicated by probe analysis, ranging from sodic labradorite to oligoclase. Olivine occurs as phenocrysts up to 3 mm across, averaging 0.6 mm across. It is altered to brown vermiculite(?) on its rims. Diopsidic augite occurs in equal amounts as phenocrysts (commonly in clusters) and groundmass grains. The phenocrysts are close in size to those of olivine. An unidentified secondary mineral of low refractive index, low birefringence, light-brown color, and cryptocrystalline to radial-fibrous habit is commonly found in interstices between plagioclase laths and is generally occluded by red hematite dust and apatite needles. The texture of the rock is pilotaxitic.

In contrast to rock of flow 1, clasts of the volcanic breccia have a groundmass consisting of light-yellow-brown to dark-red-brown glass, subalined plagioclase laths, a felt of diopsidic augite prisms and apatite needles, and opaque minerals. Crystalline phases have sharp relief against the glass. Rock of flow 2 is similar to rock of the volcanic breccia except that cryptocrystalline material, which is heavily occluded by red hematite dust, occurs in the groundmass in the place of glass.

CHEMICAL COMPOSITION

In three chemically analyzed samples of this unit (table 3), silica, recalculated on a water-free and cal-

⁴The rock classification by Williams and others (1954) is used in this text for the naming of all igneous rocks.

TABLE 2.—*Modal composition of the Crater Pasture Formation*

[Analyses by G.S. Fuis; Tr., trace; --, not detected]

| Unit sampled | Volcanic breccia and flow of Road End Gap: flow 1 | Flow of Eight O'Clock Gorge | Flow of Meadow Dam | Tuff and flow of Two O'Clock Gap: flow | Flow of Annex Ridge | Flow of Buffalo Ridge | Flow of Lion Ridge | Flow of Fault Canyon |
|----------------------------------|---|-----------------------------|--------------------|--|---------------------|-----------------------|--------------------|----------------------|
| Sample number 1/ | 190 | Ao | 227 | 178b | 154c | 235 | 154f | 406b |
| Points counted | 989 | 500 | 501 | 972 | 991 | 500 | 1001 | 500 |
| Mineral | Percent | | | | | | | |
| Glass | -- | 6.2 | -- | -- | -- | -- | -- | -- |
| Plagioclase | 18.3 | 6.0 | 7.6 | 11.2 | 14.9 | 20.0 | 20.9 | 0.6 |
| Sanidine | 14.3 | -- | 13.2 | 14.4 | 25.3 | 14.8 | 12.8 | 57.2 |
| Unspecified feldspar | 28.9 | 18.4 | 29.8 | 35.4 | 35.7 | 40.0 | 29.1 | -- |
| Olivine 2/ | 8.3 | 6.8 | 5.2 | 2.0 | -- | -- | -- | 9.6 |
| Clinopyroxene 2/ | 22.3 | 32.2 | 19.4 | 19.4 | 1.0 | 3.4 | 16.6 | 17.8 |
| Orthopyroxene 2/ | -- | -- | -- | 1.3 | -- | -- | -- | -- |
| Hornblende 2/ | -- | -- | 16.8 | 10.0 | 16.3 | 14.6 | 11.6 | -- |
| Biotite 2/ | -- | 2.6 | 2.0 | -- | -- | -- | .2 | 3.0 |
| Apatite | .7 | .4 | .6 | .7 | 2.8 | Tr. | 1.5 | 1.4 |
| Zircon | -- | -- | .2 | -- | -- | -- | -- | -- |
| Opaque minerals | 4.5 | 18.6 | 2.4 | 5.1 | 3.9 | 5.8 | 7.2 | 7.8 |
| Analcime | -- | .6 | -- | -- | -- | -- | -- | -- |
| Calcite | -- | 2.2 | -- | -- | -- | -- | -- | -- |
| Secondary minerals | 2.2 | -- | 3.0 | .1 | -- | -- | .2 | 2.6 |
| Unknown minerals | -- | 6.0 | -- | -- | -- | 1.4 | -- | -- |
| Total | 99.5 | 100.0 | 100.2 | 99.6 | 99.9 | 100.0 | 100.1 | 100.0 |
| Color index 3/ | 35.1 | 66.2 | 46.0 | 37.8 | 21.2 | 23.8 | 35.6 | 38.2 |
| Plagioclase/total feldspar (pct) | ≥29.8 | ≥24.6 | ≥15.0 | ≥18.3 | ≥19.6 | ≥26.7 | ≥33.3 | 1.0 |
| Sanidine/total feldspar (pct) | ≥23.3 | 0 (?) | ≥26.1 | ≥23.6 | ≥33.3 | ≥19.8 | ≥20.4 | 99.0 |

1/ Sample locations:

| | | | |
|------|---|------|---|
| 190 | Northwest side of Four O'Clock Hill | 154c | Northeast bank of Four O'Clock Wash |
| Ao | Northwest bank of wash in Eight O'Clock Gorge | 235 | Base of Buffalo Ridge flow on top of Buffalo Ridge |
| 227 | Southeast end of Meadow Dam flow on Buffalo Ridge | 154f | Northeast bank of Four O'Clock Wash |
| 178b | Base of Two O'Clock Gap flow northwest of Two O'Clock Gap | 406b | North side of Six O'Clock Wash east of Cinder Basin |

2/ Includes alteration products, if any.

3/ Sum of olivine, pyroxenes, hornblende, biotite, opaque minerals, and dark unknown minerals.

cium-carbonate-free basis⁵, ranges from 56 to 58 percent, well within the range of intermediate composition (52-66 percent). Potassium oxide averages around 3 percent, and normative potassium feldspar averages around 19 percent. A lower limit of 10 percent modal or normative potassium feldspar is used by Williams and others (1954, p. 97) for trachyandesite. Chemical and modal data are thus in accord in classifying rock of this unit as a trachyandesite.

FLOW OF EIGHT OCLOCK GORGE

DISTRIBUTION, STRATIGRAPHY, AND PHYSICAL FEATURES

The flow of Eight O'Clock Gorge crops out on the southwest and west rim of the crater from the middle

⁵Water contents range considerably among rocks analyzed in table 3. Compare, for example, the samples of tuff and conglomerate of Hidden Pasture (samples 166a, and 165, 286, and 289a1) with preceding samples of flow rocks. In order to compare silica contents among the various rocks, an anhydrous basis of comparison was therefore chosen. Rocks with appreciable carbon dioxide usually have calcite vesicle fillings; therefore, a calcium-carbonate-free basis of comparison also seems reasonable. Note that the recalculated values vary much less among rocks of the same unit than raw silica values.

of Buffalo Ridge to the north flank of Nine O'Clock Hill. It consists of flow and minor infolded agglomerate (up to 21 m thick) and a thin (3-m-thick) overlying deposit of sandstone and granule conglomerate. This unit is thickest and best exposed in the vicinity of Eight O'Clock Gorge.

The flow is poorly resistant to weathering and is generally covered by colluvium; it forms low, black, grussy outcrops. The sandstone is generally non-resistant but does form a ledge on the northeast flank of Nine O'Clock Hill.

RELATION TO OTHER UNITS

The Eight O'Clock Gorge flow overlies Precambrian rocks and pockets of basal tuffaceous breccia and sandstone of the Crater Pasture Formation. It is overlain by the flow of Meadow Dam in the southeast and by a pyroxene-trachyandesite sandstone and conglomerate of the Crater Pasture Formation in the northeast.

SOURCE

This unit is thickest in the vicinity of Eight O'Clock Hill and Eight O'Clock Gorge. This area may have

TABLE 3.—*Chemical and normative composition of the Crater Pasture Formation*

[Rapid analyses (Shapiro and Brannock, 1962) were performed by D.J. Emmons, R.L. Swenson, and Frank Cuttitta in laboratories operated by the U.S. Geological Survey. Normative minerals are calculated after subtracting CaCO₃ from the oxides. *, single clast; ---, not detected.]

| Unit sampled Sample number L/ | Volcanic breccia and flow of Road End Gap | | | | Flow of Eight O'Clock Gorge Ao 294 |
|----------------------------------|--|---------------|----------------|------|---------------------------------------|
| | Breccia 189 | Flow 1 190 | Flow 2 195a | | |
| Oxide | Weight percent | | | | |
| SiO ₂ | 54.5 | 56.2 | 56.6 | 47.2 | 49.0 |
| Al ₂ O ₃ | 14.0 | 13.9 | 13.7 | 12.5 | 13.0 |
| Fe ₂ O ₃ | 4.2 | 3.6 | 4.0 | 6.3 | 5.8 |
| FeO | 2.79 | 3.24 | 2.25 | 3.33 | 3.61 |
| MgO | 7.7 | 7.4 | 7.4 | 6.7 | 8.1 |
| CaO | 6.4 | 6.6 | 5.6 | 11.6 | 10.3 |
| Na ₂ O | 2.7 | 3.2 | 2.9 | 1.8 | 2.1 |
| K ₂ O | 2.6 | 3.1 | 3.6 | 2.9 | 3.0 |
| TiO ₂ | 1.03 | 1.02 | .93 | 1.78 | .11 |
| P ₂ O ₅ | .37 | .34 | .36 | .64 | .76 |
| MnO | .11 | .11 | .10 | .14 | .15 |
| H ₂ O+ | 1.54 | .72 | 1.19 | 1.83 | 1.97 |
| H ₂ O- | 1.30 | .67 | .96 | 1.52 | 1.09 |
| CO ₂ | .19 | <.05 | <.05 | 1.41 | .56 |
| Total | 99.4 | 100.1 | 99.6 | 99.7 | 99.6 |

| Normative mineral | Weight percent | | | | |
|-------------------|----------------|--------|--------|--------|--------|
| Qz | 7.53 | 4.36 | 6.63 | 2.44 | -- |
| Or | 15.98 | 18.56 | 21.84 | 18.41 | 18.62 |
| Ab | 23.77 | 27.44 | 25.19 | 16.37 | 18.67 |
| An | 19.15 | 14.61 | 14.11 | 18.77 | 18.06 |
| Co | -- | -- | -- | -- | -- |
| Dp | 7.89 | 12.81 | 9.34 | 22.55 | 20.99 |
| Hy | 16.45 | 14.19 | 14.58 | 7.47 | 11.33 |
| Ol | -- | -- | -- | -- | 1.45 |
| Mt | 6.33 | 5.29 | 5.01 | 6.48 | 8.83 |
| Ht | -- | -- | .65 | 2.30 | -- |
| Il | 2.04 | 1.96 | 1.81 | 3.63 | .22 |
| Sph | -- | -- | -- | -- | -- |
| Rut | -- | -- | -- | -- | -- |
| Ap | .88 | .78 | .84 | 1.57 | 1.82 |
| Total | 100.00 | 100.00 | 100.00 | 100.00 | 100.00 |

| | | | | | |
|---|-------|-------|-------|-------|-------|
| Color index | 32.70 | 34.25 | 31.40 | 42.44 | 42.82 |
| An/(Ab + An) | 44.62 | 34.74 | 35.90 | 53.42 | 49.18 |
| Or/(Or + Ab + An) | 27.13 | 30.63 | 35.72 | 34.38 | 33.64 |
| SiO ₂ (H ₂ O-, CaCO ₃ -free) | 56.68 | 56.93 | 58.09 | 50.70 | 51.46 |

| Unit Sampled Sample number | Flow of Annex Ridge | | | |
|--------------------------------|---------------------|-------------------|----------------------------------|---------------------------------------|
| | Lower flow 154c | Upper flow 167 | Dike on Six O'Clock Hill 326a | Intrusion in Five O'Clock Wash 328 |
| Oxide | Weight percent | | | |
| SiO ₂ | 55.3 | 56.2 | 56.0 | 52.1 |
| Al ₂ O ₃ | 16.8 | 16.9 | 16.3 | 16.0 |
| Fe ₂ O ₃ | 6.5 | 6.8 | 6.9 | 7.1 |
| FeO | 1.17 | <.05 | .86 | .95 |
| MgO | 2.6 | 2.9 | 3.1 | 3.5 |
| CaO | 5.4 | 5.9 | 5.2 | 3.9 |
| Na ₂ O | 4.0 | 4.1 | 3.6 | 2.4 |
| K ₂ O | 3.2 | 2.9 | 3.1 | 3.1 |
| TiO ₂ | 1.12 | .96 | 1.15 | 1.04 |
| P ₂ O ₅ | .64 | .57 | .71 | .66 |
| MnO | .12 | .11 | .12 | .15 |
| H ₂ O+ | 1.27 | 1.80 | 1.42 | 2.80 |
| H ₂ O- | 1.41 | 1.12 | .95 | 4.19 |
| CO ₂ | <.05 | <.05 | .12 | .44 |
| Total | 99.5 | 100.3 | 99.5 | 98.3 |

| Normative mineral | Weight percent | | | |
|-------------------|----------------|--------|--------|--------|
| Qz | 7.27 | 7.47 | 10.34 | 17.45 |
| Or | 19.53 | 17.61 | 18.91 | 20.28 |
| Ab | 34.96 | 35.65 | 31.45 | 22.49 |
| An | 19.05 | 19.68 | 19.79 | 13.57 |
| Co | -- | -- | -- | 4.66 |
| Dp | 3.35 | 2.78 | .84 | -- |
| Hy | 5.14 | 6.13 | 7.58 | 9.65 |
| Ol | -- | -- | -- | -- |
| Mt | .95 | -- | -- | .59 |
| Ht | 6.06 | 6.99 | 7.12 | 7.45 |
| Il | 2.20 | .24 | 2.14 | 2.19 |
| Sph | -- | 2.11 | .15 | -- |
| Rut | -- | -- | -- | -- |
| Ap | 1.15 | 1.33 | 1.67 | 1.66 |
| Total | 100.00 | 100.00 | 100.00 | 100.00 |

| | | | | |
|---|-------|-------|-------|-------|
| Color index | 17.68 | 18.25 | 17.83 | 19.88 |
| An/(Ab + An) | 35.27 | 35.57 | 38.62 | 37.64 |
| Or/(Or + Ab + An) | 26.56 | 24.14 | 26.96 | 36.00 |
| SiO ₂ (H ₂ O-, CaCO ₃ -free) | 57.10 | 57.74 | 57.80 | 57.67 |

| Unit sampled Sample number | Flow of Meadow Dam | | | Tuff and flow of Two O'Clock Gap | |
|--------------------------------|--------------------------|---------------|---------------|-------------------------------------|--------------|
| | Undivided flow 227 | Flow 1 439 | Flow 2 440 | Tuff 148 | Flow 178b |
| Oxide | Weight percent | | | | |
| SiO ₂ | 51.8 | 51.8 | 50.0 | 52.3 | 54.9 |
| Al ₂ O ₃ | 13.8 | 15.1 | 14.7 | 15.0 | 15.3 |
| Fe ₂ O ₃ | 7.5 | 8.7 | 6.9 | 5.3 | 5.1 |
| FeO | .99 | .60 | 1.2 | 1.80 | 2.16 |
| MgO | 6.7 | 4.5 | 4.6 | 6.4 | 5.8 |
| CaO | 8.1 | 6.2 | 8.7 | 7.2 | 6.7 |
| Na ₂ O | 3.4 | 3.3 | 2.9 | 2.9 | 3.8 |
| K ₂ O | 2.3 | 2.5 | 3.1 | 2.8 | 2.4 |
| TiO ₂ | 1.25 | 1.6 | 1.2 | .85 | 1.25 |
| P ₂ O ₅ | .66 | .74 | .99 | .49 | .44 |
| MnO | .13 | .14 | .13 | .11 | .10 |
| H ₂ O+ | 1.26 | 2.4 | 1.6 | 2.42 | 1.05 |
| H ₂ O- | 1.47 | 2.4 | 1.8 | 2.19 | .96 |
| CO ₂ | .26 | <.05 | 1.6 | <.05 | <.05 |
| Total | 99.6 | 100.0 | 99.4 | 99.8 | 100.0 |

| Normative mineral | Weight percent | | | | |
|-------------------|----------------|--------|--------|--------|--------|
| Qz | 2.56 | 6.95 | 5.19 | 4.10 | 4.70 |
| Or | 14.12 | 15.53 | 19.84 | 17.39 | 14.48 |
| Ab | 29.89 | 29.35 | 26.58 | 25.80 | 32.84 |
| An | 16.21 | 19.99 | 19.44 | 20.66 | 17.98 |
| Co | -- | -- | -- | -- | -- |
| Dp | 15.05 | 3.44 | 7.27 | 10.53 | 10.14 |
| Hy | 10.35 | 10.18 | 9.03 | 11.87 | 10.05 |
| Ol | -- | -- | -- | -- | -- |
| Mt | -- | -- | .88 | 3.89 | 3.74 |
| Ht | 7.79 | 9.14 | 6.86 | 2.89 | 2.63 |
| Il | 2.46 | 1.65 | 2.47 | 1.70 | 2.43 |
| Sph | .01 | 2.00 | -- | -- | -- |
| Rut | -- | -- | -- | -- | -- |
| Ap | 1.56 | 1.77 | 2.44 | 1.17 | 1.02 |
| Total | 100.00 | 100.00 | 100.00 | 100.00 | 100.00 |

| | | | | | |
|---|-------|-------|-------|-------|-------|
| Color index | 35.66 | 26.41 | 26.52 | 30.87 | 28.98 |
| An/(Ab + An) | 35.17 | 40.51 | 42.24 | 44.47 | 35.39 |
| Or/(Or + Ab + An) | 23.44 | 23.94 | 30.13 | 27.24 | 22.18 |
| SiO ₂ (H ₂ O-, CaCO ₃ -free) | 53.79 | 54.42 | 54.12 | 54.97 | 56.05 |

| Unit sampled Sample number | Flow of Buffalo Ridge | | | |
|--------------------------------|-----------------------|--------------------------|-----------------------------|---|
| | Flow 235 | Massive intrusion 232 | Blocks on Noon Hill 291a | Dike south-east of Crater Divide 429 |
| Oxide | Weight percent | | | |
| SiO ₂ | 56.0 | 54.1 | 55.7 | 53.9 |
| Al ₂ O ₃ | 15.8 | 16.3 | 16.1 | 16.0 |
| Fe ₂ O ₃ | 6.6 | 5.2 | 7.5 | 5.2 |
| FeO | 1.25 | 2.44 | .03 | 2.72 |
| MgO | 3.4 | 4.3 | 4.0 | 4.4 |
| CaO | 5.7 | 6.9 | 6.9 | 7.6 |
| Na ₂ O | 3.9 | 3.7 | 4.3 | 4.2 |
| K ₂ O | 3.2 | 2.9 | 2.7 | 2.9 |
| TiO ₂ | 1.10 | 1.13 | 1.05 | 1.25 |
| P ₂ O ₅ | .74 | .75 | .71 | .65 |
| MnO | .11 | .13 | .14 | .13 |
| H ₂ O+ | .91 | .86 | .84 | .58 |
| H ₂ O- | 1.00 | .69 | .39 | .32 |
| CO ₂ | .20 | .29 | .29 | .44 |
| Total | 99.9 | 99.7 | 100.7 | 100.1 |

| Normative mineral | Weight percent | | | | |
|-------------------|----------------|--------|--------|--------|--------|
| Qz | 7.90 | 5.51 | 4.85 | 2.35 | 10.44 |
| Or | 19.39 | 18.00 | 16.16 | 16.25 | 17.79 |
| Ab | 33.84 | 33.52 | 36.86 | 36.21 | 32.51 |
| An | 16.58 | 18.13 | 16.88 | 17.16 | 20.62 |
| Co | -- | -- | -- | -- | -- |
| Dp | 4.82 | 7.23 | 6.39 | 10.97 | 1.19 |
| Hy | 6.45 | 7.01 | 7.13 | 6.07 | 6.43 |
| Ol | -- | -- | -- | -- | -- |
| Mt | 1.23 | 3.64 | -- | 5.67 | .71 |
| Ht | 5.92 | 2.97 | 7.59 | 1.38 | 6.15 |
| Il | 2.14 | 2.32 | .37 | 2.82 | 2.37 |
| Sph | -- | -- | 2.14 | -- | -- |
| Rut | -- | -- | -- | -- | -- |
| Ap | 1.73 | 1.67 | 1.64 | 1.51 | 1.80 |
| Total | 100.00 | 100.00 | 100.00 | 100.00 | 100.00 |

| | | | | | |
|---|-------|-------|-------|-------|-------|
| Color index | 20.56 | 23.18 | 23.61 | 26.52 | 16.85 |
| An/(Ab + An) | 32.88 | 35.10 | 31.41 | 32.15 | 38.81 |
| Or/(Or + Ab + An) | 27.78 | 25.85 | 23.12 | 23.35 | 25.09 |
| SiO ₂ (H ₂ O-, CaCO ₃ -free) | 57.41 | 56.24 | 56.40 | 54.89 | 57.71 |

TABLE 3.—Chemical and normative composition of the Crater Pasture Formation—Continued

| Unit sampled Sample number | Flow of Lion Ridge | | | Tuff and conglomerate of Hidden Pasture | |
|-------------------------------------|--------------------|-------------|--|--|--------------------------|
| | Flow 154f | Flow 171 | Intrusion in Eight O'clock Basin NE | Hornblende trachyan- desite tuff 166a | Undivided tuff 165 |
| Oxide | Weight percent | | | | |
| SiO ₂ | 54.8 | 54.9 | 52.4 | 50.3 | 51.5 |
| Al ₂ O ₃ | 16.0 | 16.1 | 16.0 | 14.8 | 12.6 |
| Fe ₂ O ₃ | 6.3 | 5.6 | 6.6 | 6.2 | 7.2 |
| FeO | 1.71 | 2.16 | 1.62 | 1.35 | .90 |
| MgO | 3.7 | 4.4 | 4.6 | 4.8 | 6.1 |
| CaO | 7.1 | 7.8 | 7.4 | 8.1 | 8.1 |
| Na ₂ O | 3.8 | 3.8 | 3.8 | 1.9 | 1.4 |
| K ₂ O | 2.9 | 2.8 | 2.8 | 2.2 | 2.2 |
| TiO ₂ | 1.11 | 1.13 | 1.19 | 1.05 | 1.11 |
| P ₂ O ₅ | .59 | .59 | .54 | .56 | .44 |
| MnO | .13 | .13 | .13 | .12 | .12 |
| H ₂ O+ | .75 | .31 | .78 | 3.49 | 2.97 |
| H ₂ O- | 1.21 | .44 | 1.42 | 4.25 | 4.84 |
| CO ₂ | <.05 | .06 | <.05 | .29 | <.05 |
| Total | 100.1 | 100.2 | 99.3 | 99.4 | 99.5 |
| Normative mineral | Weight percent | | | | |
| Qz | 5.51 | 4.08 | 1.64 | 11.76 | 14.31 |
| Or | 17.47 | 16.66 | 17.05 | 14.29 | 14.19 |
| Ab | 32.78 | 32.38 | 33.13 | 17.67 | 12.93 |
| An | 18.39 | 18.74 | 18.90 | 27.88 | 23.58 |
| Co | -- | -- | -- | -- | -- |
| Dp | 10.57 | 12.41 | 11.90 | 7.98 | 13.34 |
| Hy | 4.49 | 5.28 | 6.28 | 9.44 | 10.39 |
| Ol | -- | -- | -- | -- | -- |
| Mt | 2.77 | 4.14 | 2.26 | 1.87 | .08 |
| Ht | 4.51 | 2.78 | 5.24 | 5.52 | 7.80 |
| Il | 2.15 | 2.16 | 2.33 | 2.19 | 2.30 |
| Sph | -- | -- | -- | -- | -- |
| Rut | -- | -- | -- | -- | -- |
| Ap | 1.37 | 1.35 | 1.27 | 1.40 | 1.09 |
| Total | 100.00 | 100.00 | 100.00 | 100.00 | 100.00 |
| Color index | 24.49 | 26.77 | 28.02 | 27.00 | 33.91 |
| An/(Ab + An) | 35.95 | 36.66 | 36.32 | 61.21 | 64.59 |
| Or/(Or + Ab + An) | 25.45 | 24.58 | 24.68 | 23.88 | 27.98 |
| SiO ₂ (H ₂ O- | 55.84 | 55.27 | 53.98 | 55.27 | 56.18 |
| CaCO ₃ -free) | | | | | |

| Unit sampled Sample number | Tuff and agglomerate of Cinder Basin | | Tuff and conglomerate of Hidden Pasture | | Tuff and agglomerate of Cinder Basin | |
|-------------------------------------|--------------------------------------|--|--|---|---|--|
| | Flow 286 | *Olivine trachyan- desite clast 289a1 | Undivided tuff 250 | Undivided trachyan- desite clast 240 | Agglomerate 409 | |
| Oxide | Weight percent | | | | | |
| SiO ₂ | 49.4 | 52.9 | 50.6 | 47.2 | 49.5 | |
| Al ₂ O ₃ | 14.5 | 16.1 | 13.2 | 12.1 | 14.6 | |
| Fe ₂ O ₃ | 9.6 | 7.5 | 8.2 | 7.5 | 9.5 | |
| FeO | .36 | 1.20 | 1.10 | 2.53 | .68 | |
| MgO | 5.6 | 4.1 | 5.7 | 7.2 | 4.5 | |
| CaO | 5.2 | 7.4 | 9.2 | 11.2 | 5.8 | |
| Na ₂ O | 1.1 | 1.5 | 2.2 | 2.9 | 2.4 | |
| K ₂ O | .8 | 1.9 | 3.0 | 1.5 | 3.1 | |
| TiO ₂ | 1.29 | 1.22 | 1.51 | 1.52 | 1.6 | |
| P ₂ O ₅ | .27 | .41 | 1.27 | 1.08 | 1.4 | |
| MnO | .15 | .10 | .15 | .15 | .15 | |
| H ₂ O+ | 5.03 | 2.79 | 1.41 | 1.98 | 3.0 | |
| H ₂ O- | 6.22 | 2.56 | 1.84 | 1.86 | 3.4 | |
| CO ₂ | .20 | .32 | .23 | .38 | <.05 | |
| Total | 99.7 | 100.00 | 99.6 | 99.1 | 99.6 | |
| Normative mineral | Weight percent | | | | | |
| Qz | 24.73 | 18.16 | 6.61 | 0.56 | 9.10 | |
| Or | 5.37 | 11.96 | 18.51 | 9.39 | 19.66 | |
| Ab | 10.58 | 13.52 | 19.44 | 26.01 | 21.80 | |
| An | 25.85 | 33.65 | 18.05 | 16.51 | 21.07 | |
| Co | 3.97 | -- | -- | -- | .11 | |
| Dp | -- | .33 | 14.79 | 25.20 | -- | |
| Hy | 15.85 | 10.72 | 7.96 | 7.32 | 12.03 | |
| Ol | -- | -- | -- | -- | -- | |
| Mt | -- | .70 | -- | 4.49 | -- | |
| Ht | 10.91 | 7.50 | 8.56 | 4.85 | 10.19 | |
| Il | 1.23 | 2.47 | 2.76 | 3.06 | 1.89 | |
| Sph | -- | -- | .30 | -- | -- | |
| Rut | .82 | -- | -- | -- | .72 | |
| Ap | .70 | .99 | 3.02 | 2.61 | 3.42 | |
| Total | 100.00 | 100.00 | 100.00 | 100.00 | 100.00 | |
| Color index | 28.80 | 21.72 | 34.38 | 44.92 | 24.83 | |
| An/(Ab + An) | 70.96 | 71.34 | 48.15 | 38.83 | 49.15 | |
| Or/(Or + Ab + An) | 12.85 | 20.22 | 33.05 | 18.10 | 31.44 | |
| SiO ₂ (H ₂ O- | 56.13 | 56.32 | 52.80 | 50.00 | 53.09 | |
| CaCO ₃ -free) | | | | | | |

| Unit sampled Sample number | Tuff and agglomerate of Cinder Basin | | Shonkinite intrusion under the Fault Canyon powerlines | | Unmapped rocks | |
|-------------------------------------|--------------------------------------|-------------|--|---------------------------------|----------------|------|
| | Flow 414 | Dike 410 | *Dacite clast from sedimentary breccia 416a | Flow of Fault Canyon 406a | 459b | 459c |
| Oxide | Weight percent | | | | | |
| SiO ₂ | 51.9 | 49.3 | 62.4 | 54.1 | 52.4 | |
| Al ₂ O ₃ | 13.3 | 13.7 | 15.4 | 13.3 | 13.4 | |
| Fe ₂ O ₃ | 8.9 | 9.3 | 4.7 | 5.6 | 5.4 | |
| FeO | .36 | .88 | .92 | 1.4 | 1.36 | |
| MgO | 5.5 | 6.0 | 2.0 | 6.2 | 6.3 | |
| CaO | 4.3 | 8.3 | 5.0 | 6.5 | 7.9 | |
| Na ₂ O | 1.8 | 2.7 | 3.5 | 2.1 | 1.7 | |
| K ₂ O | 2.8 | 1.7 | 3.5 | 5.5 | 5.9 | |
| TiO ₂ | 1.2 | 1.5 | .86 | .95 | 1.02 | |
| P ₂ O ₅ | .54 | 1.3 | .42 | .74 | .69 | |
| MnO | .09 | .13 | .05 | .03 | .10 | |
| H ₂ O+ | 3.4 | 2.3 | .73 | 1.5 | .90 | |
| H ₂ O- | 5.1 | 2.8 | .47 | 2.0 | 1.21 | |
| CO ₂ | <.05 | <.05 | .08 | <.05 | 1.05 | |
| Total | 99.2 | 99.9 | 100.0 | 99.9 | 99.3 | |
| Normative mineral | Weight percent | | | | | |
| Qz | 16.35 | 7.08 | 17.67 | 3.50 | 2.10 | |
| Or | 18.25 | 10.60 | 20.95 | 33.72 | 36.78 | |
| Ab | 16.80 | 24.11 | 30.00 | 18.44 | 15.18 | |
| An | 19.64 | 21.37 | 16.19 | 11.03 | 12.15 | |
| Co | .87 | -- | -- | -- | -- | |
| Dp | -- | 9.14 | 4.79 | 13.55 | 13.57 | |
| Hy | 15.11 | 11.53 | 2.82 | 9.73 | 10.26 | |
| Ol | -- | -- | -- | -- | -- | |
| Mt | -- | -- | .64 | 1.93 | 1.85 | |
| Ht | 9.81 | 9.81 | 4.32 | 4.48 | 4.42 | |
| Il | 1.05 | 2.26 | 1.65 | 1.87 | 2.04 | |
| Sph | -- | .97 | -- | -- | -- | |
| Rut | .77 | -- | -- | -- | -- | |
| Ap | 1.36 | 3.12 | .97 | 1.75 | 1.66 | |
| Total | 100.00 | 100.00 | 100.00 | 100.00 | 100.00 | |
| Color index | 26.74 | 33.71 | 14.23 | 31.57 | 32.14 | |
| An/(Ab + An) | 53.89 | 46.99 | 35.05 | 37.43 | 44.46 | |
| Or/(Or + Ab + An) | 33.37 | 18.90 | 31.20 | 53.37 | 57.37 | |
| SiO ₂ (H ₂ O- | 57.23 | 52.00 | 63.19 | 56.11 | 55.26 | |
| CaCO ₃ -free) | | | | | | |

| Unit sampled Sample number | Tuff and conglomerate of Hidden Pasture | | Tuff and agglomerate of Cinder Basin | | Unmapped rocks 334 |
|-------------------------------------|--|--|---|--|-----------------------|
| | Undivided tuff 286 | *Olivine trachyan- desite clast 289a1 | Undivided tuff 250 | *Olivine trachyan- desite clast 240 | |
| Oxide | Weight percent | | | | |
| SiO ₂ | 55.9 | 41.5 | 48.6 | 46.4 | 49.4 |
| Al ₂ O ₃ | 13.8 | 10.3 | 12.5 | 12.1 | 13.1 |
| Fe ₂ O ₃ | 5.8 | 5.6 | 9.7 | 5.9 | 8.6 |
| FeO | 1.33 | 6.54 | .92 | 4.1 | 1.41 |
| MgO | 5.3 | 14.9 | 6.9 | 11.4 | 7.4 |
| CaO | 6.6 | 11.5 | 8.8 | 9.8 | 9.6 |
| Na ₂ O | 1.8 | 2.7 | 2.0 | 2.9 | 3.2 |
| K ₂ O | 6.3 | .9 | 3.5 | 1.2 | 1.6 |
| TiO ₂ | .98 | 2.99 | 2.0 | 1.9 | 1.80 |
| P ₂ O ₅ | .69 | .77 | .89 | .86 | .89 |
| MnO | .10 | .18 | .16 | .15 | .14 |
| H ₂ O+ | <.01 | 1.96 | 2.2 | 2.5 | 2.04 |
| H ₂ O- | 1.12 | .62 | 1.8 | .81 | 1.18 |
| CO ₂ | .18 | .33 | <.05 | <.05 | .13 |
| Total | 99.9 | 100.8 | 100.0 | 100.00 | 100.5 |
| Normative mineral | Weight percent | | | | |
| Qz | 5.28 | -- | 1.99 | -- | 1.22 |
| Or | 37.86 | 5.46 | 21.56 | 7.34 | 9.75 |
| Ab | 15.49 | 7.75 | 17.64 | 25.39 | 27.94 |
| An | 11.16 | 13.69 | 15.43 | 17.03 | 17.19 |
| Co | -- | -- | -- | -- | -- |
| Dp | 12.76 | 29.48 | 16.44 | 21.37 | 19.31 |
| Hy | 7.51 | -- | 10.29 | 2.52 | 10.06 |
| Ol | -- | 19.16 | -- | 11.87 | -- |
| Mt | 1.80 | 8.33 | -- | 8.48 | -- |
| Ht | 4.65 | -- | 10.11 | .25 | 8.87 |
| Il | 1.89 | 5.83 | 2.38 | 3.73 | 3.38 |
| Sph | -- | -- | 2.04 | -- | .19 |
| Rut | -- | -- | -- | -- | -- |
| Ap | 1.60 | 1.80 | 2.11 | 2.03 | 2.09 |
| Total | 100.00 | 91.50 | 100.00 | 100.00 | 100.00 |
| Color index | 28.61 | 62.80 | 41.26 | 48.22 | 41.81 |
| An/(Ab + An) | 41.89 | 63.83 | 46.65 | 40.15 | 38.09 |
| Or/(Or + Ab + An) | 58.68 | 20.29 | 39.46 | 14.74 | 17.77 |
| SiO ₂ (H ₂ O- | 56.83 | 42.58 | 50.64 | 47.98 | 50.94 |
| CaCO ₃ -free) | | | | | |

been the site of an old valley, which the flow followed to the northeast. The source of the flow is presumed to be west of Eight O'clock Hill.

PETROGRAPHY

The flow is massive and black with white calcite amygdules up to 1 cm across and abundant red-brown pseudomorphs after olivine phenocrysts up to 5 mm across. It contains brown glass, plagioclase, sanidine(?), pseudomorphs after olivine, augite, biotite, apatite, opaque minerals, analcime, and calcite (table 2). The rock is a limburgite (Williams and others, 1954, p. 74). In thin section, olivine is seen to be completely altered, and its pseudomorphs range in size from 50 μm to 5 mm. The pseudomorphs are rimmed by very fine grained red and yellow-brown minerals, which may be iddingsite and vermiculite, respectively. The interiors of the grains are serpentine. Augite occurs as microphenocrysts ranging in size from 50 μm up to 0.5 mm. These microphenocrysts generally have distinctive hourglass zonation and commonly occur in stellate to cruciform clusters. The groundmass consists of brown glass, arborescent opaque microlites, or scapolites, plagioclase laths, anhedral, weakly birefringent feldspar, tiny biotite flakes, and apatite needles. The scapolites are generally arranged in fanlike clusters and pla-

gioclase laths are intergrown with them. Rarely, plagioclase forms larger laths arranged in a regular crisscross pattern, or house of cards. In some samples plagioclase occurs predominantly as lathlike microphenocrysts, and the arborescent form of the scapolites is suppressed. Much of the anhedral feldspar, which appears as patches of low birefringence in the glass and in interstices between scapolites, probably is sanidine. Biotite flakes commonly are arranged in a house of cards pattern in the glass. A trace of analcime is associated with the calcite amygdules. The 6 percent of unknown minerals reported in the modal analysis (table 2) refers to apparent hematite alteration of the scapolites and of biotite.

The sandstone and granule conglomerate is orange, maroon, and olive buff. It consists dominantly of red-brown microvesicular ash that contains pseudomorphs after olivine phenocrysts and microphenocrysts and also microphenocrysts of augite, commonly in stellate to cruciform clusters. The ash most commonly has an occluded, glassy matrix, but holocrystalline ash is also present.

CHEMICAL COMPOSITION

In two chemically analyzed samples of the Eight O'clock Gorge flow (table 3), silica, recalculated on a water-free and calcium-carbonate-free basis, is about 51 percent, or within the range of basic composition (45-52 percent). Potassium oxide content, about 3 percent in these samples, is relatively high for the silica content and is reflected in high normative potassium feldspar (about 18 percent) and in the presence of sanidine(?) in the groundmass of the rocks.

FLOW OF MEADOW DAM

DISTRIBUTION, STRATIGRAPHY, AND PHYSICAL FEATURES

The flow of Meadow Dam underlies a low hill on the west side of Meadow Dam and a large hill south of the dam, where it forms high cliffs on the west side of Fort Rock Creek. It also crops out for about 300 m along the base of low cliffs on the east side of the creek below the dam. Additionally, this unit is exposed on the rim of the crater, where it is tilted to the southwest, from near the crest of Buffalo Ridge to near the top of Eight O'clock Hill.

The unit consists chiefly of two flows, or two parts of one flow, which can be distinguished in outcrops along Fort Rock Creek. A lower flow is separated from an upper flow by a thin agglomeratic(?) volca-

TABLE 3.—*Chemical and normative composition of the Crater Pasture Formation—Continued*

| 1/ Sample locations | |
|---------------------|---|
| 189, 190, 195a | Northwest side of Four O'clock Hill |
| Ao | Northwest bank of wash in Eight O'clock Gorge |
| 294 | Top of Nine O'clock Hill |
| 227 | Southeast end of Meadow Dam flow on Buffalo Ridge |
| 439 | East bank of Fort Rock Creek south of Eight O'clock Wash |
| 440 | High cliffs on west side of Fort Rock Creek south of Eight O'clock Wash |
| 148 | Near base of Two O'clock Gap flow northwest of Two O'clock Gap |
| 178b | Base of Two O'clock Gap flow northwest of Two O'clock Gap |
| 154c | Northeast bank of Four O'clock Wash |
| 167 | Northeast end of Hidden Pasture |
| 326a | Dike on north side of Six O'clock Hill northeast of Road End Gap |
| 328 | Gully at head of Five O'clock Wash |
| 235 | Base of Buffalo Ridge flow east of high point on Buffalo Ridge |
| 232 | Boot-shaped intrusive body on Buffalo Ridge |
| 291a | Reddened base of Buffalo Ridge flow on Noon Hill |
| 291c | Massive upper part of Buffalo Ridge flow on Noon Hill |
| 429 | Dike southeast of Crater Divide |
| 154f | Base of flow on northeast bank of Four O'clock Wash |
| 171 | Base of flow on east wall of Noon Gorge west of One O'clock Hill fault |
| NE | Intrusive body in Eight O'clock Basin |
| 166a, 165 | North end of Hidden Pasture |
| 286, 289a1 | East side of Noon Hill |
| 250 | Head of Cinder Basin Wash |
| 240 | Head of Tyra Wash |
| 409 | West side of Cinder Basin |
| 414 | East bank of wash in Fault Canyon |
| 410 | Cinder Basin near head of Fault Canyon |
| 416a | East wall of Fault Canyon |
| 406a | North bank of Six O'clock Wash east of Cinder Basin |
| 246 | Head of Tyra Wash |
| 280a | North bank of Eight O'clock Wash |
| 331 | Outcrop at northernmost end of mapped area (pl 1) |
| 459b, 459c | West side of large wash southeast of Number One Well |
| 334 | Cliff 120 m northwest of Indian ruins in northwest corner of map (pl 1) |

2/ Contains 8.5 weight percent normative nepheline, making the normative mineral total 100.00 weight percent.

nic breccia. Where there is no breccia separating the upper from the lower flow, the unit is mapped as undivided flow. On the rim of the crater, rocks of this unit are mapped as undivided flow, although they have been correlated with the lower flow (see pl. 2). On the rim, flow rocks overlie a thin basal volcanic breccia and minor sandstone. The rim of the crater provides the only exposure of the base of the Meadow Dam unit.

The maximum thickness of the flow of Meadow Dam on the rim of the crater is 40 m. On the large hill south of the dam, the maximum thickness of the upper flow is 40 m, and the lower flow may be as much as 75 m thick (see pl. 2).

The flow of Meadow Dam is relatively resistant to erosion and tends to form blocky outcrops. The upper flow is the most resistant part of this unit and is responsible for the high cliffs on the west side of Fort Rock Creek.

RELATION TO OTHER UNITS

On the rim of the crater, the Meadow Dam flow overlies the Eight O'Clock Gorge flow and is overlain by pockets of a pyroxene-trachyandesite sandstone of the Crater Pasture Formation and by the Buffalo Ridge flow. Along Fort Rock Creek, it is overlain by pockets of conglomerate of the Cinder Basin unit and by the Fault Canyon flow. On the southwest, west, and northwest sides of the large hill south of Meadow Dam, it is overlain by and in one place faulted against the Old Stage Road Member of the Fort Rock Creek Rhyodacite.

SOURCE

The large hill south of Meadow Dam apparently represents the thickest accumulation of the Meadow Dam flow; the vent for the flow probably underlies the hill. Outcrops of this flow in the rim of the crater may represent a lobe which, like the Eight O'Clock Gorge flow, flowed northeast up an old valley in Precambrian rocks.

PETROGRAPHY

Outcrops along Fort Rock Creek are massive, whereas outcrops in the rim of the crater have flow cleavage. All rock in this unit is medium gray on fresh surfaces and brownish gray on weathered surfaces. None of the flow is vesicular, although the upper flow has calcite-filled vugs. Phenocrysts of hornblende are abundant. They are altered red-brown or dark gray and are in some hand samples difficult

to distinguish from the groundmass. Phenocrysts of green diopsidic(?) augite are also present but sparse.

The rock is made up of plagioclase, sanidine, clinopyroxene, altered olivine, altered hornblende, biotite, opaque minerals, and accessory minerals (table 2). On the basis of its high color index (46), the absence of quartz, and the presence of more than 10 percent sanidine, the rock is classified as a trachybasalt (Williams and others, 1954, p. 57), or, in particular, a hornblende trachybasalt. In the sample examined, most hornblende grains are totally altered to a mixture of granular opaque minerals, pyroxene, and brown biotite. The outlines of the original grains are preserved, but their centers are ragged. Two generations of altered hornblende grains are present. One-third occurs as larger stubby prisms up to 1 cm in width; two-thirds occurs as smaller prisms and needles less than 1 mm long. Clinopyroxene, including both augite and pigeonite, occurs rarely as phenocrysts but abundantly and in approximately equal amounts as microphenocrysts, which range in size from 20 μ m to 0.5 mm, and as groundmass grains. Pseudomorphs after olivine microphenocrysts, up to 0.2 mm across, are red-brown biotite. Plagioclase occurs as subhedral, poorly twinned laths, arranged in sheaflike masses that sweep around phenocrysts. Sanidine(?) occupies interstices, but the identity of this mineral has not been confirmed by probe analysis. Secondary minerals include a pinkish-brown cryptocrystalline mineral of high negative relief. This unit is petrographically homogeneous, although the upper flow is somewhat finer grained than the lower flow.

CHEMICAL COMPOSITION

In three chemically analyzed samples (table 3), silica, recalculated on a water- and calcium-carbonate-free basis, averages 54 percent, which falls at the low end of the intermediate range of composition (52-66 percent). Potassium oxide and normative potassium feldspar average 2¹/₂ and 17 percent, respectively.

TUFF AND FLOW OF TWO O'CLOCK GAP

DISTRIBUTION, STRATIGRAPHY, AND PHYSICAL FEATURES

The tuff and flow of Two O'Clock Gap consists chiefly of basal tuff and, locally, tuff-breccia overlain by flow. The tuff reaches a maximum thickness of perhaps 15 m on Outer Hill, where it is most extensively exposed. It is exposed on the rim of the crater as a thin bed that extends from One O'Clock

Wash to Four O'Clock Wash. The flow is confined to the southeast end of Lion Ridge, where it probably reaches a thickness of about 40 m. The flow has a vuggy zone on its northeast flank that may be flow-top zone.

The tuff is poorly resistant to erosion; in many locations, its presence is revealed only by digging or by observing rocks clinging to the roots of uprooted trees. The flow is relatively resistant and, in a few locations, forms blocky outcrops.

RELATION TO OTHER UNITS

The tuff and flow of Two O'Clock Gap overlies Precambrian rocks everywhere where it is mapped (pl. 1), but in the vicinity of Four O'Clock Wash, it occurs in pockets too small to map on top of the Road End Gap unit. It is overlain by Lion Ridge flow in most places and by Annex Ridge flow on the south flank of Three O'Clock Hill. The unmapped pockets of the tuff in the vicinity of Four O'Clock Wash are overlain in places by a pyroxene-trachyandesite sandstone and conglomerate of the Crater Pasture Formation.

SOURCE

A vent for the tuff is probably located in the vicinity of Outer Hill, where the tuff is thickest. The flow must overlie its own vent on the southeast end of Lion Ridge, as the flow is entirely restricted to this area.

PETROGRAPHY

The basal tuff is characterized by lapilli that weather olive green and contain rare green pyroxene phenocrysts up to several millimeters across. Other clasts are olive-buff, olive-gray, and charcoal gray. Most clasts are microvesicular. The tuff also contains some clasts of Precambrian rocks; some of them appear deformed in the tuff and hence may be xenoliths that were stripped of enclosing magma. The flow is nonvesicular. Flow cleavage is developed poorly at its base. It varies in color from light bluish gray to light maroon on fresh surfaces and has a varnished exterior. Rocks in the vuggy zone are charcoal gray on fresh surfaces.

The flow is made up of plagioclase, sanidine, altered olivine, clinopyroxene, orthopyroxene, hornblende, opaque minerals, and apatite (table 2). The rock is a pyroxene trachyandesite, with a color index of about 38 and over 14 percent interstitial

sanidine (identified with the electron microprobe). Plagioclase ranges in composition from sodic labradorite to sodic andesine, as indicated by the microprobe. In the modal analysis, about three-fourths of the pyroxene phenocrysts counted, about 1 percent of the rock, is orthopyroxene, including enstatite and hypersthene (determined by microprobe analysis), and the other fourth is augite. Less than one-sixth of the pyroxene microphenocrysts, (0.1-0.5 mm) however, is orthopyroxene. Groundmass pyroxene grains (smaller than 0.1 mm) are apparently all augite. Rims of augite and altered olivine occur around some orthopyroxene grains. Altered olivine and hornblende occur in the rock as microphenocrysts. The altered olivine is a red-brown mineral, and the pseudomorphs in places attain sizes as large as 0.15 mm across. The hornblende occurs as needles and is altered on the rims to granular opaque minerals and pyroxene. Fresh hornblende occurs only in the cores of the larger needles, some of which reach 1 mm in length. The texture of the rock is pilotaxitic.

In contrast to the flow rock, clasts of the tuff that were examined in thin section have fresh hornblende and a glassy matrix that ranges in color from yellow-brown to occluded reddish brown.

CHEMICAL COMPOSITION

In two samples (table 3), recalculated silica averages 55¹/₂ percent, well within the range of intermediate composition. Potassium oxide content, averaging about 2¹/₂ percent, and normative potassium feldspar content, averaging about 16 percent, are similar to contents in Meadow Dam hornblende trachybasalt and in Road End Gap olivine trachyandesite.

PYROXENE-TRACHYANDESITE SANDSTONE AND CONGLOMERATE

DISTRIBUTION AND PHYSICAL FEATURES

A minor unit of light-maroon to red-orange pyroxene-trachyandesite sandstone and granule conglomerate is found in a few places around the rim of the crater. In the north wall of Four O'Clock Wash, a 12-m-thick section of this unit is exposed. In many places on Four O'Clock Hill along the contact between the Road End Gap volcanic breccia and flow and the Annex Ridge flow, a few centimeters of this sandstone and conglomerate can be exposed by digging. Discontinuous outcrops occur on Six O'Clock Hill and Buffalo Ridge. The unit is exposed continu-

ously from Eight O'Clock Gorge to the top of Nine O'Clock Hill, becoming at least 8 m and possibly 27 m thick on Eight O'Clock Hill. Except for local ledges, it is poorly resistant to erosion.

RELATION TO OTHER UNITS

The sandstone and conglomerate overlies the volcanic breccia and flow of Road End Gap on the southeast and south rim of the crater. Near Four O'Clock Wash, it also overlies local pockets of the Two O'Clock Gap unit. On the southwest and west rim, it overlies the Meadow Dam and Eight O'Clock Gorge flows. It is overlain by the Annex Ridge flow in the southeast and south and by the Buffalo Ridge flow in the southwest and west.

PETROGRAPHY

The sandstone and conglomerate are well bedded and moderately well sorted. These rocks consist dominantly of microvesicular gray, red, and red-orange ash that contains abundant pseudomorphs after olivine microphenocrysts scattered phenocrysts of augite, and rare phenocrysts of orthopyroxene. A few clasts contain abundant microphenocrysts of hornblende. The matrix of the ash is dominantly red-brown, dark, occluded glass with abundant tiny laths of plagioclase. Ash from this unit differs from ash in lower tuffaceous sandstone units in containing no pseudomorphs after olivine phenocrysts and in containing pyroxene almost exclusively as phenocrysts.

In outcrops on Six O'Clock Hill and Buffalo Ridge, this unit is a breccia; it contains coarse clasts, including blocks, of Road End Gap olivine trachyandesite.

FLOW OF ANNEX RIDGE

DISTRIBUTION, STRATIGRAPHY, AND PHYSICAL FEATURES

The flow of Annex Ridge underlies the southeast quadrant of the crater rim. It is about 120 m thick on Six O'Clock Hill and pinches out abruptly on Three O'Clock Hill and at Six Thirty Wash. It is a steep-sided dome, viewed nearly in cross section on the geologic map (pl. 1) owing to its high dip. The flow also underlies Annex Ridge and crops out in many places around the base of the Buttox Hills and the hills farther east, beyond the area mapped.

This flow has been subdivided into a basal facies, a lower flow, a flow-top zone, and an upper flow. The lower flow underlies the rim of the crater. The upper flow crops out southeast of the crater rim.

A dike-like intrusive body on the north flank of Six O'Clock Hill and a similar intrusive body largely altered to clay minerals in the gully at the head of Five O'Clock Wash are petrographically similar to the Annex Ridge flow and are correlated with it.

The lower flow is slabby and is somewhat less resistant to erosion than the adjacent Lion Ridge and Buffalo Ridge flows; consequently, Four O'Clock Hill and Six O'Clock Hill are low areas on the rim of the crater. The upper flow is massive and more resistant to erosion than the lower flow.

RELATION TO OTHER UNITS

The Annex Ridge flow overlies the Road End Gap volcanic breccia and flow in most places. Locally, it overlies a pyroxene-trachyandesite sandstone and conglomerate of the Crater Pasture Formation and pockets of tuff of the Two O'Clock Gap unit. At the north tip of its outcrop area it overlies Precambrian rocks in a few places. On the rim of the crater, it is overlain by Lion Ridge flow on the north and Buffalo Ridge flow on the west. On the flanks of the dome and beyond, it is overlain in different places by tuff and conglomerate of Hidden Pasture, sedimentary breccia of One O'Clock Wash, tuff and agglomerate of Cinder Basin, and the Fault Canyon flow of the Crater Pasture Formation, and by sedimentary breccia of Noon Gorge, the Old Stage Road Member, and an unnamed rhyodacite-bearing sandstone, conglomerate, and breccia of the Fort Rock Creek Rhyodacite. It is intruded by a dike related to the basalt of Buttox Hills and by a dike of trachybasalt related to the Fault Canyon flow.

SOURCE

The upper flow probably overlies a major vent for the Annex Ridge flow in the region southeast of the crater rim. The Annex Ridge flow appears to have been extruded as a viscous dome in two stages, which are represented by the upper and lower flows. The small intrusive bodies on the north flank of Six O'Clock Hill and in Five O'Clock Wash may occupy small vents for this unit.

PETROGRAPHY

The basal facies is characteristically a soft, buff to light-pinkish-brown clastic to microscopically vuggy rock. It contains phenocrysts and microphenocrysts of black hornblende, as does all rock of the Annex Ridge flow. In Six Thirty Wash, the basal

unit also includes volcanic and tuffaceous sedimentary rocks. The lower flow is light bluish gray to very light gray on both weathered and fresh surfaces. It is nonvesicular and has flow cleavage, which is best developed toward the base of the flow. The flow-top zone is characterized by microscopic vugs, some microscopic brecciation, a light-pinkish-brown color on fresh surfaces, and a brownish weathering rind with a rough, warty appearance. The warty appearance comes largely from the selective preservation of hornblende phenocrysts, which have, in many localities, resistant brownish-red to scarlet rims. Crude vertical partings in the flow-top zone distinguish it, albeit faintly, from the overlying flow, which is very similar in all respects but is massive.

A sample of the lower flow contains plagioclase, sanidine, hornblende, opaque minerals, apatite, and almost no pyroxene (table 2). The rock is a hornblende trachyandesite, with a color index of about 21 and interstitial sanidine (identified by electron microprobe). All sharp laths of plagioclase over 5 μm wide are sodic labradorite (identified by probe), but smaller grains of plagioclase may well be andesine or oligoclase. Hornblende occurs as phenocrysts up to nearly 1 cm in length. All hornblende is altered on the rim to very fine granular opaque minerals; in the larger grains the cores are augite, plagioclase, opaque minerals, and vermiculite(?), giving the hornblende phenocrysts the appearance of rotted wood. Zoning, with up to three zones, is observed in a number of hornblende grains. Radial (spokelike) strings of very fine granular opaque minerals are also seen in these grains. Needlelike hornblende microphenocrysts less than 0.5 mm long are present and are distinct from the phenocrysts in size and shape. They are almost totally altered to opaque minerals. About one-third of the hornblende occurs as microphenocrysts; two-thirds occurs as phenocrysts. About one-fourth of the apatite in this rock occurs as stubby prisms up to 0.25 mm in length with a purple to violet tinge and characteristic striations parallel to their long axes. Three-fourths of the apatite occurs as needles in the groundmass. The texture of the rock is pilotaxitic.

The dikelike intrusive body on Six O'Clock Hill consists of blue-gray rock with abundant prisms of black hornblende. In thin section, the rock is identical to the modally analyzed sample of the Annex Ridge flow, except that the hornblende is olive green and unaltered. The altered intrusive body in Five O'Clock Wash is similar to this dikelike body, except that the feldspar in the groundmass is totally altered to clay minerals. Outlines of plagioclase laths

are still plainly visible. The hornblende in this rock is unaltered.

CHEMICAL COMPOSITION

In two samples of the Annex Ridge flow (samples 154c, 167, table 3), recalculated silica averages about 57 percent, well within the intermediate range of composition. Potassium oxide is about 3 percent, and normative potassium feldspar is between 18 and 19 percent. In silica content and normative potassium feldspar content, rock of this unit is most similar to the olivine trachyandesite of the Road End Gap unit. The color index, however, which averages about 18, is about half that of Road End Gap rocks.

Rock from the dikelike body on Six O'Clock Hill is chemically similar to rock of the Annex Ridge flow (sample 326a, table 3). Rock from the altered intrusive body in Five O'Clock Wash (sample 328, table 3), however, is relatively low in calcium and sodium oxides, reflecting alteration of its feldspar to clay (montmorillonite?). Depletion of these oxides is the reason for lower normative albite, anorthite, and diopside and higher normative quartz in this rock.

FLOW OF BUFFALO RIDGE

DISTRIBUTION AND PHYSICAL FEATURES

The flow of Buffalo Ridge crops out continuously on the rim of the crater from the head of Six Thirty Wash to Wedge Basin. In Six Thirty Wash, it pinches out abruptly against the steep side of the Annex Ridge flow. Northwest of Buffalo Ridge, the flow thins somewhat more gradually. In addition, a petrographically similar body of rock rests, somewhat jumbled, on top of deposits of the Hidden Pasture tuff and conglomerate on Noon Hill and is correlated with the flow of Buffalo Ridge.

The Buffalo Ridge flow is divided into five sub-units, a basal facies, an intrusive breccia that is an intrusive equivalent of the basal facies, a flow, a flow-top zone, and a massive intrusive body that is an intrusive equivalent of the flow. The intrusive rocks of this unit are exposed on Buffalo Ridge. The extrusive rocks reach a maximum thickness of about 100 m atop Buffalo Ridge.

A dike in the vicinity of Crater Divide and a small intrusive body at the south end of Eight O'Clock Basin are petrographically similar to rock of the Buffalo Ridge unit and are correlated with it.

The flow, flow-top, and massive intrusive body are resistant to erosion and tend to form blocky,

commonly varnished outcrops. These rocks are responsible for the presence of Buffalo Ridge and the series of flatironshaped hills that form the rim of the crater north of Buffalo Ridge.

RELATION TO OTHER UNITS

From south to north, the Buffalo Ridge flow overlies the Annex Ridge flow, the Road End Gap volcanic breccia and flow, which its vents also cut, the Meadow Dam flow, a pyroxene-trachyandesite sandstone and conglomerate of the Crater Pasture Formation, the Eight O'Clock Gorge flow, and Precambrian rocks. It is overlain in different places on the flank of the dome by the One O'Clock Wash sedimentary breccia and the Cinder Basin tuff and agglomerate of the Crater Pasture Formation and by the Noon Gorge sedimentary breccia and the Old Stage Road Member of the Fort Rock Creek Rhyodacite. It is intruded by a dike of trachybasalt related to the Fault Canyon flow.

Blocks of the Buffalo Ridge flow are embedded in a conglomeratic bed at the top of the exposed section of the Hidden Pasture tuff and conglomerate on Noon Hill. It thus appears that the Hidden Pasture unit is at least partly younger than the Buffalo Ridge flow. The blocks embedded in this unit probably were deposited prior to a landslide that brought the large jumbled body of Buffalo Ridge flow to rest on top of the Hidden Pasture deposits in this location.

A tiny fragment of hornblende trachyandesite similar to that of the Buffalo Ridge flow was identified in the basal clastic unit of the Lion Ridge flow, suggesting that the Lion Ridge flow is younger than the Buffalo Ridge flow.

SOURCE

The intrusive breccia and the massive intrusive body occupy vents for the Buffalo Ridge unit on Buffalo Ridge. These intrusions can be traced continuously into extrusive rocks. They represent the only explicit sources for any of the Crater Pasture extrusive rocks on the dome with the exception of the source for the Fault Canyon flow, to be discussed below. The intrusive breccia penetrates the Road End Gap volcanic breccia and flow and, in many places, follows the bedding in this unit. This breccia can be traced laterally into tuff of the basal facies. The massive intrusive body occupies a boot-shaped vent on the inner flank of Buffalo Ridge and a vent of indefinite shape on the crest of the ridge where massive

hornblende trachyandesite can be traced continuously into lava flow. A patch of flow breccia on the southwestern side of Buffalo Ridge near the head of Tyria Wash is associated with changes in flow-banding attitudes in its vicinity; this breccia may occupy still another vent. The small dike in the vicinity of Crater Divide and the small intrusive body at the south end of Eight O'Clock Basin may have been minor sources for the Buffalo Ridge unit. Small concealed vents may also lie west of the rim of the crater.

PETROGRAPHY

The basal facies includes tuff, minor tuffaceous sandstone, and local flow-base breccia. The tuff is characterized by moderately sorted microvesicular coarse ash and lapilli that weather yellow to buff and contain abundant black hornblende prisms. The tuff contains rare accidental clasts of Precambrian rocks and Road End Gap olivine trachyandesite. The intrusive equivalent of the basal facies is a breccia consisting of lapilli-sized clasts of Buffalo Ridge rock, which also weather yellow to buff, mixed with abundant maroon fragments of Road End Gap olivine trachyandesite. The latter fragments were apparently reddened during intrusion of the breccia. They range in amount from less than 10 to almost 100 percent of the breccia. The breccia is distinguishable from the basal facies in its lack of sorting and in its high content of these xenoliths. The flow ranges from a blue-gray rock with flow cleavage at its base to a massive medium-gray rock with a varnished exterior in its middle and upper parts. The middle and upper parts of the flow are microvesicular and have largely altered hornblende phenocrysts. The flow-top zone is a brownish microvuggy rock. The intrusive equivalent of the flow is a massive medium- to dark-gray rock that weathers gray-buff.

The sample of flow presented in table 2 is from atop Buffalo Ridge. It is petrographically similar to the sample of the Annex Ridge flow listed in the table but has a slightly higher color index; groundmass clinopyroxene (3¹/₂ percent) and opaque minerals (6 percent) are more abundant than in the Annex Ridge sample. The hornblende content resembles that of the Annex Ridge sample in every way except that a slightly greater proportion of the mineral (three-fourths) occurs as phenocrysts rather than microphenocrysts. Apatite microphenocrysts (trace) and groundmass apatite grains (trace?) are less abundant in the Buffalo Ridge sample.

In Eight O'Clock Gorge, flow rock is somewhat more mafic than the sample described above. It con-

tains a few small clinopyroxene phenocrysts and also abundant (5 to 10 percent) groundmass pyroxene. Microphenocrysts of hornblende and apatite are much fewer than those in the sample from atop Buffalo Ridge. This rock is petrographically transitional to rock of the Lion Ridge flow (discussed below).

Rock from the north end of the Buffalo Ridge flow in Wedge Basin is similar to the modally analyzed rock from atop Buffalo Ridge. It contains no phenocrysts of clinopyroxene; however, it does contain abundant (5 to 10 percent) groundmass pyroxene.

The outcrop of flow on Noon Hill preserves the gross stratigraphy of the Buffalo Ridge flow, with an identifiable basal facies in at least two places. Attitudes of flow banding within the outcrop area, however, are not consistent, indicating that this body of flow is broken and structurally disarrayed. Most of the rock in this outcrop resembles the rock atop Buffalo Ridge with its abundant hornblende microphenocrysts, its trace of purplish apatite microphenocrysts, and its low pyroxene content. Other rock in this outcrop resembles the more mafic rock of the Buffalo Ridge flow seen in Eight O'Clock Gorge or rock of the Lion Ridge flow.

The dike near Crater Divide consists of blue-gray rock with abundant black hornblende prisms. In thin section, the hornblende is olive green and unaltered. The rock resembles the modally analyzed rock from atop Buffalo Ridge, except that it does not contain hornblende microphenocrysts. The intrusive body at the south end of Eight O'Clock Basin is a breccia containing abundant contact-metamorphosed clasts of Precambrian rocks and multicolored clasts of altered hornblende trachyandesite. The latter clasts contain abundant pseudomorphs after hornblende phenocrysts consisting of a light-yellow-green clay mineral. The groundmass, like the groundmass of the altered intrusive body in the gully at the head of Five O'Clock Wash, has been completely altered to clay minerals, but outlines of original plagioclase laths are still plainly visible.

CHEMICAL COMPOSITION

Three samples of the Buffalo Ridge flow (samples 235, 232, and 291a, table 3) are closely similar in chemistry and also resemble the hornblende trachyandesite of the Annex Ridge flow. These samples have slightly less silica, averaging 56¹/₂ percent, and slightly higher color indices, averaging 22¹/₂, than the Annex Ridge flow. One of these samples (291a) is from the jumbled body of Buffalo Ridge flow on Noon Hill. Another sample from this jumbled body

(sample 291c, table 3) is similar to the hornblende trachyandesite of the Lion Ridge flow (see below).

The dike rock (sample 429) is similar to rock from Buffalo Ridge, although its lower modal hornblende content is reflected in a lower normative color index.

FLOW OF LION RIDGE

DISTRIBUTION, STRATIGRAPHY, AND PHYSICAL FEATURES

The flow of Lion Ridge crops out in several large areas on the rim of the crater between Noon Gorge and Four O'Clock Hill. On One O'Clock Hill and Lion Ridge, the outcrop is of fairly uniform width, thinning out in Noon Gorge and pinching out against the Two O'Clock Gap tuff and flow on the southeast end of Lion Ridge. On a small knob extending southwest from Lion Ridge near its southeast end, this flow forms two northwest-southeast-trending strips of outcrop that terminate on the northwest side of the knob and converge in Two O'Clock Gap. Two faults, the Upper and Lower Two O'Clock Gap faults, are responsible for the repetition of the flow in this area; blocks are faulted successively downward toward the southwest, or toward the interior of the crater. A similar repetition of the flow, caused by these two faults, is seen on Outer Hill. The Lion Ridge flow is also present on Three O'Clock Hill, where it is apparently continuous, beneath the colluvium in Two O'Clock Gap, with flow in the lower fault block both on Outer Hill and on the small knob southwest of Lion Ridge. The flow pinches out against the Annex Ridge Flow on the east side of Four O'Clock Hill.

A basal facies, a reddened flow-base zone and a flow-top zone have been recognized in this unit. The unit is about 45 m thick at the head of One O'Clock Wash; its maximum thickness is probably attained on Three O'Clock Hill where it may be as much as 60 m thick.

An intrusive body in Eight O'Clock Basin is petrographically similar to the Lion Ridge flow and is correlated with it.

The Lion Ridge flow is resistant to weathering and tends to form blocky, varnished outcrops. It forms One O'Clock Hill, Lion Ridge, Outer Hill, and Three O'Clock Hill.

RELATION TO OTHER UNITS

From south to north, the Lion Ridge flow overlies the Annex Ridge flow, the tuff and flow of Two O'Clock Gap, and Precambrian rocks. It is overlain

in Four O'Clock Wash by the Old Stage Road Member of the Fort Rock Creek Rhyodacite and on Lion Ridge by the One O'Clock Wash sedimentary breccia.

The field relation of the Lion Ridge flow to the Hidden Pasture tuff and conglomerate is problematical. In the east wall of Noon Gorge, a jumbled body of Lion Ridge flow rests on Hidden Pasture deposits in a fashion similar to that of the body of Buffalo Ridge flow across the gorge; however, no blocks of Lion Ridge flow were actually found embedded in the Hidden Pasture deposits as was the case across the gorge. In Hidden Pasture, Hidden Pasture deposits conspicuously overlie Annex Ridge flow on the southeast side of Four O'Clock Hill and appear to overlie the tip of the Lion Ridge flow, although excavating in this location would be necessary to determine whether this deposit overlies or underlies the flow. On Outer Hill the Lion Ridge flow overlies a distinctive blue-gray hornblende trachyandesite tuff. Although this tuff resembles a distinctive tuff of the Hidden Pasture unit, it has been mapped as part of the basal facies of the Lion Ridge flow. At the southeastern tip of Outer Hill, some blocks of Lion Ridge flow, along with distinctive basal blue-gray tuff, overlie deposits like the Hidden Pasture unit, but these blocks have been interpreted tentatively as a landslide. In summary, the Lion Ridge flow may be older than the Hidden Pasture tuff and conglomerate. Like the Buffalo Ridge flow, it may have been thrust over these deposits in some places by landsliding.

SOURCE

A major vent for the Lion Ridge flow may be located beneath Three O'Clock Hill, where the flow is apparently thickest. A second vent beneath Lion Ridge may have been the source for the northern segment of the flow, which is geographically higher than and somewhat removed from the postulated Three O'Clock Hill vent. A relatively thicker sequence of basal tuff-breccia on Outer Hill may indicate the presence of a small vent in that area. The small plug in Eight O'Clock Basin may have also been a source for this unit.

PETROGRAPHY

Rocks of the Lion Ridge flow are similar to those of the Buffalo Ridge flow. The basal facies includes tuff, minor tuff-breccia, and minor flow-base breccia. The tuff is yellow-buff to pink and is moderately

sorted. On Outer Hill, the basal tuff is blue-gray and moderately well sorted. The reddened flow-base zone resembles the overlying part of the flow but has a distinctive reddish to lavender color, which makes it a useful mapping unit. The main part of the flow is dark blue-gray at its base and has well-developed flow cleavage. In its middle and upper parts, it is medium to dark gray and massive with varnished surfaces. The base of the flow is nonvesicular, whereas the middle and upper parts are sparsely vesicular. Generally, the vesicles are flattened. The flow-top zone is dark steel-gray on a fresh surface, has microscopic vugs, and shows some microscopic brecciation. Largely altered hornblende prisms are present throughout this flow; they are less altered toward the base and toward the top of the flow.

This flow is hornblende trachyandesite, similar to the Annex Ridge and Buffalo Ridge hornblende trachyandesites, but it contains considerably more pyroxene and more opaque minerals (table 2). The hornblende has a thick alteration rind consisting of fine-grained opaque minerals and pyroxene. The cores of the hornblende grains generally are opaque minerals, pyroxene, feldspar, and biotite. These cores give the phenocrysts the appearance of rotted wood. Unlike that in the Buffalo Ridge and Annex Ridge flows, the hornblende of the Lion Ridge flow occurs almost exclusively as phenocrysts, up to $1/2$ cm across; microphenocrysts are rare. Augite occurs as small phenocrysts, generally less than 1 mm in size, commonly in clusters, and as groundmass grains. Phenocrysts of augite make up about $1\frac{1}{2}$ percent of the rock; groundmass grains make up about 15 percent. Groundmass feldspar includes interstitial sanidine and plagioclase ranging in composition from sodic labradorite to oligoclase (both identified by probe). Apatite in this rock occurs as needles in the groundmass and only very rarely as purplish microphenocrysts of the type found in the Buffalo Ridge and Annex Ridge hornblende trachyandesites. The texture of the rock is pilotaxitic.

Rock from the intrusive body in Eight O'Clock Basin is somewhat similar to the Lion Ridge flow but contains half again to twice as much hornblende (15-20 percent). The hornblende in this rock is, furthermore, olive green and fresh except for some "worm-hole" cores.

CHEMICAL COMPOSITION

Two modally analyzed samples of the Lion Ridge flow (samples 154f, 171, table 3) show recalculated silica to be about $55\frac{1}{2}$ percent, which is lower than

the average value for the Buffalo Ridge hornblende trachyandesite (56¹/₂ percent) or the Annex Ridge hornblende trachyandesite (57 percent). The lower silica content in this flow is reflected in a higher normative color index, which averages 25¹/₂. Potassium oxide averages about 3 percent, and normative potassium feldspar averages 17 percent; both are slightly lower than in the Buffalo Ridge and Annex Ridge flows.

The intrusive body (sample NE, table 3) is somewhat more basic than any of the samples of the Lion Ridge flow; it has a recalculated silica content of 54 percent.

TUFF AND CONGLOMERATE OF HIDDEN PASTURE

DISTRIBUTION, STRATIGRAPHY, AND PHYSICAL FEATURES

The tuff and conglomerate of Hidden Pasture crops out in several relatively small areas. In Hidden Pasture, up to 23 m of this tuff and conglomerate overlies the Annex Ridge flow. Another outcrop area is the vicinity of Noon Gorge, where as much as 27 m of this unit occupies an ancient valley or hollow in the Precambrian rocks. The deposits in the Noon Gorge area were tilted and faulted during doming, and their upper beds incorporate landslide material that was emplaced during doming. Two small outcrops of the unit are also found on the east flank of Short Hill.

This unit is poorly resistant and is generally covered by colluvium. Where it does crop out, however, it is fairly distinctive. It consists of tuff, tuffaceous sandstone, and fine-pebble conglomerate. Yellow and olive-brown tuffs occur at several horizons. The tuffaceous sandstone and conglomerate are light-gray to light-brown overall and contain multicolored clasts. Two distinctive beds in the unit have been mapped, a blue-gray hornblende-trachyandesite tuff in Hidden Pasture and in the Noon Gorge area, and a fine-pebble conglomerate.

RELATION TO OTHER UNITS

In Hidden Pasture, the tuff and conglomerate overlies the Annex Ridge flow and possibly the Lion Ridge flow and is overlain by ash-flow tuff of the Fort Rock Creek Rhyodacite. In the Noon Gorge area, Hidden Pasture deposits overlie Precambrian rocks. In the east wall of Noon Gorge, these deposits are conformably overlain by the sedimentary breccia of One O'Clock Wash. In most places in the Noon Gorge area, however, their upper contact is a fault contact

with either Precambrian rocks or landslide bodies of the Buffalo Ridge and Lion Ridge flows.

SOURCE

A unit of undivided Hidden Pasture and Cinder Basin deposits has been mapped in a number of scattered locations from the northeast flank of Annex Ridge to the southeast corner of Outer Hill. Similar deposits are also found farther east, beyond the area mapped, and appear to be associated with a large trachybasalt eruptive center located about 1 km east of the dome (see fig. 3). At least some of the Hidden Pasture tuff probably originated from that center. Some also could be derived from the Cinder Basin eruptive center south of the dome (discussed below).

PETROGRAPHY

Beds in this unit range in thickness of millimeters to several tenths of a meter. Sorting ranges from moderate to good; the tuffs are the best sorted. Two chief petrographic types of ash are present in the tuffs, hornblende trachyandesite and olivine trachyandesite. The first type constitutes the hornblende-trachyandesite tuff that is mapped, and the second constitutes yellow tuffs that are found at several horizons in the section. Sandstone and conglomerate in this unit contain mixtures of these two types of ash and also ash that is petrographically transitional between the two.

Hornblende-trachyandesite tuff forms a thin bed (less than 30 cm thick) of well-sorted blue-gray to blue-green microvesicular ash that contains abundant euhedral hornblende prisms. In thin section, the hornblende is greenish brown and is different from the brown variety of hornblende found in the Annex Ridge, Buffalo Ridge, and Lion Ridge flows. Subhedral groundmass hornblende granules are also present. Tiny phenocrysts of clinopyroxene are present but rare. In addition to hornblende granules, the groundmass contains plagioclase laths, pyroxene prisms, and abundant apatite prisms in a clear, glassy to cryptocrystalline matrix.

Yellow tuff consists of yellow, yellow-brown, and olive-brown to black, microvesicular olivine-trachyandesite ash containing in thin section abundant red-brown pseudomorphs after olivine microphenocrysts and rare phenocrysts and microphenocrysts of clinopyroxene. The groundmass is yellow-brown, red-brown, or occluded glass, commonly altered to clay minerals; plagioclase laths are generally present.

The unit of fine-pebble conglomerate contains rounded, fine pebbles that weather out to form a characteristic pebbly float. The pebbles are light gray to charcoal gray, light brown to red brown, or, more rarely, bluish green or yellow. Typically, the pebbles are microvesicular and devoid of phenocrysts or microphenocrysts. They are composed of glass, tiny laths of plagioclase, and tiny grains of hornblende(?) and (or) altered olivine. The texture of the ash is pilotaxitic. Ash in the matrix of the conglomerate includes types with abundant olivine and clinopyroxene microphenocrysts.

Other beds in the Hidden Pasture unit include gray to brownish sandstone and conglomerate. In hand specimen, multicolored clasts are visible that contain either hornblende, green pyroxene, red-brown (altered) olivine, or any combination of these. Hornblende occurs both as small phenocrysts and as microphenocrysts; pyroxene occurs dominantly as phenocrysts up to several millimeters across but is rare; (altered) olivine occurs mostly as microphenocrysts and generally is abundant.

All deposits in this unit are cemented by tridymite and potassium feldspar.

CHEMICAL COMPOSITION

Recalculated silica in this unit (samples 166a, 165, 286, and 289a1, table 3) averages about 56 percent. Potassium oxide ranges from 1 to 2 percent and is low compared to all older rocks of the Crater Pasture Formation. Normative potassium feldspar contents are correspondingly low; nevertheless, all but the sample of yellow tuff (286) contain more than 10 percent normative potassium feldspar and are classed as trachyandesites. In a sample of yellow tuff (286) and a clast from the conglomerate (289a1), depletion(?) of sodium and potassium oxides relative to silica and alumina may reflect the alteration to clay minerals seen in these samples. This depletion(?) results in lower normative albite and orthoclase and higher quartz in these samples relative to other trachyandesites of the Crater Pasture Formation.

SEDIMENTARY BRECCIA OF ONE OCLOCK WASH

DISTRIBUTION AND PHYSICAL FEATURES

The sedimentary breccia of One OClock Wash is a local deposit on the flanks of the Fort Rock dome that was formed during uplift of the dome. It is distributed around three-fourths of the periphery of the dome in outcrops of various sizes and thicknesses.

The most extensive outcrop is found on the north flank of the crater, where it crops out continuously from near Two OClock Gap to Wedge Basin. Thicknesses of preserved breccia in this area are estimated at 23 m in One OClock Wash, 60 m on Noon Hill, and 73 m on Short Hill. From Wedge Basin southward to Six OClock Wash, the breccia is exposed chiefly in the walls of the valleys that cut into the flanks of the dome. In Eight OClock Gorge, the breccia ranges in thickness from a meter or so to 60 m. In the vicinity of Six Thirty Wash, it is about 18 m thick.

The breccia is poorly resistant to weathering; it is covered by colluvium in almost all places except where it is made up of coarse angular blocks. It generally crops out in the banks of washes or on slopes that have been washed clean of colluvium. Cliffrose grows preferentially on soil underlain by this breccia (and by other clastic units) and is of help in locating outcrops. It is commonly necessary to dig shallow pits 25 to 50 cm deep to determine the presence and nature of the breccia; hundreds of pits were dug in the hills on the north side of the crater. Float from this unit consists, in most places, of a mixture of dark volcanic rocks and light-colored pink and orange Precambrian rocks.

RELATION TO OTHER UNITS

The breccia overlies numerous units on the dome. The youngest unit is the tuff and conglomerate of Hidden Pasture in Noon Gorge. The oldest units are Precambrian rocks, in Noon Gorge, on Short Hill, and in Wedge Basin. The breccia also overlies the Lion Ridge flow and the tuff and flow of Two OClock Gap on Lion Ridge, the Buffalo Ridge flow on Noon Hill, Ten OClock Hill, Nine OClock Hill, Eight OClock Hill, and Buffalo Ridge, and the Annex Ridge flow in Six OClock Wash and vicinity. The breccia is overlain by the tuff and agglomerate of Cinder Basin in Six OClock Wash and in a number of nearby places to the west. Throughout most of its area of outcrop, it is overlain by the Noon Gorge sedimentary breccia of the Fort Rock Creek Rhyodacite and locally by the Old Stage Road Member of the Fort Rock Creek Rhyodacite.

The contact of the One OClock Wash sedimentary breccia with the underlying Hidden Pasture tuff and conglomerate can be readily studied in the east wall of Noon Gorge by digging shallow pits. The contact appears to be gradational over a narrow interval. Ash content diminishes upward, and clasts of recognizable flow rock, which are the chief constituent of the breccia, increase. The gradation takes place over an interval of about 15 m on the ground. There is

some alternation of ash-rich and clast-rich lithology within this interval.

Near its contact with underlying volcanic flow, the One O'Clock Wash unit locally includes small bodies of authigenic breccia, which are indicated by a special symbol on the geologic map (pl. 1). These bodies include discrete fillings of large cracks, such as those created by the Eight O'Clock Gorge faults and the Eight O'Clock Hill fault. They also include rock in the uppermost part of some flows in which there is widespread filling of small cracks or in which extensive open brecciation is accompanied by inclusion of small amounts of foreign ash. Defined in this fashion, the One O'Clock Wash breccia includes rock in the uppermost part of the Buffalo Ridge flow in Ten O'Clock Wash and Nine O'Clock Wash and in the uppermost part of the Lion Ridge flow in Four O'Clock Wash.

PROVENANCE AND CLAST CONTENT

Most of the breccia appears to be sedimentary in origin, hence the name of the unit. Most is a mixture of clasts from older units and small amounts of volcanic ash. Subaerial transport of the components of the breccia seems necessary to explain this mixture, but absence of clear bedding and clast rounding and sorting makes it difficult to determine if water was the transporting agent. Patterns of occurrence of various clasts in the breccia do, however, suggest a crude stratigraphy that can be explained by sedimentation on the flanks of an uplifted, eroding dome. The poor sorting and bedding and the angularity of clasts are interpreted to indicate a short distance of transport and (or) rapid deposition.

Clasts in the breccia include both volcanic and Precambrian rocks; they appear to reflect the areas on the dome from which they were derived. The Lion Ridge flow apparently underlay most of the roof of the dome, as clasts of this flow are generally most abundant in the breccia. Clasts of the Lion Ridge flow cannot be distinguished in all cases, however, from clasts of the Buffalo Ridge flow. Clasts of Precambrian rocks generally are second in abundance in the breccia. Volume percentages of these clasts have been contoured on the geologic map (pl. 1); variation in their abundance represents the only stratigraphic variation easily observable in the breccia. Two patterns of variation can be seen. The first pattern is best developed in the vicinity of Lion Ridge, where the content of Precambrian rocks is almost nil in the basal part of the breccia and increases relatively smoothly in successively higher parts. This pattern is also seen in the vicinities of

Eight O'Clock Wash and Six O'Clock Wash. The second pattern is best developed in the area between Noon Hill and Wedge Basin, where the content of Precambrian rocks is high at the base of the breccia, lower somewhat higher in the section, and then increases rather smoothly in still higher parts. The first pattern probably reflects progressive erosion of a source area on the dome in which volcanic rocks initially overlay Precambrian rocks; the second pattern probably reflects progressive erosion of a source area on the dome in which Precambrian rocks were initially exposed but where volcanic rocks cropped out in nearby high areas on the dome.

Block patches have been mapped in the One O'Clock Wash breccia. A block patch is defined to be an area containing five or more blocks of volcanic flow, each 1.2 m (four feet) or more across, in which the blocks constitute 30 percent or more of the area. Clasts as large as 3 m across are seen in some block patches. Block patches probably originated as disaggregated landslide bodies, similar to the bodies of Buffalo Ridge flow and Lion Ridge flow in the Noon Hill-Noon Gorge area. Block patches are confined to the north flank of the crater.

LITHOLOGY

The sedimentary breccia of One O'Clock Wash is unbedded and unsorted; it contains angular to subangular clasts. In a few localities, lenticular clasts show a weak preferred orientation that is interpreted as bedding. In most outcrops that are not in the vicinity of block patches, clasts do not exceed 30 cm across, and the most of the breccia is made up of clasts 2.5 cm or smaller in size. Clasts of Precambrian rocks tend to be smaller than clasts of volcanic rocks. Where the breccia is relatively fine grained and made up mostly of volcanic clasts, it has an overall pinkish-brown color. In these rocks, there is a continuous gradation in clast size from silt to large clasts; a matrix is not easily distinguishable from large clasts. Induration is strong enough in some places that the rock fractures through its clasts, although in most places it is possible to break clasts out. Large volcanic clasts are medium gray to maroon, and smaller ones (1 cm or less across) have additional colors of red-brown, yellow-brown, pink, and light-gray. Mafic to intermediate⁶ ash is present

⁶Mafic is used here to refer to dark rocks; ideally, it refers to rocks with color indices greater than 40, although color indices cannot be determined in glassy specimens. Intermediate here refers to dark rocks with a color index between 10 and 40. Felsic refers to rocks with a color index less than 10

everywhere in the finer grained part of the breccia in amounts rarely exceeding a trace. The ash is petrographically similar to olivine-trachyandesite ash in the Hidden Pasture tuff and conglomerate and also to olivine-trachybasalt ash in the Cinder Basin tuff and agglomerate (discussed below). The ash is best observed in thin section but can also be seen in hand specimen on close scrutiny. In hand specimen, it shows up as tiny green, yellow, and olive-brown clasts less than 1 mm across. Some are pyroxene phenocrysts, some are serpentine(?) pseudomorphs after olivine phenocrysts, but most are microvesicular ash containing green and red-brown microphe-nocrysts. The breccia is cemented by tridymite and potassium feldspar(?).

TUFF AND AGGLOMERATE OF CINDER BASIN

DISTRIBUTION, STRATIGRAPHY, AND PHYSICAL FEATURES

The tuff and agglomerate of Cinder Basin is exposed in several inliers in the Fault Canyon flow and along the base of the Fault Canyon flow from Annex Ridge to the head of Tyria Wash. It also forms a few narrow outcrops at the base of the Fault Canyon flow in Fort Rock Creek. The outcrop belt of the Cinder Basin unit extends well beyond the mapped area (pl. 1) to the south and southeast.

The tuff and agglomerate is divided into several intertonguing subunits. (See the explanation for the geologic map, pl. 1.) Three principal subunits are tuff, agglomerate, and sedimentary breccia. Several small flows and a dike have also been mapped, as well as a distinctive bed of sedimentary breccia that contains a mixture of rhyodacite, dacite, and trachy-basalt clasts. The three principal subunits are found throughout the outcrop area of the Cinder Basin tuff and agglomerate, whereas the minor subunits are local in occurrence.

None of the subunits of the tuff and agglomerate is resistant to erosion, although the agglomerate, the minor flows, and the dike tend to be more resistant than the tuff and sedimentary breccia. Where it is exposed as inliers in the Fault Canyon flow, this unit forms basins, of which Cinder Basin is one.

RELATION TO OTHER UNITS

The tuff and agglomerate of Cinder Basin overlies the One O'Clock Wash sedimentary breccia in Six O'Clock Wash and in nearby places to the west. On the southwest flank of Buffalo Ridge it overlies the Buffalo Ridge flow in a few places. It overlies the

Annex Ridge flow on the south side of Six O'Clock Hill and along the west flank of Annex Ridge. In Fort Rock Creek, thin lenses of this unit overlie the flow of Meadow Dam. The Cinder Basin unit is overlain in most places by the Fault Canyon flow; it is also cut by vents for the Fault Canyon flow on the southwest flank of Buffalo Ridge. Locally on the flank of the dome, it is overlain by the Noon Gorge breccia and the Old Stage Road Member of the Fort Rock Creek Rhyodacite.

The contact of the Cinder Basin tuff and agglomerate with the underlying One O'Clock Wash sedimentary breccia is not exposed but may be gradational over a narrow interval. In Six O'Clock Wash, over a distance of about 6 m on the ground, one passes from the One O'Clock Wash sedimentary breccia, which contains only a trace of ash, to a tuffaceous breccia assigned to the Cinder Basin unit that contains 40 percent or more ash. Beds of sedimentary breccia in the Cinder Basin unit probably correlate with parts of the One O'Clock Wash sedimentary breccia at other locations around the dome.

Some rocks of the Cinder Basin tuff may be present in a unit mapped as undivided Crater Pasture Formation found in a large area extending northeastward from Annex Ridge. The undivided unit consists of blue-green tuff and associated sedimentary rocks. It is not clear whether these beds belong to the Hidden Pasture tuff and conglomerate or to the Cinder Basin tuff and agglomerate.

SOURCE FOR VOLCANIC UNITS

The agglomerate of the Cinder Basin unit forms two hills beneath the Fault Canyon flow, one between Six O'Clock and Annex Washes and the other between Six O'Clock and Cinder Basin Washes. Parts of the flanks of these hills are exposed as inliers in the Fault Canyon flow. The hills are probably spatter cones and may have also been sources for the tuff and some of the small flows. The youngest of the small flows may have been fed by the dike (see pl. 1).

PROVENANCE FOR SEDIMENTARY UNITS

Where it crops out on or near the south flank of the dome, the sedimentary breccia contains abundant clasts similar to those in the sedimentary breccia of One O'Clock Wash, which are clearly derived from the dome. The small outcrop of sedimentary breccia in Cinder Basin, however, is devoid of these

clasts; it contains only ash and angular clasts of trachybasalt. This area apparently was not supplied by a drainage from the dome.

The sedimentary breccia that contains a mixture of rhyodacite, dacite, and trachybasalt clasts was probably derived in part from an area to the south-east, in which two intrusive(?) bodies of rhyodacite and dacite are located (fig. 3).

PETROGRAPHY

Rocks of the Cinder Basin tuff and agglomerate are characterized by pseudomorphs after olivine phenocrysts and microphenocrysts. Commonly the pseudomorphs are light-green serpentine(?), but in some specimens they are very fine grained red-brown minerals. The altered phenocrysts occur in sizes up to several millimeters and are relatively sparse; the altered microphenocrysts occur in sizes up to 0.5 mm and are abundant. In rocks of most subunits, clinopyroxene is present as phenocrysts, microphenocrysts, and groundmass grains but is somewhat less abundant than olivine and much less visible in hand specimen. A trace of biotite is present in most rocks and is locally visible in hand specimen. Color, texture, and groundmass composition differ from subunit to subunit.

The subunit designated tuff includes tuff, agglomeratic tuff, sandstone, and conglomerate. Tuff, sandstone, and conglomerate are in most places well bedded and moderately to moderately well sorted, whereas agglomeratic tuff is massive and unsorted. These deposits have colors of light bluish green, maroon, yellow, and white. In thin sections of tuff, ash grains are seen to be chiefly light-brown glass, occluded red-brown glass, or pale-brown altered glass. Some tuffs consists mostly of glassy ash and some mostly of altered ash. Scattered bombs in the agglomeratic tuff are as large as 1.5 m across; they are vesicular, banded, and are dark bluish gray to reddish gray. Bombs contain, on the average, 1/2 percent serpentinized(?) olivine phenocrysts, 15 percent serpentinized(?) olivine microphenocrysts, 1/2 percent clinopyroxene phenocrysts, 10 percent clinopyroxene microphenocrysts, 20 percent groundmass clinopyroxene, 15 percent plagioclase laths (less calcic than An_{44}), 8 percent opaque minerals, and a trace of biotite phenocrysts; the remaining 30 percent is cryptocrystalline interstitial minerals. Sanidine is probably present among the interstitial minerals; normative potassium feldspar is calculated to be about 18.5 percent (table 3, sample 250). This

rock is trachybasalt, if one uses a modal color index of 40 to separate trachybasalts from trachyandesites.

A minor unit designated granule and fine-pebble conglomerate is a distinctive sedimentary bed in the tuff, consisting of red to multicolored, rounded clasts of olivine trachybasalt and olivine trachyandesite. Some beds of this conglomerate contain ash similar to ash of the fine-pebble conglomerate of the Hidden Pasture unit.

None of the deposits mapped as tuff contain more than 10 percent foreign clasts. A deposit with more than 10 percent foreign clasts is mapped as sedimentary breccia.

The subunit mapped as agglomerate consists of bombs up to 3 m across. The bombs are microvesicular and gray, or they are vesicular and banded in colors red-brown and dark-gray. They are embedded in a lighter colored red-brown matrix of ash. The bombs are similar in petrography to those in the tuff, but pseudomorphs after olivine are hematite(?) and biotite(?) and tend to weather out of the rock leaving prismatic holes lined with alteration products. A few embayed hornblende phenocrysts are also present. A zone of welded agglomerate has been mapped in places where the bombs become difficult to distinguish from the matrix and from each other. In this zone of welding both the matrix and bombs are bluish gray.

The subunit mapped as sedimentary breccia consists of breccia and sandstone. It is composed dominantly of clasts of olivine trachybasalt but contains more than 10 percent foreign clasts, including hornblende-trachyandesite clasts and Precambrian rocks. The breccia has an overall orange color. Most of the foreign clasts apparently were derived by erosion from the dome, although some could have been accidental clasts in the eruption of the trachybasalt. On the south flank of the dome the foreign clasts reach 1.2 m in diameter.

Three small flows have been mapped. The lowest of these, a massive, vesicular, light-maroon rock crops out in Fault Canyon. It contains no pyroxene except for a possible trace in the groundmass. Serpentine(?) pseudomorphs after olivine phenocrysts and microphenocrysts are abundant (15 percent total). It has a lower proportion of mafic minerals than other trachybasalts in the unit. The middle flow also crops out in Fault Canyon. It is a dark-bluish-gray sparsely vesicular rock similar to the agglomerate. It occurs at the same stratigraphic horizon as the agglomerate and may be a related spatter flow. The third flow crops out in Cinder Basin. It is a nonvesicular dark-gray rock similar to rock of a nearby dike. The dike rock contains phenocrysts and abundant

microphenocrysts of clinopyroxene and fairly abundant tiny anhedral flakes of biotite. The groundmass consists dominantly of pyroxene, opaque minerals, plagioclase(?) laths, and apatite with interstitial anhedral grains of feldspar.

A sedimentary breccia mapped in Fault Canyon is distinguished from other sedimentary breccia in this unit by its clast content. This breccia is a massive, unsorted, pinkish-buff rock containing clasts of olivine trachybasalt (and olivine trachyandesite?), rhyodacite, and dacite; it is referred to here as mixed breccia. Dark olivine-trachybasalt clasts are the dominant visible clasts in the breccia and are relatively dark shades of gray, brown, red brown, yellow brown, and maroon. These clasts are as large as 13 cm across but generally are about 1 cm across. Rhyodacite clasts make up most of the matrix of the breccia but are found in sizes up to 25 cm across. These clasts include gray-white, gray, and red nonvesicular clasts as well as scattered fragments of white pumice. They are similar to rocks of the overlying Fort Rock Creek Rhyodacite. In thin section, they contain 10 to 15 percent phenocrysts and microphenocrysts of plagioclase, 2 percent biotite, 2 percent clinopyroxene, and rare phenocrysts of sanidine and quartz(?). The groundmass is cryptocrystalline. Dark-maroon dacite clasts up to 25 cm across constitute less than 15 percent of the breccia. They are slightly more mafic than the rhyodacite clasts. One dacite clast that was examined in thin section contains 25 percent plagioclase (less calcic than An_{48}), 5(?) percent potassium feldspar, 3 percent clinopyroxene, 2 percent biotite, 1 percent pseudomorphs after olivine (red and opaque minerals), 3 percent opaque minerals, and cryptocrystalline groundmass with some opaque dust. The feldspar and pyroxene in this rock occur bimodally as phenocrysts and microphenocrysts. Biotite and pseudomorphs after olivine occur as microphenocrysts, seen as brown specks in hand specimen.

CHEMICAL COMPOSITION

Exclusive of the dacite sample (sample 416a, table 3) from the mixed sedimentary breccia, the range in recalculated silica content among rocks of the Cinder Basin unit is 50 to 57 percent (table 3). Four of the rocks in this range have recalculated silica contents between 50 and 53 percent; these rocks are near the division (52 percent) between intermediate and basic rocks. A minor flow (sample 414) has a recalculated silica content of 57 percent, reflecting its low modal abundance of mafic minerals. On the

average, rocks of the Cinder Basin unit are more basic than any older unit of the Crater Pasture Formation except the flow of Eight O'Clock Gorge. Potassium oxide content in these rocks averages about 2¹/₂ percent, and normative potassium feldspar averages 15 percent.

FLOW OF FAULT CANYON

DISTRIBUTION, STRATIGRAPHY, AND PHYSICAL FEATURES

The flow of Fault Canyon covers much of the southwestern part of the map (pl. 1). The flow is approximately bounded by Fort Rock Creek on the west, the flank of the Fort Rock dome on the north, and Annex Ridge on the east. It extends about 1¹/₂ km to the southeast beyond the area mapped. It probably reaches a maximum thickness of about 60 m in the vicinity of Tyria Wash. Several minor subdivisions have been recognized in addition to flow. They include an agglomerate on top of the flow, dikes, and other intrusive bodies, intrusive tuff-breccia or breccia, and a flow-base zone.

The Fault Canyon flow is resistant to erosion; it forms high cliffs along the east side of Fort Rock Creek and along east tributaries of Fort Rock Creek.

RELATION TO OTHER UNITS

Throughout most of its outcrop area, the Fault Canyon flow overlies the Cinder Basin tuff and agglomerate. Locally, along Fork Rock Creek, it overlies the flow of Meadow Dam. It probably overlies the One O'Clock Wash sedimentary breccia in the vicinity of Eight O'Clock Wash, but the contact is covered here by the Noon Gorge sedimentary breccia. It is overlain in places along the flank of the dome by the Noon Gorge sedimentary breccia and the Old Stage Road Member of the Fort Rock Creek Rhyodacite. Elsewhere it is overlain only by the Old Stage Road Member of the Fort Rock Creek Rhyodacite.

SOURCE AND RELATION TO DOMING

A vent for the Fault Canyon flow is exposed at the head of Tyria Wash. An associated dike northeast of this vent and two small sills in the vicinity of Road End Gap may have been small vents for the flow. Topographically high areas on the flow on either side of Six O'Clock Wash may overlie concealed vents.

Intrusive contacts at the head of Tyria Wash dip moderately to gently to the northeast under Buffalo

Ridge; it appears that this lava was erupted from a magma chamber beneath the dome (pl. 2). Extrusion of the Fault Canyon flow is closely associated in time with uplift of the Fort Rock dome. Sedimentary breccias formed by erosion of the dome both underlie and overlie the flow. I conclude from a study of structure of the dome and of the Fault Canyon flow that the flow was extruded near the end of doming and that the magma that erupted the Fault Canyon flow uplifted the dome.

PETROGRAPHY

The flow is massive, nonvesicular to sparsely vesicular, and colored black, dark brownish gray, medium brownish gray, or greenish gray. In Six O'clock Wash, Tyria Wash, and other canyons, it is greenish gray and jointed near its base and brownish gray and massive at its top. Joints at the base of the flow occur in two or more directions and, in places, are spaced as closely as 1 to 2 cm. Red stain commonly occurs along one of the joint sets.

The Fault Canyon flow is characterized by abundant pseudomorphs after olivine microphenocrysts occurring singly and in clusters. The single pseudomorphs are easily seen under a hand lens and are yellow brown to red brown. The clusters of pseudomorphs are, on the whole, either yellowish green with a yellow-brown rim or red brown. Green pyroxene phenocrysts and microphenocrysts, which are in some cases clustered, also are abundant but are less evident in hand specimen.

Petrographic analysis of a sample of the flow (table 2) shows this rock to be made up of sanidine and mafic minerals, with a color index of about 38. It resembles, in its lack of plagioclase, the trachybasalts of the Navajo country described by Williams (1936, p. 148). It is here given the name of olivine-sanidine trachybasalt. Sanidine occurs as subhedral laths, averaging 0.1 mm in length, and as anhedral grains. The mafic minerals include augite, pigeonite, altered olivine, altered biotite, and opaque minerals. In the sample examined, augite occurs as clear euhedral to subhedral phenocrysts up to 1 mm and microphenocrysts averaging 0.2 mm; pigeonite occurs as yellow-green overgrowths on the augite and as anhedral groundmass granules. Pigeonite is over twice as abundant as augite. In other samples of this flow, augite and pigeonite are not easily distinguished optically. Pseudomorphs after olivine microphenocrysts in the sample studied average 0.2 mm in length. Alteration minerals include opaque minerals plus a small amount of translucent brown mineral. In other

samples, olivine is altered to serpentine(?). In the sample analyzed, pseudomorphs after biotite microphenocrysts are similar in size to the pseudomorphs after olivine. They are granular opaque material and are in many cases hard to distinguish from the pseudomorphs after olivine. In some samples, these pseudomorphs are absent, but in others they are more plentiful than in the sample analyzed, retain some patches of unaltered biotite, and occur with fresh phenocrysts and microphenocrysts of biotite, some of which protrude into vesicles.

Agglomerate occurs in thin, scattered patches on top of the flow. It consists of dark-brown vesicular bombs of olivine-sanidine trachybasalt in a matrix of fine-grained white ash that contains abundant tiny biotite flakes. In addition to biotite, the white ash contains microscopic plagioclase, sanidine, and quartz grains and probably is rhyodacite or dacite. In several localities, the ash has been metamorphosed to a hard, very fine grained hornfels adjacent to bombs of trachybasalt. The ash may have been a thin regional deposit laid down very shortly after extrusion of the Fault Canyon flow. It was incorporated into an agglomerate in a subsequent eruption of bombs.

The intrusive bodies of the Fault Canyon flow are identical petrographically to the flow. The body at the head of Tyria Wash has a contact aureole 15 to 30 cm thick of bright-yellow, chertlike hornfels. The hornfels is contact-metamorphosed tuff of the Cinder Basin unit.

Intrusive tuff-breccia or breccia contains red scoria, a few bomblike clasts, abundant angular clasts, and, adjacent to one of the sills, accidental clasts of Annex Ridge flow. The largest body of tuff-breccia is associated with the intrusive body at the head of Tyria Wash.

The flow-base zone is characterized by vugs or breccia. It is found not only at the base of the flow but also at the base of faint flow lobes within the flow.

CHEMICAL COMPOSITION

The Fault Canyon flow is easily distinguishable chemically from all other rocks of the Crater Pasture Formation. It contains about twice as much potassium oxide and normative potassium feldspar as other rocks of the formation. Potassium oxide average 6 percent; normative potassium feldspar averages 36 percent (samples 406a, 246, 280a, table 3). Although this rock has been classified as a trachybasalt, its recalculated silica content average 56 per-

cent, which is well within the intermediate range of composition.

MISCELLANEOUS UNITS

In the vicinity of Fort Rock dome are outcrops of the Crater Pasture Formation that cannot be correlated with certainty with rocks mapped on the dome. Many of these rocks are petrographically different from rocks on the dome. Outcrops located within one diameter of the Fort Rock dome are described briefly below.

SHONKINITE INTRUSION UNDER THE POWERLINES

An outcrop of dark intrusive(?) rock is found at the northern tip of the area mapped, near the powerlines (pl.1; powerlines not shown). This outcrop continues northwestward beyond the mapped area for about 1 km parallel to the powerlines. It is located on the edge of a low escarpment of Precambrian granitic rock that forms the eastern boundary of a large basin drained by Fort Rock Creek (fig. 3). The powerline intrusion is apparently overlain in the mapped area by the Noon Gorge sedimentary breccia of the Fort Rock Creek Rhyodacite; 0.8 km to the northwest it is overlain by ash-flow tuff of that formation. In a few places to the northwest, it is overlain by tuff and conglomerate containing intermediate to mafic ash and clasts.

In the mapped area, this intrusion is poorly resistant to weathering; it underlies a low saddle between a hill underlain by Noon Gorge sedimentary breccia and the escarpment of Precambrian rock. Where gullies have cut into it, it forms grass. Surface float consists of detached blocks. Farther northwest, this rock forms a resistant ridge.

The intrusion is massive, nonvesicular, and black (brownish on a weathered surface) with abundant visible red-brown olivine phenocrysts. It is classified as a shonkinite. In thin section, it is seen to contain 15 percent olivine, 50 percent augite, 5 percent opaque minerals, 3 percent biotite, 27 percent orthoclase, and a trace of analcime. Olivine occurs as phenocrysts, up to 3 mm across, and as microphe-nocrysts. The olivine phenocrysts are altered to a red-brown mineral on their rims, and a few microphe-nocrysts are totally altered to chlorite. Augite occurs as distinctive elongated prisms in a continuous size distribution from groundmass grains to phenocrysts. Biotite occurs as ragged, poikilitic flakes up to 0.5 mm across. Orthoclase also forms anhedral poikilitic grains up to 0.5 mm across. Petrographi-

cally this rock is similar to the flow of Eight O'clock Gorge, which is a limburgite, although it is more mafic and contains no glass.

The recalculated silica content for a sample of this body (sample 331, table 3) is about 42¹/₂ percent, which is well within the range of ultrabasic composition (less than 45 percent). This rock is the only sample of the Crater Pasture Formation that is undersaturated in silica.

OTHER ROCKS

Other outcrops of Crater Pasture rocks that cannot be definitely correlated with rocks mapped on the dome are numbered below in order of their occurrence in a clockwise sense around the dome, beginning in the east.

1. A large body of olivine-trachybasalt flow and agglomerate underlies a basin about 1 km in diameter located about 1 km east of the Fort Rock dome (fig. 3). A high hill in the center of the basin and two smaller adjoining hills may overlie a vent area for this unit. In some locations on the edge of the basin, these rocks are overlain by tuff and conglomerate similar to the tuff and conglomerate of Hidden Pasture on the Fort Rock dome. In places, this tuff and conglomerate contains olivine-trachybasalt bombs; hence its source may be associated with the vent for the underlying trachybasalt and may be found somewhere near the basin. In most places on the edge of the basin, the trachybasalt and the tuff and conglomerate are overlain by ash-flow tuff of the Fort Rock Creek Rhyodacite.

This body of olivine trachybasalt occurs in vesicular and nonvesicular varieties. Vesicular rocks are dark bluish gray, charcoal gray, light brownish gray, or red; nonvesicular rocks are dark gray or black. Color and texture vary markedly over distances of a few meters. Petrographically, the rock is similar to the shonkinite intrusion under the powerlines, only slightly finer grained. Olivine occurs as phenocrysts up to 1 mm across and as microphe-nocrysts. In vesicular samples, olivine is totally altered to red-brown minerals on its rims and to serpentine in its interior. Clinopyroxene occurs only as groundmass grains. Interstitial minerals include potassium feldspar, analcime, and a mineral of moderate birefringence and high negative relief.

Two chemically analyzed samples of this rock (samples 459b and 459c, table 3) have recalculated silica contents averaging 49 percent, which is in the range of basic composition. One of these rocks has

less than 10 percent normative potassium feldspar and is technically not a trachybasalt.

2. A massive hornblende-trachyandesite body, which is similar in hand specimen to the upper, massive hornblende-trachyandesite flow of the Annex Ridge unit, crops out as a small inlier in the terrace gravels about 2 km southeast of the dome (fig. 3). This flow differs from the flow of Annex Ridge in containing scattered green pyroxene phenocrysts.

3. A massive pyroxene-trachyandesite flow, similar in hand specimen to the flow of the Two O'Clock Gap unit on Fort Rock dome, crops out beneath agglomerate and minor flows of the Cinder Basin unit about 1½ km south-southeast of the dome. Its outcrop area is about 1.3 km long and 0.4 km wide and straddles the major drainage in this area. A deep canyon cuts the flow on the south but does not expose its base; the flow is at least 23 m thick in this area.

4. A small outcrop of hornblende-trachyandesite flow, similar in hand specimen to the Buffalo Ridge flow on the Fort Rock dome, is exposed beneath Cinder Basin extrusive rocks on the northeast side of the Fort Rock Creek fault about 2 km south of the dome.

5. An agglomerate composed of red to charcoal-gray bombs underlies a low mound about 60 m across, located about ½ km southwest of the Fort Rock Ranch headquarters (fig. 3). The agglomerate is overlain by ash-flow tuff of the Fort Rock Creek Rhyodacite. The rock is an aphanitic trachyandesite. In thin section it is composed of tiny plagioclase laths, opaque minerals, and glass.

6. An agglomerate composed of brown to red-brown bombs underlies a large hill, 0.5 km across, located 1 km northeast of the ranch headquarters (fig. 3; pl. 1, the hill underlying the Indian ruins). Two low mounds northeast of this hill are composed of similar agglomerates. This agglomerate is overlain by ash-flow tuff of the Fort Rock Creek Rhyodacite. The rock is olivine trachybasalt, petrographically similar to both the shonkinite intrusion under the powerlines and the olivine trachybasalt flow and agglomerate east of the Fort Rock dome. It contains 15 percent biotite pseudomorphs after olivine, 40 percent clinopyroxene, 10 percent plagioclase, 30 percent potassium feldspar, 3 percent opaque minerals, and 2 percent calcite. The biotite pseudomorphs range in size from 0.1 mm to 1 mm. Clinopyroxene occurs only in the groundmass as prisms up to 0.2 mm. Plagioclase occurs as scattered laths. Potassium feldspar is anhedral and fills interstices between other minerals. Calcite fills scattered vesicles. The rock has a recalculated silica content of nearly 51

percent and a normative potassium feldspar content of nearly 10 percent (sample 334, table 3).

7. A pyroxene-trachyandesite lapilli tuff and tuff-breccia, similar in hand specimen to the tuff at the base of the tuff and flow of Two O'Clock Gap, underlies a low mound over 100 m across, located beneath the powerlines about 1 km north of the dome. It is overlain by ash-flow tuff of the Fort Rock Creek Rhyodacite.

FORT ROCK CREEK RHYODACITE

Fort Rock Creek Rhyodacite is a name applied by Fuis (1973) to a series of ash-flow and other massive tuffs, volcanic breccias, lava flows, and associated intrusive and sedimentary rocks in the Aquarius Mountains. The composition of volcanic rocks in these units is chiefly rhyodacite, although rhyolite is present in some units.

This formation is subdivided into two formally named and two informally named members, listed below with the oldest at the bottom:

- Breccia and conglomerate of the Crossing
- Three Sisters Butte Member (chiefly massive tuff and breccia)
- Old Stage Road Member (chiefly ash-flow tuff)
- Sedimentary breccia of Noon Gorge

In addition to these members, the formation includes, in the vicinity of the Fort Rock dome, a rhyodacite intrusive body and an unnamed unit of rhyodacite-bearing sedimentary breccia and sandstone that differs in lithology and age from the other members of this formation.

TYPE SECTION

The easternmost of the three buttes known as the Three Sisters (figs. 2 and 3) is the type section for the Fort Rock Creek Rhyodacite. This butte is located about 3 km west-southwest of the Fort Rock Ranch headquarters. The type section was measured and described on the north side of the butte beginning at a 6-m high white bluff located in the NW¼ NW¼SW¼ sec. 5, T. 20 N., R. 10 W. The traverse followed in describing this section runs southward up the low bluff and then west-southwestward from the top of the bluff for about 300 m along a low rise. At the end of the rise, the traverse runs southward again for about 500 m up a topographic rib to the

top of the butte, which is located in the SE¹/₄SE¹/₄ SE¹/₄, sec. 6, T. 20 N., R. 10 W.

At the type section the Fort Rock Creek Rhyodacite rests on intermediate to mafic lava flows, agglomerates, and volcanic breccias of the Crater Pasture Formation. The contact between the two formations dips gently to the east and has local relief of about 10 m. Most beds in the Fort Rock Creek Rhyodacite also dip gently to the east or are horizontal. Dips are locally steeper at the base of the section.

Three members are present in the type section, the Old Stage Road Member, the Three Sisters Butte Member, and the breccia and conglomerate of the Crossing, which forms the cap rock of the butte.

Fort Rock Creek Rhyodacite Feet

- 22. Massive tuff; white; unsorted; slope former. Clasts greater than 2 mm in diameter make up over half the rock: in this size range, 35 to 45 percent of the rock is white pumice, 15 to 35 percent is accessory gray rhyodacite clasts, and a trace is accidental clasts of Precambrian rocks and dark-brown to gray rocks from the Crater Paster Formation. The rest of the rock is matrix, which consists of clasts of all compositions that are less than 2 mm in diameter. Modal diameter ill-defined; matrix grades in grain size into the larger clasts; pumice generally smaller than accessory and accidental clasts; maximum clast size about 30 cm. Indian ruins atop the butte are built on this unit..... 15.0 preserved

Breccia and conglomerate of the Crossing

- 21. Breccia; slope former; largely unexposed; blocks of gray to red rhyodacite up to 2 m across occur in the colluvium covering this unit; the presence of pumice in the breccia probably accounts for lack of resistance to weathering 25.0
- 20. Breccia; poorly sorted; crudely bedded; forms the cap rock of the butte; chiefly blocks of red to gray rhyodacite, a few clasts of Precambrian rocks and dark-brown to gray rocks from the Crater Pasture Formation, and no observable pumice; modal diameter 10 cm at the base, 50 cm in the middle, and 10-15 cm at the top; maximum clast size 3 m 41.5

Total breccia and conglomerate of the Crossing .. 66.5

Unconformity(?); contact has relief of less than 2 cm where exposed.

Three Sisters Butte Member

- 19. Sandstone; light gray brown; very fine to very coarse grained; moderately well to well sorted; bed thickness 1-15 mm; notch former; gray rhyodacite and one percent grains of Precambrian rock; total thickness 8-40 cm 1.0
- 18. Massive tuff; similar to unit 22; upper 100 feet covered by colluvium and may include breccias similar to units 15 or 17 (see below);

- light-gray-brown sandstone similar to unit 19 with a thickness of 1.5-15 cm four feet below the top..... 169.0
 - 17. Breccia; pumiceous⁷; crudely bedded; slope former; grades into unit 18; mostly gray rhyodacite clasts and white pumice, and a few clasts of Precambrian rocks and clasts of dark-brown to gray rocks from the Crater Pasture Formation; modal diameter 12 cm at the base, 7 cm at the top; maximum clast size 60 cm 12.5
 - 16. Massive tuff; similar to unit 22; grades upward into pumiceous breccia and includes ill-defined lenses of rock transitional to pumiceous breccia 23.5
 - 15. Breccia; pumiceous; slope former; largely unexposed; grades upward and laterally into massive tuff; mostly clasts of gray rhyodacite and white pumice, and a few clasts of Precambrian rocks and dark-brown to gray rocks from the Crater Pasture Formation; modal diameter 5-10 cm; maximum clast size 40 cm 46.0
 - 14. Fine-pebble conglomerate; moderately to moderately well sorted; pumiceous; slope former; 75 percent gray to red rhyodacite pebbles, 17 percent white pumice, 5 percent pebbles of Precambrian rocks, and 3 percent pebbles of dark-brown to gray rocks from the Crater Pasture Formation; modal diameter 0.5 cm 1.0
 - 13. Breccia; dark red; moderately to moderately well sorted; ledge former; contains red rhyodacite clasts and a few clasts of Precambrian rocks; modal diameter 1-1.5 cm; maximum clast size 3 cm 0.25
 - 12. Sandstone⁸; light brown; very fine to very coarse grained; moderately to moderately well sorted; bed thickness 1-5 mm; notch former; 90 percent grains of gray to red rhyodacite, 7 percent white pumice, and 3 percent clasts of Precambrian rock 0.25
- Total Three Sisters Butte Member 253.50

⁷The following arbitrary definition was used to separate units described as massive tuff from units described as pumiceous breccia: A massive tuff contains less than 35 percent accidental and accessory clasts (excluding pumice) greater than 2 mm in diameter; a pumiceous breccia contains more than 35 percent of these clasts. The remaining part of both rocks consists of a matrix of grains of all compositions less than 2 mm in diameter. Defined in this fashion, massive tuff is similiar, except for its field relations, to ash-flow tuff.

⁸Units 12 through 15 occur on an outlier, about 100 m across, located on a low southwest-trending rise above the white bluff at the base of the section. The outlier is about halfway between the bluff and the topographic rib described above on the north side of the butte. At the north end of the topographic rib, an 8-cm-thick, fine-grained, well-sorted, resistant, dark-gray sandstone crops out at the base of the Three Sisters Butte Member. Neither units 13 nor 14 are exposed, although excavation might reveal them. The sandstone is overlain by unit 15.

On -east side of the butte, in an area not measured in the type section, the basal sandstone of The Three Sisters Butte Member, unit 12, is about 4 m thick.

Old Stage Road Member

11. Ash-flow tuff⁹; white; unsorted (lower part) to poorly sorted (upper part); graded bedding; nonwelded; cliff former in many places. Clasts greater than 2 mm in diameter make up a little over half the rock on the average: in this size range, 25 percent of the rock is white pumice, 25 percent is gray to red rhyodacite accessory clasts, 3 percent is accidental clasts of Precambrian rocks, and a trace is accidental clasts of dark-brown to gray rocks from the Crater Pasture Formation. The remainder of the rock is pinkish-gray matrix, which includes all clasts less than 2 mm in size. Modal diameter 0.75 cm at the bottom, 1 cm at the top; maximum clast size about 5 cm; horizon containing abundant cobble-sized angular clasts of rhyodacite, Precambrian rocks, and rocks from the Crater Pasture Formation one half meter above its base 8.3
10. Massive (ash-flow?) tuff, ash-fall lapilli tuff, and sandstone; interbedded; cliff former; massive tuff similar to but finer grained than unit 11; modal diameter less than 5 mm; contact with sandstone gradational; average bed thickness 30 cm for massive tuff; ash-fall lapilli tuff similar to but finer grained than unit 6 or 8 (see below); modal diameter for lapilli 5-10 mm; average bed thickness 15 cm for lapilli tuff; sandstone, white, pumiceous, nonfissile; average bed thickness 3 cm for sandstone 3.5
9. Ash-flow tuff; similar to unit 11 17.0
8. Ash-fall lapilli tuff; white to pinkish-brown; moderately to moderately well sorted; bed thickness 30 cm at the base, about 2 cm at the top; notch former; 75 percent white pumice, 10 percent gray to red rhyodacite accessory clasts, 12 percent accidental clasts of dark-brown to gray rocks from the Crater Pasture Formation, and 3 percent accidental clasts of Pre-cambrian rocks; modal diameter 1 cm 2.7
7. Ash-flow tuff; similar to unit 11 6.0
6. Ash-fall lapilli tuff; white to pinkish brown; moderately to moderately well sorted; graded bedding; notch former; base of unit slightly better sorted and contains less pumice than top; top grades into ash-flow tuff; 79 percent white pumice, 15 percent gray to red rhyodacite accessory clasts, 5 percent clasts of Precambrian rocks, and one percent clasts of dark-brown to gray rocks from the Crater Pasture Formation; modal diameter 2 cm 1.5
- Unconformity; angular; dips of beds on either side differ by a few degrees; contact has only a few centimeters relief.
5. Sandstone; light gray; very fine to very coarse grained; moderately well sorted; fissile;

- pumiceous; notch former; bed thickness 1-30 mm; lower beds thicken regularly toward the east; upper beds are cross-laminated and indicate a westerly current direction; 46 percent white pumice, 50 percent gray to red accessory rhyodacite grains, 3 percent grains of Precambrian rocks, and less than one percent grains of dark-brown to gray rocks from the Crater Pasture Formation 11.0
4. Sandstone; white; very fine to very coarse grained; moderately sorted; nonfissile; pumiceous; slope-former; bed thickness 1 mm to 30 cm 5+
3. Sedimentary breccia¹⁰; massive; slope former; 70 percent clasts of Precambrian rocks, 20 percent gray to red rhyodacite clasts, 10 percent clasts of dark-brown to gray rocks from the Crater Pasture Formation; modal diameter 1.5-2 cm 2+
- Total Old Stage Road Member 57.0+
- Total Fort Rock Creek Rhyodacite 392.0+ preserved

Crater Pasture Formation Feet

2. Sedimentary breccia; massive; slope former; clasts of olivine trachybasalt(?) in an orange, sandy matrix; clast colors include red, yellow brown, and dark gray; modal diameter several centimeters 1.0
1. Volcanic breccia and agglomerate; red to red brown; unsorted; massive; strongly indurated; forms hills and ridges; angular clasts and bombs of olivine trachybasalt(?) in a matrix of ash 20+

REFERENCE SECTION

Penitentiary Butte, 15 km west-southwest of the Fort Rock dome (fig. 3), is the reference section for the Fort Rock Creek Rhyodacite. This section was measured and described on the west side of the butte beginning in the $W^{1/2}NW^{1/4}NW^{1/4}$ sec. 19, T. 20 N., R. 11 W. and proceeding eastward up a gully. At the base of the Three Sisters Butte Member, which is marked only by a 6-cm thick bed of breccia in this gully, the traverse jogs abruptly to the north approximately 180 m and proceeds eastward again up another gully that lies roughly along the line between sec. 19 and sec. 18. In this gully the basal breccia in the Three Sisters Butte Member is much thicker (1.1 m) and more distinctive.

The reference section of the Fort Rock Creek Rhyodacite rests on agglomerate of the Crater Pasture Formation. The contact has about 100 m of relief. Most beds in the Fort Rock Creek Rhyodacite

⁹For justification in applying the terms "ash-flow tuff" and "ash-fall tuff" to the rocks described here, one must invoke some broad field relations that are not evident in the type section. These relations are briefly described in the section entitled "Mode of Emplacement of Extrusive Rocks."

¹⁰This unit is in fault contact with the overlying sandstone. Fault displacements in this area are generally small, and missing section is probably only a few feet thick at most.

| | | | |
|---|-------|--|------|
| 2 percent accidental clasts of Precambrian rocks; modal diameters 7.5 mm for pumice and accidental clasts, 1 mm for the crystals; modal diameters and sorting differ slightly from bed to bed | 0.5 | 22 percent of the rock is white pumice (light-buff-weathering), 8 percent is accessory clasts of red to gray rhyodacite, a few clasts are accidental clasts of Precambrian rocks, and there are no conspicuous accidental clasts of rocks from the Crater Pasture Formation. The remainder of the rock is matrix including coarse and fine ash and accessory fragments less than 2 mm in diameter. Modal diameters 4 mm for pumice, 1 cm for accessory clasts; maximum clast size 1.5 cm for pumice, 2.5 cm for accessory clasts. 1.5-m-thick beds characterized by abundant large pumice fragments (up to 5 cm in diameter) occur 1.5 meters above base and at top | 38.8 |
| 20b. Pumice tuff; white; poorly sorted; faintly bedded; cliff former with knobby appearance like unit 22. Clasts greater than 2 mm make up 60 percent of the rock: in this size range, 40 percent of the rock is white (buff weathering) pumice, 20 percent is accessory clasts of gray rhyodacite; bimodal: modal diameters 1 and 3 cm for pumice, 0.75 and 3 cm for accessory clasts; maximum clast size 5 cm for pumice, 7 cm for accessory clasts | 52.8 | 15. Ash-flow tuff; similar to unit 16; lower 2.5 m of section cliff former, upper 13 m slope former; among clasts greater than 2 mm in diameter, 15 percent of the rock is pumice, 15 percent is accessory clasts of rhyodacite, and there are rare accidental clasts of Precambrian rocks and no conspicuous clasts of rocks from the Crater Pasture Formation; modal diameters 0.5 cm for pumice, 1 cm for accessory clasts; maximum clast sizes 3 cm for pumice clasts, 5 cm for accessory clasts; a bed up to 30 cm in thickness characterized by large angular clasts of rhyodacite (up to 30 cm in diameter) occurs 2 m above the base; 2-m-thick beds characterized by abundant large pumice fragments (up to 5 cm in diameter) occur near the center and at the top of the section | 50.0 |
| 20a. Pumice tuff; similar to unit 20b; modal diameters 1 and 3 cm for pumice, 0.75 and 2 cm for accessory clasts; maximum clast size 15 cm for pumice, 3 cm for accessory clasts | 4.0 | 14. Sedimentary breccia; gray; very poorly sorted; massive; notch former; 65 percent subangular clasts of gray to red rhyodacite and 35 percent pumiceous sand and silt; maximum clast size 2 cm | 1.0 |
| 19. Ash-fall tuff; white; moderately sorted; well bedded; notch former; bed thickness 3-4 mm; 70 percent white pumice, 30 percent angular accessory fragments of gray rhyodacite, and a few accidental clasts of Precambrian rocks; modal diameter 3 mm | 1.3 | 13b. Ash-flow tuff; similar to unit 16; maximum clast size 4 cm for pumice, 8 cm for accessory clasts | 18.1 |
| 18e. Pumice tuff; similar to unit 22 | 44.0 | 13a. Ash-flow tuff; similar to unit 16; cliff former; among clasts greater than 2 mm in diameter, 20 percent of the rock is pumice, 15 percent is accessory clasts of rhyodacite, and there are a few accidental clasts of red-brown rocks of the Crater Pasture Formation and rare accidental clasts of Precambrian rocks. Modal diameters 0.5 cm for pumice, poorly defined but approximately 1.5 cm for accessory clasts; maximum clast sizes 1 cm for pumice, 8 cm for accessory clasts. | 10.0 |
| 18d. Pumice tuff; similar to unit 22; among clasts greater than 2 mm in diameter, 15 percent of the rock is clasts of rhyodacite; modal diameters 1 cm for pumice, 2.5 cm for accessory clasts; maximum clast size 2 cm for pumice, 4 cm for accessory clasts | 10.0 | 12. Pumiceous conglomerate; poorly sorted; notch former; 2 beds of subequal thickness; 8 percent granules and pebbles of red to gray rhyodacite and 92 percent white pumiceous sand; granules and pebbles subangular and have poorly defined mode | 0.15 |
| 18c. Pumice tuff; similar to unit 22; among clasts greater than 2 mm in diameter, 1 percent of the rock is accessory clasts of rhyodacite; modal diameters 1.5 cm for pumice, 2 cm for accessory clasts; maximum clast size 4 cm for pumice, 3 cm for accessory clasts | 13.5 | 11. Ash-flow tuff; white; poorly sorted; graded bedding; nonwelded; cliff former. Clasts greater than 2 mm in diameter make up 60 percent of the rock: in this size range, 57 percent of the rock is pumice, 3 percent is accessory clasts of rhyodacite, and there are rare accidental clasts of Precambrian rocks and no conspicuous accidental clasts from the Crater Pasture | |
| 18b. Pumice tuff; white; poorly sorted; bedded; slope former; contains 90 percent white pumice and 10 percent accessory clasts of rhyodacite; composition changes slightly from bed to bed; modal diameters also change from bed to bed: 2-5 mm for pumice, 3-10 mm for accessory clasts; maximum clast size 2 cm | 3.0 | | |
| 18a. Pumice tuff; white; similar to unit 22 but very poorly sorted; among clasts greater than 2 mm, 3 percent of the rock is accessory clasts of rhyodacite; modal diameter 1 cm; maximum clast size 20 cm for pumice, 3 cm for accessory clasts | 5.5 | | |
| 17. Breccia; light red brown; unsorted; ledge former; bed thickness 6-36 cm; angular clasts of red to gray rhyodacite; some of the sand and smaller interstitial grains may be fragments of pumice; modal diameter poorly defined, 0.5-1 cm in different beds; maximum clast size 10 cm | 3.6 | | |
| Total Three Sisters Butte Member | 379.3 | | |
| Old Stage Road Member | | | |
| 16. Ash-flow tuff; white; unsorted; massive; nonwelded; slope former in most places. Clasts greater than 2 mm in diameter make up 30 percent of the rock: in this size range, | | | |

Formation. The remainder of the rock is light-gray-white matrix, which includes coarse and fine pumice ash and other clasts less than 2 mm in size. Modal diameters 1 cm for pumice and accessory clasts, 2 cm for accidental clasts; maximum clast size 4 cm; scattered large pumice fragments (up to 10 cm in diameter) in the upper meter 80.0

10. Granule and fine-pebble conglomerate; gray; poorly sorted (lower part) to moderately sorted (upper part); bimodal; notch former; 25 percent granules and fine pebbles of gray rhyodacite, 10 percent granules and fine pebbles of white pumice, and 65 percent pumiceous sand and silt 0.4

9. Ash-flow tuff; white; unsorted; nonwelded; cliff former. Clasts greater than 2 mm in diameter make up 45 percent of the rock: in this size range, 40 percent is white pumice, 5 percent is accessory clasts of rhyodacite and there are a few accidental clasts of Precambrian rocks and clasts from the Crater Pasture Formation. The remainder of the rock is light-gray-white matrix, which includes coarse and fine pumice ash and other clasts less than 2 mm in diameter. Modal diameters 0.75 cm for pumice and accessory clasts, 2 cm for accidental clasts; maximum clast size 4 cm 5.8

8. Ash-flow tuff; similar to unit 11 43.8

7. Granule and fine-pebble conglomerate; similar to unit 10 0.8

6. Ash-flow tuff; similar to unit 9; slightly finer grained; among clasts greater than 2 mm in diameter, 7 percent of rock is accessory clasts of rhyodacite and there are rare accidental clasts from the Crater Pasture Formation; scattered large clasts of rhyodacite (up to 18 cm in diameter) near its base 9.1

5. Granule and fine-pebble conglomerate; gray; poorly sorted; bimodal; notch former; 25 percent granules and fine pebbles of gray rhyodacite and 75 percent pumiceous sand and silt 0.1

4c. Ash-flow tuff; similar to unit 9; slightly finer grained; among clasts greater than 2 mm in diameter, 7 percent of rock is accessory clasts of rhyodacite and there are rare accidental clasts from the Crater Pasture Formation; scattered large pumice fragments (up to 20 cm in diameter) in the upper meter 36.1

4b. Ash-flow tuff; somewhat similar to unit 11; pumice bimodal, 0.5 cm and 2.5 cm; maximum size 4 cm. Large pumice weathers to holes; the unit is generally a notch former 4.5

4a. Ash-flow tuff; similar to unit 9; among clasts greater than 2 mm in diameter, 10 percent of rock is accessory clasts of rhyodacite; scattered large clasts of rhyodacite and clasts from Crater Pasture Formation (up to 30 cm in diameter) near its base 50.6

3. Sedimentary breccia; gray; very poorly sorted; notch former; bed thickness 1.5-4.5 cm; 25 percent light-green to light-orange pyroxene trachyandesite(?) pumice, 25 percent white

rhyodacite pumice, 25 percent gray to red rhyodacite (nonpumiceous) clasts, 10 percent gray to red-brown clasts from the Crater Pasture Formation, and 1 percent clasts of Precambrian rocks; remainder of the rock is light-gray ash; modal diameters 8 mm for pyroxene trachyandesite pumice, 3 mm for rhyodacite pumice, 1 mm for rhyodacite (nonpumiceous) clasts, poorly defined for clasts of Crater Pasture Formation and Precambrian rocks, with clasts of Crater Pasture Formation up to 15 cm in diameter 0.85

2. Ash-flow tuff; white; unsorted (lower part) to poorly sorted (upper part); graded bedding; nonwelded; slope former. Composition changes from base (b) to top (t); clasts greater than 2 mm in diameter make up 50 percent (b) to 75 percent (t) of the rock: in this size range, 40 percent (b) to 74.5 percent (t) of the rock is white pumice, 10 percent (b) to 0.5 percent (t) is accessory clasts of red to gray rhyodacite, a trace is accidental clasts of red-brown to gray rocks from the Crater Pasture Formation, and a trace is accidental clasts of Precambrian rocks. The remainder of the rock is light-gray-white matrix, which includes coarse and fine pumice ash and other clasts less than 2 mm in size. Modal diameters 0.75 (b) to 1 cm (t) for pumice and accessory clasts, 2 cm for accidental clasts; maximum clast size 3 cm 21.4

Total Old Stage Road Member 371.5

Total Fort Rock Creek Rhyodacite 750.8

Crater Pasture Formation

1. Agglomerate; red brown to gray; unsorted; massive; strongly indurated (welded?); forms hills and ridges; contains bombs and angular clasts of olivine trachybasalt(?) in a matrix of ash; bombs and clasts are compact to scoriaeous; maximum size 0.5 m; bombs and clasts are 80 percent dark-gray lithic groundmass and 20 percent red-brown-altered olivine microphenocrysts; modal diameter for microphenocrysts 0.1 mm and maximum size 2 mm .. 50+

SEDIMENTARY BRECCIA OF NOON GORGE

DISTRIBUTION AND PHYSICAL FEATURES

The sedimentary breccia of Noon Gorge is a local unit of the Fort Rock Creek Rhyodacite found on or near the flanks of the Fort Rock dome. Distribution of this breccia is similar to the sedimentary breccia of One O'clock Wash of the Crater Pasture Formation, which it overlies. It is distributed around three-fourths of the periphery of the dome in outcrops of differing size. The most extensive outcrop occurs on

the north flanks of One O'Clock Hill and Lion Ridge. In this area, the Noon Gorge breccia reaches an estimated thickness of about 15 m. Although thinner than the parts of the One O'Clock Wash sedimentary breccia that are preserved in this area (estimated thickness, 23 m), the Noon Gorge sedimentary breccia crops out over a somewhat larger area because of its lower dip. From Noon Gorge in a counterclockwise direction around the crater to the southwest flank of Buffalo Ridge, this breccia crops out as a narrow belt high on the flank of the dome adjacent to the One O'Clock Wash breccia. The chief exposures are in valleys on the flank of the dome. Estimated maximum thicknesses are 9 m on Noon Hill, 23 m on Short Hill, 30 m in Eight O'Clock Wash, and 5 m at the head of Tyria Wash. In addition to outcrops high on the flanks of the dome, a large inlier of Noon Gorge breccia occurs in the Old Stage Road Member about 450 m north of Wedge Basin, and a large outlier of the unit occurs at the north edge of the mapped area (pl. 1).

Like the One O'Clock Wash breccia, the Noon Gorge breccia is poorly resistant to weathering and is in most places covered by colluvium. Uprooted trees, which are numerous on the lower part of the flanks of the dome, were used to determine the presence and character of this breccia in many places. Shallow excavations were necessary elsewhere. Float from this unit consists of gray clasts of volcanic rocks and clasts of pink, orange, and black Precambrian rocks.

RELATION TO OTHER UNITS

In most places on the dome, the Noon Gorge sedimentary breccia overlies the One O'Clock Wash sedimentary breccia. Locally, it overlies the Buffalo Ridge flow, the Fault Canyon flow, the Cinder Basin tuff and agglomerate, and the Annex Ridge flow. North of Lion Ridge, it overlies Precambrian rocks. This unit is overlain by sedimentary breccia, sandstone, ash-fall tuff, and ash-flow tuff of the Old Stage Road Member.

Contrasts in lithology between the Noon Gorge sedimentary breccia and the underlying One O'Clock Wash sedimentary breccia are subtle (table 4). The contact between these two units appears to be gradational through at least one meter of section on the flanks of Lion Ridge, One O'Clock Hill (east of the One O'Clock Hill fault), Noon Hill, Short Hill, and Wedge Basin. The contact is somewhat sharper west of the One O'Clock Hill Fault, in Ten O'Clock Wash, and in Eight O'Clock Wash.

PROVENANCE AND CLAST CONTENT

Like the underlying One O'Clock Wash sedimentary breccia, the Noon Gorge sedimentary breccia consists chiefly of clasts eroded from the dome during its uplift, including clasts of volcanic and Precambrian rocks. Volume percentages of Precambrian clasts in this breccia are contoured on the geologic map (pl. 1), as they are in the underlying One O'Clock Wash breccia. In general, the volume percentage of Precambrian clasts increases smoothly upward through the Noon Gorge breccia. This pattern probably reflects the widening of the exposure of Precambrian rocks on the dome as the covering of volcanic rocks was being stripped back by erosion.

Distinctive black clasts of olivine trachyandesite are found in the Noon Gorge breccia in an area extending from Noon Hill to the north side of Lion Ridge. Their lowest occurrence coincides with the basal contact of the breccia through most of the area in which they are found, and they are thus useful in mapping the basal contact of this unit. These clasts are petrographically and chemically similar to rock of the Road End Gap volcanic breccia and flow. They are interpreted as detrital clasts derived from this unit by erosion during uplift of the dome. The Road End Gap volcanic breccia and flow presently crops out only on the southern rim of the crater. In order for this unit to have been a source for the clasts in the breccia, a lobe of volcanic breccia (or flow) must have originally extended northward more than half-way across the site of the present crater.

SOURCE FOR VOLCANIC ASH

In addition to detrital clasts from the Fort Rock dome, the Noon Gorge sedimentary breccia contains small amounts of mafic to intermediate ash and small amounts of felsic volcanic clasts. Locally, mafic and intermediate ash are concentrated in tuffaceous beds in the breccia. Two such beds have been mapped. A tuffaceous sandstone and conglomerate consisting chiefly of dark-colored olivine-trachyandesite (or olivine-trachybasalt) clasts occurs in the breccia at one locality on the north flank of One O'Clock Hill. Bomblike clasts from this subunit are petrographically similar to the shonkinite intrusive body under the powerlines to the northeast and also to a body of olivine-trachybasalt agglomerate to the west-northwest (underlying the hill with Indian ruins in pl. 1). The latter body may have been the source of the ash and clasts in this bed, as the shonkinite intrusion

appears to be overlain by the Noon Gorge breccia. A tuffaceous granule and fine-pebble conglomerate consisting chiefly of light-colored trachyandesite ash was mapped in isolated localities on the southwest and south flanks of the dome. The source of this ash is unknown. Rhyolite and rhyodacite clasts scattered through the breccia most likely had their source in the large rhyodacite eruptive center in the Aquarius Mountains to the southwest; they apparently represent the onset of volcanism in that center. Sedimentary breccia containing more than about 1/2 percent of these clasts is mapped as a subunit of the overlying Old Stage Road Member.

LITHOLOGY

The breccia is massive to poorly bedded and unsorted to poorly sorted; it contains angular clasts. In most outcrops, clasts do not exceed 30 cm in diameter, and most of the breccia is made up of clasts 15 cm or smaller in size. Owing to slightly better sorting in this breccia than in the One OClock Wash sedimentary breccia, the matrix is sandy in most locations and contains little silt. The matrix is commonly light pinkish brown, light gray-brown, or buff. The large volcanic clasts in the breccia, which are light to medium gray, stand out against the matrix. Because of its sandy matrix, this breccia is in most locations not as well indurated as the One OClock Wash sedimentary breccia; individual clasts break out easily. It is cemented by tridymite and potassium feldspar(?), which make up as much as 20 percent of the rock; small cavities are abundant. The lithology of the Noon Gorge breccia is contrasted with that of the One OClock Wash breccia in table 4.

PETROGRAPHY OF CLASTS AND ASH

The distinctive black olivine-trachyandesite clasts that occur in the breccia on the north side of the crater are dark gray to black on fresh surfaces and gray-brown to yellow-brown on weathered surfaces, with abundant red-brown grains of olivine (up to 1 mm across). They are vesicular to nonvesicular. In thin section they contain 6 percent olivine, 12 percent clinopyroxene, 25 percent plagioclase, 55 percent reddish brown glass, and 2 percent opaque minerals. Olivine occurs as small phenocrysts and microphenocrysts with light-brown rim alteration. Clinopyroxene occurs chiefly as microphenocrysts and groundmass prisms. The plagioclase laths, pyroxene prisms, and opaque minerals have sharp relief against the reddish-brown glass. The modal compo-

TABLE 4.—*Contrasts between the lithologies of the sedimentary breccia of One OClock Wash (Crater Pasture Formation) and the sedimentary breccia of Noon Gorge (Fort Rock Creek Rhyodacite)*

| Sedimentary breccia of One OClock Wash | Sedimentary breccia of Noon Gorge |
|--|--|
| Contains a trace or more of mafic to intermediate ash; contains no felsic volcanic clasts (rhyolite or rhyodacite). | Contains a trace to a few percent mafic to intermediate ash; contains a few beds rich in this ash; contains in many localities traces of felsic volcanic clasts (rhyolite or rhyodacite); on the north flank of the dome, contains distinctive black olivine-trachyandesite clasts, thought to be detrital clasts from the Road End Gap volcanic breccia and flow. |
| Massive. | Massive to very crudely bedded. |
| Unsorted; clasts commonly not easily distinguished from the matrix; the matrix contains a continuous clast-size distribution from silt size on up. | Unsorted to poorly sorted; clasts easily distinguished from the matrix; matrix sandy and contains little silt. |
| Moderately well indurated and poorly resistant to erosion; clasts do not break out easily; up to 5% tridymite and potassium feldspar(?) cement. | Poorly indurated and very poorly resistant to erosion; clasts break out relatively easily; up to 20% tridymite and potassium feldspar(?) cement; small cavities abundant. |
| In most areas characterized by clasts 3 cm in diameter or smaller, although much larger clasts are present; block patches abundant. | In most areas characterized by clasts 15 cm in diameter or smaller, although much larger clasts are present; no mappable block patches. |
| Clasts angular to subrounded. | Clasts angular. |
| Pinkish-brown with multicolored clasts; gray, red-brown, yellow-brown. | Gray clasts and light-brown to buff matrix; matrix commonly has white specks (rhyodacite or rhyolite). |

sition of this rock and the distinctive appearance of its groundmass makes it petrographically very similar to rock of the Road End Gap volcanic breccia and flow. Its chemistry (sample 325a, table 5) is also similar. Its recalculated silica content, 59 percent, is most similar to that of flow 2 (sample 195a, table 3) of the Road End Gap unit.

A small amount of mafic to intermediate ash is commonly present in the matrix of the breccia in most places. In hand specimen, it shows up as small grains, rarely larger than 2 mm, that are green, yellow-green, buff, gray-brown, and olive-brown in color and contain tiny orange (altered olivine) specks. Petrographically, this ash is identical to the olivine-trachyandesite ash in the Hidden Pasture tuff and conglomerate and in the One OClock Wash sedimentary breccia.

A bomblike clast that was taken from the tuffaceous sandstone and conglomerate on the north flank of One OClock Hill is an olivine trachyandesite or olivine trachybasalt. In hand specimen, it is dark brownish gray and vesicular. In thin section, it is seen to contain 5 percent pseudomorphs after olivine, 25 percent clinopyroxene, 25 percent plagioclase, 40 percent cryptocrystalline interstitial feldspar, and 5 percent opaque minerals. The pseudomorphs

TABLE 5.—Chemical and normative composition of the Fort Rock Creek Rhyodacite and other units

[Rapid analyses (Shapiro and Brannock, 1962) were performed by D.J. Emmons, R.L. Swenson, and Frank Cuttitta in laboratories operated by the U.S. Geological Survey. Normative minerals are calculated after subtracting CaCO₃ from the oxides. *, single clast; --, not detected.]

| Unit sampled Sample number 1/ | Sedimentary breccia of Noon Gorge | | Old Stage Road Member | | |
|---|------------------------------------|---|--|----------------------|----------------------|
| | *Olivine trachyandesite clast 325a | *Olivine trachybasalt clast from tuffaceous sandstone and conglomerate 452b | *Rhyolite clast from basal sedimentary breccia 300 | Ash-flow tuff 318 2/ | Ash-flow tuff 332 2/ |
| Oxide | Weight percent | | | | |
| SiO ₂ | 58.5 | 47.0 | 73.7 | 67.0 | 66.1 |
| Al ₂ O ₃ | 13.1 | 15.2 | 14.1 | 14.2 | 13.5 |
| Fe ₂ O ₃ | 2.8 | 9.1 | 1.0 | 1.6 | 1.9 |
| FeO | 3.10 | 1.2 | 1.4 | .52 | .54 |
| MgO | 6.4 | 4.3 | 3 | 1.2 | 2.0 |
| CaO | 5.7 | 6.1 | 1.2 | 2.2 | 2.2 |
| Na ₂ O | 3.2 | 1.6 | 4.2 | 3.4 | 2.8 |
| K ₂ O | 3.9 | 2.8 | 4.8 | 3.9 | 3.8 |
| TiO ₂ | .99 | 1.8 | .09 | .25 | .39 |
| P ₂ O ₅ | 3.4 | 1.1 | .06 | .08 | .13 |
| MnO | 10 | .14 | .05 | .10 | .07 |
| H ₂ O+ | 1.18 | 5.3 | .16 | 3.02 | 3.06 |
| H ₂ O- | .38 | 4.2 | .19 | 1.79 | 2.90 |
| CO ₂ | .35 | <.05 | .41 | .15 | .10 |
| Total | 100.00 | 99.8 | 100.4 | 99.4 | 99.5 |
| Normative mineral | Weight percent | | | | |
| Qz | 7.43 | 11.73 | 29.42 | 28.03 | 30.24 |
| Or | 23.60 | 18.32 | 28.62 | 24.45 | 24.07 |
| Ab | 27.73 | 15.00 | 35.86 | 30.53 | 25.40 |
| An | 10.11 | 25.56 | 3.01 | 10.02 | 10.10 |
| Co | -- | 1.20 | .91 | .98 | 1.43 |
| Dp | 11.26 | -- | -- | -- | -- |
| Hy | 13.00 | 11.86 | .75 | 3.17 | 5.34 |
| Ol | -- | -- | -- | -- | -- |
| Mt | 4.16 | -- | .36 | 1.36 | .90 |
| Ht | -- | 10.08 | .76 | .76 | 1.42 |
| Il | 1.93 | 3.14 | .17 | .50 | .79 |
| Sph | -- | -- | -- | -- | -- |
| Rut | -- | 3.4 | -- | -- | -- |
| Ap | .79 | 2.77 | .14 | .19 | .32 |
| Total | 100.00 | 100.00 | 100.00 | 100.00 | 100.00 |
| Color index | 30.34 | 25.41 | 2.05 | 5.79 | 8.45 |
| An/(Ab + An) | 26.71 | 63.02 | 7.74 | 24.72 | 28.45 |
| Or/(Or + Ab + An) | 38.41 | 31.12 | 42.41 | 37.62 | 40.41 |
| SiO ₂ (H ₂ O-, CaCO ₃ -free) | 59.89 | 52.03 | 74.35 | 71.08 | 70.85 |

TABLE 5.—Chemical and normative composition of the Fort Rock Creek Rhyodacite and other units—Continued

| Unit sampled Sample number | Old Stage Road Member | | | | Peach Springs Tuff of Young (1966) 5 |
|---|--|---|---|---------------------------------|--------------------------------------|
| | Vapor-phase-crystallized ash-flow tuff 333 | Rhyodacite intrusion on Three O'Clock Hill 187a | Rhyodacite intrusion in Five O'Clock Wash 207 | Basalt of Buttox Hills flow 205 | |
| Oxide | Weight percent | | | | |
| SiO ₂ | 70.3 | 66.6 | 67.1 | 47.4 | 67.0 |
| Al ₂ O ₃ | 10.8 | 14.8 | 15.9 | 15.5 | 13.8 |
| Fe ₂ O ₃ | 1.4 | 1.7 | 2.2 | 7.6 | 1.0 |
| FeO | .36 | 1.26 | .54 | 2.70 | .22 |
| MgO | 1.2 | 1.2 | 1.0 | 5.7 | 1.3 |
| CaO | 2.5 | 3.2 | 2.3 | 10.4 | 1.4 |
| Na ₂ O | 1.7 | 4.1 | 3.8 | 3.5 | 3.6 |
| K ₂ O | 2.7 | 4.1 | 4.1 | 1.4 | 4.4 |
| TiO ₂ | .26 | .44 | .33 | 1.83 | .21 |
| P ₂ O ₅ | .11 | .20 | .19 | .98 | .04 |
| MnO | .07 | .06 | .07 | .15 | .08 |
| H ₂ O+ | 4.37 | 1.62 | .57 | 1.22 | 3.53 |
| H ₂ O- | 3.39 | .53 | 1.90 | 1.62 | 3.15 |
| CO ₂ | .06 | .06 | .07 | .19 | .44 |
| Total | 99.2 | 99.9 | 100.1 | 100.2 | 100.2 |
| Normative mineral | Weight percent | | | | |
| Qz | 47.54 | 20.43 | 24.23 | -- | 27.67 |
| Or | 17.47 | 24.83 | 24.87 | 8.54 | 28.11 |
| Ab | 15.76 | 35.56 | 33.01 | 30.57 | 32.94 |
| An | 12.36 | 10.13 | 9.98 | 23.18 | 4.22 |
| Co | 1.04 | -- | 1.69 | -- | 1.82 |
| Dp | -- | 3.46 | -- | 17.31 | -- |
| Hy | 3.27 | 1.74 | 2.56 | 2.58 | 3.50 |
| Ol | -- | -- | -- | 2.83 | -- |
| Mt | .70 | 2.53 | 1.04 | 4.01 | .39 |
| Ht | 1.05 | -- | 1.54 | 5.08 | .81 |
| Il | .54 | .86 | .64 | 3.59 | .43 |
| Sph | -- | -- | -- | -- | -- |
| Rut | -- | -- | -- | -- | -- |
| Ap | .27 | .47 | .44 | 2.30 | .10 |
| Total | 100.00 | 100.00 | 100.00 | 100.00 | 100.00 |
| Color index | 5.56 | 8.58 | 5.78 | 35.40 | 5.13 |
| An/(Ab + An) | 43.96 | 22.17 | 23.22 | 43.13 | 11.36 |
| Or/(Or + Ab + An) | 38.33 | 35.21 | 36.65 | 13.71 | 43.07 |
| SiO ₂ (H ₂ O-, CaCO ₃ -free) | 76.98 | 68.25 | 68.86 | 48.91 | 72.44 |

1/ Sample locations:

| | |
|------|---|
| 325a | North side of Noon Hill |
| 452b | North side of One O'Clock Hill near the road |
| 300 | North bank of Ten O'Clock Wash. |
| 318 | Basal bed of ash-flow tuff on northwest side of Noon Hill |
| 332 | Bed of ash-flow tuff above basal bed in vicinity of Old Stage Road Butte. |
| 333 | Old Stage Road Butte. |
| 187a | Southeast flank of Three O'Clock Hill |
| 207 | West end of gully at head of Five O'Clock Wash |
| 205 | Base of Buttox Hills basalt flow on southwest side of Buttox Hills. |
| 5 | Partially welded ash-flow tuff from lower part of low cliff on top of Penitentiary Butte. |

2/ Visible accessory and accidental fragments (generally greater than 2 mm across) were removed by hand from these samples after the samples were disaggregated

after olivine are brown material on the rims and serpentine in the interiors; they occur as microphe-nocrysts up to 0.55 mm in length. Clinopyroxene occurs as prisms generally less than 0.3 mm in length and tiny (5 μm) orange groundmass granules. Plagioclase occurs as laths in the groundmass. The habit and abundance of clinopyroxene makes this rock pet-

rographically similar to the shonkinite intrusive body under the powerlines to the north and to the trachybasalt agglomerate to the west. It has a recalculated silica content of about 52 percent (sample 452b, table 5).

Light-gray trachyandesite ash constitutes most of the subunit mapped as tuffaceous granule and fine-

pebble conglomerate. An unmapped thin bed of this unit in Eight O'Clock Wash was examined in thin section. The ash contains scattered phenocrysts and microphenocrysts of hornblende (up to 1 mm long), and 5 percent tiny (50 μ m) red-brown pseudomorphs after olivine in a glassy microvesicular matrix containing feldspar microlites.

A few felsic clasts are scattered through the breccia in most places. In hand specimen, these clasts are white to light gray and range in size from specks to about 1 cm. They are characterized by small white feldspar phenocrysts, scattered biotite books and rarer hornblende prisms. In thin section, they are seen to contain rare plagioclase phenocrysts, as much as 25 percent microphenocrysts of sanidine (stubby laths up to 0.1 mm in length), scattered biotite books, and rare hornblende prisms. The matrix is glassy to cryptocrystalline.

OLD STAGE ROAD MEMBER

DISTRIBUTION, STRATIGRAPHY, AND PHYSICAL FEATURES

The Old Stage Road Member is here named after the Old Beale Wagon Road, which is preserved as deep ruts in ash-flow tuff on the north flank of the Fort Rock dome and in other places (see "Introduction"). Its type section is the easternmost butte of the Three Sisters; a reference section is Penitentiary Butte.

The Old Stage Road Member crops out over most of the area mapped as Fort Rock Creek Rhyodacite on the reconnaissance geologic map of the region (fig. 3). Outcrops extend from Penitentiary Butte on the west to near Cross Mountain on the east and from near the Kingman-Seligman county road on the north to near Trout Creek on the south. This member is 113 m (372 ft.) thick at Penitentiary Butte and 17 m (57 ft.) thick at the easternmost butte of the Three Sisters. It is thickest in areas where it fills basins, and it thins to a feather edge on the flanks of high hills on underlying rocks.

The Old Stage Road Member consists in most places of a basal pumiceous sandstone or tuff, or, on the flanks of the Fort Rock dome, a basal sedimentary breccia, overlain by beds of ash-flow tuff interlayered with thin beds of ash-fall lapilli tuff and sandstone. In the vicinity of Fort Rock Creek, lens-shaped regions within the beds of ash-flow tuff have undergone vapor-phase crystallization and have been mapped. Minor units that have been mapped include a lapilli breccia in the southwest part of the mapped area, and boulder patches on the southeast flank of the dome.

The basal pumiceous sandstone or tuff is generally poorly resistant to weathering, as it is thinly bedded and commonly fissile. In some places it weathers to slabs and has been quarried for building stone. Several buildings on the Fort Rock Ranch have been built with this stone. Ash-flow tuff is generally moderately resistant to weathering owing to its massive character; it tends to form low white bluffs. The zone of vapor-phase crystallization in the ash-flow tuff is resistant to weathering and underlies numerous low buttes in the vicinity of Fort Rock Creek.

RELATION TO OTHER UNITS

In the northeast part of its outcrop area, the Old Stage Road Member overlies chiefly the Crater Pasture Formation and Precambrian rocks (fig. 3). In most places on the flanks of the Fort Rock dome, it overlies the Noon Gorge sedimentary breccia of the Fort Rock Creek Rhyodacite. In the west and south parts of its outcrop area, it overlies the Crater Pasture Formation and undivided volcanic and sedimentary rocks. This member is overlain in the area west, south, and southeast of the Three Sisters by the Three Sisters Butte Member of the Fort Rock Creek Rhyodacite. In the area north of the ranch it is locally intruded and capped by younger andesite. In the area immediately southeast of the Fort Rock dome, it is overlain by rhyodacite-bearing sedimentary breccia and rhyodacite sandstone and by the basalt of Buttox Hills. In a large area east and southeast of the dome, it is overlain by Quaternary terrace deposits.

On the flanks of the Fort Rock dome, the contact between the basal unit of the Old Stage Road Member and the sedimentary breccia of Noon Gorge is gradational, characterized either by a gradual increase in the content of the felsic volcanic clasts by alternation of rhyodacite-poor sedimentary breccia with rhyodacite tuff or pumiceous sandstone. In One O'Clock Wash, the content of rhyolite (or rhyodacite?) clasts in the Noon Gorge breccia increases gradually. The contact with the basal sedimentary breccia of the Old Stage Road Member is placed at the horizon where the content of these clasts exceeds about 1/2 percent by volume. On the northwest side of Eight O'Clock Wash, rhyodacite-poor sedimentary breccia is interbedded with thin beds of white rhyodacite tuff and pumiceous sandstone. Here, the proportion of rhyodacite (or rhyolite?) fragments in the breccia follows a cyclic pattern whereby it is initially high (5 percent or more) above each rhyodacite tuff or sandstone bed and decreases upward to as little as a

trace; however, there is an overall increase in rhyodacite (or rhyolite?) fragments upward through the breccia in the section here. In this locality, the contact between the Noon Gorge sedimentary breccia and the basal sedimentary breccia of the Old Stage Road Member is placed at the base of the first pumiceous sandstone in the section.

LITHOLOGY

The basal sandstone or tuff is generally white, pumiceous, and fissile. The basal sedimentary breccia on the flank of the dome is generally similar in lithology to breccia of the underlying Noon Gorge unit, except that it is poorly to moderately sorted, crudely to well bedded, and contains white felsic specks and large light-gray, reddish-gray, and dark-red felsic volcanic clasts (up to 5 cm across; commonly 1 cm across). Locally, this sedimentary breccia includes pumiceous sandstone or tuff equivalent to the basal sandstone or tuff elsewhere. Ash-fall tuff in the Old Stage Road Member (not mapped separately) is well bedded, well sorted and is composed of white lapilli of pumice and up to 50 percent lapillized clasts of rhyodacite and (or) rhyolite, Precambrian rocks, and rocks of the Crater Pasture Formation. Ash-flow tuff is massive, unsorted, and nonwelded and contains 10 to 25 percent white pumice, a trace to 35 percent red to gray rhyodacite and (or) rhyolite accessory fragments, a trace to 10 percent accidental clasts of Precambrian rocks, and a trace to 10 percent accidental clasts of rocks from the Crater Pasture Formation. The remaining fraction of the tuff is gray to light pinkish gray matrix consisting of ash less than 2 mm across. Parts of the ash-flow tuff adjacent to the Fort Rock dome that contain more than about 35 percent detrital clasts from the dome and (or) rhyodacite accessory clasts are mapped as part of the basal unit. Ash-flow tuff that has undergone vapor-phase crystallization is mapped in places where 50 percent or more of the pumice in the tuff is crystallized; cavities occur in place of the pumice. Crystallized ash-flow tuff is porous, yellow-brown, and very hard. The lapilli breccia that is mapped is massive and consists chiefly of angular lapilli of rhyodacite and (or) rhyolite. It appears to grade, by decrease in lapilli and increase in ash, into ash-flow tuff, generally crystallized ash-flow tuff. Like the crystallized ash-flow tuff, the lapilli breccia is very hard. Boulder patches that are mapped are defined in the same way as block patches in the Noon Gorge and One OClock Wash sedimentary breccias. The boulders in these patches are dark-gray to dark-red rhyodacite containing abundant (20

to 25 percent) white plagioclase phenocrysts, up to 5 mm across, and fairly abundant (5 percent) black biotite books and hornblende prisms, up to 2 mm in largest dimension.

PETROGRAPHY

A fragment of light-gray, banded rhyolite, 4 cm in diameter, from the basal sedimentary breccia on the dome contains 1 percent oligoclase phenocrysts, up to 2 mm in length, $\frac{1}{2}$ percent sanidine phenocrysts, up to 2 mm in length, $\frac{1}{2}$ percent biotite phenocrysts, up to 1.5 mm across, 25 percent sanidine microphenocrysts averaging 0.1 mm in length, 3 percent biotite microphenocrysts, and a trace of quartz microphenocrysts. The matrix is cryptocrystalline.

A specimen from the lowest bed of ash-flow tuff on the Fort Rock dome contains 20 percent white pumice and almost no visible accessory or accidental fragments in a uniformly fine-grained gray matrix. The pumice is up to 3 cm across but averages $\frac{1}{2}$ cm across. In terms of identifiable grains in thin section, the rock is rhyodacite. Pumice fragments contain scattered phenocrysts of sanidine, plagioclase, biotite, and quartz, listed in order of abundance. The order of abundance of these grains in the matrix, where they are plentiful, is plagioclase, sanidine, quartz, and biotite. The overall volume percentage of grains is $1\frac{3}{4}$ percent plagioclase, $1\frac{1}{2}$ percent sanidine, 1 percent quartz, and $\frac{1}{2}$ percent biotite. The matrix also contains scattered clasts of Precambrian rocks, olivine trachyandesite, and rhyolite similar to the small fragment described above. It is difficult to separate Precambrian xenocrysts from volcanic crystals; the overall percentages of various crystal fragments given above includes some contamination from Precambrian rocks.

A specimen from a higher bed of ash-flow tuff on the Fort Rock dome contains 25 percent white pumice, 5 percent accessory fragments, and 2 percent accidental fragments in a light-pinkish-gray matrix of mixed grain size. Pumice and accessory and accidental fragments are up to 3 cm across but average $\frac{1}{2}$ cm across. In terms of identifiable grains in thin section, this tuff is also a rhyodacite. Pumice contains scattered phenocrysts of quartz, biotite, hornblende, plagioclase, and sanidine (rare), listed in order of abundance. The order of abundance in the matrix, where these grains are plentiful, is quartz, plagioclase, sanidine, biotite, and hornblende. The overall volume percentages of grains is $1\frac{1}{4}$ percent quartz, 1 percent plagioclase, $\frac{1}{2}$ percent sanidine, $\frac{1}{4}$ percent biotite, and $\frac{1}{8}$ percent hornblende. The matrix also contains scattered clasts of Precambrian

rocks, olivine trachyandesite, and rhyolite similar to the specimen described above. In other specimens of ash-flow tuff, some of the accessory fragments contain abundant phenocrysts of plagioclase and probably are rhyodacite rather than rhyolite.

A sample of vapor-phase-crystallized ash-flow contains 25 percent cavities by volume. Most cavities are at least partly lined by tridymite and potassium feldspar(?). These minerals occur as small (25 μm) clear, weakly birefringent, low-index tablets showing striations parallel to their longest dimensions. In some cases, the tablets are intergrown in a bladed habit on the cavity walls; in other cases, they occur as shingly aggregates. In areas where cavities are thickly lined with tridymite and potassium feldspar(?), the matrix of the rock is finely crystalline, and accessory fragments are recrystallized to relatively coarse interbladed aggregates of tridymite and potassium feldspar(?). Where cavities are only thinly or partly lined by these minerals, the matrix is glassy.

CHEMICAL COMPOSITION.

A chemically analyzed sample of the rhyolite clast described above from the basal breccia on the Fort Rock dome has a recalculated silica content of about 74 percent (sample 300, table 5). Its normative potassium feldspar content is about 28^{1/2} percent, which constitutes 42^{1/2} percent of the total normative feldspar in the rock. In an average rhyolite (Nockolds, 1954), normative potassium feldspar is 32 percent of the whole rock and about 51^{1/2} percent of the total normative feldspar. For comparison, in an average rhyodacite, normative potassium feldspar is 18 percent of the whole rock and 26^{1/2} percent of the total normative feldspar. Thus, this clast is chemically closer to the average rhyolite.

A sample of the lowest bed of ash-flow tuff of the Old Stage Road Member (sample 318, table 5) and a sample of a higher bed of ash-flow tuff (sample 332) are chemically similar. Both have a recalculated silica content of about 71 percent. Normative potassium feldspar in both rocks is about 24 percent and constitutes 37^{1/2} to 40^{1/2} percent of the total normative feldspar; thus they are intermediate between the average rhyolite and the average rhyodacite.

A sample of vapor-phase-crystallized ash-flow tuff (sample 333, table 5) is high in silica and low in alkali oxides compared to noncrystallized ash-flow tuff collected nearby (sample 332). Recalculated silica is about 77 percent in this rock. Total alkali oxides are two-thirds that of the sample 332. These differ-

ences presumably reflect a leaching of alkaline elements during vapor-phase crystallization.

THREE SISTERS BUTTE MEMBER

DISTRIBUTION, STRATIGRAPHY, AND PHYSICAL FEATURES

The Three Sisters Butte Member crops out over an area bounded by the Fort Rock Creek fault on the northeast, the Three Sisters on the north, Penitentiary Butte on the west, and Trout Creek on the south. This member is 116 m (379 ft) thick in the reference section measured at Penitentiary Butte and 77 m (253 ft) thick in its type section measured at the easternmost butte of the Three Sisters.

This member consists chiefly of interbedded volcanic breccia and massive tuff that grade laterally and vertically into one another. In addition, deposits of ash-fall lapilli tuff are thick enough to map in some places. In the type section, relatively thin beds of sandstone and conglomerate are locally present at or near the base of the member.

The Three Sisters Butte Member is poorly resistant to erosion and forms steep-sided hills covered by colluvium made up of angular rhyodacite lapilli and blocks. Volcanic breccia forms resistant ledges in some locations. At Penitentiary Butte and throughout most of the vicinity of Knight Creek, a resistant ledge of volcanic breccia occurs at the base of this member. Massive tuff is rarely exposed. Where it does crop out, it rarely forms bluffs like those that characterize ash-flow tuff of the underlying Old Stage Road Member.

RELATION TO OTHER UNITS

Throughout most of its outcrop area, the Three Sisters Butte Member overlies the Old Stage Road Member. In the vicinity of Trout Creek, it locally overlies older rocks. It is overlain at the Three Sisters and in a large area south of Three Sisters and southwest of the Fort Rock Creek fault by the breccia and conglomerate of the Crossing. It is capped at Penitentiary Butte and several other nearby buttes by the Peach Springs Tuff of Young (1966).

The contact between the Three Sisters Butte Member and Old Stage Road Member is chosen in the type section at the base of thin sandstone and breccia beds (total thickness 15 cm) that separate ash-flow tuff from a sequence consisting chiefly of interbedded volcanic breccia and massive tuff. On the east side of the butte the sandstone bed is considerably thicker (4 m). At Penitentiary Butte, the contact is placed at the base of a ledge-forming breccia.

cia (up to 3 m thick) that separates ash-flow tuff from a bedded pumiceous tuff overlain by volcanic breccia. Along Fort Rock Creek, the contact between the two members appears to be in part gradational. Here, a lapilli breccia assigned to the Old Stage Road Member grades downward into vapor-phase-crystallized ash-flow tuff of the Old Stage Road Member and upward into volcanic breccia of the Three Sisters Butte Member.

LITHOLOGY

In general, the volcanic breccia is poorly sorted and weakly indurated. Where it is moderately sorted, it is commonly a strongly indurated, ledge former, dark red on a fresh surface and dark red to buff on a weathered surface. In general, clasts in the breccia are angular to locally subrounded. The modal diameter ranges from 1 to 12 cm but commonly is 5 cm. Maximum clast size is commonly around 30 to 60 cm. Clasts are chiefly red to gray rhyodacite, containing abundant (25 percent) white plagioclase phenocrysts up to 5 mm across, and fairly abundant (5 percent) biotite books and hornblende prisms up to 2 mm in largest dimension. The matrix in these rocks is glassy to lithic. None of the clasts were studied in thin section, but the petrography is similar to that of a rhyodacite intrusion on Three OClock Hill (see below). Only a few clasts of Precambrian rocks and rocks from the Crater Pasture Formation are found in the breccia.

The massive tuff lithologically resembles ash-flow tuff of the underlying Old Stage Road Member, except that accessory clasts are more heterogeneous in size and include large clasts similar to those found in beds of volcanic breccia, into which the massive tuff grades. Additionally, accidental clasts of Precambrian rocks and rocks from the Crater Pasture Formation are rare (generally a trace to 1 percent), whereas these clasts are fairly abundant (generally a few percent) in ash-flow tuff of the Old Stage Road Member. At Penitentiary Butte, the tuff beds in the Three Sisters Butte Member are faintly laminated, whereas the tuff beds in the Old Stage Road Member are faintly graded. Pumice is more heterogeneous in size in the Three Sisters Butte tuff.

BRECCIA AND CONGLOMERATE OF THE CROSSING

DISTRIBUTION AND PHYSICAL FEATURES

The breccia and conglomerate of the Crossing forms the caprock of the Three Sisters and caps an

east-southeast-trending, fault-bounded escarpment south of the Three Sisters (figs. 2, 3). This escarpment swings to the southeast near Fort Rock Creek and is parallel to the creek in the vicinity of the Crossing (pl. 1). On the east side of the creek, the breccia and conglomerate of the Crossing underlies the top of the high hill bounded on the east by Fault Canyon (pl. 1). The unit crops out over most of the area between the escarpment and the large eruptive center in the Aquarius Mountains.

The breccia and conglomerate of the Crossing is characterized by very coarse angular blocks of red to gray rhyodacite reaching diameters of 3 meters. The unit is poorly resistant to weathering except where it forms the caprock of the Three Sisters. Generally it is covered by coarse colluvium.

RELATION TO OTHER UNITS

This unit overlies the Three Sisters Butte Member. It is overlain at the Three Sisters by small outcrops of massive tuff similar to massive tuff in the Three Sisters Butte Member.

At the Three Sisters, the basal contact of the breccia and conglomerate of the Crossing is sharp and probably unconformable. In a cliff on the north side of a major wash that joins Fort Rock Creek from the west at a location 270 m south of the Crossing (pl. 1), the contact is unconformable on top of massive (ash-flow?) tuff of the Three Sisters Butte Member. In cross section B-B' (pl. 2), the contact is interpreted to be an unconformity; the breccia and conglomerate of the Crossing is interpreted to fill an ancient valley in the top of the Three Sisters Butte Member at the site of present-day Fort Rock Creek.

LITHOLOGY

Except for local conglomerate beds, this unit is poorly to moderately poorly sorted and consists of angular clasts. The modal diameter ranges from 10 to 50 cm. Clasts are gray to red rhyodacite that appears to be petrographically similar to rock of the small intrusion on Three OClock Hill (described below).

MISCELLANEOUS UNITS

RHYODACITE INTRUSION ON THREE O'CLOCK HILL

An intrusive body of rhyodacite crops out on the southeast flank of Three OClock Hill. It is elongated in a northeast-southwest direction; it measures 100

by 45 m. The outcrop consists of blocks of rhyodacite up to 1.5 m across that appear to fit together as parts of blocks as large as 6 m across. Although contacts are not exposed, this body is assumed to be an intrusion because of its isolated occurrence.

The rock is gray to red-brown with abundant white phenocrysts of plagioclase, black books of biotite, and black prisms of hornblende. It is massive to locally banded. In terms of grains that can be identified in thin section, the rock is a dacite, although it is chemically a rhyodacite. In thin section, it is seen to contain 30 percent oligoclase, 6 percent hornblende, 5 percent biotite, $\frac{1}{2}$ percent sanidine, and traces of quartz, augite, and hypersthene in a glassy matrix. Oligoclase occurs as euhedral to broken or rounded phenocrysts up to 4 mm in length and as smaller fragments in the glassy matrix. Sanidine occurs as broken or rounded microphenocrysts up to 0.5 mm and as smaller fragments in the matrix. Biotite and hornblende occur as books and prisms, often broken, up to 3 mm in maximum dimension. Quartz occurs as embayed microphenocrysts 0.5 mm across. Augite occurs as microphenocrysts 0.5 mm across partly altered to hornblende. Hypersthene occurs as small grains 0.1 mm across in the matrix. The glass of the matrix was analyzed using an electron microprobe and was found to contain 77 percent silica, 12 percent alumina, $3\frac{1}{2}$ percent potassium oxide, 1 percent sodium oxide, $\frac{1}{2}$ percent each of calcium oxide and iron oxide, and about 5 percent water(?). This glass has the composition of a mixture of quartz and sanidine.

A chemically analyzed whole-rock sample contains 68 percent recalculated silica (sample 187a, table 5). Normative potassium feldspar is about 25 percent, and constitutes about 35 percent of the total normative feldspar. Chemically, the rock is most similar to the average rhyodacite (Nockolds, 1954).

SEDIMENTARY BRECCIA, SANDSTONE, AND CONGLOMERATE

A thin deposit of rhyodacite-bearing sedimentary breccia and rhyodacite sandstone and conglomerate overlies ash-flow tuff of the Old Stage Road Member in the Buttox Hills. It ranges in thickness from a feather edge to 9 m at most. It is rarely exposed but is characterized by abundant float of massive rhyodacite (including boulders), Precambrian rocks, and rocks from the Crater Pasture Formation. Clasts in this deposit are derived from units on the dome and on the flank of the dome to the northwest and north. Rhyodacite clasts appear to be petrographically similar to rhyodacite of the intrusion on the

flank of Three O'clock Hill. This deposit is overlain by the basalt of Buttox Hills.

SOURCE OF THE FORT ROCK CREEK RHYODACITE

The Fort Rock Creek Rhyodacite is distributed around a large eruptive center in the Aquarius Mountains (fig. 3). Some units can be traced to extrusive rocks on the flanks of the eruptive center, and others cannot; however, the center has only been studied in reconnaissance by the author. In addition to the large eruptive center, several smaller intrusive bodies in the western part of the Aquarius Mountains were sources of parts of the Fort Rock Creek Rhyodacite. Rocks within this formation were emplaced chiefly as ash flows, ash and block falls, and volcanic mudflows.

AQUARIUS MOUNTAINS ERUPTIVE CENTER

The Aquarius Mountains eruptive center is a complex body of massive intrusive rocks, shown by a hachure pattern on the reconnaissance geologic map (fig. 3), flanked by pumiceous agglomerate, volcanic breccia, and lava flows. Radiating rhyodacite dikes cut all rocks in this center.

Stratigraphy in the pumiceous agglomerate, volcanic breccia, and lava flows on the flanks of the center is complicated owing to rapid facies changes, intrusion of dikes, and faulting. Two sequences of rocks can be recognized on the west flank of the center, however, and these sequences are similar to one another. The oldest sequence consists of a basal pumiceous agglomerate overlain by a lava flow. The agglomerate appears to grade into the flow through a zone where its clasts become compressed, welded, and ultimately indistinguishable from one another and from overlying banded flow rock. The second sequence overlies the first and consists of a basal volcanic breccia overlain by a lava flow. As in the first sequence, the breccia becomes indistinguishable from overlying flow rock in a zone of welding near its top.

These two sequences of extrusive rocks can be correlated, in part, with the Old Stage Road and Three Sisters Butte Members of the Fort Rock Creek Rhyodacite. A distinctive ledge-forming bed of volcanic breccia at the base of the Three Sisters Butte Member (unit 17 in the reference section), traceable throughout most of the vicinity of Knight Creek, has been tentatively traced to breccia on the west flank

of the eruptive center that overlies rocks of the older sequence and underlies rocks of the younger sequence. On the northwest flank of the eruptive center, the lava flow in the younger sequence is underlain on its distal (northwest) end by massive tuff of the The Three Sisters Butte Member and is overlain by breccia and massive tuff of this member. Thus, the Three Sisters Butte Member correlates, at least in part, with the younger sequence. The Old Stage Road Member probably correlates in a similar fashion with the older sequence, although none of its beds of ash-flow tuff can be traced directly into the eruptive center. On the other hand, it is entirely likely that the ash flows represented by the Old Stage Road Member were rootless.

MINOR INTRUSIVE BODIES

Three relatively small bodies of intrusive breccia and banded rocks occur to the west of the large eruptive center. One body, located 2.8 km west (fig. 3), is a rhyodacite neck that intrudes the Three Sisters Butte Member at that location. This neck may have been a source for a higher part of this member. A second body, located 6 km west of the center, near Knight Creek, was the source for a local sequence of rhyolitic sandstone, tuff, volcanic breccia, and flow, all of which is older than the Old Stage Road Member. The largest intrusive body, Austin Peak, a rhyodacite neck located about 2¹/₂ km southwest of Penitentiary Butte, rises 300 m above surrounding Precambrian rocks. It is not conspicuously related to any nearby deposits of the Fort Rock Creek Rhyodacite.

MODE OF EMPLACEMENT OF EXTRUSIVE ROCKS

The basal pumiceous sandstone or tuff of the Old Stage Road Member blankets underlying topography and is very evenly bedded with little channeling. Cross-lamination is seen in one or two localities. The sandstone or tuff probably was emplaced as an ash-fall or as a "base surge."

ASH-FLOW TUFF

The beds of unsorted to poorly sorted tuff in the Old Stage Road Member were emplaced as ash flows. They are homogeneous over large distances; they have graded structure suggestive of single, shortlived episodes of emplacement; they fill basins and thin to a feather edge on the flanks of high hills; and

they were emplaced with entrapped steam, as is indicated by zones of vapor-phase crystallization. (Refer to Ross and Smith, 1961, for characteristics of ash-flow tuffs.)

The beds of unsorted to poorly sorted tuff in the Old Stage Road Member are similar throughout most of its outcrop area. Compare, for example, unit 7 in the type section with unit 2 in the reference section. These beds are not correlatable, but they are very similar. They have the same clast-size distribution; both have a subtle graded structure. They also have similar clast composition, except that the bed exposed at the Three Sisters contains more accessory and accidental fragments. These tuff beds in the Old Stage Road Member contrast in their homogeneity with the beds of massive tuff in the Three Sisters Butte Member. The latter beds undergo lateral and vertical facies changes into volcanic breccias over short distances.

That the unsorted to poorly sorted tuffs of the Old Stage Road Member were emplaced as fluids is apparent from the fact that these beds fill basins and thin out on the flanks of hills that existed prior to eruption. Thinning can be seen in several locations near the Fort Rock dome, most notably at an outcrop along the ranch road 330 m north of Casa Grande (pl. 1) and at an outcrop at the east end of Annex Ridge, beyond the mapped area. No outcrops of unsorted to poorly sorted tuff are found above an elevation of about 5,150 ft (1,570 m) on the Fort Rock dome, Annex Ridge, and the escarpment on the Precambrian rocks north of the dome (see fig. 9, map 10). Apparently the top of the Old Stage Road Member was a level surface, as one might expect of a fluid.

Crystallization of pumice and glass shards in ash-flow tuff has been described in some localities as a phenomenon associated with welding (see, for example, Smith and Bailey, 1966, and Fisher, 1966). Crystallization results from slow cooling of the tuff under the influence of entrapped steam. It commonly occurs in a zone adjacent to the zone of welding where steam is expelled during compaction. In other localities, crystallization in tuff is not associated with welding (see Fenner, 1948). In these cases, entrapped steam is presumably also responsible for the crystallization, but temperatures are not high enough to cause welding. Such conditions apparently prevailed during emplacement of the Old Stage Road Member. In addition to the zones of vapor-phase crystallization shown on the geologic map (pl. 1), an extensive zone occurs immediately northwest of the Fort Rock Ranch headquarters and another about 3 km northeast of the headquarters. These zones transect the

contacts between individual beds; hence, some of the beds were emplaced in rapid succession.

VOLCANIC BRECCIA

The distinctive ledge-forming volcanic breccia at the base of the Three Sisters Butte Member in the vicinity of Knight Creek (unit 17 in the reference section) has the characteristics of a flow. It is relatively homogeneous over a large area, and it thins to a feather edge on the flanks of high hills. This breccia may have been emplaced as a lahar, or volcanic mudflow. The breccia and conglomerate of the Crossing may likewise represent a volcanic mudflow on the northeast flank of the eruptive center; it apparently fills at least one canyon in the top of the Three Sisters Butte Member (pl. 2).

MASSIVE TUFF

Some of the massive tuff of the Three Sisters Butte Member may have been emplaced as ash flows, but unlike ash-flow tuff of the underlying Old Stage Road Member, beds cannot be traced for large distances laterally; they grade into beds of volcanic breccia. No zones of vapor-phase crystallization are observed; therefore, evidence of emplacement with entrapped steam is lacking. This tuff and associated volcanic breccia were probably emplaced chiefly as massive ash and block-fall deposits. Local ash flows and volcanic mudflows may also have occurred.

MISCELLANEOUS UNITS

RHYODACITE INTRUSION IN FIVE OCLOCK WASH

A body of rhyodacite is located at the west end of the gully at the head of Five OClock Wash (pl. 1). It intrudes Precambrian rocks, also exposed in the gully. It is light gray and contains abundant white phenocrysts of plagioclase, black books of biotite, and black prisms of hornblende. The larger grains in thin section include 12 percent oligoclase phenocrysts, a trace of small phenocrysts of sanidine, 3 percent biotite books, and 1 percent hornblende prisms. The matrix constitutes 84 percent of the rock, of which 25 percent is microphenocrysts of sanidine, 30 percent is microphenocrysts of quartz, 2 percent is opaque minerals, less than 1 percent is apatite prisms, and 27 percent is cryptocrystalline minerals. Oligoclase phenocrysts are euhedral to broken and rounded and are up to 5 mm in length. Biotite

and hornblende are up to 2 mm in maximum dimension. In the matrix, sanidine occurs as relatively sharp, stubby, rectangular grains averaging 0.1 mm across. Quartz occurs as indistinct equant grains about 0.1 mm across that are heavily occluded with dust and difficult to identify. These grains may have formed during contact metamorphism by nearby intrusive bodies of the basalt of Buttox Hills. Contact metamorphism in adjacent Precambrian rocks is seen in a conversion of microcline to sanidine and in oxidation of mafic minerals.

Except for apparent contact-metamorphic features, this rhyodacite is petrographically similar to tiny fragments found in the basal tuffaceous breccia and sandstone of the Crater Pasture Formation in Four OClock Wash. On this basis, this rhyodacite body is thought to be older than the Crater Pasture Formation.

A chemically analyzed specimen of this rock (sample 207, table 5) has a recalculated silica content of 69 percent. Normative potassium feldspar is about 25 percent of the whole rock and constitutes 36¹/₂ percent of the total normative feldspar. Chemically, the rock is intermediate between the average rhyodacite and the average rhyolite (Nockolds, 1954).

BASALT OF BUTTOX HILLS

DISTRIBUTION, STRATIGRAPHY, AND PHYSICAL FEATURES

The basalt of Buttox Hills underlies the Buttox Hills, part of a narrow ridge east of the Buttox Hills and part of Three OClock Hill. It also forms a dike roughly parallel to Five OClock Wash, and a series of plugs aligned with the dike inside the crater. The dike varies in width from a meter or so to 60 m, and the distance from the southeast end of the dike to the northwesternmost plug is 1¹/₂ km. The maximum preserved thickness of basalt flow in the Buttox Hills is about 23 m.

This unit consists of basalt flow, intrusive basalt, tuff and tuff-breccia, and undivided basalt. The flow and intrusive rocks are generally resistant to erosion, but the tuff and tuff-breccia are not.

RELATION TO OTHER UNITS

In most places, this unit overlies a rhyodacite-bearing sedimentary breccia and rhyodacite sandstone and conglomerate of the Fort Rock Creek Rhyodacite. Locally it overlies ash-flow tuff of the latter formation or Annex Ridge flow of the Crater

Pasture Formation. The dike of Buttox Hills basalt intrudes ash-flow tuff, Annex Ridge flow, and Precambrian rocks. In a concealed body of tuff-breccia northwest of the dike and 120 m southwest of Sams Camp, fragments of basalt include small clasts of rhyodacite that are identical in hand specimen to the rhyodacite intrusion in the gully at the head of Five O'Clock Wash. Contact metamorphism of both the rhyodacite and Precambrian rocks in the area between the end of the dike and the concealed body of tuff-breccia appears to be related to intrusion of the basalt.

This basalt is overlain on the narrow ridge east of Buttox Hills by terrace deposits.

SOURCE

Intrusive basalt, characterized by irregular contacts and steeply dipping banding, where banding is present, occurs in the northwest part of the Buttox Hills. Relatively flat-lying basalt flow occurs in the southeast part of these hills and on the narrow ridge to the east. The flow can be traced continuously into the intrusive body. The dike may have also been a small source for the flow. Bodies of tuff and tuff-breccia in the northwest part of the Buttox Hills probably are partly intrusive and partly extrusive in nature. A thin blanket of reddened tuff that underlies the flow to the southeast can be traced continuously, except where it is covered by colluvium, into these bodies of tuff and tuff-breccia. These bodies probably also were the source for the patch of tuff on the east flank of Three O'Clock Hill.

PETROGRAPHY

Basalt flow and intrusive basalt are steel-gray on weathered surfaces and dark gray to black on fresh surfaces. Near the base of the flow and near the edges of the intrusive basalt, the rock has flow cleavage and bands of tiny vesicles. The tuff and tuff-breccia contain red to olive-brown vesicular ash, lapilli and (rare) bombs of basalt, and as much as 5 percent angular fragments of Precambrian rocks (up to several centimeters across), Annex Ridge flow (up to more than 30 cm across), and olivine trachyandesite (up to several centimeters across).

In thin section, a sample of the basalt flow is seen to contain 1 percent pseudomorphs after olivine phenocrysts, 23 percent clinopyroxene grains (all sizes), 12 percent pseudomorphs after olivine microphenocrysts, 49 percent groundmass labradorite (determined by microprobe), and 15 percent opaque minerals. The pseudomorphs after olivine are red-brown to red min-

erals on their edges and serpentine in their centers. The phenocrysts reach a size of 1 mm across. The microphenocrysts are distinctive in that they are uniform in size, about 0.1 mm across; they can be seen as red specks in hand specimen. Clinopyroxene is distributed continuously in sizes from 1 mm down to groundmass grains, but only about 3 percent occurs as grains greater than 0.1 mm. The larger grains are diopsidic augite and commonly occur as glomerophenocrysts. The texture of the rock is intergranular to pilotaxitic.

In rock of the dike and rock of the small plugs northwest of the dike, clinopyroxene commonly occurs abundantly (10 percent) in sizes greater than 0.1 mm and the total content of pseudomorphs after olivine is only about 5 percent.

CHEMICAL COMPOSITION

A sample of the Buttox Hills basalt (sample 205, table 5) contains 49 percent recalculated silica, which is well within the range of basic composition. Potassium oxide is only 1.4 percent, in contrast to rocks of the Crater Pasture Formation. This rock is chemically similar to an average alkali basalt (Nockolds, 1954).

QUATERNARY SEDIMENTARY DEPOSITS

Quaternary sedimentary deposits in the vicinity of the Fort Rock dome include alluvium, colluvium, and high terrace deposits. The unit mapped as "alluvium" includes modern alluvium in washes and older alluvium on low terraces on the flanks of the dome. The unit mapped as "colluvium and high terrace deposits" includes all surficial cover not mapped as alluvium. Alluvium is shown on the geologic map where it exceeds a thickness of about 15 cm; colluvium and high terrace deposits are shown where they exceed a thickness of 30 to 45 cm.

Alluvium is distinguished from colluvium by composition and sorting. It contains clasts that have been transported some distance and, in many locations, are foreign to local rock types. For example, on the west and northwest flanks of the dome, alluvial fans contain chiefly clasts of Precambrian rocks from the interior of the crater, whereas colluvium is composed chiefly of rocks of the Crater Pasture Formation from nearby areas on the rim and flank. Additionally, alluvium is better sorted than colluvium. Its finest particles are silt, whereas the finest particles in the colluvium are clay. Colluvium also contains abundant caliche.

High terrace deposits generally contain abundant clasts of Paleozoic rocks, chiefly dark-red fragments of Tapeats Sandstone. Locally these deposits are cemented by caliche or calcite and are well indurated. An extensive area east of the Fort Rock dome is underlain by these high terrace deposits. Within the area mapped (pl. 1), these deposits occur on the north flank of One O'Clock Hill, on the northeast flank of Lion Ridge, and in the area east of Three O'Clock Hill. The clasts in these deposits were derived from Cross Mountain or from terrain to the east and north-east.

STRUCTURE

PRECAMBRIAN STRUCTURES

On the Fort Rock dome, Precambrian structures were deformed during doming, but in most cases it is possible to distinguish them from younger structures. A large fold or fault is apparent in the vicinity of Lion Ridge, but the rotation of attitudes that occurred during doming must be removed, using a stereonet, in order to observe this structure clearly. Small folds are seen in layered metamorphic rocks. These are unaffected by doming except for rotation. A broad shear zone characterized by fractured and veined rocks crosses the south half of the crater. Fractures are in most cases distinct from the largely unmineralized fractures and breccia lenses that were formed during doming.

FOLDS

A large structure in the Precambrian rocks is apparent in the vicinity of Lion Ridge. In the exposure of the Precambrian rocks northeast of the crater, the foliation dips, on the average, about 75° to the west-northwest. In the north half of the crater, however, the foliation presently dips about 60° to the south. The effect of doming can be removed from attitudes inside the crater by rotating each attitude, using a stereonet, in a direction counter to the rotation caused by doming; the amount of rotation necessary is determined from the cross sections (pl. 2). This procedure leaves the strike of the foliation of rocks inside the crater nearly unchanged but steepens the dip to an average of 75° to 80° south (fig. 4). A large difference in attitude between rocks inside and outside of the crater remains, reflecting a structure that predates the formation of the dome. This structure might be a fold or a fault. It is also pos-

sible that two different foliations were developed in the rocks, in which case no large structure is required to explain the observations. If a structure is present, its axis must lie beneath Lion Ridge, where the two sets of attitudes are separated by less than 270 m. Such a structure would lie along the north-west projection of the Upper Two O'Clock Gap fault, which is a Tertiary structure (see below). More of the Precambrian rocks northwest of the crater must be mapped to interpret this structure fully.

Small folds, measuring centimeters to meters in amplitude, occur in the layered metamorphic rocks. These folds are most easily seen in the well-exposed gneiss in the northwest quadrant of the dome. They are largely isoclinal and may reflect large-scale isoclinal folding. The lack of distinct units in the layered metamorphic rocks, however, prevents the recognition of large folds. Some folds can be observed in which foliation locally bends to follow the margins of pegmatites.

SHEAR ZONE

A broad shear zone crosses the south half of the Fort Rock crater, characterized by Precambrian rocks that have been fractured and veined. These fractured and veined rocks are covered by Tertiary volcanic rocks on the rim of the crater. Seven kilometers north of the crater, rocks in a similar shear zone are covered by Tapeats Sandstone of Cambrian age. Minor hematite-veined fractures seen in places in the Tapeats Sandstone indicate minor renewed movement in this zone in Phanerozoic time.

The spatial density of veined fractures in the shear zone in the Fort Rock crater has been mapped (fig. 4). Isopleths marking the divisions between different levels of vein density (refer to fig. 4 for definitions) trend largely east-west in the center of the crater, swing around to the southwest in the west and southwest part of the crater and appear to be discontinuous in the east part. From north to south across the shear zone there is a fairly regular increase in the density of veins from low to very high, followed by a more erratic decrease in density to moderate. Veins are moderately dense in most of the exposed Precambrian rocks in the south part of the crater. Rock type influences to some extent the density of veins. In Eight O'Clock Basin, for example, the cataclastite of Eight O'Clock Basin forms an elongate pocket of moderate vein density within a zone of high vein density.

The shear zone may be part of a major Precambrian fault zone. Rocks in the north half of the crater generally are different from those in the south half. For example, pegmatites are abundant north of the shear zone but are nearly absent in the south. No Precambrian unit that was mapped in the north can be traced across the zone. In addition, metamorphic grade differs slightly between rocks in the north and south halves of the crater. North of the shear zone, the layered metamorphic rocks belong entirely to the epidote-amphibolite facies, whereas in the south half of the crater, within the shear zone, some rocks of greenschist facies are found.

A discontinuity of large proportions passing through the vicinity of the Fort Rock dome is apparent on an aeromagnetic map of Arizona (Sauck and Sumner, 1971). The dome lies on a line bounding a series of positive magnetic anomalies that trends west-southwest from the vicinity of Ashfork, Ariz., to the west border of the Aquarius Mountains. The magnetic anomalies have low gradients and bear no direct relation to volcanic rocks in the region; they are apparently caused by differences in the properties of the Precambrian basement rocks (Shoemaker and others, 1974). Linear margins on the anomalies imply linear discontinuities of rock type that probably correspond to an ancient fault zone. In support of this hypothesis, Tertiary volcanic rocks are offset by west- and west-southwest-trending normal faults in places along the margins of the anomalies. Examples of such faults are seen in the northwest part of the Aquarius Mountains and in the south part of the Cottonwood Cliffs (fig. 3). These faults are believed to have been formed by renewed movement on the ancient system of faults (see Shoemaker and others, 1974).

The shear zone exposed on the Fort Rock dome may be similar in structure to the Shylock fault zone, which is exposed for a distance of about 80 km between Black Canyon and Mingus Mountain in central Arizona. The Shylock fault zone trends north-south and is covered at the north end by Tapeats Sandstone of Cambrian age. This structure separates Precambrian rocks of widely differing composition at its north end and rocks of similar composition but differing metamorphic grade at its south end. A minimum of 8 km of right-lateral displacement can be documented at its north end, although displacement may be less at its south end (Anderson and Creasey, 1958, p. 77; Anderson, 1967). A pronounced linear boundary of aeromagnetic anomalies is present along the entire exposed length of the fault zone. Movement along this fault zone produced foliation and

fissility in the rocks that were sheared, whereas movement along the shear zone on the Fort Rock dome produced only brittle fractures that were subsequently veined.

The shear zone on the Fort Rock dome was presumably a zone of weakness along which the body of magma that ultimately caused doming was intruded. It is not clear, however, what structural feature within the shear zone caused the magma to be restricted to a plug shape during intrusion rather than a dike. Perhaps the offset in the shear zone on the east side of the dome (fig. 4, queried buried fault) was such a feature. The rhyodacite eruptive center in the Aquarius Mountains and other intrusive bodies to the west-southwest (fig. 3; see "Source of the Fort Rock Creek Rhyodacite") were possibly also controlled by this shear zone. It is interesting to note that accidental clasts of Precambrian rocks in the Fort Rock Creek Rhyodacite commonly are fractured and veined in a manner similar to the Precambrian rocks exposed in the shear zone on the Fort Rock dome.

TERTIARY PRE-DOME FAULTS

A number of faults on the rim of the crater offset rocks as young as the Two O'Clock Gap tuff and flow of the Crater Pasture Formation but are either covered or intruded by rocks that predate the uplift of the dome. One such fault, on Four O'Clock Hill, may have been ancestral to the Four O'Clock Hill fault, which formed during doming. Another fault, the Upper Two O'Clock Gap fault, underwent movement prior to doming in a direction opposite to its movement during doming. These and other pre-dome faults are discussed below in order of the age of the rocks that cover them; faults covered by the oldest rocks are discussed first.

The Road End Gap volcanic breccia and flow is offset by three faults that are covered by the Annex Ridge flow (pl. 1). One of these faults, a north-south-trending fault on Six O'Clock Hill, offsets the Road End Gap volcanic breccia and flow by as much as 23 m stratigraphically. A second, east-west-trending fault on Four O'Clock Hill offsets this unit by about 15 m stratigraphically, and a third fault, which trends west-northwest and lies about 120 m farther northeast on the same hill, offsets this unit and is accompanied by a change in attitude of rocks on either side. Rocks along these faults are displaced down on the east, north, and northeast, respectively. No fault scarps are preserved beneath the Annex Ridge flow; the Road End Gap unit is thinner on

upthrown sides of the faults, indicating a period of erosion between faulting and emplacement of the Annex Ridge flow. A reverse-facing fault-line scarp is, however, preserved along the east-west-trending fault on Four O'Clock Hill, as there is a small buried hill on the downthrown side of this fault beneath the Annex Ridge flow. The east-west-trending fault is closely associated geographically and in trend with the structurally complex southwesternmost part of the Four O'Clock Hill fault. The Four O'Clock Hill fault offsets the Annex Ridge and Lion Ridge flows and apparently was formed during doming. The east-west-trending fault may have been ancestral to this fault.

The Eight O'Clock Gorge flow is offset by two faults that are covered by the Buffalo Ridge flow (pl. 1). One, on the top of Nine O'Clock Hill, trends east-west and has a stratigraphic displacement of about 21 m. A smaller fault is seen near the top of Eight O'Clock Hill. No scarps are preserved on these faults beneath the Buffalo Ridge flow.

Atop Buffalo Ridge, the Road End Gap unit is offset of by a number of faults that are associated with intrusive bodies that fed the Buffalo Ridge flow (pl. 1; pl. 2, cross section *B-B'*). Five small north-south-trending faults east of the boot-shaped intrusion atop this ridge drop the Road End Gap unit successively down in the direction of the intrusion. On the west side of the boot-shaped intrusion, an 18- by 15-m block of the Road End Gap unit is dropped down along an east-west and a north-south-trending fault, which are both intruded by intrusive breccia. Farther west, three similar-sized blocks have been faulted successively down to the west in the direction of another intrusive body. On the northwest side of the latter body, a block of Road End Gap volcanic breccia has been dropped and rotated parallel to the margin of the intrusion such that the basal contact of the breccia now strikes perpendicular to Buffalo Ridge. All of this faulting adjacent to Buffalo Ridge intrusives seems to represent collapse of wallrock into eruptive vents.

In Two O'Clock Gap, the Two O'Clock Gap tuff thins abruptly across the Upper Two O'Clock Gap fault (pl. 1; pl. 2, cross section *C-C'*). This unit is overlain here by Lion Ridge flow. In order to explain the thinning, it is estimated that prior to emplacement of the Lion Ridge flow, the rocks in the southwest wall of the fault moved up relative to those on the northeast by an amount ranging from 15 m along the northwest exposure of the fault to 9 m along the southeast exposure. Later movement on this fault during doming took place in the opposite direction.

THE FORT ROCK DOME

The Fort Rock dome is a structural dome, 2.4 km in diameter, whose central part has been deeply excavated by erosion. The edge of the dome is in most places a monocline, whose steeply dipping limb has been preserved as the "rim" of the "crater." Most faults shown on the geologic map (pl. 1) are related in origin to the dome. They are mappable only in the vicinity of the monocline, perhaps partly as a result of poor exposure and lack of structural control in the deeply eroded central part of the dome. In addition to the mapped faults, abundant small faults, with displacements of a meter or less, and lenses of unmineralized breccia occur everywhere in the structure. These features are also related in origin to doming. All units of the Crater Pasture Formation older than the Fault Canyon flow are strongly uplifted and deformed on the dome; the Fault Canyon flow and units of the Fort Rock Creek Rhyodacite are uplifted and deformed by much smaller amounts.

THE MONOCLINE

Volcanic rocks older than the Fault Canyon flow in the rim of Fort Rock crater have dips that range from 43° to 90°(?) and average about 60° (table 6).¹² In one or two places, it can be seen that these rocks form the steeply dipping limb of a monocline. This monocline nearly encircles in dome. In most places, the gently dipping inner limb of the monocline has been removed by erosion, and the gently dipping outer limb is buried beneath younger units.

On Nine and Ten O'Clock Hills, the entire monocline is exposed. The structure is best observed on the northeast wall of Ten O'Clock Wash, where it is defined by the contact of the Buffalo Ridge flow on Precambrian rocks (pl. 1; pl. 2, cross section *D-D'*). On this wall, the gently dipping outer limb of the monocline is exposed just above the bottom of the wash and dips about 15° to the northwest. The steeply dipping limb lies between 5,100 and 5,200 ft (1,554 and 1,585 m) elevation and dips about 60° to

¹² It should be noted that attitudes of flow cleavage in volcanic rocks cannot, in general, be used to determine structure. On Ten O'Clock Hill, flow cleavage dips steeply (40° or more) into the contact between the flow and the Precambrian rocks near the top of the hill (pl. 1). This phenomenon is also seen on Outer Hill, on the top of Four O'Clock Hill, and on the small knob extending southwest of the southeast end of Lion Ridge. Furthermore, in most places the attitudes of flow cleavage change directions from the bottom to the top of a flow. This phenomenon can be easily seen, for example, in rocks on the southwest side of the Upper Two O'Clock Gap fault on Outer Hill (pl. 1).

TABLE 6.—Dips of volcanic units older than the Fault Canyon flow on the dome

| Location | Dip (degrees) | Dip obtained from |
|-------------------------------------|------------------|--|
| Nine O'Clock Wash | 52 | Basal tuffaceous sandstone of Crater Pasture Formation. |
| | 68, 50 | Pyroxene-trachyandesite sandstone of Crater Pasture Formation. |
| Eight O'Clock Gorge | 51 | Basal contact of Buffalo Ridge flow. |
| | 52 | Basal tuffaceous sandstone of Crater Pasture Formation. |
| Six Thirty wash | 74, 80 | Sandstones within basal facies of Buffalo Ridge and Annex Ridge flows. |
| Six O'Clock Hill, near Road End Gap | 52 | Basal tuffaceous sandstone of Crater Pasture Formation. |
| Hidden Pasture | 55, 50 73, 56 | Tuff and tuffaceous sandstone of Hidden Pasture tuff and conglomerate. |
| Four O'Clock Wash | 56 | Basal tuffaceous sandstone of Crater Pasture Formation from a pit in bottom of wash. |
| Three O'Clock Hill, southwest flank | 76 | Basal contact of Crater Pasture Formation exposed in 1-m-deep pit. |
| One O'Clock Wash | 90 (?) | Basal contact of Lion Ridge flow |
| Noon Hill, east side | 90 (?) | Isopleths in One O'Clock Wash sedimentary breccia. |
| | 43, 63, 90 | Hornblende-trachyandesite tuff and tuffaceous sandstone of Hidden Pasture tuff and conglomerate. |

the northwest. The gently-dipping inner limb lies above 5,200 ft, and dips about 28° to the northwest. The monocline can be viewed in its entirety by standing on Nine O'Clock Hill and looking to the northeast. It can also be seen on the southwest wall of Ten O'Clock Wash from Ten O'Clock Hill. On the southwest wall, the steeply dipping limb lies approximately between 5,200 and 5,300 ft (1,585 and 1,615 m) elevation. The monocline is, thus, warped or possibly displaced along a concealed fault in the vicinity of the wash; however, the initial surface on the Precambrian rocks over which the Buffalo Ridge flow was emplaced at this locality was somewhat hilly, and structural interpretation must be made with caution.

The only other location where the gently dipping inner limb of the monocline is well preserved is Four O'Clock Hill (pl. 2, cross section *D-D'*). On top of this hill, contacts of the Road End Gap volcanic breccia and flow and Precambrian rocks and of the Annex Ridge flow and Road End Gap rocks dip as gently as 7° to the southeast. Hidden Pasture deposits on the southeast side of this hill, which dip 55° to the southeast, are on the steeply dipping limb of the monocline.

Cross sections *A-A'*, *B-B'*, *C-C'*, and *D-D'* (pl. 2) show the monocline in profile at various locations around the dome. In cross section *D-D'*, enough

ground control on the inner limb of the monocline on Ten O'Clock Hill and on Four O'Clock Hill is available to project contacts inward and reconstruct the form of the now-eroded central part of the dome. Cross section *C-C'* is also well controlled by exposures in Eight O'Clock Gorge and on Lion Ridge. In the southeast wall of Eight O'Clock Gorge, a double monocline can be observed; here the flank of the dome has a structural terrace. Near Lion Ridge, the flank of the dome has collapsed, as shown in the cross section. Reconstruction of the dome above ground in the remaining two cross sections, *A-A'* and *B-B'*, is somewhat conjectural and is done with the aid of cross sections *C-C'* and *D-D'*.

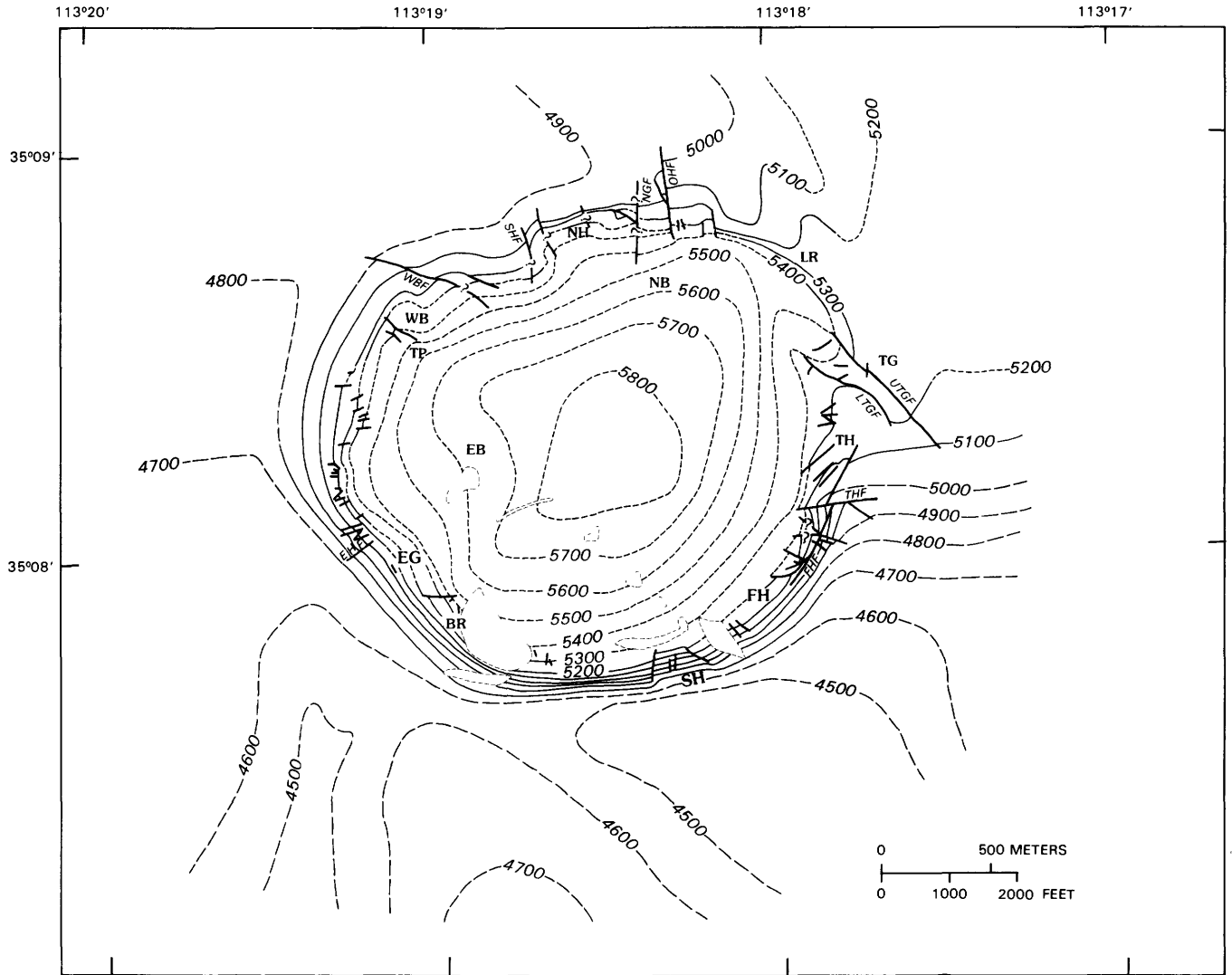
Cross sections *A-A'*, *B-B'*, *C-C'*, and *D-D'*, along with the geologic map, can be used to construct a structure contour map of the dome (fig. 5). Asymmetry of the dome is apparent on this map. A monocline is well developed along the south margin of the dome but diminishes in amplitude and sharpness in both directions around the dome. To the east, it diminishes rapidly over a relatively steep initial slope on the basement; it dies out abruptly on Three O'Clock Hill. To the west, it gradually gives way to a broad monocline interrupted by a small, sharp monocline, as is seen in the vicinity of Ten O'Clock Peak. Irregularities characterize the north side of the dome, although control for the structure contour map is somewhat sketchy here. Noon Hill appears to be underlain by a sharp monocline, offset successively on the west by two faults. West of these faults, the monocline is very broad. The monocline is also offset by several faults east of Noon Hill. Between the One O'Clock Hill fault and a fault farther east, the monocline is anomalously broad. East of the latter fault, the monocline is again sharp but becomes gradually broader along Lion Ridge. It dies out at Two O'Clock Gap. Maximum structural relief on the dome is about 400 m (1,300 ft).

A topographic map of the prevolcanic surface on the Precambrian rocks can be constructed using the structure contour map for undeformed areas outside the dome and using a few inferences about the initial topography inside the dome (see fig. 9, map 1). The topographic relief on this surface can be subtracted from the structural relief (fig. 5) to determine the vertical uplift that occurred during doming. A contour map of this vertical uplift (fig. 6) is similar in its configuration to the structure contour map but with contours shifted southwestward. Maximum vertical uplift is about 280 m (over 900 ft) and is centered in the south half of the dome. The concentration of uplift in the south half of the dome may

be due in part to geometry: the dome was created on a sloping surface and the downhill side might expect more uplift from a plug rising vertically. On the other hand, concentration of uplift in the south may be due in part to the presence of the shear zone there, along which the plug that created the Fort Rock dome presumably rose.

MAPPED FAULTS

Most faults shown on the geologic map (pl. 1) offset rocks younger than the Two O'Clock Gap tuff and flow in the rim of the crater. Where ages can be determined, these faults formed during or shortly



EXPLANATION

---100--- Contour on contact between Precambrian and Tertiary rocks—Short dashed above present ground surface; long dashed below present ground surface where uncertain. Elevation given in feet above sea level

 Intruded area

— Fault—Queried where uncertain
 EHF, Eight O'Clock Hill fault; FHF, Four O'Clock Hill fault; LTGF, Lower Two O'Clock Gap fault; NGF, Noon Gorge fault; OHF, One O'Clock Hill fault; SHF, Short Hill fault, THF, Three O'Clock Hill fault; UTGF, Upper Two O'Clock Gap fault; WBF, Wedge Basin fault

Geographic locations—BR, Buffalo Ridge; EB, Eight O'Clock Basin; EG, Eight O'Clock Gorge; FH, Four O'Clock Hill; LR, Lion Ridge; NB, Noon Basin; NH, Noon Hill; SH, Six O'Clock Hill; TG, Two O'Clock Gap; TH, Three O'Clock Hill; TP, Ten O'Clock Peak; WB, Wedge Basin

FIGURE 5.—Structure contour map of Fort Rock dome.

after uplift of the dome. These faults have chiefly radial and tangential strikes. Dips are steep where they can be determined. Block rotations are observable along faults that are traceable for long distances.

Faults differ significantly on different sides of the dome (pl. 1, fig. 5). On the east side, tangential faults are traceable for relatively long distances. Radial and subradial faults, also traceable for relatively long distances, offset these faults in places. On the north side, relatively long radial and subradial faults occur. On the west side, relatively short radial faults

are numerous compared to faults in other areas on the dome. On the south side, relatively short radial faults occur but are rare.

EAST SIDE OF THE DOME

Tangential faults, traceable for up to 700 m, occur on the east side of the dome (pl. 1, fig. 5). These faults include the Upper Two O'Clock Gap fault, the Lower Two O'Clock Gap fault, and the Four O'Clock Hill fault. The Three O'Clock Hill fault and a fault

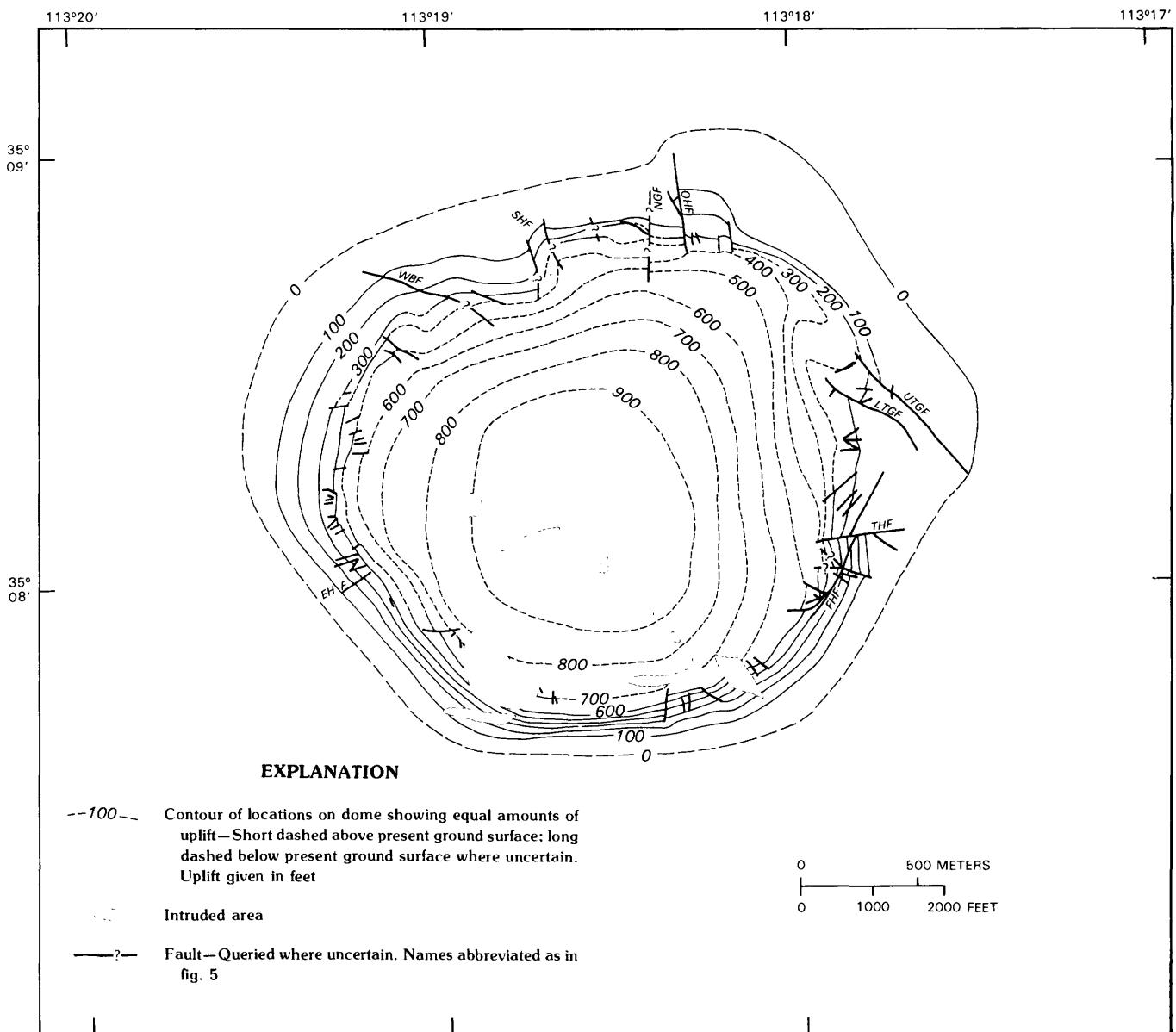


FIGURE 6.—Uplift map of Fort Rock dome.

in Four OClock Wash offset the Four OClock Hill fault.

The Upper Two OClock Gap fault trends northwest-southeast from the saddle between Lion Ridge and the small knob on the southwest side of this ridge to the south side of Outer Hill. This fault offsets the contact between Precambrian and Tertiary rocks by about 6 m along its northwest exposure and by less than 1½ m along its southeast exposure (pl. 2, cross section C-C'). The contact of Lion Ridge flow and the Two OClock Gap tuff is offset along this fault by as much as 21 m on the northwest and by 8 m on the southeast. All contacts are offset relatively downward on the southwest. In addition to offset, there is a persistent angular discordance between contacts on either side of this fault that varies from 18° in the northwest to 7° in the southeast; units on the southwest side of this fault have been rotated to the southwest relative to units on the northeast side. The fact that younger units are offset by greater amounts than older units along this fault implies a history of faulting. Early movement occurred between emplacement of the Two OClock Gap tuff and flow and the Lion Ridge flow, as noted above. Rocks on the northeast side of the fault were displaced relatively downward during this episode. Movement after emplacement of the Lion Ridge flow occurred in the opposite direction and apparently involved rotation.

The Lower Two OClock Gap fault is exposed on the west side of Outer Hill and along the southwest flank of the small knob southwest of Lion Ridge. It probably extends beneath the colluvium in Two OClock Gap but has been queried there, as the resulting fault is quite crooked. This fault offsets all contacts by about 11 m along its northwest exposure and by about 5 m along its southeast exposure. Displacement is relatively down on the southwest.

The Four OClock Hill fault extends north-northeastward from the top of Four OClock Hill to the east side of Three OClock Hill. Displacement tapers off at either end and is as great as 75 m on the north bank of Four OClock Wash. The displacement changes abruptly across several radial and subradial faults that offset this fault; the largest displacement occurs between the Three OClock Hill fault and a concealed fault in Four OClock Wash. Angular discordance is observed in the flow cleavage in the Annex Ridge flow on either side of this fault (pl. 1). Rocks on the northwest side of the fault have apparently been rotated down to the east relative to rocks on the southeast side of the fault. Struc-

ture at the southwest end of the fault is complicated by echelon faults and by the presence of older faults. The Four OClock Hill fault may be in part a reactivated pre-dome fault, as noted above.

NORTH SIDE OF THE DOME

Radial and subradial faults, traceable for as much as 600 m, occur on the north side of the dome (pl. 1, fig. 5). These faults include One OClock Hill, Noon Gorge, Short Hill, Wedge Basin, and other faults.

The One OClock Hill fault trends north-south and is located high on the west flank of One OClock Hill. Rocks on the west side of the fault have been either downthrown with respect to rocks on the east side or moved left-laterally along the fault or both. Along the south exposure of the fault, rocks on the west side have steep dips (60°), whereas rocks on the east side have moderate dips (30°), as inferred from isopleths within the One OClock Wash sedimentary breccia. Along the north exposure of the fault, rocks on both sides of the fault appear to have gentle dips (15°). On the structure contour map (fig. 5), the contact of Tertiary rocks with Precambrian rocks is interpreted as a broad monocline on the east side of the One OClock Hill fault and on the west side a sharp monocline. The author's conception of this fault is shown in figure 7.

The Noon Gorge fault is a concealed north-south-trending fault in Noon Gorge. Rocks on the east side have been either downthrown with respect to rocks on the west side or moved right-laterally along the fault or both. Dips within units on opposite sides of the fault are similar. On the structure contour map (fig. 5), this fault is interpreted to offset the axes of the monoclines on either side.

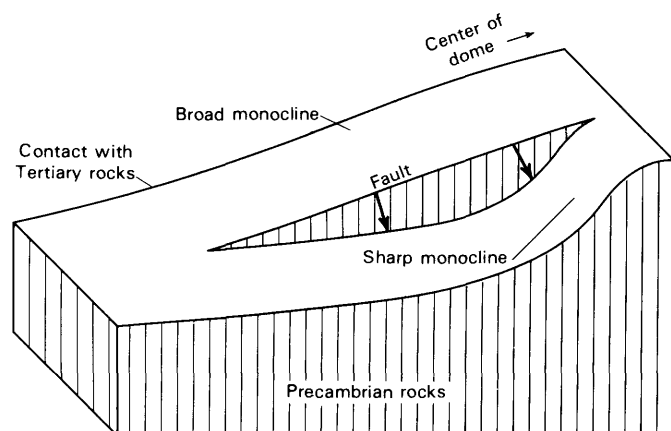


FIGURE 7.—Author's conception of the One OClock Hill fault

The Short Hill fault is an apparent fault that trends north-south to northwest-southeast along the crest of Short Hill. It is similar to the One O'Clock Hill fault in that rocks on the west side have been either downthrown or moved left-laterally along the fault or both; they also dip more steeply than rocks on the east side along the south exposure of the fault.

The Wedge Basin fault can be traced along the northeast edge of Wedge Basin. Toward its southeast end, rocks on the northeast side appear to be downthrown, whereas toward its northwest end rocks on the southwest side are downthrown. Excellent exposures of the fault in the wash draining Wedge Basin show it to be a normal fault with a displacement of 3 to 6 m in this area.

WEST AND SOUTH SIDES OF THE DOME

Except for the Eight O'Clock Gorge faults, faults on the west side of the dome have radial and subradial trends (pl. 1, fig. 5). Generally, they are more numerous and traceable for shorter distances (100 m or less) than faults on other sides of the dome. They have normal or strike-slip offsets, or combinations of the two. One of the largest faults on this side of the dome is the Eight O'Clock Hill fault, which trends northeast-southwest and is located on the northwest wall of Eight O'Clock Gorge. Rocks on its southeast side are downthrown or offset left-laterally along the fault. Most other faults on Eight O'Clock Hill show a similar sense of displacement. Faults on Nine O'Clock Hill, on the other hand, are downthrown on the north or show right-lateral movement. Thus, rocks in the region between Eight and Nine O'Clock Hills were uplifted slightly more or moved laterally farther away from the center of the dome than rocks on either side (see pl. 1, fig. 5).

The Eight O'Clock Gorge reverse faults are exposed as three breccia-filled fissures in the upper part of the Buffalo Ridge flow in Eight O'Clock Gorge. The fissures strike tangentially to the dome and dip steeply to the southwest. Rocks on their southwest sides have moved relatively up.

Faults on the south side of the dome that are not associated with intrusion of the Buffalo Ridge flow and that do not predate emplacement of the Annex Ridge flow are rare. The largest is an east-west-trending fault at the northwest end of Buffalo Ridge that is traceable for over 100 m. Four or five radial and subradial faults of similar length occur on the rim of the crater in the vicinity of Five O'Clock Wash.

AGES OF FAULTS.

Several faults in the rim of the crater have well-determined ages that range from the beginning of doming to well after major doming was finished. Other faults do not have well-known ages but are presumed to be related to doming because of their local extent and because they have radial or tangential trends. Faults are discussed below in order of their age, oldest first.

The Eight O'Clock Hill fault and the Eight O'Clock Gorge faults offset the Buffalo Ridge flow but are covered (and locally filled) by One O'Clock Wash sedimentary breccia; fault scarps are preserved beneath the breccia. These faults formed at the beginning of doming, which is indicated by the deposition of this breccia.

The Short Hill fault offsets most of the section of the One O'Clock Wash sedimentary breccia on Short Hill but is apparently covered by about 15 m of this unit. The isopleth pattern in the breccia is suggestive of a low fault scarp preserved beneath the upper 15 m. Thus, this fault is inferred to have formed during the major part of doming.

The youngest unit offset by the One O'Clock Hill fault is the lower part of the basal sedimentary breccia of the Old Stage Road Member. The fault is covered by a higher part of this basal breccia. Movement thus occurred after the major part of the uplift of the dome, represented by deposition of the One O'Clock Wash and Noon Gorge sedimentary breccias. Possible coarsening of the Noon Gorge sedimentary breccia on the west side of this fault may or may not indicate earlier movement. The Noon Gorge fault, concealed by alluvium, is probably the same age as the One O'Clock Hill fault. Another fault, atop Noon Hill, is covered by the basal sedimentary breccia of the Old Stage Road Member and, thus, moved at about the same time as the One O'Clock Hill fault.

The Wedge Basin fault offsets ash-flow tuff of the Old Stage Road Member; it formed well after doming ceased but caused only minor offset.

Ages of the Lower Two O'Clock Gap fault, the Four O'Clock Hill fault, and the latest movement on the Upper Two O'Clock Gap fault are unknown and must be inferred from the geologic history of the dome or from a model of doming (see the appropriate sections below). The Three O'Clock Hill fault and a concealed fault in Four O'Clock Wash offset the Four O'Clock Hill fault. Although these faults are younger than the Four O'Clock Hill fault, all three may be very close in age.

UNMAPPED FAULTS AND BRECCIA LENSES

Numerous small faults with displacements of centimeters to meters and lenses of largely unmineralized breccia occur on the dome. These features are most abundant and most easily observed in the Precambrian rocks but are also seen in the volcanic rocks. Their distribution on the dome and their occurrence in both the Precambrian and Tertiary rocks indicate that they are related in origin to the dome.

The average spatial density of small faults and the maximum thicknesses of breccia lenses were recorded in traverses through Eight O'Clock Gorge, Eight O'Clock Basin, Noon Basin, and the area northeast of Lion Ridge. The faults and breccia lenses were observable only in the banks and bottoms of washes where recent floods had locally removed all surficial cover. In most cases, exposures were in the form of narrow strips parallel to the washes. Generally, the faults and lenses of breccia seen were those oriented nearly perpendicular to the strip of outcrop; these faults and breccia lenses almost invariably had steep dips. The total number of faults seen in a given strip of outcrop was divided by the length of that outcrop to give a density measured in number of faults per meter. The fault density and breccia-lens thickness are plotted versus distance from the center of the dome (fig. 8), where the center of the dome is determined from the structure contour map (fig. 5).

The dome is well defined on these plots. Beyond the dome the density of faults is low, generally less than 0.3 fault per meter of outcrop; there are almost no breccias. On the dome, the density of faults is commonly between 0.3 and 1.6 faults per meter of outcrop; breccia lenses are numerous and range from a few centimeters in maximum thickness to as much as 24 m. Fault density and maximum thickness of breccia lenses generally decrease from the rim of the crater toward the center; however, because of thick deposits of alluvium in the center of the crater, no data are available there. In addition, fault density and the number of relatively thick breccia lenses are higher in the region of Eight O'Clock Gorge and Eight O'Clock Basin than in the region of Noon Basin.

The fact that small faults are more numerous and that breccia lenses are thicker toward the edges of the dome is consistent with the fact that a monocline is found on the edge of the dome in most places, where rock deformation was presumably most severe. The fact that small faults and thick breccia lenses are most numerous in the southwest part of

the dome is consistent with the fact that the best developed monocline occurs in that area.

UPLIFT AND TILTING OF THE FAULT CANYON FLOW AND UNITS OF THE FORT ROCK CREEK RHYODACITE

Rocks of the Fault Canyon flow and the Fort Rock Creek Rhyodacite are not as strongly uplifted and tilted on the dome as rocks of the Crater Pasture Formation that are older than the Fault Canyon flow. These rocks may not, in fact, be uplifted or tilted at all.

The topography on the Fault Canyon flow after it was extruded (see below: fig. 9, map 9) consisted chiefly of lobes extending away from feeder vents. A slightly anomalous long narrow ridge extending northwest from the main feeder vent is probably best explained by uplift of the order of 8 m adjacent to the dome subsequent to extrusion of the flow. Explanations that do not involve uplift, however, are possible. For example, additional vents could underlie this ridge.

The basal contact of the Noon Gorge sedimentary breccia dips away from the dome in all quadrants where it is exposed at average of about 33°; the maximum dip is 45° (table 7). Dips on the basal contact of the overlying Old Stage Road Member and on sandstone beds within this unit range from 6° to 34°, depending on how high on the flank of the dome the dip is measured. Generally, dips are steeper higher on the flanks of the dome. Most of the dips on the base of the Noon Gorge sedimentary breccia could be explained as initial dips, assuming that the angle of repose on the One O'Clock Wash sedimentary breccia was between 30° and 40° at the time the Noon Gorge breccia was deposited. Although the Noon Gorge breccia probably was, indeed, deposited on a steep slope, it is reasonable to believe that some subsequent tilting took place. Dips on the base of the Old Stage Road Member and on sandstone within this unit are all easily explainable as initial dips on the dome.

MAJOR NORMAL FAULTS

Major normal faults near the Fort Rock dome include the Fort Rock Creek fault and an east-west-trending fault south of the Three Sisters (pl. 1; fig. 3). The youngest unit offset by Fort Rock Creek fault is a basalt that postdates the Fort Rock Creek Rhyodacite. The youngest unit offset by the fault south of the Three Sisters is the Fort Rock Creek

Rhyodacite. The downthrown sides of these two faults are the southwest and south sides, respectively. Units within the Fort Rock Creek Rhyodacite appear to thin abruptly on the downthrown sides of both faults, suggesting that during emplacement of the Fort Rock Creek Rhyodacite movements took place on the faults

in directions opposite to the presently observed displacements.

On the Fort Rock Creek fault, the displacement of rocks of the Crater Pasture Formation is estimated to be about 45 m in the area southeast of Fault Canyon (pl. 2; cross section A-A'). Maximum dis-

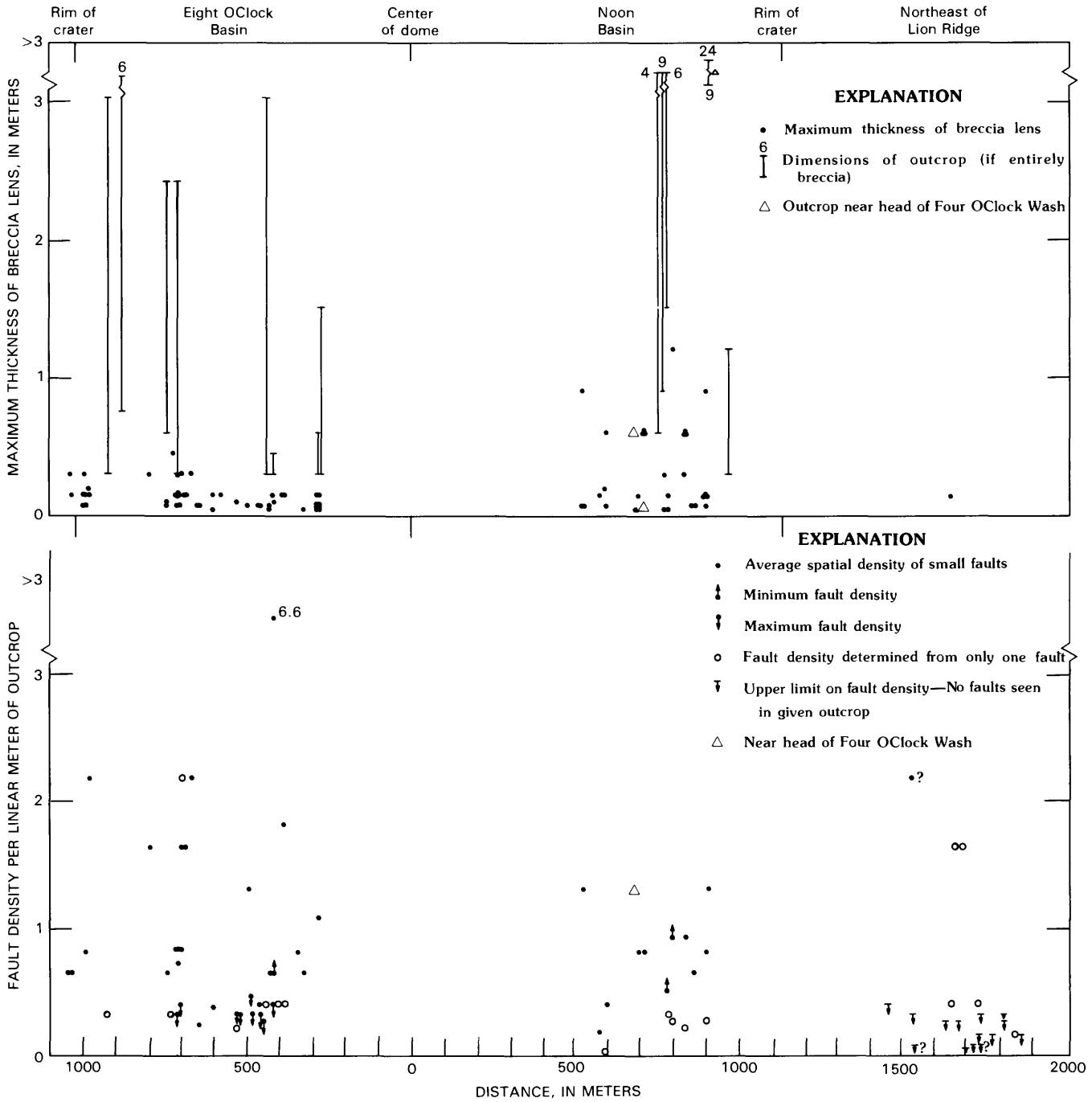


FIGURE 8.—Average spatial density of small faults and maximum thicknesses of breccia lenses on the Fort Rock dome. The number of faults seen in a given outcrop is divided by the length of that outcrop to give an average spatial density. (Outcrops tend to occur as narrow strips in the bottoms and the banks of washes.) Faults spaced closer than 15 cm apart were considered a single fault zone.

placement of rocks of the Fort Rock Creek Rhyodacite is unknown at this location but probably is over 100 m. The fault passes into a monocline on the hill west and northwest of Fault Canyon (pl. 2; cross section *B-B'*). West of the hill, the fault offsets rocks of the Crater Pasture Formation by more than 8 m and dies out about 300 m northwest of the point where it crosses Fort Rock Creek. The southeast part of the fault consists of two branches (fig. 3). Displacement is small on the northeast branch. The southwest branch offsets young (post-Fort Rock Creek Rhyodacite) basalt by as much as 30 m.

On the fault south of the Three Sisters, the displacement of rocks of the Crater Pasture Formation ranges from zero to 120 m. At a point immediately south of the Three Sisters the displacement is zero. Five kilometers west, the displacement is 120 m; 8 km west, it is zero; 11 km west, it is small but reversed, with the downthrown side on the north. In contrast to rocks of the Crater Pasture Formation, the breccia and conglomerate of the Crossing, a member of the Fort Rock Creek Rhyodacite, is displaced 90 m downward across the fault at the point immediately south of the Three Sisters.

GEOLOGIC HISTORY

HISTORY BEFORE TERTIARY VOLCANISM

The oldest geologic event that can be inferred from rocks on the Fort Rock dome is the deposition in Precambrian time of a sequence of volcanic and (or) sedimentary rocks. These rocks were subsequently deeply buried, folded, and metamorphosed to the epidote-amphibolite facies. The layered metamorphic rocks that were produced were then intruded by a number of relatively small bodies of granitic rocks. Both the layered metamorphic rocks and the granitic intrusive rocks were next subjected to cataclastic deformation. Near the end of the episode of cataclastic deformation, these rocks were in some areas intruded by granites and then by swarms of pegmatites. Uplift and erosion ensued. At some time during the uplift, shearing and veining occurred, which probably was produced by major (strike-slip?) faulting. The shear zone that passes through the Fort Rock dome probably was part of an active fault zone that extended from near present-day Ashfork, Ariz., to the west edge of the present-day Aquarius Mountains, a distance of about 110 km. Prior to deposition of the Tapeats Sandstone, in Cambrian time, a surface of very low relief

TABLE 7.—Dips of units in the Fort Rock Creek Rhyodacite on the dome

| Location | Dip (degrees) 1/ | Dip obtained from |
|---------------------------------------|------------------|---|
| Wash between Noon Hill and Short Hill | 32 | Basal contact of Noon Gorge sedimentary breccia |
| | 10 (11 → 8) | Basal contact of Old Stage Road Member |
| | 10 | Sandstone in Old Stage Road Member |
| Wash on west side of Short Hill | 33 | Basal contact of Noon Gorge sedimentary breccia |
| | 14 | Sandstone in Old Stage Road Member |
| Wash draining Wedge Basin | 34 (43 → 29) | Basal contact of Noon Gorge sedimentary breccia |
| | 32 | Basal contact of Old Stage Road Member |
| | 32, 17 | Sandstone in Old Stage Road Member |
| Ten O'Clock Wash | 30 | Basal contact of Noon Gorge sedimentary breccia |
| Nine O'Clock Hill, west side | 20 → 12 → 6 | Sandstone in Old Stage Road Member |
| Eight O'Clock Hill, southwest side | 12 → 16 | Sandstone in Old Stage Road Member |
| | 27 → 23 → 14 → 9 | |
| Eight O'Clock Gorge | 38 (36 → 45) | Basal contact of Noon Gorge sedimentary breccia |
| | 17 (22 → 12) | Basal contact of Old Stage Road Member |
| Buffalo Ridge southwest side | 15 | Sandstone in Old Stage Road Member |
| | 34 | Sandstone in Old Stage Road Member |
| | 18 | Sandstone in Noon Gorge sedimentary breccia |
| Four O'Clock Wash | 14 | Sandstone in Old Stage Road Member |

1/ The first number is an average dip for the given location. The numbers in parentheses are a selected dip higher on the flank of the dome (left) and lower on the flank of the dome (right). Arrows point to dips measured successively lower on the flank of the dome.

was produced on the faulted metamorphic and plutonic rocks.

The similarity between older Precambrian rocks in the Grand Canyon and Precambrian rocks on the Fort Rock dome suggests similar geologic histories for the two areas. One might infer the timing of Precambrian events at the Fort Rock dome from the timing of events at the Grand Canyon. At the Grand Canyon, volcanic and sedimentary rocks were buried, folded, and metamorphosed to produce layered metamorphic rocks. These rocks were then intruded by the Zoroaster Granite of Campbell and Maxson (1936) and other granites, which have reported uranium-lead ages of around 1,725 Ma (Pasteels and Silver, 1965; Silver, oral commun., 1973). This age may apply to intrusions now represented by some of the cataclasites on the Fort Rock dome. The next event at the Grand Canyon was metamorphism at about 1,695 Ma and intrusion at about the same time by pegmatites (Pasteels and Silver, 1965). At the Fort Rock dome, cataclastic metamorphism preceded and in part accompanied intrusion of pegmatites. Uplift and erosion occurred next at the

Grand Canyon. There is evidence that large-scale strike-slip faulting may also have occurred at about this time (Shoemaker and others, 1974). Strike-slip(?) faulting may have occurred at this time at the site of the Fort Rock dome to produce the shear zone seen. At the Grand Canyon, erosion continued, and a surface of very low relief, the Arizonan Plain (Maxson, 1961), was produced. Subsidence and deposition of rocks of the Grand Canyon Supergroup followed; these rocks are not present at the Fort Rock dome. This deposition apparently began no earlier than 1,400 Ma (Elston and others, 1973; D.P. Elston, written commun., 1973) and no later than 1,150 Ma (L.T. Silver, oral commun., 1973). Uplift, tilting, normal and reverse faulting, and erosion occurred next at the Grand Canyon. A surface of very low relief was present on the Precambrian rocks at the time the Tapeats Sandstone was deposited, in Cambrian time, as was true at the Fort Rock dome.

Early Phanerozoic events at the Fort Rock dome, recorded at nearby Cross Mountain, were subsidence and the deposition of sedimentary rocks. In Cambrian time, the Tapeats Sandstone, Bright Angel Shale, and Muav Limestone were deposited. Unnamed carbonate rocks were deposited in Devonian time. In Mississippian time, the Redwall Limestone was deposited. Younger Paleozoic units probably were deposited but were subsequently removed by erosion. Likewise, Mesozoic and early Tertiary units may have been deposited, but have not been preserved.

In middle Tertiary time, uplift and erosion occurred. An erosional surface was formed over a wide area in northwest Arizona. In the vicinity of the Fort Rock dome, Cross Mountain was a butte on this surface. West and south of Cross Mountain, Phanerozoic rocks were completely removed by erosion. From the relief that can be seen on the Precambrian-Tertiary contact in the vicinity of the Fort Rock dome, it appears that the topography that was developed on Precambrian rocks was similar to the topography seen today on these rocks. Locally at the Fort Rock dome, the erosion surface sloped to the west, southwest, and south away from a high area in the vicinity of present-day Lion Ridge (see pl. 2, cross section *B-B'*). Relief was about 200 m. Two lines of evidence indicate that a northeast-trending valley, extending well inside of the limits of the present crater, existed near present-day Eight O'Clock Gorge. First, the flows of Eight O'Clock Gorge and Meadow Dam are locally thick in Eight O'Clock Gorge. Second, an isolated outcrop of the flow of Buffalo Ridge occurs on Noon Hill. In order for this flow to have arrived here from

its vent near present-day Buffalo Ridge, it would have had to flow uphill unless a valley were present.

Map 1 (fig. 9) illustrates the topography on the Precambrian rocks prior to volcanism in the area. This map and all subsequent paleotopographic-paleogeologic maps (fig. 9, maps 1-10) are constructed using plates 1 and 2 and a few inferences about the geologic history such as described above.

TERTIARY VOLCANIC HISTORY

BEGINNING OF VOLCANISM AND ERUPTION OF THE CRATER PASTURE FORMATION

Volcanism in the vicinity of the Fort Rock dome apparently began with the intrusion of one or more small rhyodacite plugs. One plug was intruded inside the limits of the present-day crater and is seen today at the head of Five O'Clock Wash. A period of minor(?) erosion followed, and fragments of this rhyodacite were deposited in the thin tuffaceous basal sandstone of the Crater Pasture Formation. Mafic ash in this sandstone signaled the beginning of eruption of rocks of the Crater Pasture Formation.

The first major volcanic units to be erupted in the vicinity of the Fort Rock dome were the volcanic breccia and flow of Road End Gap and the flow of Eight O'Clock Gorge (fig. 9, map 2). The vent for the Road End Gap unit is located south of the rim of the present crater. Volcanic breccia was apparently deposited well to the north inside the limits of the present crater, because probable clasts of this unit are now found in the Noon Gorge sedimentary breccia on the north flank of the Fort Rock dome. The clasts were apparently transported from the top of the dome to the north flank during erosion of the dome. The vent for the Eight O'Clock Gorge flow is west of the rim of the present crater. A lobe of this flow extended up the valley through the site of present-day Eight O'Clock Gorge. The relative age of the Road End Gap and Eight O'Clock Gorge units is unknown.

Minor faulting occurred next, followed by erosion. A fault that may have been ancestral to the Four O'Clock Hill fault (which formed during doming) formed at this time. Map 2 (fig. 9) depicts the paleogeology and paleotopography after faulting and erosion of the Road End Gap and Eight O'Clock Gorge units.

The flow of Meadow Dam and the tuff and flow of Two O'Clock Gap were erupted next (fig. 9, map 3).

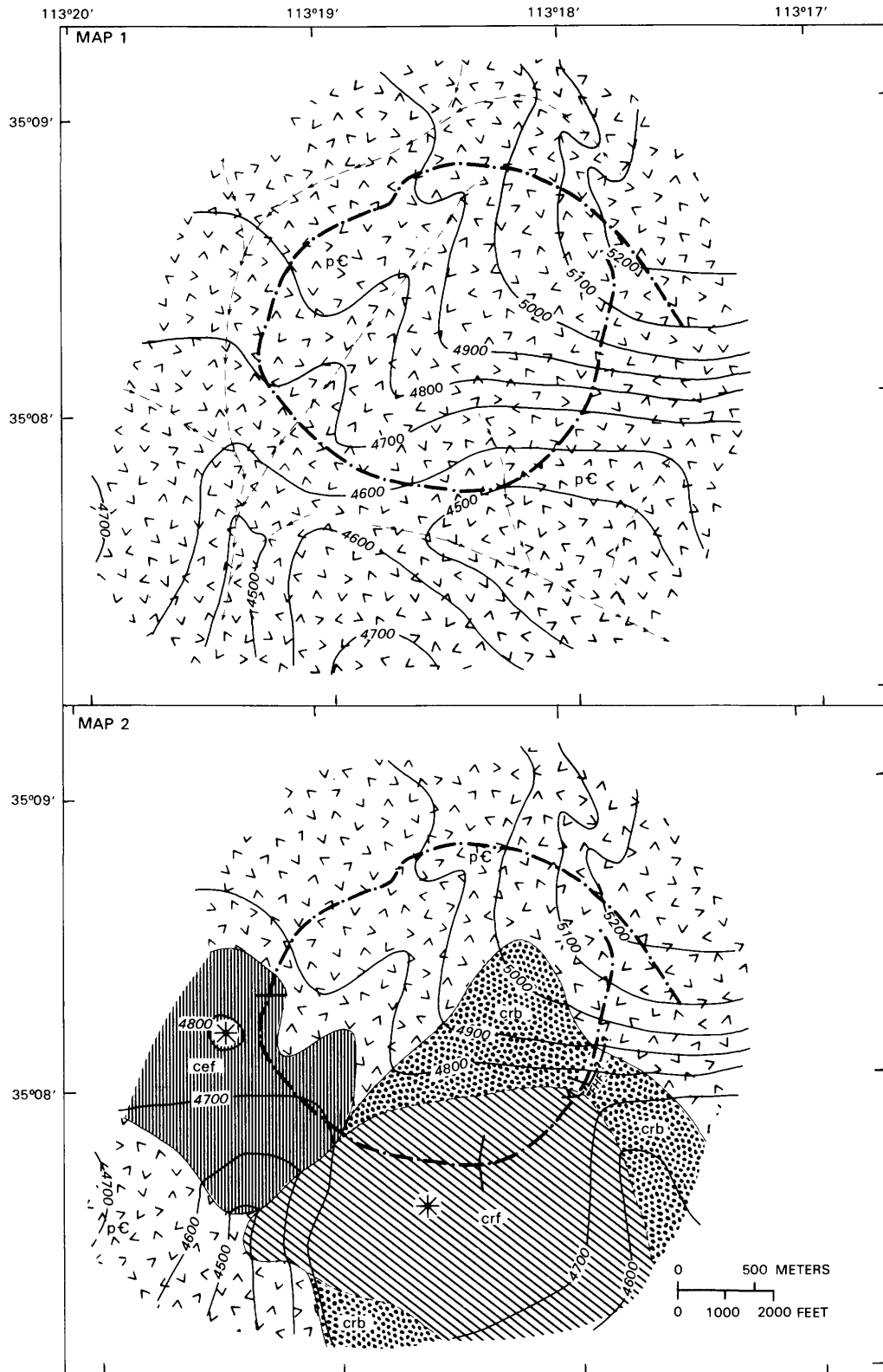


FIGURE 9.—Paleogeology and paleotopography at the Fort Rock dome in middle Tertiary time, before, during, and after eruption of the Crater Pasture Formation.

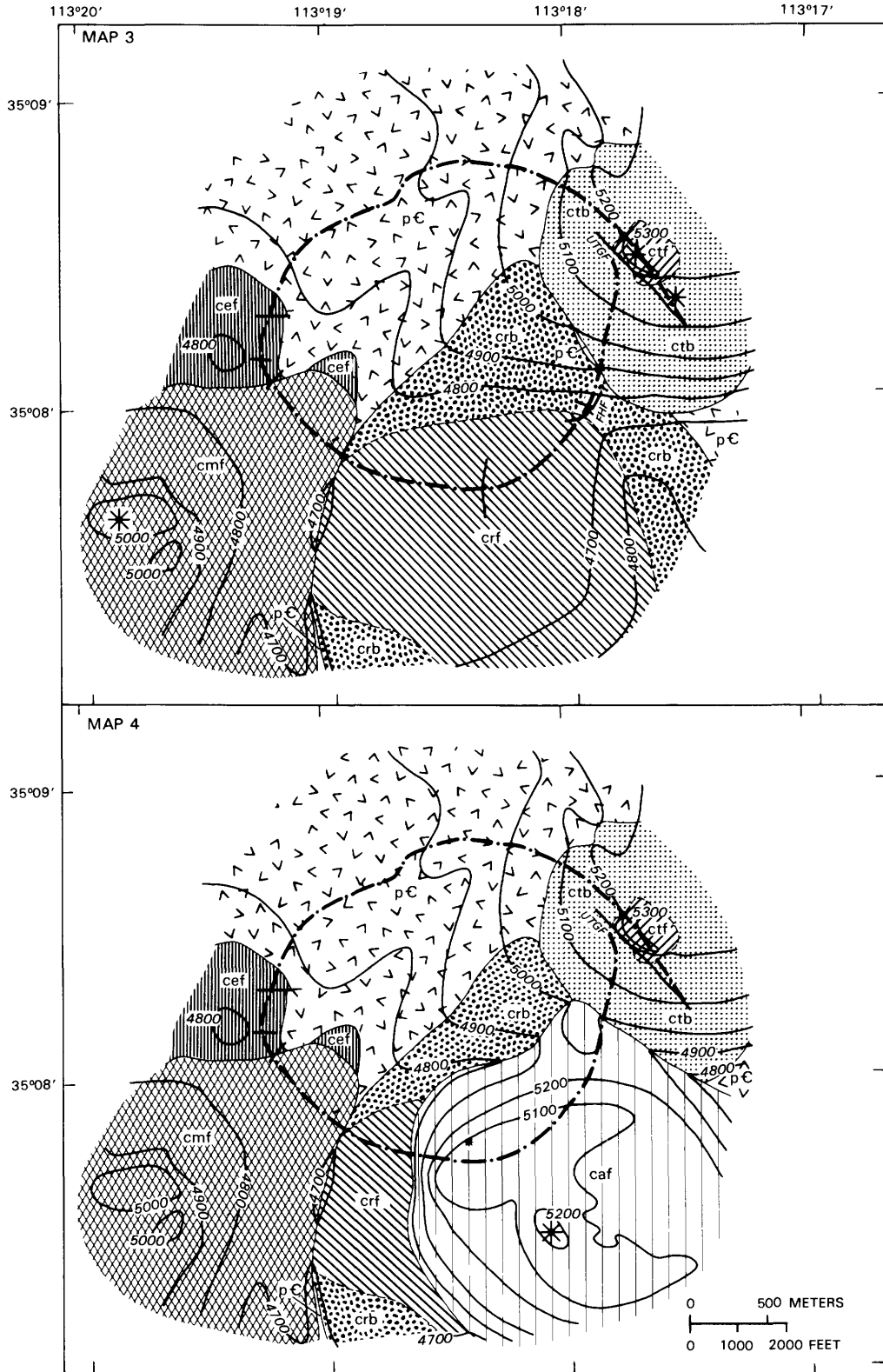


FIGURE 9.—Continued

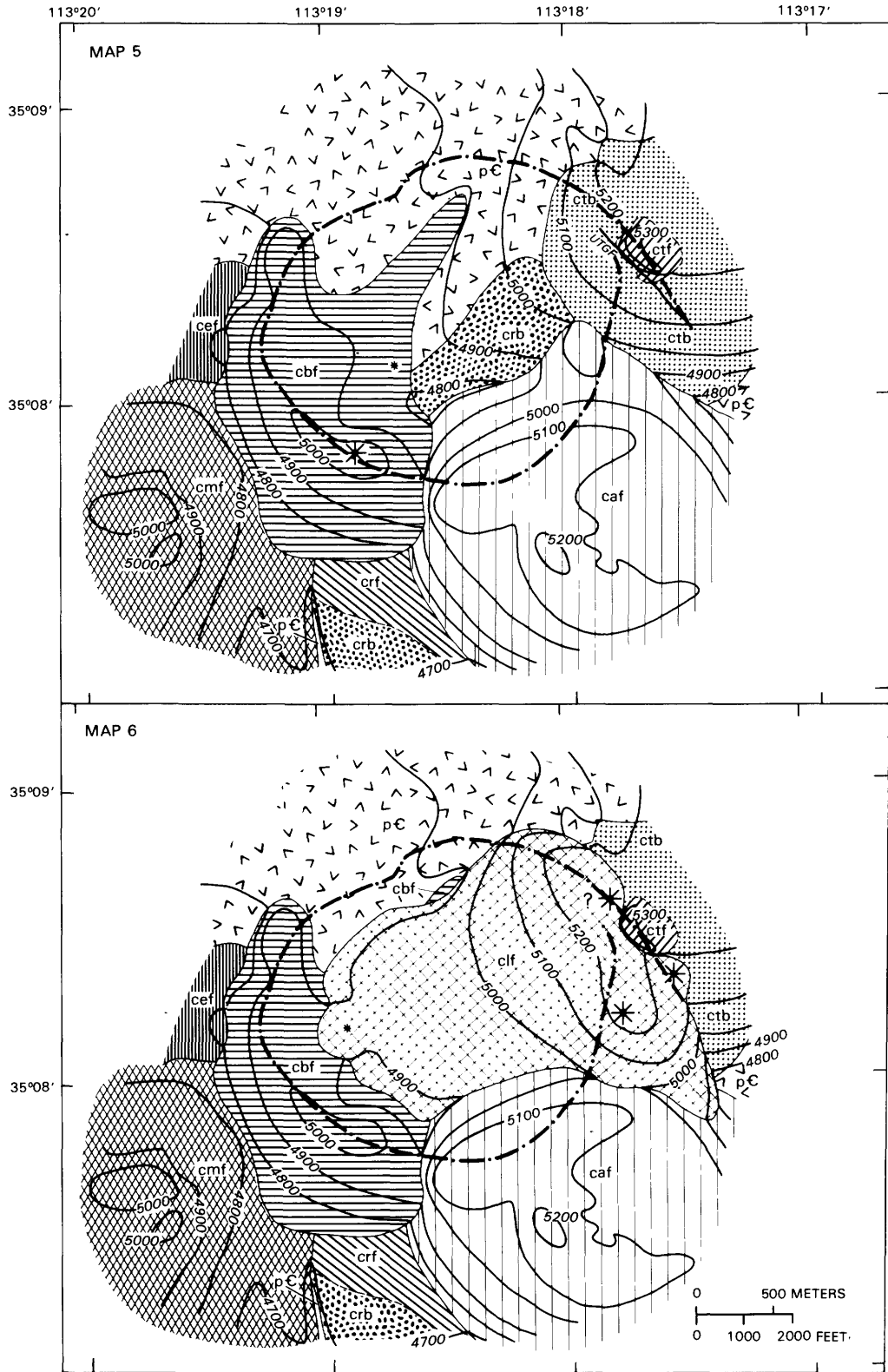


FIGURE 9.—Continued

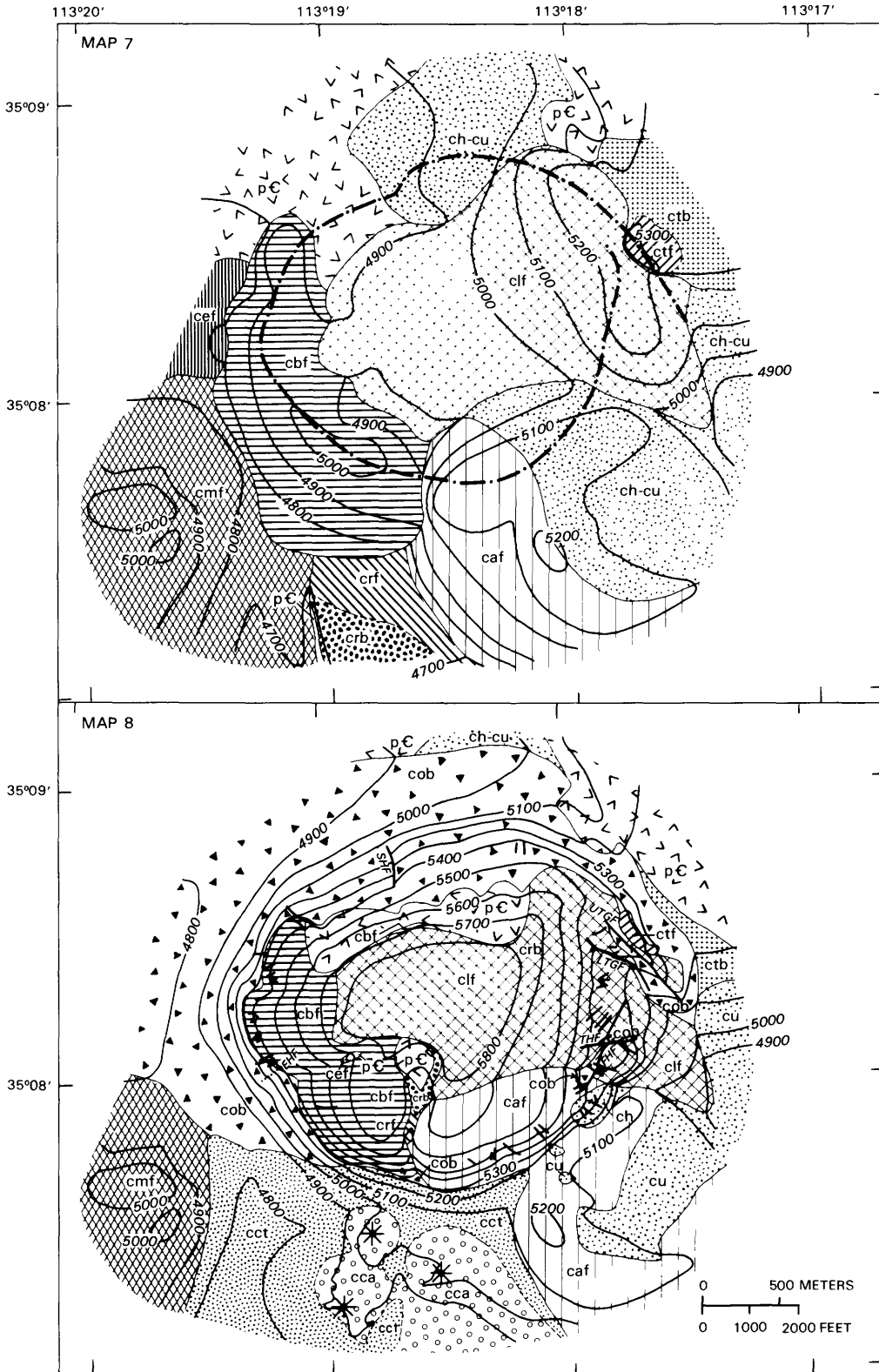


FIGURE 9.—Continued

GEOLOGY AND MECHANICS OF FORT ROCK DOME, ARIZONA

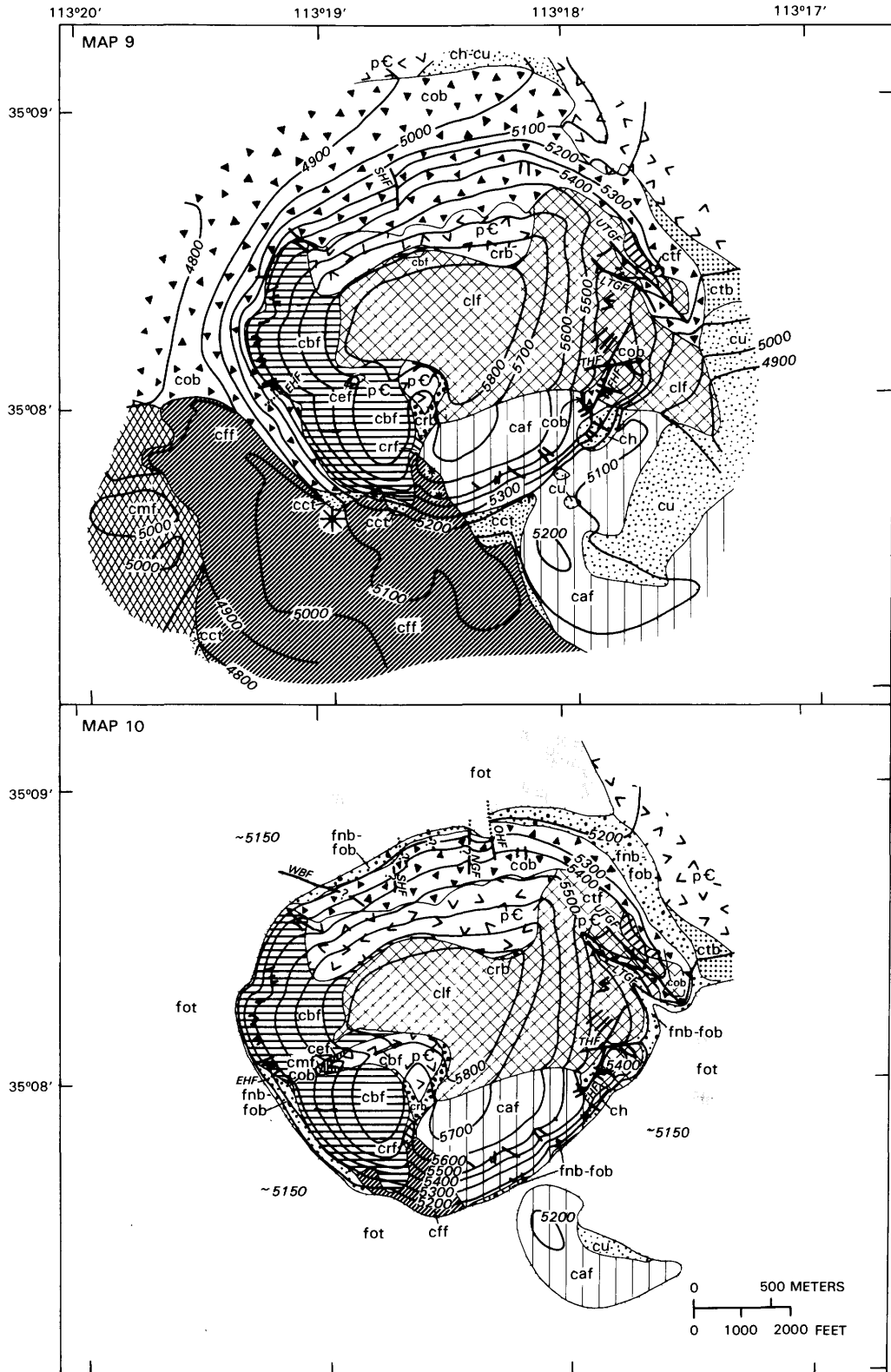


FIGURE 9.—Continued

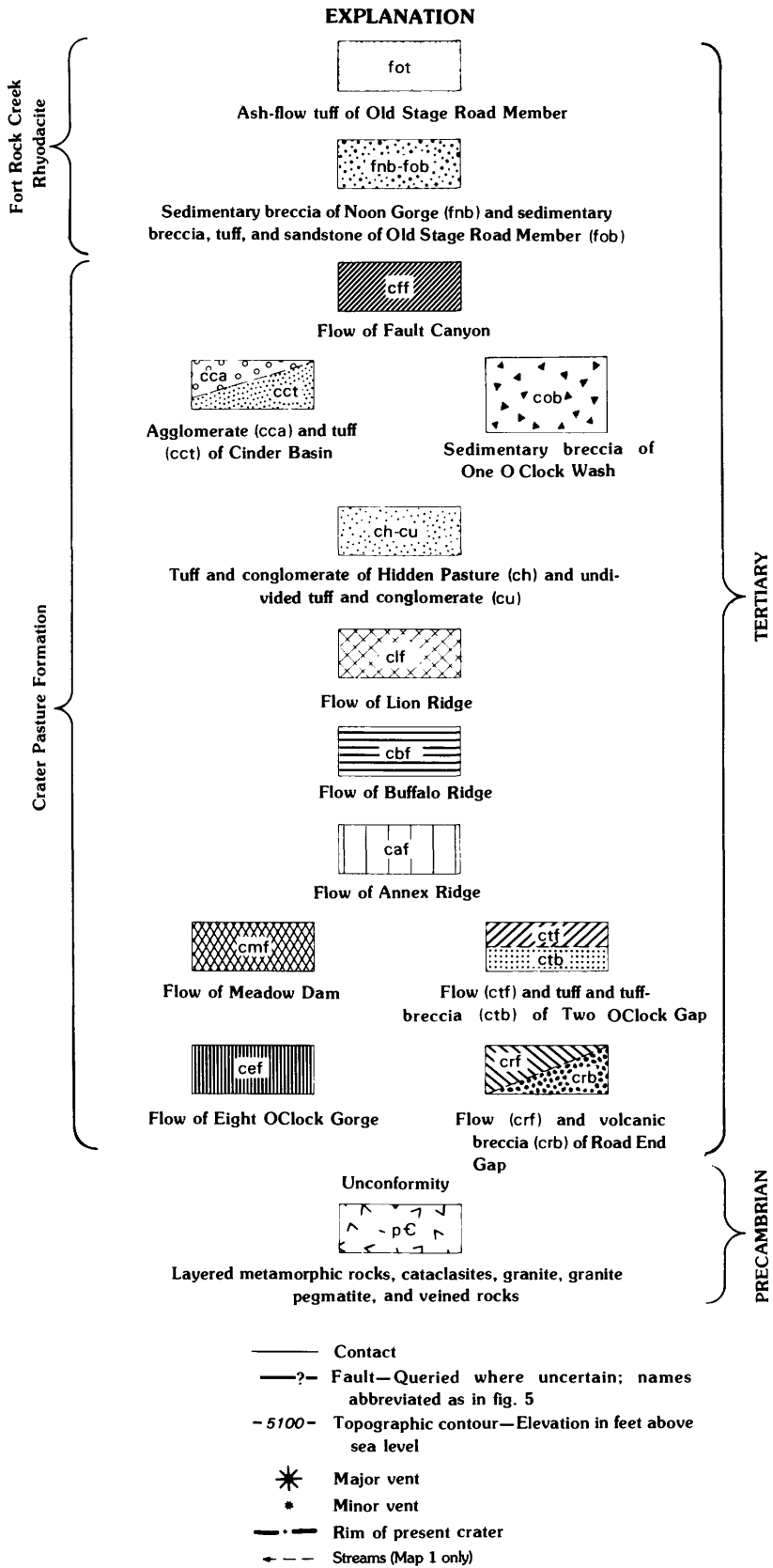


FIGURE 9.—Continued

The Meadow Dam flow had its source about 1.2 km southwest of the rim of the present crater. A small volcanic dome with a relief of about 90 m was extruded above the vent for this unit. This dome presently forms a high hill south of Meadow Dam. A lobe of this flow extended up the valley through the site of present-day Eight O'Clock Gorge. The tuff of Two O'Clock Gap formed a thin blanket on top of nearby rocks. It apparently had its source near present-day Outer Hill. The flow of Two O'Clock Gap formed a small volcanic dome about 30 m high above its vent, which is located near the southeast end of present-day Lion Ridge. The flow did not extend beyond the small dome.

The Upper Two O'Clock Gap fault was formed some time during or after eruption of the tuff and flow of Two O'Clock Gap. If it was formed after the eruption, then minor erosion occurred to cause a thinning of the tuff on the upthrown, or southwest, side of the fault. Map 3 (fig. 9) depicts the paleogeology and paleotopography after faulting and erosion, if erosion occurred, on the Two O'Clock Gap tuff and flow.

The flow of Annex Ridge was erupted next as a high, viscous dome (fig. 9, map 4). The vent for this flow is located somewhere southeast of the rim of the present crater, perhaps beneath present-day Annex Ridge. In addition, a small vent, occupied by an intrusive body of hornblende trachyandesite on present-day Six O'Clock Hill may have been a local source for this flow. The relief on the volcanic dome was about 150 m.

The flow of Buffalo Ridge was erupted next from a vent now exposed on Buffalo Ridge (fig. 9, map 5). In addition to this vent, a dike of hornblende trachyandesite near present-day Crater Divide may have been a local source for this flow. This flow apparently formed a volcanic dome, with a relief of about 60 m, above the vent exposed on Buffalo Ridge. The flow pinched out against the steep side of the Annex Ridge dome to the east. A low tongue of the flow apparently extended well up the valley northeast of present-day Eight O'Clock Gorge, because a jumbled body of the flow is found today in deposits on the north flank of the Fort Rock dome. During doming, this body of flow apparently moved to the north as a landslide from a position high on the dome. That the Buffalo Ridge flow did not extend into the valley to the south is purely speculative. There is no evidence for or against the presence of this flow in cross section A-A' (pl. 2), which is the control for this part of map 5.

The flow of Lion Ridge was erupted next from vents located near the east and northeast margins

of the present crater (fig. 9, map 6). A small vent occupied by a plug of hornblende trachyandesite in present-day Eight O'Clock Basin may have been a local source for this flow. The flow moved downhill from its main vents, which were located on relatively high ground, and formed a shallow pool against the volcanic domes of the Buffalo Ridge and Annex Ridge flows. This flow apparently covered much of the area that was subsequently domed, as rocks from this unit occur as clasts in beds of sedimentary breccia on several sides of the dome (fig. 10).

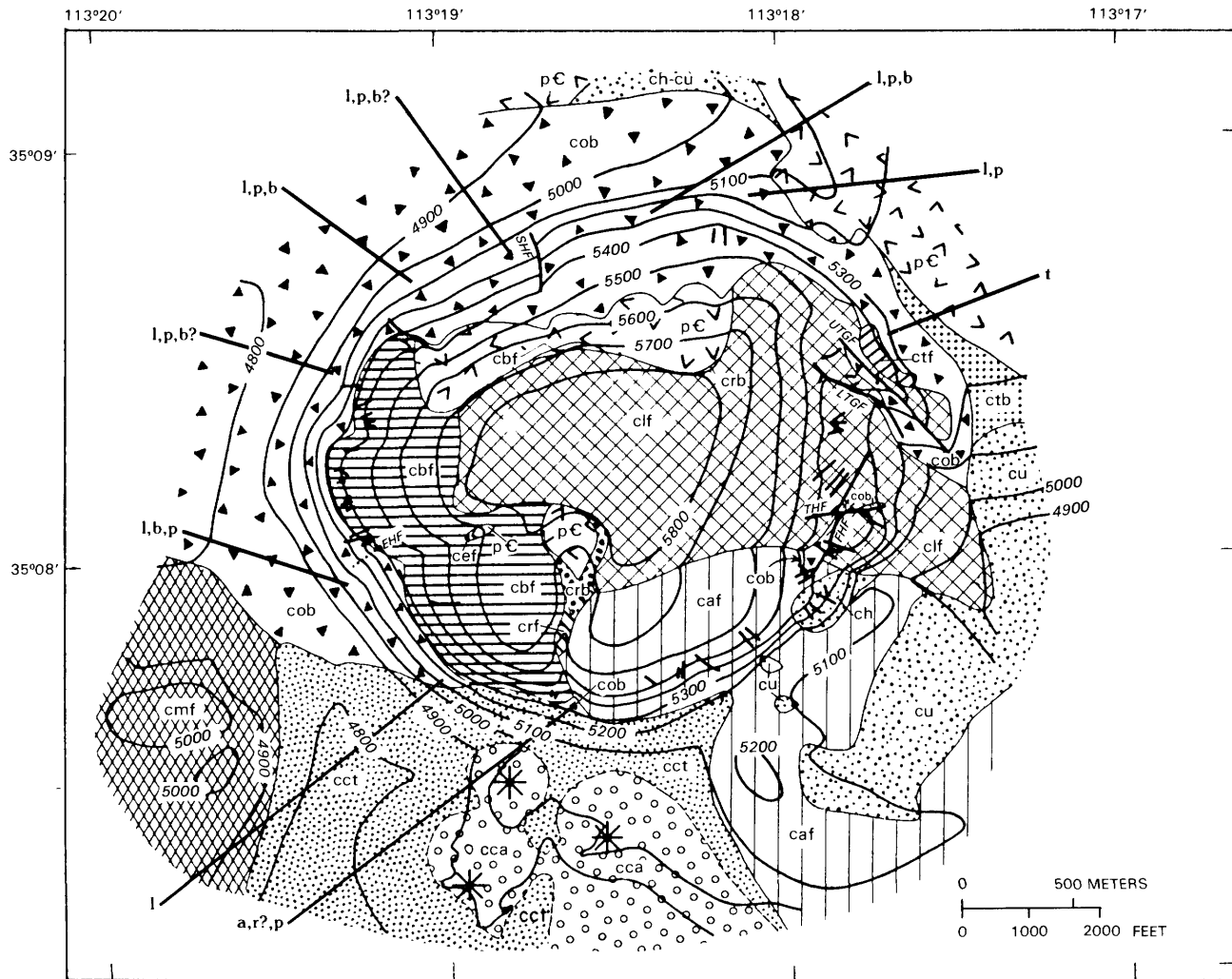
After emplacement of the Lion Ridge flow, patches of the tuff and conglomerate of Hidden Pasture and undivided tuff were deposited (fig. 9, map 7). These units are trachyandesite in composition. One patch was deposited over a large area east and southeast of the present crater. Another was deposited north of the present crater. Ash and bombs in the deposit on the east and southeast appear to have come from a source in or near a large trachybasalt eruptive center approximately 1 km east of the Fort Rock dome (fig. 3). Some ash may have come from vents now covered by the Cinder Basin tuff and agglomerate south of the dome. Ash in the deposit on the north may have come from the same source(s) or possibly from a vent now occupied by the intrusive shonkinite body under the powerlines north of the Fort Rock dome.

Uplift of the Fort Rock dome followed the deposition of the Hidden Pasture tuff and conglomerate. Landsliding, or gravity thrusting, signaled the beginning of the uplift. One large landslide body, mentioned above, apparently broke away from an outcrop of the Buffalo Ridge flow located in a former valley near the north side of the present crater (fig. 9, map 6). This body slid out over thin Hidden Pasture deposits, which probably initially covered the outcrop (fig. 9, Map 7), and came to rest on top of these deposits at the site of present-day Noon Hill. A second large landslide body slid away from the north edge of the Lion Ridge flow and now also rests on Hidden Pasture deposits in the east wall of Noon Gorge. This landslide body is contiguous on its east end with Lion Ridge flow that is in place.

As uplift continued, the sedimentary breccia of One O'Clock Wash was deposited on the flanks of the dome, and the tuff and agglomerate of Cinder Basin was erupted on the south side of the dome (fig. 9, map 8). Deposition of the breccia began earlier than eruption of the tuff and agglomerate, but throughout the last stages of uplift these units apparently were being emplaced simultaneously, as the tuff and agglomerate of Cinder Basin contains beds similar to the One O'Clock Wash breccia.

On the north side of the dome, erosion proceeded rapidly as volcanic rocks were undermined by weathering and erosion of poorly resistant Precambrian rocks. The One O'Clock Wash breccia is, therefore, relatively thick on this side of the dome. The initial concentration of clasts of Precambrian rocks in the detritus from the dome was high because the slopes

here were initially underlain by Precambrian rocks. As uplift proceeded, volcanic rocks on the dome supplied most of the detritus, including disaggregated landslide bodies now seen as "block patches" in the breccia. As exposures of Precambrian rocks on the dome widened, clasts of Precambrian rocks again became abundant in the material eroded from the



EXPLANATION

- l Clasts of Lion Ridge flow
 - b Clasts of Buffalo Ridge flow
 - a Clasts of Annex Ridge flow
 - t Clasts of Two O'Clock Gap tuff and flow
 - r Clasts of Road End Gap volcanic breccia and flow
 - p Clasts of Precambrian rocks
- Note: See figure 9 for explanation of geologic units and symbols

FIGURE 10.—Composition of the One O'Clock Wash sedimentary breccia at various places around the Fort Rock dome (shown on map 8 from figure 9). Clasts in the breccia are listed in order of most abundant to least abundant.

dome. On other sides of the dome, erosion proceeded more slowly because of mantling by resistant volcanic flows, and the One O'Clock Wash sedimentary breccia is relatively thin. Drainages were cut slowly through the flows. Precambrian rocks were gradually exposed as inliers, and clasts of Precambrian rocks appeared in gradually increasing amounts in the detritus. Hence, two patterns of isopleths are seen today in the One O'Clock Wash sedimentary breccia; the pattern on the north side of the dome is different from the pattern on other sides of the dome (see the section describing this unit). On the southeast side of the dome, breccia was not deposited or was deposited and removed before younger units were emplaced. In this location, the Annex Ridge flow is very thick and apparently resisted significant erosion.

The drainage pattern developed on the growing dome appears to have been ancestral to the pattern seen today. On the north side of the dome, where rocks were poorly resistant, numerous drainages developed. Numerous drainages are seen in this area of the dome today. In locations where the dome was mantled by volcanic rocks, widely spaced gorges were cut. From the clast content of the sedimentary breccia on the flanks of the dome, it appears that one gorge was cut in the vicinity of present-day Eight O'Clock Gorge and another in the vicinity of Six O'Clock Wash. None of the drainages on the dome were deeply entrenched, as there is no evidence today of old valleys on the rim of the crater. Drainage profiles apparently were similar to the profile of the dome, that is, they were convex upward rather than concave upward. Such abnormal gradients could be explained only if doming took place too rapidly for drainage gradients to keep pace. In the postulated sequence of events shown in figure 11, a normal, concave-upward profile forms first on a low dome but is unable to keep pace with uplift at some point in time and becomes convex upward.

Both the One O'Clock Wash sedimentary breccia and the Cinder Basin tuff and agglomerate were deformed as the dome grew. The oldest beds were deformed the most. On present-day Noon Hill, successively greater tilting of older beds in the One O'Clock Wash breccia is apparent. At the same time, the Eight O'Clock Hill fault and the Eight O'Clock Gorge faults formed as open fissures that were subsequently filled by sedimentary breccia. The Short Hill fault formed next, offsetting a thick section of the One O'Clock Wash unit. Numerous relatively short radial faults on the west side of the dome probably formed during growth of the dome. The timing of down-to-the-west movement on the relatively long

tangential faults on the east side of the dome, the Upper and Lower Two O'Clock Gap faults and the Four O'Clock Hill fault, is uncertain but may have coincided with uplift. The absence of a thick deposit of breccia on the northeast flank of Lion Ridge and the absence of clasts of the Lion Ridge flow in this breccia (fig. 10) could be explained if drainage from the dome were diverted to the southeast by in-facing scarps along the Upper and Lower Two O'Clock Gap faults (fig. 9, map 8). A similar drainage diversion could have occurred along the Four O'Clock Hill fault, as there is no breccia on the southeast flank of Four O'Clock Hill (fig. 9, map 8). It may be possible, on the other hand, to explain the absence of thick deposits of breccia on Lion Ridge and on Four O'Clock Hill as the result of retarded erosion owing to resistant volcanic rocks or as the result of deposition and subsequent removal of breccia before the emplacement of younger units. Down-to-the-west movement on the Upper Two O'Clock Gap fault, whatever its precise age, was opposite the pre-dome movement on this fault. The Four O'Clock Hill fault may also represent reactivation of a pre-dome fault.

At the time when the Fort Rock dome had attained a topographic relief of about 300 m (1,000 ft.) (fig. 9, map 8) and a structural relief comparable to that today, the Fault Canyon flow was erupted on the south flank (fig. 9, map 9). The major vent for this flow is at the head of Tyria Wash. Sills and dikes of this unit on Buffalo Ridge may have been additional small sources for the flow. A large lobe of the flow extended to the north between the Fort Rock dome and the volcanic dome over the vent for the Meadow Dam flow. Most of the flow extended to

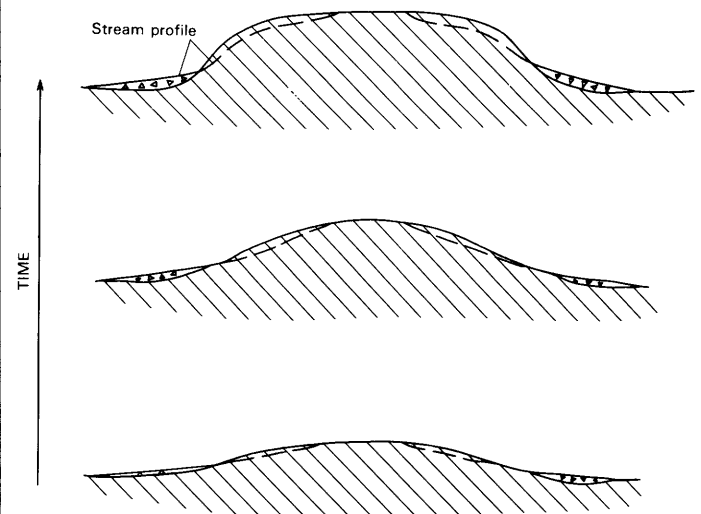


FIGURE 11.—Stream profiles on a dome undergoing accelerating uplift. Bedrock, diagonal lines; breccia, triangles.

the southwest and south. Nearly 0.1 km³ of trachybasalt was erupted.

This flow apparently was erupted from beneath the dome, as the wall of the vent exposed at the head of Tyria Wash dips gently to the northeast beneath Buffalo Ridge. Major uplift of the dome halted after this flow was extruded, and some collapse may even have occurred. It is concluded from the close geographic and temporal association of the Fault Canyon flow with doming that the magma that fed this flow was responsible for the uplift of the dome.

The relative subsidence of rocks toward the center of the dome that occurred along the Upper and Lower Two O'Clock Gap faults and the Four O'Clock Hill fault may represent collapse of the east part of the dome. Thus, a second plausible age for movement on these faults is the time during or after the extrusion of the Fault Canyon flow.

ERUPTION OF THE FORT ROCK CREEK RHYODACITE

Erosion of the Fort Rock dome continued after the eruption of the Fault Canyon flow. Clasts eroded from the dome at this time comprise the sedimentary breccia of Noon Gorge. Widening exposures of Precambrian rocks on the dome contributed increasing quantities of Precambrian clasts to this deposit. On the north, the Lion Ridge flow was eroded southward to uncover the volcanic breccia of Road End Gap (fig. 9, maps 9 and 10), probable clasts of which appear at the base of the Noon Gorge breccia in this area. In the vicinity of present-day Eight O'Clock Gorge, Six O'Clock Wash, and Two O'Clock Gap, gorges on the dome deepened.

Mafic ash of at least two different compositions, trachybasalt and trachyandesite, was incorporated in the Noon Gorge breccia. Small amounts of this ash were sprinkled through the breccia as it accumulated, but occasionally discrete beds were deposited. A tuffaceous bed on the north flank of One O'Clock Hill contains ash and bombs of trachybasalt that may have been erupted from a vent beneath a hill of agglomerate located 1 km northwest of the dome. Trachyandesite ash of unknown source was incorporated in beds on the southwest flank of the dome. In addition to mafic ash, small fragments of rhyodacite were included in trace amounts in the breccia. These clasts probably were erupted from the large rhyodacite eruptive center in the Aquarius Mountains.

As eruptions increased in frequency and volume at the large rhyodacite eruptive center, rhyodacite fragments were deposited in increasing quantities

in the breccia, and pumice began to appear. Ash flows were next erupted. One or more thin flows reached the Fort Rock dome, followed by one or more massive flows that buried all of the vicinity of the dome below an elevation of about 5,150 ft (1,570 m). These flows constitute the ash-flow tuff of the Old Stage Road Member (fig. 9, map 10). In places enough steam was trapped in the ash flows to crystallize some of the pumice.

Deformation of rocks on the flanks of the Fort Rock dome continued until after the ash flows were emplaced. Deformation included minor uplift, tilting, and faulting. The Noon Gorge sedimentary breccia probably was uplifted and tilted by a small amount, but uplift had apparently ceased by the time the Old Stage Road Member was laid down. Faulting occurred at several intervals. Movement on the One O'Clock Hill fault occurred during emplacement of the basal sedimentary breccia of the Old Stage Road Member. Movement on the Noon Gorge fault probably occurred at the same time. The scarps of these two faults created a small embayment in the north flank of the dome that was subsequently invaded by the ash flows. Further movement on the Lower Two O'Clock Gap fault may have occurred at this time. Such movement appears necessary to explain the presence of a small outcrop of the basal member of the Old Stage Road Member at a low elevation inside the present crater (see pl. 1). Movement on the Wedge Basin fault occurred after the emplacement of the ash flows but caused only minor offset.

After the ash flows, massive ash and block falls(?) were erupted from the Aquarius Mountains center, together with occasional ash flows and volcanic mudflows of differing thicknesses and extents. The rocks erupted during this episode constitute the Three Sisters Butte Member of the Fort Rock Creek Rhyodacite.

A period of erosion followed eruption of the Three Sisters Butte Member, during which a valley was carved at the site of present-day Fort Rock Creek. A volcanic mudflow(?), which now constitutes the breccia and conglomerate of the Crossing, subsequently filled this valley. This mudflow originated in the Aquarius Mountains eruptive center.

At intervals throughout the emplacement of the Fort Rock Creek Rhyodacite, movement occurred on the Fort Rock Creek fault and on the fault south of the present-day Three Sisters. The south sides of both faults were uplifted, and units on the north sides of these faults, were either deposited in relatively greater thickness or were protected from erosion compared to units on the upthrown sides.

ERUPTION OF THE BASALT OF BUTTOX HILLS

On the southeast side of the dome, after emplacement of ash-flow tuff and intrusion of a small body of rhyodacite on Three O'Clock Hill (pl. 1), a period of erosion occurred, and a thin bed of detritus from the Fort Rock dome was deposited. The basalt of Buttox Hills was erupted next. The major vent for this basalt lies beneath the northwest end of the Buttox Hills. A flow went southeast from this vent, and a long dike intruded the edge and flank of the dome in a radial northwest-southwest direction. In addition, a series of small plugs aligned with the northwest end of the dike intruded rocks inside the present crater.

ERUPTION OF OTHER VOLCANIC ROCKS

Volcanic rocks that postdate the Fort Rock Creek Rhyodacite were emplaced in a number of locations in the region. These include the Peach Springs Tuff, the Mohon Mountains volcanic field, and several minor intermediate and mafic dikes.

The Peach Springs Tuff of Young (1966) originated as a regional Miocene ash flow that was emplaced in a large region of the central and eastern Mojave Desert in California and the Basin and Range province and southwest margin of the Colorado Plateau in Arizona (Young and Brennan, 1974; Goff and others, 1983; Glazner and others, 1986). Prior to emplacement of the tuff on the west flank of the Aquarius Mountains, faulting occurred along a sinuous north-south-trending fault located on the west edge of the Cottonwood Cliffs and Aquarius Mountains (fig. 3). The fault brought rocks of the Crater Pasture Formation up on the west and either formed a fault scarp against which rocks of the Fort Rock Creek Rhyodacite were emplaced or offset these rocks downward on the east. A period of erosion ensued before the Peach Springs Tuff was emplaced.

After emplacement of the Peach Springs Tuff, volcanic flows erupted south of the Aquarius Mountains to form the Mohon Mountains volcanic field (Young and Brennan, 1974; Simmons, 1990). A basalt flow at or near the base of these volcanic rocks covered an extensive area south of the Fort Rock dome (fig. 3).

Miscellaneous dikes of intermediate and mafic volcanic rocks were intruded at several locations after emplacement of the Fort Rock Creek Rhyodacite. Andesite(?) dikes were formed that fed local flows on top of the ash-flow tuff a little over 2 km north of the Fort Rock dome (fig. 3). Remnants of these flows

form the caprock of small buttes and mesas in this area today.

LATE GEOLOGIC HISTORY

After emplacement of volcanic units in the region of the Fort Rock dome, renewed movement occurred on the Fort Rock Creek fault, the fault south of the Three Sisters, and the fault along the west edge of the Cottonwood Cliffs and Aquarius Mountains. This movement, in all three cases, was down on the south or west, in a direction opposite to earlier movement.

Movement on the fault along the west edge of the Cottonwood Cliffs and Aquarius Mountains was part of an episode of faulting in which Basin and Range topography was formed. Subsidence along this fault, approximately 300 m, and along the fault at the base of the Grand Wash Cliffs to the north, which appears to be continuous with this fault, led to the formation of basins with interior drainage. Deposits such as the Muddy Creek Formation of Pliocene age near present-day Lake Mead (Longwell, 1936; Damon, 1965; Lucchita, 1972) and the Big Sandy Formation of Pliocene age west of the Mohon Mountains (Sheppard and Gude, 1972) accumulated in these basins.

An episode of significant erosion followed volcanism and faulting in the region and is continuing at the present. The deep canyons of Trout Creek, Cow Creek, Muddy Creek, and Fort Rock Creek have been cut during this episode. The volcano that was built over vents in the Aquarius Mountains has been deeply dissected to produce the present-day topography. This volcano probably was at one time as high as the volcano, still apparently largely intact, that constitutes the Mohon Mountains to the south. The Fort Rock dome was deeply dissected during this episode. In addition, erosion in the vicinity of Cross Mountain resulted in extensive deposits of gravel east of the Fort Rock dome. These gravel deposits are now being dissected but are preserved on high terraces. This regional episode of erosion is associated with the formation of the Colorado River drainage, which began in early or middle Pliocene time (Young and Brennan, 1974; McKee and McKee, 1972; Lucchita, 1972).

About two-thirds of the volume of uplifted rocks on the Fort Rock dome, or about 0.7 km³, has been removed during the recent episode of erosion. Previous erosion of the dome, which is recorded in the deposits of sedimentary breccia on the flanks of the dome, amounted merely to removing most of the relatively thin covering of volcanic rocks. Recent erosion

resulted in carving of a craterlike depression on the dome.

The sequence of erosional events leading to the present craterlike depression may have been somewhat as follows: As volcanic rocks were stripped from the dome, drainages cut deeply into the less resistant Precambrian rocks beneath. Headward convergence of drainages apparently led frequently to stream capture. The two drainages most successful at stream capture appear to have been those ancestral to Four O'Clock and Five O'Clock Washes. These two drainages appear to have captured the headward parts of the drainage on the south side of the dome, in the position of present-day Six O'Clock Wash, and the drainage along the Lower Two O'Clock Gap fault (see fig. 9, map 10). It is likely that the headward part of the drainage ancestral to Eight O'Clock Gorge was also captured. Stream capture thus diverted drainage of more than half of the dome through two gorges on the southeast. Precambrian rocks in the center continued to be dissected by these two drainages. Drainage basins widened, converged on one another, and extended outward to the steeply dipping volcanic rocks in the monocline on the edge of the dome. These rocks formed an infacing scarp around the drainage basins and created the distinctive craterlike depression seen today in the southeast half of the Fort Rock dome.

Drainages on the northwest half of the dome were probably initially small compared to the two major drainages in the southeast. High-standing hills inside the present-day crater rim on this half of the dome, such as Ten O'Clock Peak, indicate that no major northwest-draining basins comparable to those in the southeast were ever formed. In fact, it is probable that most of this half of the dome initially drained to the southeast. With the incision of Fort Rock Creek on the west side of the dome, however, the local base level for drainages on the northwest half of the dome was lowered, and deep gorges are now being cut in this area. Erosion of this half of the dome is following the same course that erosion followed on the southeast half of the dome. The drainage through Eight O'Clock Gorge has already captured the headward parts of Nine O'Clock and Ten O'Clock Washes. The drainage through Noon Gorge is presently about to capture the headward parts of One O'Clock Wash and the drainage on the west side of Noon Hill. Eight O'Clock Basin and Noon Basin are widening at the expense of the upland between them and at the expense of Crater Pasture, which is the old drainage depression on the southeast half of the dome. Crater Divide marks the present limit of

encroachment of the young drainages in the northwest upon the older drainages in the southeast.

MECHANICS OF FORMATION OF THE FORT ROCK DOME

The Fort Rock dome was apparently created by an intrusive plug pushing its way toward the surface creating an arch in overlying Precambrian and Tertiary rocks. In this chapter the results of modeling this phenomenon mathematically are described and applied to the Fort Rock dome. The reader is referred to Fuis (1973) for a detailed development of the model; only the highlights are presented below.

FORMULATION AND SOLUTION OF THE PROBLEM

The Precambrian and Tertiary rocks on the Fort Rock dome are modeled as a layer of Newtonian-viscous fluid. On the bottom of the layer an axisymmetric pressure is applied, representing the pressure of the intrusive plug against the overlying rock. This model is a rather severe idealization of the mechanics of formation of the Fort Rock dome; nevertheless, limited but useful results are obtained. Arguments justifying the use of this simple model are outlined below.

Deformation on the Fort Rock dome can be treated by continuum mechanics, as the size of individual blocks moving around is much smaller than the characteristic dimension in this problem, which is the radius of the dome. Field studies indicate faulting at scales ranging from centimeters to a few tenths of a kilometer, whereas the dome radius is slightly over 1 km. The choice of a Newtonian-viscous rheology to describe the behavior of this faulted assemblage of plutonic, metamorphic, and volcanic rocks is arbitrary but is preferable to an elastic rheology, in view of the permanent deformation seen in the rocks, and is simpler to treat than other likely rheologies, such as "pseudoplastic" or "Bingham" rheologies (see Johnson and Pollard, 1973, p. 287 ff). Without a knowledge of the actual rheology of the rocks underlying the dome, it is preferable to use a linear, viscous rheology in a first attempt at modeling and see how well it describes the behavior of the Fort Rock dome.

Navier-Stokes equations are appropriate to describe the mechanics of a Newtonian-viscous fluid. We linearize these equations by neglecting accelerations, an approximation that is commonly made when the Reynolds number of the fluid flow is low (Landau

and Lifshitz, 1959, p. 63). The Reynolds number is the ratio of the product of a characteristic length and velocity to viscosity. For the Fort Rock dome, a characteristic length is 1 km, a characteristic velocity might range from millimeters per year to meters per year, and viscosities for solid geologic substances (see, for example, Haskell, 1935) range from 10^{10} to 10^{27} poises. A maximum Reynolds number for the Fort Rock dome is thus about 10^{-10} . Hence, this linearizing approximation is reasonable for the Fort Rock dome, and our equations of motion and continuity are

$$\frac{\eta}{\rho} \nabla^2 \bar{v} = \frac{1}{\rho} \nabla p - \frac{1}{\rho} \bar{f} \quad (1)$$

$$\nabla \cdot \bar{v} = 0 \quad (2)$$

where

- η is viscosity
- ρ is average density of Precambrian and Tertiary rocks
- \bar{v} is velocity (vectors are indicated with an overhead bar)
- p is pressure
- \bar{f} is here the acceleration due to gravity, of magnitude g ,

In order to formulate tractable boundary conditions for the linearized Navier-Stokes equations, we treat the Precambrian and Tertiary rocks as a layer of viscous fluid of depth h and infinite lateral extent resting on a semi-infinite body of inviscid fluid, or magma. A pluglike intrusion of the layer is modeled by applying an axisymmetric pressure distribution on its bottom surface (fig. 12).

It would probably be more reasonable to model the Precambrian and Tertiary rocks as a semi-infinite body of viscous fluid in which a vertical cylinder of inviscid magma rests with its top at depth h below the surface of the fluid. Intrusion by the cylinder could be modeled by applying a buoyancy pressure at the top (and sides) of the cylinder. This model poses difficult boundary conditions, however. One would have to solve the equations in two regions, the region below depth h and the region above depth h , and match the solutions at h . This problem was not attempted. Rather, using the model proposed, we in effect solve half of the latter problem; namely, we obtain a solution for the region above depth h and ignore the influence of rocks below. Thus, the Precambrian and Tertiary rocks are decoupled at

depth h . This model makes no provision for stopping or injection of magma as dikes and apophyses. Intrusion is modeled simply as a concordant upwelling of magma.

From this point forward, the formulation and solution of the problem is similar to Haskell's (1935). Haskell modeled the deformation of Fennoscandia under a load of glacial ice; the Fennoscandian crust was modeled as a viscous fluid. Our problem is analogous, but the viscous fluid is bounded below, and pressure is applied to the lower surface. In Haskell's problem, the load applied to the upper surface is a constant pressure of magnitude σ_0 applied inside a radius a , representing the glacial load. In our problem, we could apply a similar pressure distribution to the bottom of the fluid, representing the pressure of an intrusive plug; however, we must compensate the net force thus applied to the layer by adding an annulus of "negative pressure" around it. (Adding an annulus of negative pressure is an artificial way of restoring some coupling between rocks above depth h and those below.) In order to obtain a relatively simple analytic solution, we approximate this pressure distribution, which we call $\sigma(\bar{r})$, with a Bessel function, J_0 ,

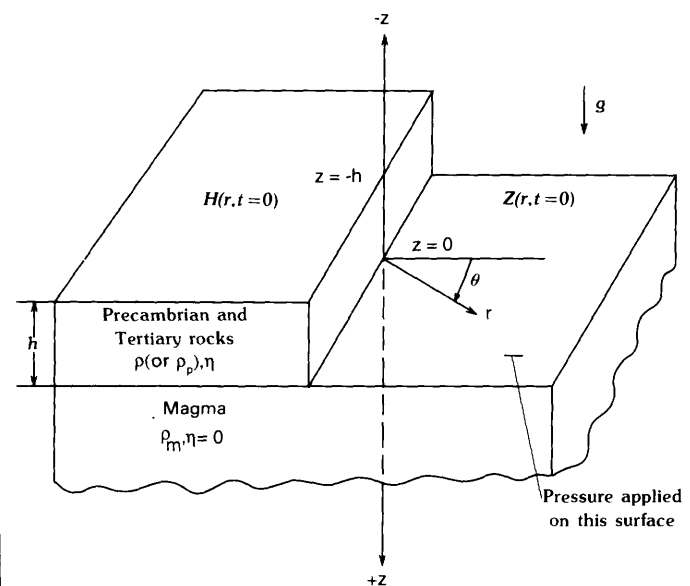


FIGURE 12.—Model used in a mathematical formulation of doming. Note that the coordinate system (r, Θ, z) remains fixed in space for all t , whereas the surfaces $H(r, t)$ and $Z(r, t)$ will move. ρ , density; η , viscosity; h , depth; g , acceleration due to gravity; subscript p denotes Precambrian and Tertiary rocks; subscript m denotes magma.

$$\sigma(\bar{r}) = \sigma_0 J_0(\alpha_0 \bar{r}) + \rho g h, \quad (3)$$

where σ_0 is the maximum magmatic driving pressure, that is the excess of lithostatic pressure $\rho g h$, \bar{r} is the radial coordinate normalized by plug radius a ($\bar{r} = r/a$), and α_0 is the first root of the Bessel function. This Bessel-shaped pressure distribution peaks at the center of the plug, falls to zero at $\bar{r} = 1$, the edge of the plug, has an annulus of negative values just beyond $\bar{r} = 1$, followed at greater \bar{r} by annuli of alternately positive and negative pressure of diminishing amplitude. The pressure is turned on at $t = 0$.

Finally, the idealized boundary conditions for the problem can be stated as follows (see Fuis, 1973, pp. 204-208): (1) the normal stress (T_{zz} , see fig. 16) and shear stresses (T_{rz} , T_{zr}) at the top surface of the layer of fluid are zero, (2) the normal stress (T_{zz}) at the bottom of the layer is equal to the applied magmatic pressure; the shear stresses (T_{rz} , T_{zr}) are zero, and (3) the velocity at the top and bottom surfaces is equal to the partial time derivative of displacement of these surfaces. Let the displacement of the top surface be described by the function $H(\bar{r}, t)$ and the displacement of the bottom surface by $Z(\bar{r}, t)$. Then in all the boundary conditions make the simplification that normals to the surfaces H and Z be approximated by the vertical unit vectors $(0, 0, \pm 1)$ and that the values of the unknown quantities on these surfaces, including p and \bar{v} and their derivatives, be replaced by their values on the flat surfaces $z = 0, -h$ (refer to figure 12). The latter simplifications clearly limit our study of doming to its early stages, where displacements are small compared to the radius of the plug.

The final solution for the displacement of the upper surface of the fluid, or the dome, is

$$H(\bar{r}, t) = \frac{2\sigma_0}{\rho g} J_0(\alpha_0 \bar{r}) \Omega_{H1}(\gamma) \sinh(\tau) \quad (4)$$

and for the lower surface of the fluid, or the roof of the magma chamber, is

$$Z(\bar{r}, t) = \frac{\sigma_0}{\rho g} J_0(\alpha_0 \bar{r}) \left\{ [e^\tau - 1] \Omega_{Z1}(\gamma) + [1 - e^{-\tau}] \Omega_{Z2}(\gamma) \right\} \quad (5)$$

where

$$\bar{r} = r/a$$

t is time

σ_0 is maximum magmatic driving pressure

ρ is average density of Precambrian and Tertiary rocks

g is acceleration due to gravity

$\alpha_0 = 2.4048$, the first root of J_0

$\tau \equiv$

$$\frac{1}{2} \rho g h (t/\eta) (G/\gamma), \quad G \equiv \left[1 + \frac{4\gamma^2 e^{-\gamma}}{e^\gamma (1 - e^{2\gamma})^2 - 4\gamma^2 e^{-\gamma}} \right]^{1/2}$$

$\gamma \equiv \alpha_0 h/a$

$\Omega_{H1}(\gamma)$, $\Omega_{Z1}(\gamma)$, $\Omega_{Z2}(\gamma)$ are given by expressions in Fuis (1973, p. 226) and are shown graphically in figure 13.

Expressions for velocities and pressures in the fluid layer (see Fuis, 1973, p. 226) along with expressions (4) and (5) can be shown to satisfy our linearized Navier-Stokes equations and to fit our simplified boundary conditions for small distortions, where "distortion" is used formally here to mean dome (or magma chamber) amplitude divided by plug radius a , that is, $H(\bar{r}=0)/a$ (or $Z(\bar{r}=0)/a$). For distortions

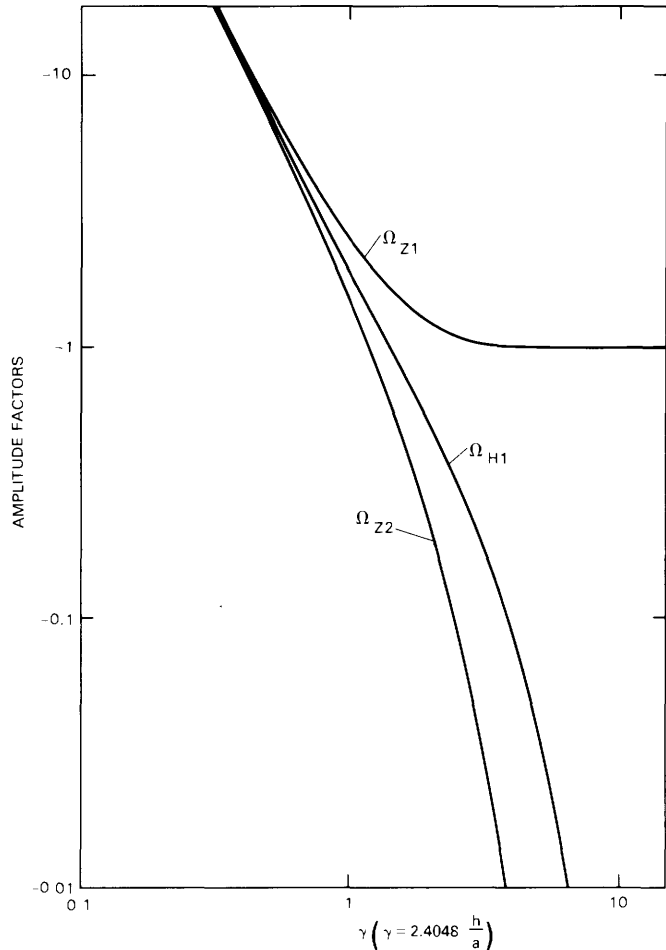


FIGURE 13.—Amplitude factors Ω_{H1} , Ω_{Z1} , Ω_{Z2} in equations (4) and (5). See text for equations.

less than about 10 percent, the model will be a physically meaningful reproduction of doming in a viscous fluid. For larger distortions, it is not clear how the model would correlate with real doming. (Mathematically, however, there are no limits on the solution, and domes as large as desired can be treated.)

BEHAVIOR OF THE DOME

Certain aspects of the behavior of the dome and magma chamber, described by equations (4) and (5) are interesting and applicable to the Fort Rock (and other) domes, and certain aspects reflect limitations of our simple model. The functions H and Z are expressed in terms of the variables \bar{r} , γ , and τ . As τ has a dependence on γ , we can define an independent variable $\tau' = (\gamma/G) \cdot \tau = \frac{1}{2}\rho gh(t/\eta)$. γ is the ratio of layer thickness h to plug radius a multiplied by a constant; τ' is the ratio of time to viscosity, scaled by half the maximum lithostatic pressure. We shall examine the behavior of the dome and magma chamber as determined by these independent variables.

DEPENDENCE ON RADIUS

H and Z are the same functions of \bar{r} ; that is, the undulations on the surface of the fluid have the same radial dimensions as those on the roof of the magma chamber below. This property is a limitation of our model arising from our choice of a Bessel-shaped pressure distribution. None of the upward broadening of features is seen that one would expect from, say, a cylindrical driving pressure. The wings of the Bessel function prevent fluid from flowing off the top of the dome to infinity. Such flow would serve to broaden the dome and lessen its height. Instead, the wings intersperse areas of positive and negative radial mass transport such that there is no net transport.

DEPENDENCE ON γ AND τ'

The amplitude of the dome converges to that of the magma chamber as the layer is made thinner than $h=a$ (i.e., $\gamma=2.4048$), but it quickly becomes negligible compared to that of the magma chamber as the layer becomes thicker than $h=a$ (fig. 14). This property has important implications for the formation of domes. One can demonstrate (Fuis, 1973, p. 233 ff.) that the quantities h/a and τ' have critical values of the order of 1 for the formation of domes like the Fort Rock dome, where distortion is signifi-

cant ($H/a > 0.1$) but the magma chamber has not arched all the way up inside the dome ($Z/h < 1$). By "critical values," we mean values that are fairly stationary over a wide range of driving pressures. The existence of critical values of h/a and τ' can be understood as follows. For relatively thin layers, where $h/a \ll 1$, the time interval t during which doming occurs must be short or the fluid viscosity η must be high to prevent the magma from arching through the layer and violating the condition that $Z/h < 1$; therefore τ' must be small. Dome distortions produced in these thin layers are small, since the shape of the dome is closely similar to that of the arched roof of the magma chamber. For relatively thick layers, at the other extreme, where $h/a \gg 1$, the time interval t must be long or the viscosity η must be low to allow significant penetration by the magma; τ' must, therefore, be large. Dome distortions in this case are also small, because a long time interval or a low viscosity permits fluid to flow away from the dome, making it flatter. Thus, maximum dome distortions occur at intermediate values of time, viscosity, and h/a , namely those such that $\tau' \sim 1$ and $h/a \sim 1$. Near these critical values, factors tending to cause low dome distortions are minimized.¹³

Several other authors have also concluded that h/a must be of the order of 1 for significant distortion to be seen at the surface due to magmatic intrusion at depth. Gilbert (1880, p. 81), using a very approximate method, concluded that a laccolith with significant distortion at the surface cannot be formed unless its diameter is of the order of the thickness of overlying rock, or $h/a \sim 2$. His model of a laccolith involves upward movement of a plug of overburden along a circular fault in response to pressure from magma below that plug. More recently Pollard and Johnson (1973) concluded that a transition occurs between sill intrusion, involving no distortion at the surface, and laccolith intrusion, with surface distortion, at around $h_e/a \sim 0.6$, where h_e is the effective thickness of the overburden. The composite model used by Pollard and Johnson involves, for sill intrusion, elastic deformation around a pressurized elliptical slit in an infinite medium, and for laccolith intrusion, elastic bending of layered overburden over a pressurized magma. The effective height of the overburden h_e is equal to the actual height h if the layers are bonded to each other but is considerably

¹³Although our model is not strictly applicable to the range $H/a > 0.1$ and $0.1 < Z/h < 1$, Fuis (1973, p. 237-238) has shown that the same critical values, $h/a \sim 1$ and $\tau' \sim 1$, are obtained for a range where the model is applicable, namely, $0.01 < H/a < 0.1$ and $Z/h < 0.1$.

less than h if the layers can slide over one another. Pollard and Holzhausen (1979) revised the above estimate of h/a for the transition from sill to laccolith intrusion to $h/a \sim 1.25$. Their model involves elastic deformation by a pressurized elliptical slit in a medium with a free surface. Thus, analyses of several different models of doming all conclude that for significant distortion at the surface, h/a must be of the order of 1.

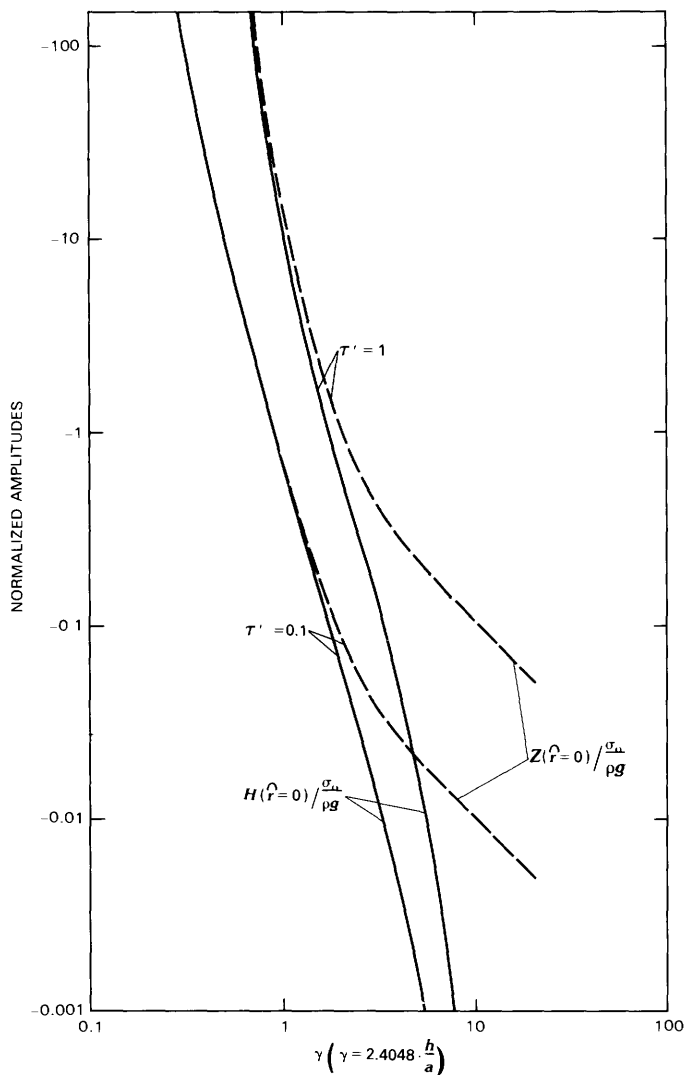


FIGURE 14.—Normalized amplitude of the dome, $H(\bar{r}=0)/(\sigma_0/\rho g)$, and the magma chamber, $Z(\bar{r}=0)/(\sigma_0/\rho g)$. H , dome surface; Z , roof of magma chamber; h , layer thickness; \bar{r} , normalized radial coordinate, $\bar{r} = r/a$; a , plug radius; t , time; η , viscosity; σ_0 , maximum magmatic driving pressure; ρ , average density of Precambrian and Tertiary rocks; g , acceleration due to gravity. Two values of τ' ($= \frac{1}{2}\rho g h(t/\eta)$), 0.1 and 1, are used for the curves.

ACCELERATION

All time derivatives of equation (4) are positive; therefore, doming in the model is an accelerating process. This acceleration is caused by the fact that the driving pressure remains constant as the layer of fluid is progressively thinned as Z approaches H . The dome will continue to grow without bound unless some other process is introduced to stop it at some point. Processes for halting doming are discussed below.

VELOCITIES AND STRESSES

Velocities in the deforming layer of fluid are given by expressions in Fuis (1973, p. 226) and are shown in fig. 15. Maximum vertical velocity is seen at $\bar{r}=0$, as is expected. Maximum radial velocity is small compared to maximum vertical velocity and is realized near $\bar{r}=0.75$. Note that velocity is purely vertical at the center of the dome and purely radial at the edge of the dome; the edge of the dome for our purposes is defined as $\bar{r}=1$. Vertical velocity decreases with height, whereas radial velocity increases with τ' .

These trends in velocity can be understood in a physical sense. Vertical velocity is imparted to the fluid by the upward push of the magma and a dome is created. Radial velocity arises from material flowing outward in response to gravity. This outward flow is highest laterally in the layer where slopes on the dome and the magma chamber are the steepest, near $\bar{r}=0.75$. In terms of depth within the layer, radial flow is highest at the surface of the dome, which is stress-free. Outward flow of material tends to flatten the dome relative to the magma chamber.

Gradients in the velocity components give rise to stresses. Refer to Fuis (1973, p. 241-243 and table 10) for expressions and evaluations for stresses. These stresses can be transformed locally into principal stresses. In our model, two of the local principal stress directions lie in the r - z plane and the third lies in the θ direction (fig. 16). Maximum shear stress S occurs on planes parallel to the local intermediate-principal-stress axis and inclined at 45° to the maximum- and minimum-principal-stress axes (see, for example, Anderson, 1942, p. 9). The local inclination i of the principal stress axes from radial and vertical directions is indicated in table 8 along with the direction of the intermediate-stress axis and the normalized value of maximum shear stress. The implications of table 8 for faulting on a dome, as-

suming faults form along planes of maximum shear stress, are summarized in figure 17. Referring to table 8 and figure 17 one notes the following:

- (1) The highest shear stress occurs near the top of the dome. At lower horizons, maximum shear stress occurs near $\bar{r}=0.75$.
- (2) Shear planes which have radial to subradial strikes and dips steeper than 45° are seen in a lens-shaped region underlying the surface of the dome.

Shear planes in deeper regions and those in the region beyond the dome have tangential strikes and various dips.

- (3) Senses of displacement are such that on all shear planes with dips greater than 45° the downthrown side is away from the center of the dome.
- (4) The region from the center of the dome to the edge of the dome is characterized by normal shear, whereas the region beyond the edge of the dome is

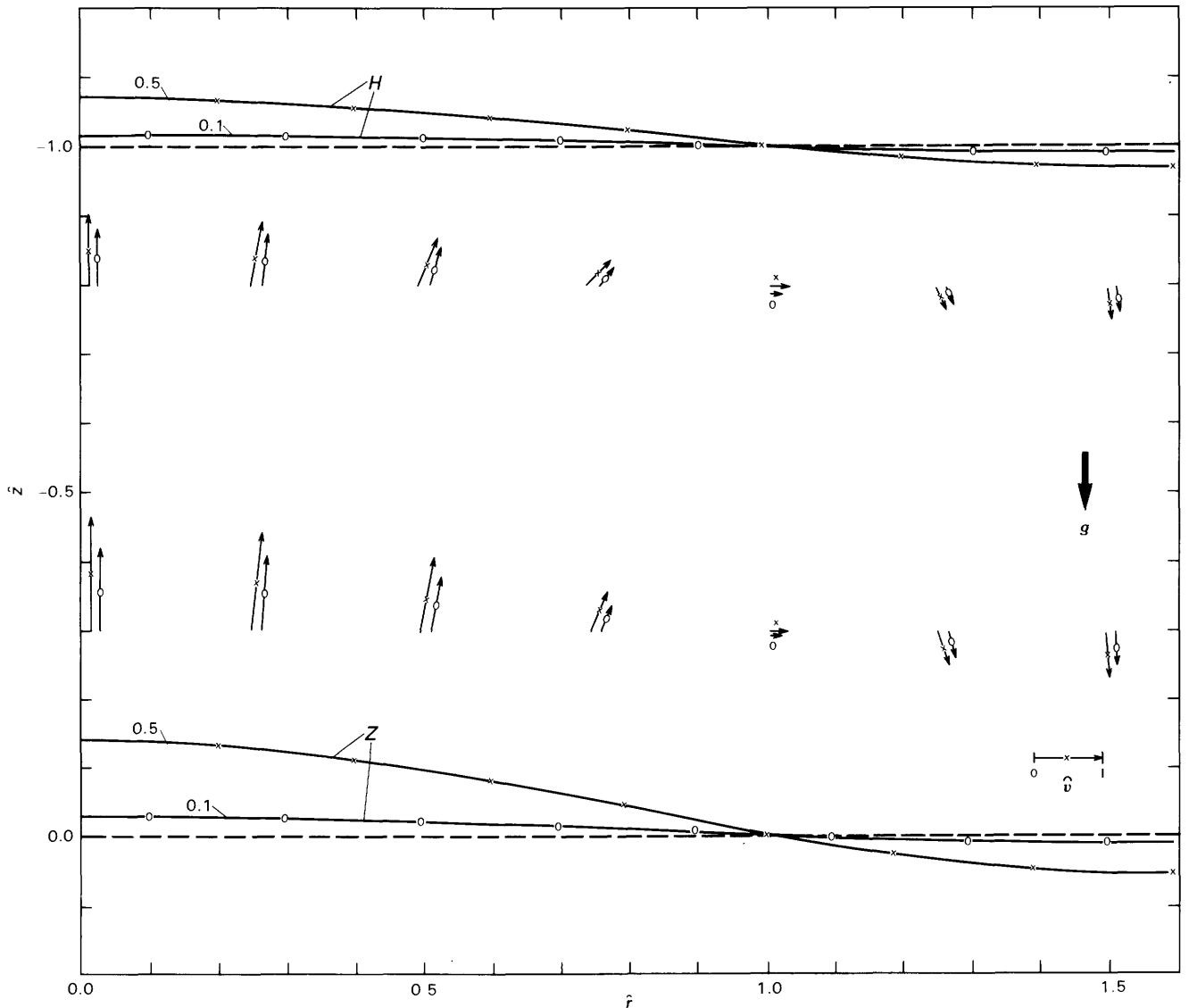


FIGURE 15.—Normalized velocity, $\bar{v} = (4\eta/\sigma_0 h)v$, in the layer of fluid for two values of τ' , 0.1, indicated by O's, and 0.5, indicated by X's. Upper and lower surfaces of the fluid are shown for these two values of τ' . In calculating velocities in this figure, we use $\sigma_0/\rho gh = 0.5$ and $h/a = 1.0$, where σ_0 is maximum magmatic driving pressure, ρ is the average density of Precambrian and Tertiary rocks, g is acceleration due to gravity, h is layer thickness, and a is plug radius. \bar{r} and \bar{z} are normalized coordinates; $\bar{r} = r/a$ and $\bar{z} = z/h$. $\bar{r} = 0.0$ is the center of the dome; $\bar{r} = 1.0$ is the edge of the dome. $\bar{z} = -1.0$ is the pre-dome surface; $\bar{z} = 0.0$ is the initial position of the magma-chamber roof in our model. H, Z are surfaces of the dome, magma-chamber, respectively.

characterized by reverse shear. Here we use the words "normal" and "reverse" as they used to describe senses of fault movement.

PROCESSES FOR HALTING DOMING

According to our model, doming continues at an accelerating rate. Acceleration is caused by the fact that the pressure applied to the base of the layer is constant as the layer is thinning above it. There are at least two processes by which the pressure applied by the magma can be made to decrease, with the result that doming is decelerated or halted completely. These processes are the formation of a vent and the solidification of the magma.

FORMATION OF A VENT

Let us examine pressures found in two different cases where a magma fills a cylindrical chamber of length ℓ in Precambrian and Tertiary rock. In both cases, the top of the cylindrical chamber rests at

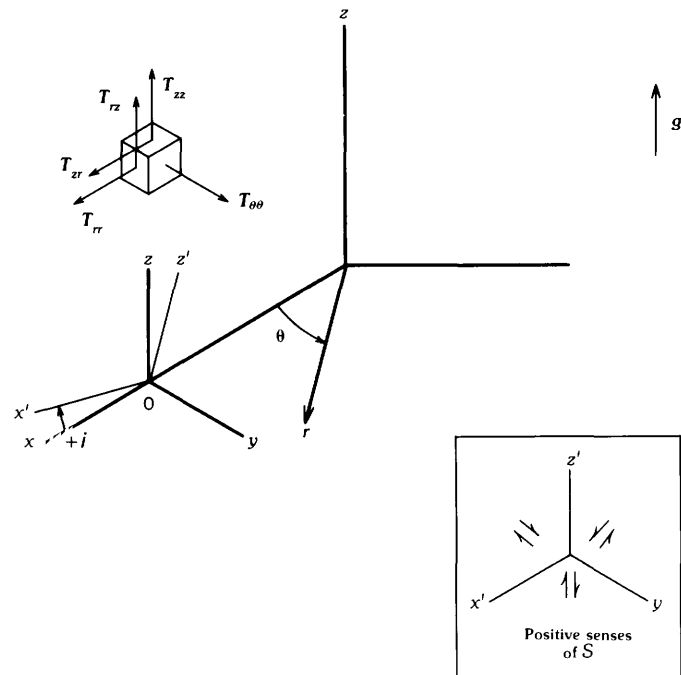


FIGURE 16.—Coordinate system used to describe principal stresses in the layer of fluid. Stresses T_{zz} , T_{rr} , $T_{r'z'}$, $T_{z'r'}$ and $T_{\theta\theta}$ can be transformed at any point O into principal stresses with directions x' , z' , and y , where x' and z' are in the r - z plane and are tilted by angle i from the radial and vertical directions, respectively, and y is the θ direction. Positive senses of shear stress S are indicated. Down is toward the top of the page; g is acceleration due to gravity.

depth h below the surface, which we take to be $z=0$, as in figure 12; the bottom rests at $z=+\ell$. In the first case, the chamber is completely surrounded by Precambrian and Tertiary rock; in the second case, it is connected by a tube to the surface. In both cases the wall of the cylinder is considered to be infinitely rigid, such that all interaction between magma and surrounding rock takes place at the top and bottom of the cylinder.

In the first case, equating magmatic pressure with the vertical normal stress T'_{zz} in the roof rock above the magma chamber gives (refer to Fuis, 1973, p. 205-206)

$$-\sigma = -\rho_p g h + T'_{zz}(z=0), \quad (6)$$

where subscript p refers to Precambrian and Tertiary rock. T'_{zz} includes all nonlithostatic stresses in the rock. Comparing this equation with (3), it is clear that

$$\sigma_0 = -T'_{zz}(z=0), \quad (7)$$

where dependence on radius is ignored for our purposes here.

Likewise, at the bottom of the magma chamber, $z = \ell$,

$$-(\sigma + \rho_m g \ell) = -\rho_p g(\ell + h) + T'_{zz}(z = \ell), \quad (8)$$

or

$$-\sigma = -g\ell(\rho_p - \rho_m) - \rho_p g h + T'_{zz}(z = \ell), \quad (9)$$

where subscript m refers to magma.

Letting

$$\sigma_r \equiv -T'_{zz}(z = \ell), \quad (10)$$

gives finally

$$\sigma_0 = g\ell(\rho_p - \rho_m) + \sigma_r. \quad (11)$$

Because the magma is buoyed upward, $T'_{zz}(z = \ell)$ will be a tensile or positive stress; hence, σ_r will be negative. The maximum value σ_0 can have is, therefore,

$$\sigma_0 \text{ max} = g\ell(\rho_p - \rho_m). \quad (12)$$

As rock strength in tension is considerably lower than rock strength in compression, equilibration is

TABLE 8. — *Inclination i of principal stress system; maximum shear stress, S/σ_0 ; and direction of shear planes in principal stress system*

[Direction of shear planes are as follows: 1--parallel to x' direction (see fig. 16), 2--parallel to y direction, 3--parallel to z' direction. The combination 12 at $r = 0$ indicates that principal stresses in the x' and y direction are identical; the shear planes in this case would dip outward in a conical fashion away from z axis. r and z are normalized coordinates; $r = r/a$, $z = z/h$. $r = 0.0$ is the center of the dome; $r = 1.0$ is the edge of the dome; $r = 1.59$ is the center of the first trough of the Bessel function. $z = -1.0$ is the predome surface; $z = 0.0$ is the initial position of the magma chamber roof in our model, which corresponds to its depth when doming becomes significant at the surface.]

| | | i (degrees) | | | | | | | S/σ_0 | | | | | | | Direction of shear planes in principal stress system | | | | | | |
|------|-----|---------------|------|-----|------|-----|------|------|--------------|------|------|------|------|------|------|--|--------------|-----|------|-----|---------------|------|
| z | r | 0.0 | 0.25 | 0.5 | 0.75 | 1.0 | 1.25 | 1.59 | 0.0 | 0.25 | 0.5 | 0.75 | 1.0 | 1.25 | 1.59 | 0.0 | 0.25 | 0.5 | 0.75 | 1.0 | 1.25 | 1.59 |
| -1.0 | 0 | 0 | 0 | 0 | 89 | 89 | 90 | | 0.44 | 0.41 | 0.32 | 0.19 | 0.12 | 0.18 | 0.23 | 12 | 1 | 1 | 1 | 1 | 2 | 2 |
| -0.9 | 0 | 6 | 14 | 29 | 56 | 75 | 90 | | .33 | .31 | .25 | .18 | .13 | .16 | .18 | 12 | 1 | 1 | 1 | 1 | 2 | 2 |
| -0.8 | 0 | 12 | 24 | 36 | 50 | 65 | 89 | | .27 | .27 | .25 | .23 | .20 | .17 | .14 | 12 | 2 | 2 | 2 | 2 | 2 | 2 |
| -0.7 | 0 | 16 | 29 | 39 | 48 | 61 | 89 | | .25 | .26 | .29 | .29 | .26 | .20 | .13 | 12 | 2 | 2 | 2 | 2 | 2 | 2 |
| -0.6 | 0 | 18 | 31 | 40 | 48 | 59 | 89 | | .24 | .27 | .32 | .34 | .30 | .22 | .13 | 12 | 2 | 2 | 2 | 2 | 2 | 2 |
| -0.5 | 0 | 19 | 31 | 40 | 48 | 58 | 89 | | .24 | .28 | .34 | .36 | .32 | .23 | .13 | 12 | 2 | 2 | 2 | 2 | 2 | 2 |
| -0.4 | 0 | 19 | 32 | 40 | 48 | 57 | 89 | | .24 | .28 | .34 | .36 | .32 | .23 | .13 | 12 | 2 | 2 | 2 | 2 | 2 | 2 |
| -0.3 | 0 | 20 | 32 | 40 | 47 | 57 | 89 | | .21 | .25 | .32 | .34 | .30 | .21 | .11 | 12 | 2 | 2 | 2 | 2 | 2 | 2 |
| -0.2 | 0 | 22 | 34 | 41 | 47 | 56 | 89 | | .15 | .19 | .26 | .28 | .25 | .17 | .08 | 12 | 2 | 2 | 2 | 2 | 2 | 2 |
| -0.1 | 0 | 34 | 40 | 43 | 45 | 49 | 89 | | .03 | .09 | .15 | .17 | .15 | .10 | .01 | 12 | 2 | 2 | 2 | 2 | 2 | 2 |
| 0.0 | 0 | 89 | 89 | 89 | 0 | 0 | 0 | | -.17 | -.15 | -.12 | -.07 | -.04 | -.07 | -.09 | 12 | 3 | 3 | 3 | 3 | 2 | 2 |
| | | | | | | | | | | | | | | | | | normal shear | | | | reverse shear | |

likely to take place more rapidly at the bottom of the magma chamber than at the top, and σ_r will remain small. Equation (12), is therefore, probably a good approximation to σ_0 and agrees, for example, with Johnson and Pollard (1973, p. 284).

In the second case, flow of magma through a tube to the surface is permitted. This flow is considered to be inviscid. Velocities in the magma chamber are assumed to be small compared to velocities in the tube. Bernoulli's equation requires that

$$\sigma = \frac{1}{2} \rho_m v^2 + \rho_m g h, \quad (13)$$

where v is the velocity of the magma as it leaves the vent. Substituting this expression into (6) and (9) and using (7) and (10) gives

$$\sigma_0 = -g h (\rho_p - \rho_m) + \frac{1}{2} \rho_m v^2 \quad (14)$$

$$\sigma_r = -g(h + \ell)(\rho_p - \rho_m) + \frac{1}{2} \rho_m v^2. \quad (15)$$

The eruption velocity v will drop at a rate determined by the size of the vent and how fast the base of the magma chamber collapses inward to maintain the flow. The rate of collapse is determined by the viscosity of the Precambrian and Tertiary rock and the pressures σ_0 and σ_r . Hypothetical graphs of σ_0

and σ_r versus time have been constructed (fig. 18) assuming that σ_r is initially zero and that v falls off smoothly with time after formation of a vent at $t=t_0$. Two examples are given, A and B. For the curves of example A, the velocity is presumed to drop rapidly after formation of a vent owing to either a large vent opening or a slow rate of collapse of the magma chamber. Equations (14) and (15) predict sharp drops in both σ_0 and σ_r in this case. These pressures will conceivably level off at a point in time where the collapse of the magma chamber, which these pressures induce, can maintain a constant flow out of the tube. Doming will continue, although at a lesser acceleration than previously, until time t_1 , after which collapse, corresponding to a negative value of σ_0 will occur. For curves of example B, the velocity drops much less rapidly owing to either a small vent opening or a high rate of collapse of the magma chamber. Doming will continue indefinitely in this case at an acceleration less than acceleration prior to venting. In both examples A and B, σ_r is negative and would induce collapse of the base of the magma chamber. Although the wall of the magma chamber has been considered rigid for the sake of analysis, it too will presumably collapse.

At time t_2 (fig. 18), the vent is closed and pressures will rise to their pre-vent values with the exception that

$$\sigma_0 = g \ell' (\rho_p - \rho_m), \quad (16)$$

where ℓ' is less than ℓ owing to magma loss through the vent. Doming will continue after t_2 , but at a somewhat lesser acceleration than prior to venting.

If the flow of the magma through the vent tube is viscous, back-pressure in the tube due to magmatic viscosity would supplant dynamic backpressure $\frac{1}{2}\rho_m v^2$ and would presumably lead to slower drops in pressures after venting than those discussed above. If a gaseous phase separates from the magma during eruption, additional complexity is expected.

CRYSTALLIZATION OF THE MAGMA

If the density difference $(\rho_p - \rho_m)$ in equation (12) decreases, σ_0 will decrease. It can be shown that if the density of the crystallized magma is about equal to the density of the Precambrian rocks, then

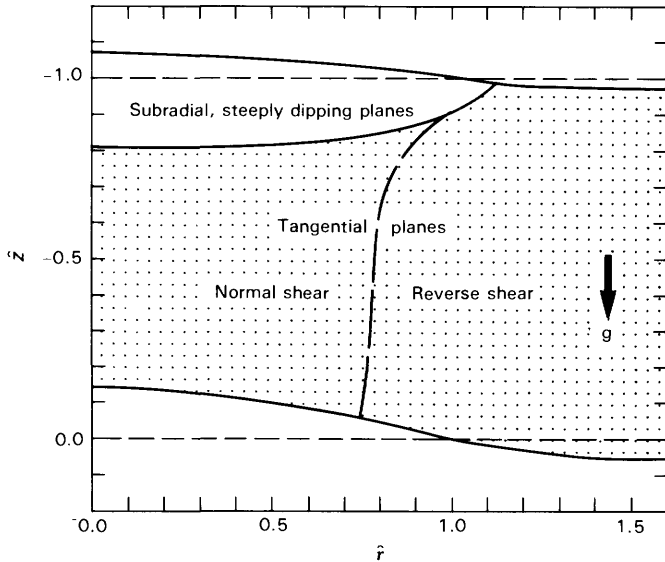


FIGURE 17.—Summary of table 8. In the lens-shaped region underlying the dome (unstippled), planes of maximum shear stress have strikes that range from radial, or in the plane of the page, at $\hat{r} = 0$, to 45° from the plane of the page at $\hat{r} = 1$. Dips of both conjugate planes range from 45° at $\hat{r} = 0$ to 90° at $\hat{r} = 1$. Shear in this region is normal shear, where we use the word “normal” as it is used to describe faults. In the rest of the layer (stippled), planes of maximum shear stress have strikes that are tangential, or perpendicular to the plane of the page. The dip of one conjugate plane ranges from 45° at $\hat{r} = 0$ to $45^\circ + i$ (see table 8) at increasing radius; the dip of the other conjugate plane ranges from 45° at $\hat{r} = 0$ to $45^\circ - i$ at increasing radius. Regions of normal and reverse shear are indicated. Senses of displacement are such that on all shear planes in the lens-shaped region and on those shear planes with dips greater than 45° in the rest of the layer, the downthrown side is away from the center of the dome. \hat{r} and \hat{z} are normalized coordinates; $\hat{r} = r/a$ and $\hat{z} = z/h$. g is acceleration due to gravity.

$$(\rho_p - \rho_m) \cong \frac{\rho_c f_l}{\rho_l / (\rho_c - \rho_l) + f_l} \cong \frac{\rho_c}{\rho_l} (\rho_c - \rho_l) f_l, \quad (17)$$

where ρ_c is the density of the crystallized magma, ρ_l is the density of the liquid magma, and f_l is the fraction of the mass of the magma that is liquid. (The quantity $(\rho_c - \rho_l) / \rho_l$ will be less than about 0.1.) According to (12) and (17), σ_0 is roughly proportional to the fraction of the magma that is liquid.

The time required to crystallize a magma is a limit on the duration of doming. This time is less than about 32,000 years for the Fort Rock dome (Fuis, 1973, p. 259 ff.). This upper limit is calculated modeling the magma chamber as a dike of half width equal to 1 km, assuming crystallization proceeds inward from the walls, and neglecting convection in the magma. For the purposes of calculations below in this report, the time of crystallization is assumed to be of the order of 10^4 years.

COMPARISON OF THE FORT ROCK DOME WITH THE MODEL

DEPTH AND DIMENSIONS OF THE MAGMA CHAMBER AND DRIVING PRESSURE

The critical value of h/a is of the order of 1 for the creation of the Fort Rock dome. This value implies that doming began significantly at the surface when the magma, working its way upward, reached a depth equivalent to its radius. The radius of the Fort Rock dome, 1 km, is an upper limit on the radius of the magma chamber. Our model indicates

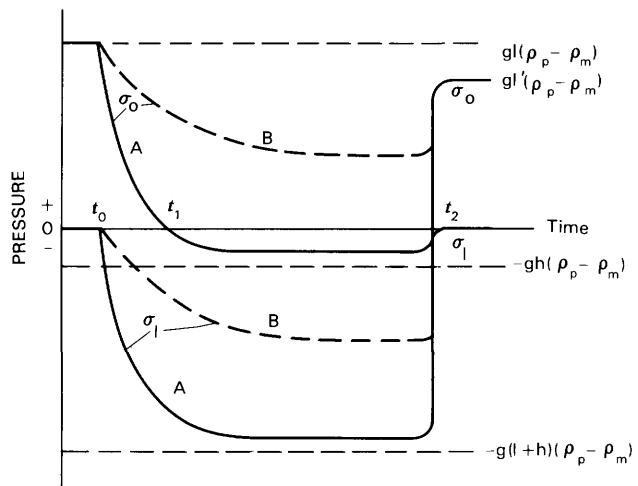


FIGURE 18.—Hypothetical graphs of σ_0 and σ_l versus time. A vent is formed at t_0 ; the vent is closed at t_2 . See text for further explanation.

identical radii for the dome and magma chamber, but it is oversimplified. Presumably some broadening of the dome over the magma chamber would occur if a more realistic model were invoked. We conclude, then, that the top of the intrusion currently rests somewhere between 1 km depth and the surface.

The volume of uplifted rock on the dome can be calculated from the uplift map (fig. 6) to be 0.79 km³. From our model we know this volume must be a lower limit on the volume of the magma chamber. It is interesting to note that the volume of the flow of Fault Canyon, which is inferred to be the extruded part of this magma, is an order of magnitude smaller than this lower limit. (The volume of this flow can be calculated from maps 8 and 9 (fig. 9) to be about 0.09 km³). An exaggerated upper limit on the volume of the magma chamber is a little over 100 km³ assuming a radius of 1 km and a length equivalent to crustal thickness in this area, which is inferred from Johnson (1967) or McCarthy and others (1991) to be about 33 km.

The driving pressure σ_0 for doming is arbitrary in our model. It has no critical values, and hence we can not make any reasonable estimates of it. Lower and upper limits that can be calculated are two orders of magnitude apart. Using the amplitude of the dome, 0.25 km (see fig. 6), as the lower limit ℓ of the magma chamber and 33 km as an exaggerated upper limit, the calculated driving pressures range from less than 0.01 kb to about 1 kb (Fuis, 1973, p. 263 ff.). For most calculations in this report, a relative driving pressure $\sigma_0/\rho gh$ of 0.5 is used corresponding to a driving pressure σ_0 of 0.15 kb.

EFFECTIVE VISCOSITY OF FRACTURED PRECAMBRIAN AND TERTIARY ROCKS

The critical value of $\tau' (= \frac{1}{2}\rho gh(t/\eta))$ is of the order of 1 for the formation of the Fort Rock dome. Thus

$$\eta \sim t(\frac{1}{2}\rho gh) \quad (20)$$

Using $t=10^4$ years, $\rho=2.84$ g/cm³ (an average crustal density; see [Stacey, 1969, p. 287]), and $h=1$ km, we obtain a value for viscosity of

$$\eta \sim 4.4 \times 10^{20} \quad (21)$$

The viscosity given here is the probable effective viscosity of the highly fractured Precambrian and Tertiary rocks underlying the Fort Rock dome.

FAULTS AND BRECCIA LENSES

Two assumptions about material properties are inherent in an assumption of perfect viscosity for the fluid in our model. The first is an assumption of zero yield strength, or continuous failure. The second is an assumption that stress is proportional to the strain rate. On the Fort Rock dome, rock is so thoroughly fractured that it is conceivable that the effective rock strength is indeed small compared to stresses developed. Of course, some doming must have occurred before the rock became thoroughly fractured. The response of fractured rock to stress is, of course, unknown. The assumption of a linear stress-rate-of-strain relationship is an approximation at best. Without understanding the physics of doming at Fort Rock, the best one can hope to do is examine structure on the dome to see if it is consistent with structure predicted by the model. In particular, are shear features in the dome, for example faults and lenses of breccia, similar to shear features in the model?

Mapped faults on the Fort Rock dome include radial to subradial faults, tangential faults, and gravity-thrust faults bounding some landslide blocks. Both radial and tangential faults dip steeply in all places where attitudes can be determined. Faults on the north side of the dome involve block rotations (fig. 7). Radial faults on the west and south sides of the dome probably involve relative movement perpendicular to contact planes, which dip steeply. These faults, therefore, show a combination of dip-slip and strike-slip movement. Faults similar to these are also seen on the north flank of Three O'Clock Hill. Tangential faults on the east side of the dome are apparently derived from pre-dome structures. The Upper Two O'Clock Gap fault is definitely a reactivated pre-dome fault, and the Four O'Clock Hill fault may also represent renewed movement on a pre-dome fault. The Eight O'Clock Gorge faults, on the other hand, are tangential reverse faults that formed during doming.

Steeply dipping subradial planes of combined normal and strike-slip shear are generated in the model near the edge of the dome (table 8; fig. 17). Displacement is such that on subradial shear planes the downthrown side occurs on the side of the plane away from the center of the dome. This sense of displacement is seen on virtually all faults on the west and south sides of the crater, on faults on the north side of Three O'Clock Hill, and on at least parts of all faults on the north side of the dome, with the exception of the One O'Clock Hill fault. On the latter fault the downthrown side is toward the

center of the dome. The Three O'Clock Hill fault is also an exception.

Tangential shear is generated in the model at horizons deeper than $\hat{z}=-0.9$ within the limits of the dome ($\hat{r}\leq 1$) and at all horizons beyond the edge of the dome ($\hat{r}> 1$) (table 8; fig. 17). Beneath the Fort Rock dome, then, one would expect to encounter tangential faulting at about 0.1 km below the pre-dome land surface, or well below the present level of exposure on the dome. One in fact finds tangential faults at the surface, namely the Upper and Lower Two O'Clock Gap faults and the Four O'Clock Hill fault. Furthermore, these faults have senses of displacement opposite to that predicted by the model for shear in the deeper horizons. These discrepancies lead one to suspect that a different stress regime than that prescribed in the model was responsible for these faults. They may represent collapse of the dome, brought about by venting of the magma, or they may represent uneven uplift due to some irregularity in the magma chamber below. Collapse is perhaps the simplest and most appealing interpretation from the standpoint of the model, but the geologic history (see the previous chapter) suggests that these faults were active throughout doming with a sense of displacement opposite that predicted by the model. Perhaps, then, irregularities in the magma chamber developed during doming because the Upper Two O'Clock Gap fault and possibly the Four O'Clock Hill fault predate doming and exerted structural control on the intrusion. The Eight O'Clock Gorge faults appear consistent with the predicted tangential reverse shear beyond the edge of the dome ($\hat{r}> 1$).

In addition to faults shown on the map, abundant small faults, with displacements of centimeters to perhaps a meter, and lenses of unmineralized breccia are found throughout the dome and were apparently caused by doming. The spatial density of these faults and the maximum thicknesses of breccia lenses is apparently greatest near a radius of about 0.75 km (fig. 8), which would correspond to $\hat{r}=0.75$ in our model. Most measurements of fault densities and breccia lenses were made at an elevation of about 5,100 feet (1,555 m), which is only about 100 feet (30 m) above the average level of the pre-dome ground surface (fig. 9, map 1). For purposes here, we shall consider that these measurements were made at the level of the pre-dome ground surface, or at $\hat{z}=-1.0$.

The model predicts the highest maximum shear stress $S=0.45\sigma_0$ at $\hat{r}=0$ and $\hat{z}=-1.0$ (table 8). S drops to less than a third of this value, $0.13\sigma_0$, at $\hat{r}=1.0$. One might expect the spatial density of faults and

maximum thicknesses of breccia lenses on the Fort Rock dome to reflect this radial decrease in shear stress, instead of peaking at $\hat{r}=0.75$. The pattern on the dome actually resembles closely a pattern predicted by the model for horizons $\hat{z}=-0.7$ and deeper, which would be found well beneath the present level of exposure on the Fort Rock dome.

The discrepancy between the fault and breccia pattern on the dome and the pattern of maximum shear predicted by the model might be explained in at least three ways. First, the assumption of a correlation between shear stress S and fault density or breccia thickness may be wrong. Secondly, the geometry of applied stress beneath the Fort Rock dome might have been different from the smooth Bessel-shaped geometry used in the model. Thirdly, the actual rheology of rocks underlying the Fort Rock dome might lead to a somewhat different pattern of deformation than that arising from the Newtonian-viscous rheology in the model. Either the second or third explanation seems most likely. The concentration of deformation toward the edge of the Fort Rock dome, including the existence of a sharp monocline, suggests, on one hand, that the magma chamber below may have sharp corners. On the other hand, a "pseudoplastic" or "Bingham" rheology, might produce such deformation without requiring sharp corners on the magma chamber. For these rheologies there is a tendency for deformation to concentrate into narrow zones. For example, a pseudoplastic or Bingham substance moving through a tube moves largely as a plug, with most or all shear occurring on the edge, near the tube walls; whereas a Newtonian-viscous substance moves through the tube with shear distributed smoothly and parabolically (see Johnson and Pollard, 1973, fig. 19). Even layered elastic materials tend to concentrate deformation in narrow zones. Koch and others (1979) have treated a model of laccolith formation in which horizontal elastic sedimentary strata above the magma can slide over one another once the shear strength of the contacts between the layers is exceeded. They find that the overburden moves upward like a piston with monoclines on its edge. The analogy to doming on the Fort Rock dome would appear to be remote, as the layering in the Precambrian rocks is vertical rather than horizontal; however, the ultimate shape produced is similar to that of the Fort Rock dome.

The monoclinical fold and chiefly radial normal faults seen on the Fort Rock dome are very similar to structures seen on salt domes. The reader is referred to any textbook on structural geology (see, for example, Billings, 1965, p. 254-262 and figs. 216-

217). In particular, the style of faulting on the Hawkins dome in Wood County, Texas, is similar to that on the Fort Rock dome (Wendlandt and others, 1946). The monoclinical fold on the Fort Rock dome is also similar to the peripheral folds on many of the laccoliths in the Henry Mountains of Utah (Hunt, 1953).

CRYSTALLIZATION OF THE MAGMA

The Fault Canyon flow is interpreted to be an extrusive part of the magma that caused doming. The flow may not, however, be a representative sample of the magma. At the time of vent formation, the Fault Canyon flow was between 12 percent and 38 percent crystallized, based on estimates from petrographic studies. (See a preceding chapter: the sum of olivine phenocrysts and colorless cores of pyroxene phenocrysts in the rock is 12 percent (table 2), whereas the sum of all mafic minerals in the rock is 38 percent; the rest of the rock is essentially sanidine, which was last to crystallize.) The body of magma beneath the dome may have been much more highly crystallized than these estimates if extensive crystal settling had taken place. In the latter case, the Fault Canyon flow may be representative only of the liquid fraction of the magma that occupied the upper part of the magma chamber.

According to the model, uplift of the Fort Rock dome would continue after the vent for the Fault Canyon flow was plugged. Acceleration would be proportional to the fraction of the magma that was still liquid. Continued doming was, however, small in magnitude. If the Fault Canyon flow is representative of the magma, a great deal of crystallization must have taken place in the magma chamber shortly after the flow was extruded. If the flow is representative only of the upper liquid fraction of the magma, then that fraction was probably relatively small at the time of venting.

HISTORY OF DOMING

Uplift of the Fort Rock dome was rapid prior to extrusion of the Fault Canyon flow. Abnormal stream gradients appear to have existed on the dome (fig. 9, maps 8 through 10) and units of massive sedimentary breccia were deposited on the flanks of the dome. It is possible that doming was actually accelerating as is suggested in figure 11, and acceleration is, indeed, predicted by the model.

Halting of uplift of the Fort Rock dome is most conspicuously related to extrusion of the Fault Can-

yon flow. Little if any continued doming is needed to explain attitudes within units on the flanks of the dome that are younger than this flow. Collapse may have, in fact, occurred. The radial faults on the north side of the dome occurred largely after extrusion of the Fault Canyon flow, but it is difficult to determine whether they represent collapse of certain segments on the dome's periphery or lagging behind of these segments during continued doming. The Upper and Lower Two OClock Gap fault and the Four OClock Hill fault are, on the other hand, inconsistent with doming as described by the model. Either doming was irregular in these areas, or these faults represent collapse.

SUMMARY

The model that is developed in this chapter is a description of doming in a Newtonian-viscous fluid. The model is physically reasonable for distortions equal to 0.1 or smaller. In this range of distortion the model fits proper boundary conditions to a good approximation and behaves in an expected fashion. For distortions greater than 0.1, the correlation of the model to real doming in a viscous fluid is uncertain.

The model is applied to the Fort Rock dome in order to make order-of-magnitude arguments for certain quantities of interest. Within a range of H/a and Z/h defined to include the Fort Rock dome, it was found that values of the quantities h/a and τ' that produce the largest domes remain close to 1 over a wide range of relative driving pressure. Assuming that these "critical" values are more or less correct for the Fort Rock dome, a "layer" thickness h and a probable effective viscosity η for the fractured Precambrian and Tertiary rocks beneath the dome are calculated. For a radius a of 1 km, the layer thickness h is 1 km. This thickness is the depth of the magma chamber when doming began to be felt significantly at the surface. For a time t of the order of 10^4 years, the estimated time required to crystallize the magma beneath the dome, an effective viscosity for the fractured Precambrian and Tertiary rocks is calculated to be 4.4×10^{20} poises.

Planes of maximum shear are generated in the model that are consistent with most mapped faults on the Fort Rock dome. Near the surface of the dome in the model, these planes are radial to subradial, dip steeply, and show a combination of normal and strike-slip shear. Deep beneath the dome, they are tangential and show normal shear. Beyond the edge of the dome, they are tangential and show reverse

shear. Several tangential faults on the east side of the Fort Rock dome are inconsistent with shear planes generated in the model and either represent collapse of the dome after a venting of the magma or reflect some irregularity in the magma chamber at depth during uplift. The spatial density of numerous unmapped faults of small displacement on the Fort Rock dome follows a pattern that appears inconsistent with the pattern of maximum shear stress predicted by the model. This discrepancy can be explained if either the magma chamber beneath the Fort Rock dome had sharp corners or the rocks underlying the dome behaved in the manner of a "pseudoplastic" or "Bingham" substance.

According to the model, doming is an accelerating process which can be halted by formation of a vent or solidification of the magma causing the uplift. Upon formation of a vent, doming decelerates, and collapse occurs in some cases. After the vent is sealed, doming continues at a lesser acceleration until the magma solidifies. On the Fort Rock dome most of this predicted sequence of events is seen. Doming was rapid and may well have been accelerating prior to extrusion of the Fault Canyon flow. After extrusion of this flow, little if any continued doming is indicated and some collapse may have occurred. From the lack of significant continued doming, it is concluded that either solidification of the magma was rapid after extrusion of the Fault Canyon flow, or the magma was largely solidified at the time of extrusion.

REFERENCES CITED

- Anderson, C.A., 1967, Precambrian wrench fault in central Arizona: U.S. Geological Survey Professional Paper 575-C, p. C60-C65.
- Anderson, C.A., Blacet, P.M., Silver, L.T., and Stern, T.W., 1971, Revision of Precambrian stratigraphy in the Prescott-Jerome area, Yavapai County, Arizona: U.S. Geological Survey Bulletin 1324-C, p. C1-C16.
- Anderson, C.A., and Creasey, S.C., 1958, Geology and ore deposits of the Jerome area, Yavapai County, Arizona: U.S. Geological Survey Professional Paper 308, 185 p.
- Anderson, C.A., Scholz, E.A., and Stobell, J.D., Jr., 1956, Geology and ore deposits of the Bagdad area, Yavapai County, Arizona: U.S. Geological Survey Professional Paper 278, 103 p.
- Anderson, E.M., 1942, The dynamics of faulting and dyke formation: London, Oliver and Boyd, 191 p.
- Babcock, R.S., Brown, E.H., and Clark, M.D., 1974, Geology of the older Precambrian rocks of the Upper Granite Gorge of the Grand Canyon, in Breed, W.J., ed., Geology of the Grand Canyon: Grand Canyon National History Association, p. 2-19.
- Barnes, W.C., (revised and enlarged by B.H. Granger), 1960, Arizona place names: Tucson, University of Arizona Press, 519 p.
- Billings, M.P., 1954, Structural geology [2d ed.]: Englewood Cliffs, N.J., Prentice-Hall, 514 p.
- Billingsley, G.H., Conway, C.M., and Beard, L.S., 1988, Geologic map of the Prescott 30- \times 60-minute quadrangle, Arizona: U.S. Geological Survey Open File Report 88-372, 13 p., 1 sheet, scale 1:100,000.
- Boyce, J. M., 1972, The structure and petrology of the older Precambrian crystalline rocks, Bright Angel Canyon, Grand Canyon, Arizona: Northern Arizona University, M.S. thesis, 88 p.
- Brown, E. H., Babcock, R. S., and Clark, M. D., 1974, A preliminary report on the older Precambrian rocks in the Upper Granite Gorge of the Grand Canyon, in Carlstrom, T. N. V., and others, eds., Geology of northern Arizona, Part I—Regional studies: Geological Society of America, p. 2-33.
- Campbell, Ian, and Maxson, J. H., 1936, Geological studies of Archean rocks at Grand Canyon: Carnegie Institute of Washington Year Book 35, p. 329-331.
- Conway, C.M., 1986, Field guide to early Proterozoic strata that host massive sulfide deposits at Bagdad, Arizona, in Nations, J. D., Conway, C.M., and Swann, G.A., eds., Geology of central and northern Arizona: Geological Society of America, Rocky Mountain Section Field Trip Guidebook, p. 140-157.
- Conway, C.M., Connelly, T.J., and Robison, L.C., 1986, An early Proterozoic volcanic-hydrothermal-exhalative system at Bagdad, Arizona: Arizona Geological Society Digest, v. XVI, p. 24-34.
- Conway, C.M., and Karlstrom, K.E., 1986, Early Proterozoic geology of Arizona: Eos, Transactions American Geophysical Union, v. 67, no. 37, p. 681-682.
- Damon, P.E., 1964, Correlation and chronology of ore deposits and volcanic rocks: Tucson, University of Arizona, Geochronology Labs., Annual Progress Report No. COO-689-42 to the Research Division, U.S. Atomic Energy Commission, 117 p.
- 1965, Correlation and chronology of ore deposits and volcanic rocks: Tucson, University of Arizona, Geochronology Labs., Annual Progress Report No. COO-689-50 to the Research Division, U.S. Atomic Energy Commission, 75 p.
- 1968, Correlation and chronology of ore deposits and volcanic rocks: Tucson, University of Arizona, Geochronology Labs., Annual Progress Report No. COO-689-100 to the Research Division, U.S. Atomic Energy Commission, p. 48-52.
- Davis, W.M., 1931, The Peacock Range, Arizona: Geological Society of America Bulletin, v. 41, p. 293-313.
- Elston, D.P., Gromme, C.S., and McKee, E.H., 1973, Precambrian polar wandering and behavior of the earth's magnetic field from stratified rocks of the Grand Canyon Supergroup, Arizona: Geological Society of America, Abstracts with Programs, v. 5, p. 611.
- Fenneman, N.M., 1931, Physiography of western United States: New York, McGraw-Hill, 1st ed., 534 p.
- Fenner, C.N., 1948, Incandescent tuff flows in southern Peru: Geological Society of America Bulletin, v. 59, p. 879-893.
- Fisher, R.V., 1966, Geology of a Miocene ignimbrite layer, John Day Formation, eastern Oregon: California University Publications in Geological Science, v. 67, p. 1-58.
- Fuis, G.S., 1973, The geology and mechanics of formation of the Fort Rock dome, Yavapai County, Arizona: California In-

- stitute of Technology, Ph.D. thesis, 278 p.
- Gilbert, G. K., 1880, Report on the geology of the Henry Mountains: Washington, U.S. Government Printing Office, 2d ed., 170 p.
- Glazner, A.F., Nielsen, J.E., Howard, K.A., and Miller, D.M., 1986, Correlation of the Peach Springs Tuff, a large-volume Miocene ignimbrite sheet in California and Arizona: *Geology*, v. 14, p. 840-843.
- Goff, F.E., Eddy, A.C., and Arney, B.H., 1983, Reconnaissance geologic strip map from Kingman to south of Bill Williams Mountain, Arizona: Los Alamos National Laboratory, Los Alamos, New Mexico, LA-9202-MAP, 5 sheets, scale 1:48,000.
- Green, C.R., and Sellers, W.D., 1964, Arizona climate: Tucson, University of Arizona Press, 503 p.
- Haskell, N.A., 1935, The motion of a viscous fluid under a surface load: *Physics*, v. 6, p. 265-269.
- Hobbs, S.W., 1944, Tungsten deposits in the Borina district and in the Aquarius Range, Mohave County, Arizona: U.S. Geological Survey Bulletin, 940-I, p. 247-264.
- Hunt, C. B., 1953, Geology and geography of the Henry Mountains region, Utah: U.S. Geological Survey Professional Paper 228, 234 p.
- Johnson, A.M., and Pollard, D.D., 1973, Mechanics of growth of some laccolithic intrusions in the Henry Mountains, Utah, I: *Tectonophysics*, v. 18, p. 261-309.
- Johnson, L.R., 1967, Array measurements of *P* velocity in the upper mantle: *Journal of Geophysical Research*, v. 72, p. 6309-6325.
- Koch, F.G., Johnson, A.M., and Pollard, D.D., 1981, Monoclinical bending of strata over laccolithic intrusions: *Tectonophysics*, v. 74, no. 3-4, p. T21-T31.
- Koons, E.D., 1948, Geology of the eastern Hualpai Reservation (Arizona): *Plateau*, v. 20, p. 53-60.
- 1964, Structure of the eastern Hualpai Indian Reservation: *Arizona Geological Society Digest*, v. 7, p. 97-114.
- Krieger, M.H., 1965, Geology of the Prescott and Paulden quadrangles, Arizona: U.S. Geological Survey Professional Paper 467, 127 p.
- 1967, Reconnaissance geologic maps of the Turkey Canyon, Camp Wood, Simmons, Iron Springs, and Sheridan Mountain quadrangles, Yavapai County, Arizona: U.S. Geological Survey, Miscellaneous Geological Investigations, Maps I-501 through I-505, scale 1:62,500.
- Landau, L.D., and Lifschitz, F.M., 1959, *Fluid mechanics*: London, Pergamon Press, 536 p.
- Longwell, C.R., 1936, Geology of the Boulder Reservoir floor, Arizona-Nevada: *Geological Society of America Bulletin*, v. 47, p. 1393-1476.
- Lucchitta, Ivo, 1972, Early history of the Colorado River in the Basin and Range Province: *Geological Society of America Bulletin*, v. 83, p. 1933-1948.
- Maxson, J.H., 1961, Geologic history of the Bright Angel quadrangle, in *Geologic map of the Bright Angel quadrangle: Grand Canyon National History Association*, 2d ed., revised 1966, 1 sheet.
- McCarthy, Jill, Larkin, S.P., Fuis, G.S., Simpson, R.W., and Howard, K.A., 1991, Anatomy of a metamorphic core complex: seismic refraction/wide-angle reflection profiling in southeastern California and western Arizona: *Journal of Geophysical Research*, v. 96, no. B7, p. 12,259-12,291.
- McKee, E.D., and McKee, E.H., 1972, Pliocene uplift of the Grand Canyon region—Time of drainage adjustment: *Geological Society of America Bulletin*, v. 83, p. 1923-1931.
- McKee, E.D., Wilson, R.F., Breed, W.J., and Breed, C.S., 1967, Evolution of the Colorado River: Flagstaff, Arizona, Museum of Northern Arizona, Bulletin 44, 67 p.
- McKee, E.H., and Anderson, C.A., 1971, Age and chemistry of Tertiary volcanic rocks in north-central Arizona and their relation to the Colorado Plateaus: *Geological Society of America Bulletin*, v. 82, p. 2767-2782.
- Moyer, T.C., and Esperanca, Sonia, 1989, Geochemical and isotopic variations in a bimodal magma system: the Kaiser Springs volcanic field, Arizona: *Journal of Geophysical Research*, v. 94, p. 7841-7859.
- Nealey, L.D., Ward, A.W., Bartel, A.J., Vivit, D.V., and Knight, R.J., 1986, Petrochemistry of rocks from the Mohon Mountains volcanic field, Yavapai and Mohave Counties, Arizona: U.S. Geological Survey Open File Report 86-423, 19 p.
- Nielson, J.E., Lux, D.R., Dalrymple, G. B., and Glazner, A. F., 1990, Age of the Peach Springs Tuff, southeastern California and western Arizona: *Journal of Geophysical Research*, v. 95, no. B1, p. 571-580.
- Noble, L.F., and Hunter, J.F., 1917, A reconnaissance of the Archean complex of Granite Gorge, Grand Canyon, Arizona: U.S. Geological Survey Professional Paper 98-I, p. 95-113.
- Nockolds, S. R., 1954, Average chemical compositions of some igneous rocks: *Geological Society of America Bulletin*, v. 45, p. 1007-1032.
- Pasteels, P., and Silver, L. T., 1965, Geochronologic investigations in the crystalline rocks of the Grand Canyon, Arizona: *Geological Society of America Special Paper* 87, p. 124.
- Pollard, D. D., and Holzhausen, Gary, 1979, On the mechanical interaction between a fluid-filled fracture and the earth's surface: *Tectonophysics*, v. 53, p. 27-57.
- Pollard, D. D., and Johnson, A. M., 1973, Mechanics of growth of some laccolithic intrusions in the Henry Mountains, Utah, II: *Tectonophysics*, v. 18, p. 311-354.
- Rascoe, J., 1968, *Old Arizona treasures*: Fort Davis, Texas, Frontier Book Co., 120 p.
- Reynolds, S.J., 1988, *Geological map of Arizona*: Arizona Geological Survey, Tucson, Arizona, map 26, scale 1:1,000,000.
- Ross, C.S., and Smith, R.L., 1961, Ash-flow tuffs: Their origin, geologic relations, and identification: U.S. Geological Survey Professional Paper 366, 81 p.
- Sauck, W.A., and Sumner, J.S., 1971, Residual aeromagnetic map of Arizona: Tucson, University of Arizona, Department of Geosciences, scale 1:1,000,000.
- Shapiro, Leonard, and Brannock, W.W., 1962, Rapid analysis of silicate, carbonate, and phosphate rocks: U.S. Geological Survey Bulletin 1144-A, p. A1-A56.
- Sheppard, R.A., and Gude, A.J., 3d, 1972, Big Sandy Formation near Wikieup, Mohave County, Arizona: U.S. Geological Survey Bulletin 1354-C, p. C1-C10.
- Shoemaker, E.M., Squires, R.L., and Abrams, M.J., 1974, The Bright Angel and Mesa Butte fault systems of northern Arizona, in Karlstrom, T. N. V., and others, eds., *Geology of Northern Arizona, Part 1—Regional studies*: Geological Society of America, p. 355-391.
- Simmons, A.M., 1986, The geology of Mount Hope, a volcanic dome in the Colorado Plateau—Basin and Range Transition Zone, Arizona: State University of New York at Buffalo, M.S. thesis, 156 p.
- Simmons, A.M., 1988, Contrast in timing, geochemistry, and eruptive style in the shift from mid-Tertiary to extension-re-

- lated volcanism in the Mohon Mountains (abs.): Geological Society of America Abstracts with Program, v. 20, no. 7, p. A306.
- Simmons, A.M., 1990, The Miocene Mohon Mountains volcanic field, west-central Arizona: geology, geochemistry, and petrogenesis: State University of New York at Buffalo, Ph.D. thesis, 274 p.
- Smith, R.L., and Bailey, R.A., 1966, The Bandelier Tuff: A study of ash-flow eruption cycles from zoned magma chambers: Bulletin Volcanologique, v. 29, p. 83-104.
- Spry, A., 1969, Metamorphic textures: New York, Pergamon Press, 350 p.
- Stacey, F.D., 1969, Physics of the Earth: New York, Wiley, 324 p.
- Ward, A.W., and Nealey, L.D., 1990a, Preliminary geologic map of the Pilot Knob quadrangle, Mohave and Yavapai Counties, Arizona: U.S. Geological Survey Open File Report 90-26, scale 1:24,000.
- Ward, A.W., and Nealey, L.D., 1990b, Preliminary geologic map of the Burro Mesa quadrangle, Yavapai County, Arizona: U.S. Geological Survey Open File Report 90-212, scale 1:24,000.
- Wendlandt, E.A., Shelby, T.H., Jr., and Bell, J.S., 1946, Hawkins Field, Wood County, Texas: American Association of Petroleum Geologists Bulletin, v. 30, p. 1830-1856.
- Williams, Howell, 1936, Pliocene volcanoes of the Navajo-Hopi country: Geological Society of America Bulletin, v. 47, p. 111.
- Williams, Howell, Turner, F.J., and Gilbert, C.M., 1954, Petrography: San Francisco, W. H. Freeman, 406 p.
- Wilson, E.D., Moore, R.T., and Cooper, J.R., 1969, Geologic map of Arizona: Arizona Bureau of Mines and the U.S. Geological Survey, scale 1:1,000,000.
- Young, R.A., 1966, Cenozoic geology along the edge of the Colorado Plateau in northwestern Arizona: Washington University, Ph.D. thesis, 167 p.
- Young, R.A., and Brennan, W.J., 1974, The Peach Springs Tuff: Its bearing on structural evolution of the Colorado Plateau and development of Cenozoic drainage in Mohave County, Arizona: Geological Society of America Bulletin, v. 85, p. 83-90.